NON POLAR AND AFFINITY MONOLITHIC STATIONARY PHASES FOR HPLC OF LARGE AND SMALL MOLECULES AND THEIR USE IN A MULTI COLUMN LIQUID PHASE SEPARATION PLATFORM FOR THE CAPTURING AND FRACTIONATION OF SIALOGLYCOPROTEINS FROM HUMAN SERUM

By

ERANDI PRASHANI MAYADUNNE

Bachelor of Science
University of Colombo
Sri Lanka
2007

Submitted to the Faculty of the
Graduate College of the
Oklahoma State University
in partial fulfillment of
the requirements for
the Degree of
DOCTOR OF PHILOSOPHY
December, 2013

NON POLAR AND AFFINITY MONOLITHIC STATIONARY PHASES FOR HPLC OF LARGE AND SMALL MOLECULES AND THEIR USE IN A MULTI COLUMN LIQUID PHASE SEPARATION PLATFORM FOR THE CAPTURING AND FRACTIONATION OF SIALOGLYCOPROTEINS FROM HUMAN SERUM

Dissertation Approved:

Dr. Ziad El Rassi

Dissertation Adviser

Dr. Barry Lavine

Dr. Richard Bunce

Dr. Nicholas Materer

Dr. Junpeng Deng

Outside Committee Member

ACKNOWLEDGEMENTS

I am sincerely and heartedly grateful to my advisor, Dr. Ziad El Rassi, for his continuous support and guidance during my studies at Oklahoma State University. I am grateful to him for directing me in research and developing the analytical thinking and scientific writing skills. I am fortunate to have the opportunity to pursue my PhD under him and I learned a lot of important concepts about bioanalytical chemistry. He always encourages and motivates me in the right direction. Thank you, Dr. El Rassi for your support and guidance.

I am grateful to the members of my committee, Dr. Barry Lavine, Dr. Richard Bunce, Dr. Nicholas Materer, and Dr. Junpeng Deng. I would also like thank for Dr. Steve Hartson for his help with the LC-MS/MS measurements. My gratitude also goes to all the staff members in the Department of Chemistry.

I would like to thank my previous labmates Samuel Karenga, Subhashini Selvaraju and Dilani Gunasena and the present members Chanida Puanpila, Renuka Rathnasekara, Nisansala Ganewatta, Shantipriya Khadka, Murthy Jonanda and Alharthi Sarah for their friendship and endless support.

My heartiest thanks go to my loving husband, Asitha Silva, who have been always there for me. Thanks for sharing my happiness and sorrows. You are the most wonderful husband one can ever get. Without your love and guidance I will not be able to

achieve my goals. Special thanks go to my little princess Seyha who brings joy and happiness to our lives, and you are the most precious gift in my life. Your priceless smiles relieve life's difficulties. Special thank goes to Mrs. Gerry Smith who has has helping me in various ways. I am also thankful to my in-laws for their love and support. Finally, my heartfelt gratitude goes to my beloved parents Prabhodhanie and Kumara Mayadunne for their unconditional love and showing me the right path in life. I am proud to be your daughter.

Acknowledgements reflect the views of the author and are not endorsed by committee members or Oklahoma State University

TABLE OF CONTENTS

Chapter Page

Chapter Page

Chapter Page

LIST OF TABLES

Chapter II

Chapter III

Table Page

Chapter IV

Chapter V

Table Page

LIST OF FIGURES

Chapter II

Chapter III

Figure Page

Chapter IV

Figure Page

Chapter V

Figure Page

LIST OF ABBREVIATIONS

4-SPV	1-(3-Sulfopropyl)-4-vinylpyridinium betaine
AAL	*Aleuria aurentia*
ACN	Acetonitrile
AIBN	2,2′-Azobis(isobutyronitrile)
AMC	Affinity monolith chromatography
AB	Alkyl benzenes
BAC	Boronate-affinity chromatography
BMA	n-Butyl methacrylate
BVBDMS	Bis (*p*-vinylbenzyl) dimethylsilane
BVPE	1, 2-Bis (*p*-vinylphenyl) ethane
CNT	Carbon nanotube
Con A	Concanavalin A
CPLL	Combinatorial peptide ligand libraries
DEP	Differentially expressed proteins

DMN-H6	1,4,4a,5,8,8a-Hexahydro-1,4,5,8-*exo*,*endo*-dimethanonaphthalene
Dns	Dansyl
DTT	Dithiothreitol
EDMA	Ethylene glycol dimethacrylate
EMA	Ethyl methacrylate
FR	Fluoroalkylsilyl-bonded
GalNAc	n-Acetylgalactosamine
GlcNAc	n-Acetylglucosamine
GMM	Glyceryl mono methacrylate
HAS	Human serum albumin
HCC	Hepatocellular carcinoma
HILIC	Hydrophilic interaction liquid chromatography
HIS	Histidine
HMA	n-Hexyl methacrylate
HPA	Agarose-bound helix pomatia agglutinin
HPLC	High performance liquid chromatography
IMAC	Immobilized metal affinity chromatography

IR	Infrared
k’	Chromatographic retention factor
LC	Liquid chromatography
LEL	*Lycopersicon esculentum* lectin
LMAA	Lauryl methacrylate additive
LMA	n-Lauryl methacrylate
LTA	*Lotus tetragonolobus* agglutinin lectin
MAL-II	*Maakia amurensis* lectin
MBA	N,N’-Methylenebisacrylamide
MeOH	Methanol
MPC	2-Methacryloyloxyethyl phosphorylcholine
MS	p-Methylstyrene
MS	Mass spectrometry
MWCNT	Multiwalled carbon nanotubes
NBE	Norborn-2-ene
ODA	Octadecyl acrylate
ODMA	n-Octadecyl methacrylate

PBB	(Pentabromobenzyloxy) propylsilyl-bonded
PETA	Pentaerithrytol triacrylate
PRISM	High-pressure, high-resolution separation with intelligent selection and multiplexing
PVA	Poly vinyl alcohol
ROMP	Ring-opening metathesis polymerization
RPC	Reversed phase chromatography
RSD	Relative standard deviation
SALDI-MS	Surface-assisted laser desorption/ionization mass spectrometry
SAX	Strong anion exchange
SDS	Sodium dodecyl sulfate
SEM	Scanning electron microscopy
Serial-LAC	Serial lectin affinity chromatography
SISCAPA	Stable isotope standards and capture by anti-peptide antibodies
SNA	*Sambucus Nigra* agglutinin lectin
SWCNT	Single walled carbon nanotubes
TCA	Trichloroacetic acid
TEM	Transmission electron microscopy

TFA	Trifluoroacetic acid
TMOS	Tetramethoxysilane
t_R	Migration time of retained solute
TRIM	Trimethylolpropane trimethacrylate
Tris	Tris (hydroxymethyl)-aminomethane
UEA-1	U*lex europaeus*
VTMS	Vinyltrimethoxysilane
WGA	Wheat germ agglutinin

CHAPTER I

BACKGROUND AND RATIONALE OF THE STUDY

Introduction

This introductory chapter aims at providing the reader with the basic knowledge and background of what is known so far about monolithic columns in HPLC and their chromatographic retention mechanisms. Also, this chapter introduces the reader to the prefractionation and concentration methodologies of complex proteomics samples prior to their analysis by LC/MS-MS.

Monolithic columns for HPLC

Introductory remarks

Monolithic stationary phases are "continuous separation media" that do not contain interstitial space (i.e., interparticle space). Two decades ago (year 1991), Hjerten and co-workers introduced monolithic stationary phases in which one piece of porous organic polymer filled the cylindrical column [1]. Five years later (year 1996), Minakuchi et al. developed monolithic columns based on inorganic silica matrices. The silica columns gave plate heights of 10-20 μm for aromatic hydrocarbons. It was observed that

the performance of silica rods was better than particle columns for high molecular weight species [2]. Even though, they have been introduced recently, monolithic columns have rapidly become popular in HPLC due to their advantages of low back pressure drop, fast mass-transfer and simple preparation [3]. They possess good flow through pores that yield good permeability and enable separation at high flow rate, withstand pressure while generating good separation efficiency. Monolithic columns possess higher porosity than densely packed particle columns. This higher porosity leads to higher permeability and lower pressure drop [4]. Due to their small sized skeletons, high separation efficiency can be expected using monolithic columns. Monoliths can be molded into disks, tubes, microfluidic channels, capillary columns or regular sized columns [5, 6]. In developing monoliths one can tailor the surface interactive sites according to the solutes to be separated. Today, organic, inorganic and hybrid monolithic separation media are primarily used in HPLC. These monoliths have their own advantages and disadvantages. Organic polymer monoliths can be made out of organic polymer matrices such as polystyrenes, polymethacrylate esters, polyacrylamides and others [7-9]. Inorganic monoliths are mainly made out of silica polymers [10]. In addition to the monoliths mentioned above, nanotubes incorporated monoliths are also being developed for the rapid separations of a wide spectrum of analytes [11].

Organic polymer monoliths are basically suited for separations of large molecules such as peptides and proteins and also they withstand high temperatures and a wide range of pH [9], while silica based monoliths show high separation efficiency towards small molecules [12]. Before monolithic columns gained popularity as stationary phases in HPLC, particulate columns were used. Particulate columns attempt to optimize the Eddy

diffusion term (A) and longitudinal molecular diffusion term (B) constants in the Van Deemter equation, but they are unable to address the mass transfer kinetics [13, 14]. Since in monolithic columns the mobile phase flowing through the stationary phase is the driving force for the mass transfer, the macropores enable a substantial increase in the separation speed of large molecules such as proteins [15, 16].

This overview attempts to summarize the types of monolithic stationary phases used in HPLC and their applications. Each section explains the monomers and crosslinkers used in the column fabrication, any new techniques used in the column development, types of the solutes analyzed and polarity of the stationary phases. Although the emphasis of this dissertation is the development of non-polar monoliths that are primarily used in RPC, for the sake of completeness polar as well as other monoliths are being overviewed in this chapter.

Organic polymer monoliths

Nonpolar organic monoliths. Organic polymer-based monoliths are becoming increasingly popular due to the fact that they show good stability towards all pH values, temperatures and easy surface modification. These features have proven advantageous for the separation conditions of macromolecules such as proteins and relatively small carbohydrates and nucleotides under gradient elution conditions [17, 18].

Organic polymer-based monoliths are usually fabricated *via* radical polymerization of crosslinking and functional monomers in the presence of a well-chosen porogenic solvent. The polymerization reaction is initiated with decomposition of a radical initiator, usually 2,2′-azobisisobutyronitrile (AIBN), and is facilitated with the

thermal initiation at a constant temperature using a water bath or a GC oven [19-21]. The polymerization begins with the formation of the nuclei, then the cross linking monomer starts to incorporate around the nuclei and gradually a heterogeneous polymer material fills the tubular column. Once the polymerization is completed, the monolith is washed extensively with organic solvent such as acetonitrile (ACN) or methanol (MeOH) to remove porogen and unreacted monomers.

Polymer monoliths can be prepared from styrene, methacrylate, acrylate, acrylamide or using cyclic monomers e.g., cyclic olefin copolymers and cyclic norborn-2-ene [8, 22, 23]. Alkyl methacrylate-based monolithic stationary phases of different hydrophobicity were constructed for reversed-phase chromatography (RPC) by thermally initiated radical polymerization. This involved the use of a series of alkyl methacrylates such as ethyl methacrylate (EMA), n-butyl methacrylate (BMA), n-hexyl methacrylate (HMA), n-lauryl methacrylate (LMA) and n-octadecyl methacrylate (ODMA), and the retention of alkyl benzenes were evaluated and found out that the ODMA-based column shows enhanced retention towards alkyl benzenes [24]. Another monolith was fabricated using the radical polymerization of ethylene dimethacrylate (EDMA) and BMA in the presence of porogenic solvent mixtures containing various concentration ratios of 1-propanol, 1, 4-butanediol, and water with AIBN as the initiator. The RPC retention of the column thus obtained was evaluated using some benzene derivatives [25]. In another investigation, a series of monoliths was fabricated *via* a radical polymerization using alkyl methacrylate based monomers and EDMA as a cross linker, with different compositions of the porogens. Hydrodynamic and chromatographic properties of these monoliths were studied. Among the prepared monoliths, BMA yielded rigid macroporous

morphology and excellent hydrodynamic characteristics (flow rate up to 5 mL min^{-1}). The monolith was evaluated using a mixture of benzene and its derivatives in the RPC mode. The separation efficiency was shown to increase with the addition of a lauryl methacrylate additive (LMA) in the polymerization mixture. The maximum separation efficiency achieved was 35 000 plates/meter for the monolith based on BMA with 7% LMA in the reaction mixture [26]. Construction of large volume monolithic columns was described using GMA-EDMA monolith. Due to the exothermic nature of the polymerization reaction, the evolved heat affected the nature of the monolith. The temperature increase depends on the thickness of the monolith. This study has analyzed the heat released during the polymerization and derived a mathematical model for the prediction of the maximal thickness of the monolithic having a uniform structure [27].

A monolith fabricated using bisphenol A epoxy vinyl ester resin as the functional monomer and EDMA as the cross-linker was used as the stationary phase for HPLC. The column showed good reproducibility and efficiency for the baseline separation of benzene derivatives and halogenated derivatives using isocratic elution. The column showed a good reproducibility in terms of relative standard deviation (RSD) for the retention times from run-to-run, column-to-column and batch-to-batch (n=3) with RSD of 0.98, 1.68, and 5.48, respectively [3]. Macroporous polymer monoliths based on poly(styrene-co-divinylbenzene) with varied styrene/divinylbenzene ratios have been prepared. The separation efficiency of small molecules (e.g., alkyl benzenes) was evaluated by HPLC under isocratic RPC mode. The use of tetrahydrofuran as a macroporogen and decanol as a microporogen for the fabrication of

poly(styrene/divinylbenzene) monolith yielded a column that enabled separation of peptides and proteins by the RPC mode [28].

Monolithic columns were prepared *via* ring-opening metathesis polymerization (ROMP) within silanized fused silica capillaries with an internal diameter of 200 μm by in situ grafting using the polymerization of norborn-2-ene (NBE) and 1,4,4a,5,8,8a-hexahydro-1,4,5,8-exo,endo-dimethanonaphthalene (DMN-H_6) in a porogenic system ROMP initiator. The column thus obtained was suitable for the separation of peptides [29].

Polar organic monolithic stationary phases. Polar organic polymer-based monolithic columns for hydrophilic interaction liquid chromatography (HILIC) can be fabricated by incorporating hydrophilic moieties in the polymer matrix. Monolithic columns were developed by an *in situ* reaction of tris (2, 3-epoxypropyl) isocyanurate with 4-[(4-aminocyclohexyl) methyl] cyclohexylamine in the presence of polyethylene glycol (PEG). The column thus obtained proved useful for the separation of nucleic bases and nucleosides [30]. In another report, a polar acrylamide based monolith was developed using *in situ* polymerization of piperazine, diacrylamide and methacrylamide with the addition of *N*-isopropyl acrylamide or a mixture of 2-hydroxymethacrylate and vinylsufonic acid, and the resulting monolith was evaluated with some aromatic polar compounds such as pyridine, 4-pyridylmethanol, 4-methoxyphenol, 2-naphthol, catechol, hydroquinone, resorcinol, 2,7-dihydroxynaphthalene [31].

In a study by Foo et al. [32], a novel stationary phase for HILIC was reported. It involved the co-polymerization of zwitterionic *N, N'*-dimethyl-N-methacryloxyethyl-*N*-(3-sulfopropyl) ammonium betaine (SPE) and the crosslinker 1, 2-bis (p-vinylphenyl)

ethane (BVPE). The chromatographic properties of the optimized poly (SPEco-BVPE) monolithic column were evaluated. Triplicate injections of the compounds thiourea, toluene and acrylamide were carried out with an average separation efficiency in the range of 26,888 to 35,930 [32].

Chemical modification is another way to increase the number of binding sites for the desired analytes. These chemical modifications are easily achieved using the monomers such as chloromethyl styrene and divinylbenzene. Reaction of poly (chloromethylstyrene-co-divinylbenzene) with ethylenediamine followed by γ-gluconolactone leads to a porous medium that has highly hydrophilic surface functionalities. The monolith thus obtained was tested with alkyl benzenes in the RPC mode and large proteins in the hydrophobic adsorption and ion exchange modes. The authors claimed that the modified monolith possessed a sufficient hydrophobicity that seems comparable to some of the existing hydrophilic HPLC packings [33].

Zwitterionic hydrophilic porous poly (SPV-co-MBA) monolithic column was fabricated by the thermal co-polymerization of 1-(3-sulphopropyl)-4-vinylpyridiniumbetaine (4-SPV) and *N, N'*-methylenebisacrylamide (MBA). An HILIC/RPC dual separation mechanism was observed on this optimized poly (SPV-co-MBA) monolithic column. The monolith yielded the baseline separation of nine benzoic acid derivatives using ACN gradient [34].

Some highlights of applications of organic polymer monoliths. Organic polymer monoliths are most suitable in the separation of relatively large molecules using linear gradient elution. The RPC separations of standard proteins have been investigated using commercial poly(styrene-co-divinylbenzene) monolithic columns (Dionex ProSwift™

RP-2H and RP-4H) [35]. Alternative solvents to acetonitrile, such as 2-propanol and methanol, coupled with elevated temperatures demonstrated complementary approaches to adjusting separation selectivity and reducing organic solvent consumption. Measurements of peak area at increasing isothermal temperature intervals indicated that only minor (<5%) decreases in detectable protein recovery occurred between 40 and 100° on the timescale of separation (2-5 min). The reduced viscosity of a 2-propanol/water eluent at elevated temperatures permitted coupling of three columns to increase peak production (defined as number of peaks/min) by 16.5%. Finally, narrow-bore (1 mm i.d.) columns were found to provide a more suitable avenue to fast, high temperature (up to 140°) separations.

A novel monolith was fabricated using the copolymerization of bis (*p*-vinylbenzyl) dimethylsilane (BVBDMS) with *p*-methylstyrene (MS) in the presence of 2-propanol and toluene, using AIBN as the radical initiator. The resulting monolith was used to separate proteins, peptides and oligonucleotides. Also, monolithic columns as applied to clinical analysis in the areas of monitoring of therapeutic drug and drug abuse and trace compound analysis have been reviewed recently [13]. Furthermore, organic polymer monoliths have recently been applied to the analysis of peptides, proteins and trace contaminants in food samples, and the field has been reviewed very recently [36]. A sensitive chromatographic method utilizing a monolithic column of the poly (glycidyl methacrylate-co-ethylene dimethacrylate) type, which was further modified with quaternary amine groups, were developed for the determination of trace level bromate in food and drinking water. GMA/EDMA type prepared using *in situ* polymerization and further modified with quaternary amine, have been used in the analysis of bromates in

drinking water. Bromate was detected after post-column reaction with potassium iodide at 352 nm. The parameters affecting the detection limit of bromate were studied in detail. This method showed good linearity over the concentration range 5.0-30 μg/L, short analysis time (8.5 min), and satisfactory relative standard deviation of the replicate analyses (n = 6, 0.043 %) with detection limit for bromate of 1.5 μg/L [37] .

Inorganic monoliths

Nonpolar inorganic monoliths. Besides silica- [10], zirconia- [38] and titania-based monoliths [39] have been recently developed. Among these materials, silica is an ideal support due to its favorable characteristics, such as good mechanical strength, high chemical and thermal stability, controllable pore structure and surface area, surface rich in silanol groups that can be modified, and non-swelling property [10]. Since it is the most widely used approach to prepare silica-based monoliths, the sol-gel method is described in next section.

In the sol-gel process, the silica monolith is usually fabricated by utilizing tetramethoxysilane (TMOS) as a silica precursor and polyethylene oxide (PEO) as a pore-forming agent [40]. The two components TMOS and PEO are dissolved under slightly acidic conditions and the resulting solution is filled into a suitable gelation tubes and heated at moderate temperature. These reaction conditions initiate the hydrolysis and polycondensation of the TMOS in the presence of the PEO. Transfer of the sol to the gel state forming the silica and the phase separation of the silica-rich phase and the solvent-rich phase happens simultaneously. The following two processes then take place in

parallel and compete with each other. The phase separation process that occurs after a specified reaction time determines the macroporous structure of the silica. In this stage, the silica-rich phase separates from the solvent-rich phase, building up the silica skeleton. Elimination of the solvent by drying in the solvent-rich phase then leads to the formation of the macropores. Further polycondensation reactions cause shrinkage of the rod, which then detaches from the inner surface of the gelation tube, allowing its removal. The polycondensation of the TMOS starts along the PEO chains forming H-bonds with the polymer and building up the silica consecutively. During this reaction, methanol is introduced to accumulate in "vacuoles" within the co-continuous silica-forming network. These "vacuoles" form the resulting macropores. Their size is determined by the concentration of the PEO added to the starting solution. An increasing amount of PEO will lead to silica monoliths with decreasing macropore sizes [10].

Recently, monolithic silica columns whose skeletons contained weakly connected porous silica microspheres were prepared [41]. The aging temperature was selected in the range of 25–30 ^{o}C, the mass ratio of PEG to TMOS in the range 0.10–0.20 and mass ratio of TMOS to H_2O less than 0.5. Then, dispersed porous silica spheres were obtained by gentle grinding of the monolithic column using a mortar. After surface modification with C18, the silica microspheres with an average diameter of 5.4 μm were packed and used for the HPLC of neutral, acidic, and basic compounds. The retention behavior was similar to that obtained on the commercially available 5 μm C18 silica particles but the 5.4 μm grounded silica microspheres showed better separation efficiency [41].

Novel silica-based monolithic columns have been produced recently to achieve fast separation with low backpressure and good resolution. Although silica monoliths are

favored over polymeric monoliths due to their chemical/mechanical stability and non-swelling property, the monolithic columns with randomly distributed pore structures were used so far, leading to eddy diffusion and peak broadening. To overcome this drawback, a directional freezing and freeze drying method was used for the first time to produce aligned porous silica monoliths in a silica capillary from commercially available silica colloidal suspension. Both silica and silica-polymer composite monoliths are produced and the full pore characterizations were performed. These monoliths contain parallel microchannels and thus minimize eddy diffusion. The HPLC tests on these monoliths under both normal phase and reversed phase conditions demonstrated the feasibility for use in chromatography. The aligned microchannel structures of the monoliths can achieve efficient separation with significantly low backpressure, compared to conventional porous monoliths [42].

In another development simple and comprehensive two-dimensional (2D)-HPLC was studied in a reversed-phase mode using monolithic silica columns for second-dimension (2nd-D) separation [43]. Every fraction from the first column, 15 cm x 4.6-mm i.d., packed with fluoroalkylsilyl-bonded (FR) silica particles, was subjected to the separation in the 2nd-D using one or two C18 monolithic silica columns (3 cm x 4.6-mm i.d.). Monolithic silica columns in the 2nd-D were eluted at a flow rate of up to 10 mL/min with separation time of 30 s that meets the fractionation every 15-30 s at the first dimension (1st-D) operated at a flow rate of 0.4-0.8 mL/min. Three cases were studied. (1) In the simplest scheme of 2D-HPLC, effluent of the 1st-D was directly loaded into an injector loop of 2nd-D HPLC for 28 s, and 2 s was allowed for injection. (2) Two six-port valves each having a sample loops were used to hold the effluent of the 1st-D alternately

for 30 s for one 2nd-D column to affect comprehensive 2D-HPLC without the loss of 1st-D effluent. (3) Two monolithic silica columns were used for 2nd-D by using a switching valve and two sets of 2nd-D chromatographs separating each fraction of the 1st-D effluent with the two 2nd-D columns alternately. In this case, two columns of the same C18 stationary phase or different phases, C18 and (pentabromobenzyloxy) propylsilyl-bonded (PBB), could be employed at the 2nd-D, although the latter needed two complementary runs. The systems produced peak capacity of approximately 1000 in approximately 60 min in cases 1 and 2 and in approximately 30 min in case 3. The three stationary phases, FR, C18 and PBB, showed widely different selectivity from each other, making 2D separations possible. The simple and comprehensive 2D-HPLC utilizes the stability and high efficiency at high linear velocities of monolithic silica columns [43].

Recently, the chromatographic properties of a new type of monolithic silica rod columns were examined [44]. In this study, silica rod columns were prepared from tetramethoxysilane, modified with octadecylsilyl moieties, and encased in a stainless-steel protective column with two polymer layers between the silica and the stainless-steel tubing. A 25 cm column provided up to 45,000 theoretical plates for aromatic hydrocarbons, or a minimum plate height of about 5.5 μm, at optimum linear velocity of about 2.3 mm/s and back pressure of 7.5 MPa in an ACN-water (80/20, v/v) mobile phase at 40 ˚C. The permeability of the column was similar to that of a column packed with 5 μm particles, while the plate height value equivalent to that of a column packed with 2.5 μm particles. Generation of 80,000-120,000 theoretical plates was feasible with backpressure <30 MPa by employing two or three 25 cm columns connected in series. The use of the long columns enabled facile generation of large numbers of theoretical

plates in comparison with conventional monolithic silica columns or particulate columns [44].

Polar inorganic monoliths. HILIC is a valuable alternative to RPC separations for polar, weakly acidic or basic samples. The retention mechanism is based on the competition between the sample and the mobile phase for localized polar adsorption centers on the adsorbent surface, such as silanol groups on the surface of silica gel [45].

Monolithic Titania columns were prepared by Randon et al. for the separation of naphthalene, caffeine, 7-(β-hydroxyethyl) theophylline and theophylline in HILIC. Titania monoliths were prepared from a mixture of titanium propoxide, hydrochloric acid, formamide and water. In order to obtain the macroporous titania monolith, synthesis parameters such as hydrolysis ratio, porogen type, precursor concentration, and drying step have been identified. Standard xanthines were separated successfully in HLIC using the titania monolith thus prepared [46].

Zirconia monolithic silica columns were fabricated to achieve a higher efficiency with a lower backpressure than traditional monoliths. In addition, zirconia has a higher thermal and chemical stability and specific surface properties. The monolith was able to separate mixture of amines, naphthalene, orthotoluidine, aniline and an alkoxybenzene mixture [47].

Highlights of applications of inorganic polymer monoliths. Inorganic polymer monoliths are useful for the high efficiency separation of small molecules. Especially, monolithic columns were used in the separation of biologically important compounds and pharmaceuticals. An HPLC method using fluorescence detection was developed for the

simultaneous determination of 21 derivatized 4-fluoro-7-nitro-2, 1, 3-benzoxadiazole (NBD-F) amino acids. The NBD-F derivatized amino acids were separated on a monolithic silica column (MonoClad C18-HS, 150 mm × 3 mm i.d.) [48]. Monolithic silica columns were used to separate mixtures of hydrophobic naturally occurring metabolites. These monolithic silica columns were able to separate polyprenols [49, 50]. Benzoic acid is a preservative and vanillin is a flavoring agent added to the food to enhance flavor. But adding synthetic vanillin to the food is illegal. Using titania based monolith, a simple and reliable method was developed to determine the benzoic acid and vanillin in food stuff [39].

Hybrid monolithic stationary phases

Monolithic columns made out of organic polymers such as polymethacrylates, polyacrylamides and polystyrenes, and the silica-based inorganic polymers were described in the above sections. These monoliths have their own advantages and disadvantages. The former monoliths can be generally prepared by *in situ* polymerization of organic monomers and crosslinkers in the presence of porogenic solvents while the latter is fabricated *via* a sol–gel process followed by a chemical modification of the matrix with different sialylation reagents. Organic polymer monoliths exhibit swelling or shrinkage while silica monoliths involve tedious fabrication procedures. An alternative to address these drawbacks is organic-silica hybrid monolithic column, which is receiving more and more attention as it possesses the advantages of easy fabrication, more pH stability, and less shrinkage. The field has been reviewed very recently [51].

Very recently, hybrid monoliths synthesized *via* a sol-gel process have been reviewed in Ref. [51]. According to a recent review article, hybrid monoliths can be classified into two classes [52] depending on the nature of the interface between the organic and inorganic moiety. Hybrid monoliths class I are based on weak interactions such as van der Waals forces, hydrogen bonding or electrostatic interactions between organic and inorganic parts, and obtained by the methods of impregnation, doping, or physical entrapment of organic species into sol–gel matrices. Hybrid monoliths of class II refer to monoliths possessing organic components strongly attached to the siloxane network *via* covalent bonds, and are typically prepared *via* co-condensation of alkoxysilane and organosilane reagents [53]. There are several chemical routes to synthesize these monoliths including (a) the encapsulation of organic components into silica monolith *via* sol–gel process, (b) the attachment of the desired organic functionality to sol–gel matrices by covalent bond formation and (c) direct synthesis into the final hybrid monoliths by using a functional organosilane. A detailed description of these routes can be found in a recent review [53].

Monolith fabricated *via* sol-gel process consisting of hydrolysis and condensation reactions of tetraalkoxysilanes such as tetramethoxysilanes or tetraethoxysilanes are commonly used in research. A novel hydroxyl functionalized organic–inorganic hybrid monolithic column was fabricated *via* free radical copolymerization with sonication-assisted] to decrease the time of the sol–gel process. Vinyltrimethoxysilane (VTMS) was used as the monomer and vinyl ester resin was used as both the monomer and crosslinker. The obtained column showed high permeability and low backpressure. The column was used to analyze lysozyme from egg white, and benzene derivatives [54]. In another

report, a hybrid monolith was fabricated using polycondensation of alkoxysilanes and *in situ* copolymerization of mono (6^A-*N*-allylamino-6^A-deoxy)-Ph-β-CD and vinyl group on the pre-condensed siloxanes yielding the hybrid monolithic column of perphenylcarbamoylated β-cyclodextrin-silica (Ph-β-CD-silica), and the column was used for the enantioseperation of 13 different racemates [55]. In a more recent report, an epoxy-based organic–inorganic hybrid monolithic column was used to monitor the beta-lactam antibiotics such as amoxicillin, cephradine, and cefazolin sodium in aquatic environment and milk using online solid phase extraction-HPLC [56]. Hybrid C8-silica monoliths functionalized with octyl groups was synthesized in a capillary column for nano-LC separations in the RPC mode. The resulting hybrid monoliths yielded retention factors comparable to those obtained on a C18 grafted silica monoliths for the nano-LC separation of alkyl benzenes. The authors reported separation efficiencies for alkyl benzenes that were the best ever recorded in nano-LC with hybrid monoliths [57]. Two zwitterionic organic-silica hybrid monolithic columns were successfully synthesized using [2-(methacryloyloxy)ethyl]dimethyl-(3-sulfopropyl)ammonium hydroxide (MSA) and 2-methacryloyloxyethyl phosphorylcholine (MPC) as the organic monomers. Polar compounds as well as neutral, acidic and basic analytes and small peptides were analyzed in the HILIC mode [58] on these columns.

Highlights of the use of monolithic stationary phases in affinity chromatography

Affinity monolith chromatography (AMC) is a type of liquid chromatography that uses a monolithic support having surface bound biologically active compounds as the stationary phase ligands. The field has been reviewed by Pfaunmiller et al. [59] and

Malik and Luke [60]. The retention mechanism is based on the specific and reversible interactions found in the biological systems, such as binding of an enzyme with a substrate, an antibody with an antigen, or binding of a glycoproteins with lectins [60]. In AMC the affinity columns can be fabricated using the monolithic materials such as organic polymers, silica, agarose and cryogels [59]. Stationary phase ligands used in AMC are antibodies, enzymes, proteins, lectins, immobilized metal ions and dyes [59]. In general, affinity columns whether made of monoliths or particulate materials are used extensively in many fields such as protein isolation, biomarker discovery, biochemical and chemical research, molecular biology, clinical testing, biotechnology, environmental analysis and biophysical measurements [61-65]. Monoliths used in affinity chromatography should exhibit high porosity, high permeability and low backpressure. Monoliths fabricated using glycidyl methacrylate (GMA) and ethylene glycol dimethacrylate (EDMA) are the most commonly used organic based affinity monoliths, and have been used in many applications. GMA/EDMA monolith is used in affinity chromatography due to several important characteristics of the monolith. The monolith is relatively easy to fabricate and hydrophilic in nature, thus eliminating nonspecific binding for most of the solutes [66]. The monolith can be easily modified to make it suitable for ligand attachment. By changing the porogen content, the monolith can be developed in various pore sizes, surface areas and shapes. The GMA/ EDMA monolith has been used in the identification of glycoprotein biomarkers from human breast cancer serum [67]. A multicolumn based fluidic system comprising GMA/EDMA monolithic micro columns with immobilized protein A, protein G′, and antibodies was used for the depletion of high abundance proteins in human serum [68]. Using metal ions as ligands

GMA/EDMA monolith was used in metal ion affinity chromatography for the simultaneous depletion and prefractionation of human serum prior to 2-DE for facilitating in-depth serum profiling [69]. GMM/ PETA monolith with specific immobilized lectins is emerging as a novel affinity monolith and was used in this dissertation for the capturing of sialylated glycoproteins from human serum. The GMM/PETA monolith was used for the capturing of human fucome form the breast cancer serum [67] .

Affinity monoliths can also be prepared from cryogels, and the preparation of such monolithic matrices has been recently reviewed [60]. Briefly, a mixture of acrylamide, allyl glycidyl ether and *N,N'*-methylene *bis*-(acrylamide) is used in making the polymer. Affinity cryogel monolith with immobilized concavalin A (Con A) was used for the chromatographic separation of the cells mixture of *Saccharomyces cerevisiae* and *Escherichia coli* [70]. The bio particle such as cells capturing properties and detaching them from the stationary phase by deforming the monolith was studied by the different ligand–receptor pairs (IgG–protein A, sugar–Con A, metal ion–chelating ligand) using cryogel monolith [71].

Nanotube incorporated monolithic columns

Carbon nanotubes (CNT) have been recognized for having high strength and unique electronic properties. The unique physicochemical properties of CNT such as large surface –to –volume ratio, porous nature, low density, high strength, good thermal stability have made them very attractive for use in developing novel stationary phases for HPLC. Boron nitride nanotubes functionalized *via* quinuclidine-3-thiol with gold nanoparticles were incorporated into monolithic columns and enhanced separation was

achieved for benzene derivatives, naphthalene derivatives and alkyl parabens [11]. Increased separation of alkyl benzenes and uracil was observed with MWCNTs incorporated into GMM/EDMA monolith [72]. Also, (MWCNTs were incorporated into a mixture containing benzyl methacrylate (BMA) and ethylene dimethacrylate (EDMA) as co-monomers. The optimized porogenic mixture was a ternary solution composed of cyclohexanol, 1,4-butandiol and butanol, which resulted in a stable and homogeneous suspension. Six capillary columns with increasing amounts of MWCNT, from 0 to 0.4 mg/mL, were prepared by thermal polymerization in 0.32 mm (i.d.) and 150 mm length fused silica tubing. The chromatographic evaluation showed that the synthesized monolithic beds were mechanically stable while their porosity and permeability increased with the MWCNTs content. The prepared capillary columns were tested for the separation of mixtures of ketones and phenols at an optimum flow rate of 2 μL/min. The results showed that incorporation of MWCNT slightly affected the retention while it enhanced the column efficiency by increasing the column efficiency by a factor of up to 9. This effect corresponded also to an improved resolution and full separation of the solutes [73]. Recently, fast enantiomeric separation of underivatized amino acids was achieved with silica based carbon nanotube (CNT) monolithic columns coated with a pyrenyl derivative as chiral selector. This column was applied to the chiral separation of underivatized amino acids. As well, ultra-fast separations in the range of seconds were achieved using high flow-rates [74].

Strategies for prefractionation and concentration of proteomic samples prior to their analysis by LC/MS-MS

Introductory remarks

Proteomics is the study of protein structures and functions, for recent review on this topic, see Ref. [75]. Proteins are important indicators of physiological or pathological states of an individual and contribute to the early diagnosis of disease, which may help for identifying the underlying mechanism of disease development. Differentially expressed proteins in serum have become an important event to monitoring the state of a certain disease(s). These differentially expressed proteins can be identified as candidate biomarkers for specific diseases. Protein biomarkers can assist in diagnosing a disease at the biochemical level or discriminating the responses of different patients to the same medical treatment, for review see [76]. Recent advances in proteomic techniques give the opportunity in biomarker research in which serum is considered as an excellent diagnostic medium for the detection of disease. Diseases are often discovered in an advanced stage because of the lack of specific biomarkers. Therefore, early detection of biomarkers is vital in disease diagnosis and reduces the severity of its impact on the patient's life or prevents and/or delay subsequent complications.

In proteomic analysis of serum, it is vital to reduce the complexity of serum sample. Several techniques have been suggested and employed to reduce the complexity of the plasma proteome, including depletion of high abundance proteins [67], nonspecific enrichment of low abundance proteins *via* combinatorial peptide ligand libraries (CPLL) from human serum and venom [77, 78] and specific enrichment of targeted peptides after

enzymatic digestion [79]. Also, the serum complexity can be reduced using the traditional methods such as centrifugation or extraction with organic solvents [80] or by immuno-depletion [68, 81]. Precipitation of high abundance proteins using organic solvents is another method to reduce the complexity of the serum sample. The simple organic precipitation is suitable for large scale studies as they are inexpensive, scalable, potentially robust and reproducible [82]. In this overview, an explanation of depletion methods to remove high abundance proteins from the serum sample as well as equalization of protein concentration will be provided. Furthermore, chromatographic fractionation prior to LC-MS/MS and capturing of specific proteome by lectin affinity chromatography will be discussed with some emphasis of the capturing of specific sub-glycoproteome.

Methodologies used to reduce the complexity of proteomic samples

Depletion methods. The wide range in protein abundance poses a tremendous challenge for plasma proteomics. However, as a relatively small number of proteins make up most of the total protein pool, the concentration range can be compressed by depletion of abundant proteins, such as albumin. To reduce sample complexity and increase the detection of low abundance proteins, the depletion methods can be applied [68, 81-87].

Solvent solubalization and precipitation methods. The main goal of proteomics is to discover disease biomarkers, which helps to identify physiological changes of cells, tissue or organisms compared to the control sample and helping to diagnose the diseases and pharmaceuticals design. Many of the abundant proteins in plasma have molecular weights exceeding 60 kDa (e.g. albumin, transferrin, and fibrinogen, IgA, α-2-

antitrypsin, apolipoproteins, and α-1-acid glycoprotein). The depletion of many of these large and highly abundant plasma proteins is possible by precipitation using organic solvents such as acetonitrile, acetone, trichloroacetic acid (TCA). To reduce sample complexity and increase the protein identification coverage, organic precipitation methods have been developed. High abundance proteins were removed using organic solvents such as acetonitrile. Authors state that up to 90% of albumin and other abundant proteins were removed by adding an equal volume of acetonitrile to the blood plasma samples adjusted to pH 5 [82]. Solubility of proteins is also affected by pH, ionic strength and temperature [88], and by adjusting one or more of these parameters, the precipitation may be optimized to efficiently remove as much as possible of the abundant proteins such as albumin in a single step, while maintaining low-abundant proteins in solution. Alternatively, several precipitation steps can be combined for a more efficient depletion of abundant proteins and increased recovery of low abundant proteins. Albumin is the highest abundance protein in serum. Albumin-TCA complex is soluble in organic solvents such as acetone. In the study carried out by Fattahi et al., acetone was added to 15 mL of serum sample and incubated at 20 ^{0}C for 90 min and then centrifuged at 4 ^{o}C. The albumin in the serum sample remains in the supernatant phase binding to TCA and other proteins were precipitated and used for proteomic analysis [89]. For protein precipitation, acetonitrile was mixed with the serum samples in 1:1 (v/v) ratio and the samples were vortexed, and then incubated in an ultrasonic bath at room temperature. These steps were repeated twice and incubated in ultrasonic bath for 10 min and centrifuged. The high abundance proteins were precipitated and low abundance proteins were collected from the precipitate [82]. Sequential depletion of osteoarthritis disease

serum was performed using two different chemical depletion methods, using acetonitrile and dithiothreitol (DTT), for the mass spectrometry analysis of human serum proteins. Records showed that ACN depletion was efficient for depleting high molecular weight proteins (over 75 kDa), whereas DTT depletion primarily promotes the precipitation of proteins rich in disulphide bonds (mainly albumin). The study combined these two chemical depletions in a sequential way with the intention of reducing the complexity of serum protein profile while removing high abundant proteins. First, the serum sample was incubated for 1 h at room temperature with DDT, and after centrifugation of these samples the supernatant was vortexed and supernatant was subjected to 2D gel followed by MALDI-TOF [83]. In order to find the candidate proteomic biomarkers in the serum of ankylosing spondylitis diseased serum were precipitated using chloroform and methanol. The serum was depleted from IgGs and albumin. The depleted serum was subjected to nano liquid chromatography and mass spectrometry analysis to detect and quantify proteins. A total of 316 proteins were identified with 22 showed significant up or down regulation [90].

Immunoaffinity depletion methods. Immunoaffinity depletion methods involve the use of immobilized antibodies to capture one or more of the high abundance proteins. This is another approach to decrease the complexity of the serum sample before proteomic analysis. There are numerous immunodepletion methods available which were reviewed recently by Selvaraju and El Rassi [91]. Holewinski et al. has conducted a study to find fast and reproducible method for albumin depletion from serum and cerebrospinal fluid. In this study, commercially available albumin depletion methods were compared in terms of their reproducibility and efficiency. Albumin and IgG were depleted from

pooled human serum samples and cerebrospinal fluid using commercially available immunoaffnity kits including ProteaPrep HSA spins columns, ProteaPrep HSA 96-well plate, ProteaPrep HSA/IgG depletion column, Vivapure anti-HSA/IgG depletion kit, and Sigma antiHSA/IgG depletion columns. Two depletion methods (e.g., Sigma and Proteaprep) showed albumin depletion of 97% or greater for both serum and cerebrospinal fluid [84]. Tan et al. used the chicken host to produce polyclonal antibodies IgY against complex mammalian antigens. The ability of chicken IgY antibody to deplete six high abundance proteins including α1-antitrypsin, albumin, transferrin, haptoglobin, IgG and IgA from serum was studied. The authors concluded that the polyclonal IgY antibodies were suited for the depletion of serum from high abundance proteins and to consequently identifying novel biomarkers [92]. Janecki et al. conducted a study using liquid chromatography setup for automated serum/plasma depletion with two immunoaffinity columns. The first column was the Seppro IgY14 for the depletion of the 14 most abundant proteins followed by the second column Seppro SuperMix to deplete the next 200-300 proteins. The authors processed nine serum samples of 1 mL each within 24 h period with excellent reproducibility. The proposed automated serum depletion setup can be used for the faster depletion of a large number of biological samples [85]. Yu at al. conducted the study for the depletion of albumin and IgG for the quantification of human serum transferrin, which is the principal ion transporter for the body. Briefly, serum was depleted using the ProteoPrep® Blue Albumin and IgG Depletion Kit according to the manufacture's protocol. The author believed this methodology can be applied to the clinical monitoring of human transferrin which is a potential biomarker for certain cancers [93]. Abundant proteins were depleted

from the serum in the process of quantifying target proteins using protein standard absolute quantification (PSAQ) method, which uses full-length isotope labeled protein standards to quantify proteins. Serum samples were depleted of the six most abundant proteins using the human Multiple Affinity Removal Spin cartridge (MARS6) in the study of quantification of cardiovascular biomarkers from serum. The authors were able to quantify six biomarkers from the serum including LDH-B, total LDH, creatine kinase B, creatine kinase M, myoglobin, and troponin 1. The authors believed that PSAQ will be a major contributor to efficiently quantify biomarkers [94]. Maternal serum proteome changes during pregnancy were studied with the intention of developing new gestational biomarkers. Serum (50 μL) was depleted from albumin, immunoglobulin IgA, IgG, α1-antitrypsin, transferrin and haptoglobin using a multiple affinity removal column with the size of 100 x 4.6 mm I.D. and subjected the depleted serum to the LC-MS/MS analysis. Mass spectrometric analysis detected 38 known proteins during pregnancy and identified one novel protein the beta 1 glycoprotein 4, which is a pregnancy specific protein. Further isotope labeling studies detected four new proteins. The authors concluded that measurement of changes in maternal serum proteome may be useful to identify birth defects, preterm delivery and reproductive health [95].

Supermacroporous cryogels are good alternative to traditional protein-binding stationary phase matrices due to many advantages such as large pores, short diffusion path, low-pressure drop, and very short residence times for both adsorption and elution. Macroporous cryogels imprinted with human serum albumin (HSA) was fabricated by copolymerization of 2-hydroxyethyl methacrylate with a functional co-monomer of *N*-methacryloyl-l-phenylalanine and used for the depletion of albumin from human serum.

The cryogel was first equilibrated with passing pH 6.0 phosphate buffer solution and then, human serum was injected [96].

Immunoaffinity fractionation of highly abundant proteins has proven to be one of the most effective approaches for overcoming the wide dynamic range of protein concentration, as well as enabling the detection of low abundance proteins. Janecki et al. developed fully integrated multi column system for the depletion of abundant proteins from plasma. The serum sample was loaded onto an immunoaffinity depletion column SepproTM IgY14 LC10 and Seppro SuperMix LC5 columns. The samples were serially depleted from 14 high abundance proteins first by SepproTM IgY14 LC10 column followed by Seppro SuperMix LC5 column [85]. Commercially available Seppro IgY14 LC10 column and SuperMix LC5 column were used to remove fourteen high abundance proteins from human serum samples including albumin, α1-antitrypsin, IgM, haptoglobin, fibrinogen, α1-acid glycoprotein, HDL, LDL, IgG, IgA, transferrin, α2-macroglobulin, and complement C3. Serum samples were diluted 6-fold with the dilution buffer, passed through a 0.45 μm spin filter, and centrifuged for 1 min at 9,200 × g to remove any particulate materials present in the sample [97]. In another investigation, novel HSA and IgG affinity sorbents were developed using epitope-imprinted polymers as artificial antibodies to deplete human serum. Acrylic acid, acrylamide, and *N*-acryl tyramide were used as monomers, *N,N'*-ehtylene bisacrylamide was the cross linker and cellulosic fibers were the supporting matrix. The adsorption capacity of these artificial antibodies were found to be 15.2 mg, 10 mg and 15 μg for human serum albumin, IgG and human serum, respectively. The authors state that rapid production, high specificity efficient depletion make them attractive for the serum depletion [87]. In the work conducted by Selvaraju

and El Rassi to identify differentially expressed fucosylated glycoproteins by lectin affinity chromatography, albumin and Igs were depleted using GMM/PETA monolithic columns with immobilized protein G', protein A and anti-human albumin [67].

Highlights of protein equalization method in proteomics. The few high-abundance proteins make up 99% of the serum, thus making it difficult to identify low-abundance proteins and protein alterations with different physiological conditions. It is important to reduce the concentration of high abundance proteins in serum to discover the low-abundance ones. One main approach to decrease the high abundance proteins are depletion methods, which are described above in this chapter. The other main approach is protein equalization [98]. The concept of combinatorial peptide ligand libraries (CPLL) combined with other fractionation methods such differential gel electrophoresis and off gel fractionation was recently reported to identify a large number of low abundance proteins in some extracts [91]. Righetti et al. have introduced CPLL for the equalization of proteins and conducted proteomics analyses for many fluids and matrices including human serum, plant and animal tissues [99-107]. Each CPLL consists of millions of baits on beads or in columns, which bind proteins to the peptide ligands of the beads. The high abundance proteins saturate the binding sites of CPLL and the remaining molecules of these proteins are washed away. This results in enrichment of low abundance proteins and in turn it reduces the concentration of high abundance proteins. CPLL approach has been applied for the quantitative comparison of the proteomic in multiple cell extracts. In one study, the reproducibility of CPLL was assessed by capturing the whole range of protein abundances from the proteome of *Saccharomyces cerevisiae*. For the quantitative

evaluation of the performance of CPLLs, the selected reaction monitoring (SRM) approach has been used in which mass spectrometric tool is employed for quantitative protein analysis [99]. Proteomic characterizations of venoms of rattlesnakes were conducted using CPLL. Captured protein fractions were subjected to the N-terminal sequence analysis using Procise instrument according to the manufactures protocol. Peptides were identified and subjected to SDS-PAGE and analyzed with tandem mass spectrometry [77]. The proteome of untreated white wines was explored via capture CPLL at four different pH values: pH 2.2, 3.8, 7.2, and 9.3. The study revealed the identification of 106 unique gene products belonging to Vitis vinifera as well as of an additional 11 proteins released by the S. cerevisiae used in the fermentation process [108]. Righetti et al. conducted an in depth analysis of proteome in banana fruit with the focus of identifying the metabolite composition and proteins causing food allergies and low abundance proteins in banana using CPLL. They were able to identify 1131 proteins, and food allergens such as mus a 1, pectinesterase, superoxide dismutase, and potentially new allergens. The authors believed that this is the first in-depth exploration of the banana fruit proteome and one of the largest descriptions of the proteome of any vegetable system [101]. In this study, CPLL has been used as a two-dimensional (2D) method for proteome analysis in which proteins capture under conditions favoring ionic interactions vs. environments inducing hydrophobic interactions. Briefly, the 2D orthogonal mode that utilizes the affinity of the multiple ligands, serum proteins were captured at physiological pH either at low ionic strength (25 mM NaCl) or at high concentrations of lyotropic salts which favor hydrophobic interaction. By comparison of the two modes the authors reported that 52% of the captured proteins are common to the

two capture modes, 20% are unique to the “ionic” interaction mode and 28% are unique to the hydrophobic mode. This orthogonal method overcome the major drawbacks of CPLL in which it diminishes the loss of protein up to 5% in ionic capture, whereas the hydrophobically engendered capture is loss-free [109]. Recently, CPLL was used in the enrichment of low abundance glycoproteins [102]. To reduce the high abundance protein concentration in swine plasma, CPLL has been used with dual-enzyme, dual-activation strategy to achieve high proteomic coverage. The CPLL treatment enriched the lower abundance proteins by >100-fold and a total of 3421 unique proteins spanning a concentration range of 9–10 orders of magnitude were identified [110]. To identify the proteins in the development of chick embryos, hen egg white proteins were analyzed by CPLL. Briefly, this method used ProteoMiner protein enrichment kits to enrich low abundance and identify the low abundance proteins in hen egg white samples. The study identified 30 proteins in five protein families including transferrin, protease inhibitor, clusterin, serpin and lipocalin family [111]. Ovarian cancer serum was equalized using CPLL, and the concentration of the most abundant serum proteins was reduced using the ProteoMiner Enrichment Kit and then submitted to 2-D gel electrophoresis followed by identifying proteins using MALDI-TOF. To identify new proteins with potential diagnostic or prognostic value for the therapy of ovarian cancer comparative proteomic analysis of sera from ovarian cancer patients and healthy women was performed [112]. In this investigation, serum samples from 10 patients diagnosed with epithelial ovarian cancer and 10 age-matched healthy women were analyzed. To decrease the extremely wide dynamic range of protein concentration in serum CPLL was used. Serum samples were then subjected to proteomic 2-DE analysis. Three proteins with differential

abundance were found and identified by mass spectrometry: α-1-antitrypsin, apolipoprotein A-IV and retinol-binding protein 4. Identification of α-1-antitrypsin and apolipoprotein A-IV confirms previous studies but the identification of significantly decreased levels of RBP4 in ovarian cancer patients represents a novel observation. The decrease of RBP4 levels in ovarian cancer patient sera was verified by two independent methods and determined absolute RBP4 concentrations in patients and healthy women. The possible non-cancer factors that could be responsible for the observed RBP4 decrease could be excluded, and consequently, a connection of RBP4 with epithelial ovarian was proposed and the potential of RBP4 as a candidate biomarker was advocated by the authors [112]. Human serum from osteoarthritis patients were subjected to protein equalization using ProteoMiner kit [83]. Serum from patients with gastric precancerous lesions, were equalized using ProteoMiner kit. The study identified altered O-glycosylation using simple mucin type carbohydrate antigen STn and T antigens in the serum from patients with gastritis and IM in opposition to minor or no reactivity in the same proteins of healthy individuals without any gastric disease [113].

A single chain variable fragment (scFv) displaying M13 phage library covalently immobilized onto magnetic microspheres was used to equalize human serum proteins. In this method, the phage library with magnetic microspheres was incubated with serum sample, eluted captured proteins on the library using eluting mobile phase, and tightly bound proteins were released with treatment of thrombin. The eluted proteins were analyzed with SDS-PAGE followed by the 2D strong cation exchange RPLC-ESI-MS/MS. The authors state that the number of proteins identified from scFv M13 treated human serum sample was improved by 100% compared with that from the untreated

sample. The spectral count of 10 high abundance proteins (serum albumin, serotransferrin, α-2-macroglobulin, α-1-antitrypsin, apolipoprotein B-100, Ig γ-2 chain C region, haptoglobin, hemopexin, α-1-acid glycoprotein 1, and α-2-HS-glycoprotein) was significantly reduced, which resulted in more protein identification. The phage library was compared to the peptide library and it shows strong binding capacity and high specificity toward proteins and also can be reproduced to obtain enough ligands for sample preparation [98].

Enrichment of proteins *via* immobilized metal ion affinity chromatography (IMAC) IMAC is a protein purification and enrichment technique. Its applications include the purification of histidine-tagged proteins, natural metal-binding proteins, and antibodies. The underlying mechanism of IMAC is the adsorption of proteins due to the interactions between an immobilized metal ion and electron donor groups located on the surface of proteins. Most commonly used metals are Cu(II), Ni(II), Zn(II), Co(II), TI(II) and IV and Fe(III) ions, for review see [114].

Enrichment of phosphoproteome Yue et al. developed an optimized method for the IMAC enrichment of the phosphoproteome of the human mammary cell line, MCF-10A, using both SCX-IMAC and optimized multistep IMAC enrichment followed by the high-pH RP fractionation method (multi-IMAC-HLB). 5519 unique phosphopeptides were identified in 13 fractions using the SCX-IMAC method from 15 mg of starting material. 8969 unique phosphopeptides were identified in 12 multi-IMAC-HLB, (HLB means hydrophilic–lipophilic-balanced reversed-phase cartridge) fractions from 3 mg of starting material. The efficiency of the SCX-IMAC method and the multistep IMAC-HLB method was compared using the number of identified unique phosphopeptides, the

phosphopeptide ratios, and the numbers of singly and multiply phosphorylated peptides. The authors concluded that multi-IMAC-HLB is a robust and efficient method of phophoproteome research [115]. In another very recent report, a novel material for IMAC for phosphoproteome research was designed using polydopamine coated on the graphene surface and functionalized with titanium ions (denoted as Ti^{4+}-G@PD). The above monolith with enhanced hydrophobicity and biological compatibility was evaluated using scanning electron microscopy (SEM), transmission electron microscopy (TEM), and infrared (IR). The performance for effective enrichment of phosphopeptides was evaluated with both standard peptide mixtures and human serum. The authors believed that there will be a possibility to design an efficient and sensitive tool for phosphoproteome analysis [116]. Sun et al. evaluated sequential IMAC using gallium based IMAC in conjunction with titanium dioxide based metal affinity chromatography for the enrichment of phosphopeptides. The quantitative performance of this approach was evaluated using tryptic peptides from casein, bovine serum albumin and standard phosphopeptides. This study evaluated the repeatability, dynamic range, and linearity of IMAC for large scale quantitative phosphoproteomics applications [117]. Zeng et al. conducted a study with immobilized TiO_2 onto poly(acrylic acid)-functionalized magnetic carbon-encapsulated iron nanoparticles as affinity probes for efficient enrichment of phosphopeptides. To evaluate the performance of magnetic TiO_2 affinity probes, tryptic digests of β-casein and BSA were used. Using the magnetic TiO_2 affinity probes to isolate the phosphopeptides from 200-mg equivalent of HeLa cell lysates from bovine fetal serum, 1415 unique phosphopeptides and 1093 phosphorylation sites were identified [118]. Zhou et al. conducted their investigation for enrichment of specific

phosphopeptides with immobilized titanium IMAC with the polymeric column chelated with Ti^{4+}. Briefly, phosphate polymer was prepared by direct polymerization of monomers containing phosphate groups through immobilize TI^{4+} through chelating interactions between phosphate groups on the polymer and Ti^{4+}. Ti-IMAC resin isolated phosphopeptides from digest mixture of standard phosphopeptides and BSA. The Ti-IMAC was also used to isolate phosphopeptides from mouse liver. The authors state that this method is highly specific to isolate phosphopeptides due to the specific interaction between immobilized Ti^{4+} ion and phosphate group on the phosphopeptides [119].

Enrichment of histidine-tagged proteins. The histidine-tag is today the most commonly used tag for recombinant proteins. It is used for the purification of recombinant expressed proteins and detection purposes [120]. Lee et al. developed a novel magnetic mesoporous silica (MMS) material with high magnetic strength for the selective His-tagged enzyme enrichment. The efficiency was compared with nickel-based MMS materials, such as Ni^{2+}-MMS and Ni-MMS, and nickel ion doped silica-coated magnetic nanoparticles (Ni^{2+}-MNPs). The efficiency was calculated to be 100 ± 1.93%, 70.94 ± 1.95%, and 37.03 ± 5.93% for Ni^{2+}-MMS, Ni-MMS, and Ni^{2+}-MNPs, respectively and identified Ni^{2+}-MMS as the suitable material for the enrichment of histidine tagged proteins. This method enables a high-throughput and advanced systematic approach for the separation and immobilization of proteins which cover a broad spectrum of polyhistidine-tagged proteins [121]. For the enrichment of histidine tagged peptides, silicon nanostructured (NanoSi) surface functionalized with an organic layer of nitrotriacetic acid (NTA) was used as an affinity surface-assisted laser desorption/ionization mass spectrometry (SALDI-MS) interface for histidine-tagged

peptide enrichment and mass spectrometry analysis. The developed platform has shown good selectivity toward His-tagged peptide and permits its enrichment from an artificial mixture of both tagged and untagged peptides and the mass spectrometry detection was obtained with good signal/noise ratio [122].

Enrichment of other subproteomes. Recently, in our laboratory Jmeian and El Rassi introduced an integrated fluidic platform with tandem affinity columns for the depletion of high abundance proteins followed by online fractionation and concentration by immobilized metal affinity chromatography (IMAC) [69]. The IMAC columns were fabricated using GMA/ EDMA monolithic columns with surface bound iminodiacetic acid ligands, which were chelated with $Zn^{2+,}$ Ni^{2+}, and Cu^{2+}. The captured fractions were analyzed by 2-DE and analyzed with MALDI-TOF and LC-MS/MS and 295 proteins were identified. While Cu^{2+}-IMAC column can bind to proteins having cysteine and methionine residues in addition to one histidine residue on their surface, the affinity of Ni^{2+}-IMAC and Zn^{2+}- IMAC columns require two histidine residues in particular position on the protein surface [69]. Wang et al. developed an IMAC method with an array of immobilized metal ions including Cd^{2+}, Ni^{2+}, Ca^{2+}, Zn^{2+}, Pb^{2+}, and Cu^{2+}. After analyzing the eluted fractions of each metal column by the LC-MS/MS, the identified proteins were compared with the published literature and observed there are published proteins as well as novel proteomic biomarkers [123].

Miscellaneous affinity for protein enrichment Boronate-affinity chromatography (BAC) is another tool for specific isolation and enrichment of *cis*-diol compounds. The boronic acid monoliths can be prepared by directly precipitate boronic-acid ligands with active groups (e.g., vinyl and amino group) or by immobilized boronic-acid ligands on a

monolithic column. Recent review by Li et al. has reviewed the advances in boronate affinity chromatography, see ref. [124].

Enrichment of peptides. Antibody free peptide enrichment platform was developed by Shi et al. for targeting specific peptides. A high-pressure, high-resolution separation with intelligent selection and multiplexing (PRISM) is a highly efficient method for quantification of target peptides. Application of this strategy to enrichment of human plasma demonstrated that the method was able to accurately and reproducibly quantitate peptides at the concentration ranges from the 50-100 pg/mL. The PRISM reduces background interferences and result in high sensitivity in quantification of low-abundance proteins in clinical serum samples [125]. Hydrophilic interaction liquid chromatography (HILIC) is a common approach for non-destructive method for glycopeptide enrichment. Kuo et al. compared HILIC methods for the enrichment of glycopeptides from serum using amine-derivatized Fe_3O_4 nanoparticles and Sepharose CL-4B resin. Glycopeptides were enriched from uterine luminal fluid of mice. 67 N-glycosylated peptides were identified with amine-derivatized Fe_3O_4 nanoparticles and 55 N-glycosylated peptides were identified with Sepharose CL-4B resin. The authors concluded that NH_2 functionalized nanoparticles are very useful for enrichment of N-glycosylated peptides [126]. Specific and sensitive immunoaffinity LC-MS/MS assay for quantification of low abundance cytokine of human and cynomologus monkey interleukin 21 was developed. Briefly, the peptide immunoaffinity enrichment of plasma/tissue extract was carried out using 96-well microtiter plate with the addition of monoclonal anti-IL 21. The cytokines were eluted and subjected to LC-MS/MS analysis. The authors state that the immunoaffinity LC-MS/MS approach is a selective and

sensitive strategy for pharmacological and clinical biomarker investigation [127]. Stable isotope standards and capture by anti-peptide antibodies (SISCAPA) is an immunoaffinity enrichment method for capturing of targeted peptides from digested tissue or bio-fluids. In the method of SISCAPA, peptide immunoaffinity enrichment of plasma was carried out using 96-well microtiter plate in triplicate. The bulk mixture of all eight anti-peptide antibodies was prepared and sixteen microliters of 1μm protein G magnetic beads (Invitrogen) were added to each sample and mixed briefly. The plates were sealed with further processed according to the manufactures procedure and subjected for LC analysis. The authors state that the developed SISCAPA method is a valuable technology that bridges the gap between discovery and clinical validation of candidate protein biomarkers [128] .

Serum fractionation methods. Serum fractionation has been proposed as a promising method to measure low-abundance proteins. There are several approaches to fractionate the serum that can be performed according to the size, polarity and the differences in the isoelectric points (pI values) of serum proteins.

Chromatographic fractionation. RPC columns have been used in the fractionation of serum samples. Selvaraju and El Rassi used proSwift^{TM} RP-1S column for the fractionation of fucosylated proteins captured from disease free and breast cancer sera. Two lectins namely *Lotus tetragonolobus* agglutinin (LTA) and *Aleuria aurentia* (AAL) lectin were used to capture the fucome. The collected RPC fractions were subjected to the LC-MS/MS analysis that led to the identification of a 35 broad panel of differentially expressed proteins (DEP) in the breast cancer serum relative to disease free serum and an eight narrower panel of DEP from both LTA and AAL captured protein

fractions [67]. Zhu et al. has developed two dimensional method with strong anion exchange (SAX) combined with RPC column to deplete high abundance proteins in human plasma and identification of low abundance proteins. Plasma was fractionated onto the SAX column producing 67 fractions. All the SAX fractions were reconstituted with suitable mobile phase and subjected to high pH RPC fractionation using a Jupiter C4 column and a linear gradient of 158 min with high UV absorption at 215 nm. The collected fractions were subjected to LC-MS/MS analysis for protein identification. Out of the 83 proteins that were identified, 68 were reported to be of the high- or middle-abundance proteins in plasma [129]. Kimura et al. used RPC in search for novel biomarkers for hepatocellular carcinoma (HCC). In this method, serum was subjected to immunoaffinity depletion to remove 10 high abundance proteins from the serum using Proteome Lab IgY-12HC LC10 column according to the manufacturer's instructions. The depleted serum was then loaded onto the Intrada WP-RP column and separation was performed using multi-segment elution gradient. The chromatograms were monitored at 218 nm and 40 fractions were collected each at 50 sec intervals. Fractions were analyzed with SDS-PAGE followed by in gel digestion and subjected to LC-MS/MS. 83 protein bands were found to be up regulated in HCC. Among the 83 protein bands clusterin was significantly overexpressed and the authors concluded that clusterin is a novel biomarker for HCC [130]. Comparison of two prefractionation methods based on RPC and SAX were carried out for the proteomic analysis of *Saccharomyces cerevisiae*. The first prefractionation separation was performed using SAX on Water BioSuite Q SAX at 50 ˚C using a gradient of ammonium acetate and 20 fractions were collected. The second prefractionation of proteins was performed by RPC on a PLRP-S column heated at 80 °C.

Fractions were collected using ACN gradient. In this study, more proteins were identified by RPC prefractionation than by SAX. The study concluded that RPC fractionation provides wider coverage than the SAX method [131].

Prefractionation by RPC was also used for peptides before subjecting them to LC-MS/MS. Ma et al. reported the RPC fractionation of peptides in the search of N-linked glycoproteome profiling of human serum. The serum was subjected to immunoaffinity depletion and the collected proteins were tryptically digested yielding peptides. N-linked peptides were captured with WGA, Con A, and RCA lectins. These enriched N-linked glycopeptides were fractionated using Durashell RP analytical column packed with 5 μm particles. The fractionation was carried out with high pH linear ACN gradient and 36 fractions were collected. The tandem enrichment methods, followed by high-pH reversed-phase prefractionation, enhanced the level of N-glycoproteome analysis from 312 N-glycosites to 615 N-glycosites using high-accuracy mass spectrometry [132]. Multidimensional separation of tryptic peptides from human serum proteins using RPC fractionation was done on an XBridge column [133]. Capillary reversed phase column of the dimension 200 μm inner diameter (i.d.) × 50 cm long, were packed in-house with 3 μm Jupiter C18 bonded particles to fractionate the non-depleted human serum [134]. In the search of cardiovascular biomarkers using nano-LC, depleted serum was subjected to tryptic digestion and fractionated using 300-μm x 5-mm PepMap C18 column at 300nL/min flow rate with a linear gradient for 60 min. The study was able to identify LDH-B, CKMB, myoglobin, and troponin I as biomarkers for the cardiovascular diseases [94].

Anion exchange chromatography is another technique for the fractionation of biological fluids including serum and cerebral spinal fluid (SPF). Ovarian cancer serum was fractionated using anion exchange chromatography for finding the highly glycosylated subproteome. A Mono Q 4.6/100 PE Tricorn high performance column connected to an HPLC system was used for the serum fractionation and four fractions of 500 μL were collected into glass vials containing 100 μL of 6% BSA [135]. With the intention of identifying breast cancer biomarkers, serum was fractionated by SAX chromatography. Six fractions were collected, based on differences in isoelectric point (pI) of the proteins. In the process of serum fractionation high-abundance proteins are segregated into a limited number of fractions, which reduces the signal suppression effects on proteins of lower abundance in the other fractions [136]. Multidimensional separation of tryptic peptides from human serum using strong cation exchange on PolySulfoethyl A column and serum protein profiling by nanoChip-LC–MS/MS resulted in the identification of 208 proteins and 1088 peptides with the lowest reported concentration of 11 ng/mL for heat shock protein 74 [133].

In this dissertation, RPC columns were used to fractionate disease free and breast cancer serum. In chapter 4, RPC columns were fabricated with ODA/TRIM monolith. Depleted serums as well as non-depleted serum were fractionated using linear ACN gradient. In chapter 5, RPC column was developed with different composition of ODA/TRM but incorporated with MWCNTs into the polymerization mixture. The data showed that the ODA/TRIM column incorporated with MWCNTs captured higher number of proteins than the blank ODA/TRIM column.

Capturing various glycoproteome by lectin affinity chromatography (LAC). Lectins are capable of recognizing specific glycan structures and serve as invaluable tools for the separation of glycosylated proteins (i.e., glycoproteome) from non-glycosylated proteins in biological samples [137]. Lectins can be considered as ideal reagents for protein-carbohydrate recognition since they can detect cell surface glycolipids and glycoproteins. They can be employed to identify minor variations in protein glycosylation including changes in the content of sialic acid and fucosyl residues present in serum glycoproteins [138]. There are around 60 commercially available lectins, which has the ability to recognize the diverse sugar structures, some are highly specific while others having overlapping selectivity for particular carbohydrate structures. Concanavalin A (Con A) is the best known plant lectin having very broad specificity while sambucus nigra (SNA) lectin has the specificity for sialic acid linked to α-2,6 galactose containing structures [139]. There are several formats of LAC used in glycoproteome research. While single LAC enriches limited number of glycoproteins, serial-LAC and multi- LAC allow capturing of large number of glycoproteins. In serial-LAC fraction from one lectin column is collected, dialyzed, dried and reconstituted and then transferred to a second lectin. This generates excessive discontinuous sample manipulation, which causes sample loss and propagation of experimental biases from column to column. M-LAC refers to using a mixture of immobilized lectins having complementary specificities in a given column (i.e., mixed bed column). After loading the sample onto the column, the M-LAC column is eluted sequentially using a specific haptenic sugar for each lectin. In this process, sequential elution may not be a clear cut, and some glycoproteins captured by another lectin may be concurrently eluted. It has been reported that serial-LAC resulted in

the identification of a higher number of proteins than M-LAC [140]. Recently, in our laboratory Selvaraju and El Rassi introduced tandem lectin affinity column using different lectin columns operating independently with switching valves whereby the sample is loaded onto the tandem columns and the pass through fraction of the first column is moved to the second column and so on by the mobile phase so that there is no need for collection, and fraction processing between columns, thus eliminating experimental biases and propagation of errors [140]. The study with the tandem lectin affinity monolithic column platform with surface immobilized Con A, wheat germ agglutinin (WGA) and *Ricinus communis* agglutinin (RCA) for identifying captured proteins from breast cancer and disease free human sera. According to the authors the suitable order of the lectin affinity columns were WGA, Con A and RCA. This tandem column format was able to capture 113 and 112 proteins from disease free and breast cancer sera, respectively, with 75 and 65 non redundant proteins, respectively [140]. A fully integrated platform comprised of a multicolumn operated by HPLC pumps and independent switching valves for the online depletion of high abundance proteins and capturing fucosylated glycoproteins *via* immobilized *Aleuria aurentia* (AAL) and *Lotus tetragonolobus lectins* (LTA) followed by fractionation of captured glycoproteins by RPC, was introduced by Selvaraju and El Rassi [67]. This investigation revealed a wide panel of 35 differentially proteins (DEP) and 8 narrow panel of DEP common to both LTA and AAL fractions which is a good representative of cancer altered fucome [67]. M-LAC methods was developed for the identification of cellular glycoproteins from MCF-7 breast cancer lysate combining three agarose bound lectins, namely, Con A, jacalin, and WGA and the captured lectin fractions were analyzed using nano LC-MS/MS. This

study revealed that M-LAC can be extended to total cell lysate to investigate the cellular proteomics [137]. With the intention of increasing the efficiency of the chromatographic process and selectivity of glyco-compounds separation, two stationary phases were compared. Con A lectin was immobilized on different macroporous stationary phase matrices of silica coated with poly vinyl alcohol (PVA), silica coated with cationic PVA (DEAE-PVA) and cellulose were compared. The authors concluded that in silica based monoliths higher flow rate and higher sorption parameters can be obtained [141]. The selectivity of recombinant forms of *Aleuria aurentia* lectin using weak-LAC on a commercial HPLC system was reported. Briefly, four different variants of *Aleuria aurentia* (AAL) which are native AAL purified from Aleuria aurentia mushrooms (n-AAL), recombinant AAL dimer (r-AAL), recombinant AAL monomer (m-AAL) and AAL site 2 protein (S2-AAL) were evaluate for the capturing of fucosylated glycoproteins. The study revealed that r-AAL forms show similar affinities toward glycoproteins but S2-AAL form has lower affinity to glycoproteins having sialic acid containing fucosylated saccharides [142]. Serial lectin affinity chromatography was performed for pooled human serum with four different types of affinity columns which are agarose-bound *Lycopersicon esculentum* lectin (LEL), agarose-bound *Helix pomatia* agglutinin (HPA), agarose-conjugated anti-Lewis x and anti-sialyl Lewis x IgM were used in serial-LAC. The numbers of glycoproteins identified were studied with columns attached in different orders. The authors believed that serial-LAC is a valuable tool in recognizing diversity in protein glycosylation, especially when the order of the columns in the serial-LAC is varied. [143]. In-depth analysis of the salivary proteome for the early diagnosis to identify disease biomarkers in different pathophysiological conditions were

conducted by Yates et al. The study utilized Con A, RCA-1, and *ulex europaeus* (UEA-1) lectins in lectin affinity chromatography. The captured glycoproteins were subjected to LC-MS/MS analysis and identified a total of 262 of O- and N-linked glycoproteins among them 224 were unique N-linked glycoproteins. It is believed that the glycoproteins identified in this study provide valuable information for more accurate diagnosis, prognosis, and treatment of local and systematic diseases [144]. Macroporous silica particles of 2-μm size, were used in LAC for the enrichment of glycoproteins. Briefly, AAL and Con A lectins were immobilized on the silica particles and tested for their binding properties with standard glycoproteins. The study revealed that the columns exhibited excellent binding capacities for microaffinity enrichment where Con A was able to bind 75 μg of a standard glycoprotein in a 50 × 1 mm column. The authors believed that 2 μm silica particles are excellent for chromatographic applications, owing to their rigidity, high surface area, large pores, and small particle diameter [145]. Hess et al. conducted a study to characterize *Mycobacterium tuberculosis* proteome using LCA and mass spectrometry based proteomic techniques. This study used WGA lectin and captured 1051 M. tuberculosis protein groups including 183 transmembrane proteins as identified by LC-MS/MS analysis. The authors state that the data set will serve as a valuable resource for *M. tuberculosis* proteome research [146]. Xu et al. conducted lectin affinity based approach to enrich and increase the number of secreted proteins detected in the media of cultured tissues of colorectal cancer patients. For the enrichment of glycoproteins, Con A and WGA lectins were used. The captured proteins were analyzed by one-dimensional gel electrophoresis coupled to LC-MS/MS and identified 123 differentially expressed secreted proteins with 68 of the differentially expressed proteins

were up-regulated in colorectal cancer tissues. EFEMP2 protein is one of the top 10 up-regulated differentially expressed proteins and the study indicated that EFEMP2 is a promising serum biomarker for the early detection of colorectal cancer [147]. The determination of glycoproteins in barley malt was conducted due to its importance in beer production. The aim of this study was to optimize separation and enrichment of individual modified proteins on a monolithic Con A affinity HPLC column and identified 10 bound protein fractions and their possible N-glycosylation sites [148].

Lectin affinity chromatography can also be employed as a fractionation method. This approach is widely used to fractionate protein glycoforms that have a specific glycan structure with binding affinity to lectin. It is becoming very attractive as a mode of fractionation to observe the difference between protein glycoforms. A number of lectins has been used to fractionate specific protein glycoforms from complex glycoproteome [129]. A pair of pooled serum samples was fractionated using phytohemagglutinin-L (L-PHA) lectin immobilized on biotin−streptavidin conjugated to magnetic beads specific for capturing of tissue inhibitor of metalloproteinase 1 (TIMP1) known to be aberrantly glycosylated in patients with colorectal cancer (CRC). Each captured glycoform was digested and enriched using a stable isotope standard and captured by the antipeptide antibody (SISCAPA) technique and analyzed with MALDI FTICR mass spectrometer. [129].

Rationale and scope of the study

Despite the progress made in the fabrication of monoliths, which was overviewed in the first part of this chapter, there is still need for monolithic columns well suited for the separation of small molecules as well as proteins by HPLC. Therefore, it is the aim of this dissertation to develop nonpolar organic polymer monoliths for RPC of small molecules that exhibit unique selectivity (see Chapter II). In this regards, multiwalled carbon nanotubes (MWCNTs) were incorporated into the organic polymer based monolithic columns prepared *via* the copolymerization of GMM/EDMA monomers in the presence of MWCNTs in the polymerization mixture. The above GMM/EDMA monolith was relatively hydrophilic with little or no RPC characteristics. The GMM/EDMA blank monolith when evaluated with alkyl benzenes did not show any retention but with the addition of MWCNTs, the monolith incorporating MWCNTs showed retention for alkyl benzenes and several other compounds such as toluene derivatives, anilines and herbicides. Chiral separation of biologically and environmentally important compounds was achieved using the novel monolith. However, the GMM/EDMA column incorporated MWCNTs did not separate proteins, and consequently cannot be used for proteomic studies. Therefore, we continued our search to find the monolithic column suitable for the separation of proteins.

In Chapter III, ODA/TRIM monolith was developed and the monolith was evaluated using alkyl benzenes and standard proteins. Although proteins exhibited good retention and separation on the ODA/TRIM monolithic column, the ODA/TRIM monolith was further optimized by incorporating in its texture small amount of MWCNTs. Protein separation was improved in terms of peak shape and retention. The

ODA/TRIM incorporated with MWCNTs thus obtained was used for the RPC fractionation of sialylated glycoproteins captured by lectin affinity columns in a multicolumn liquid phase based platform described in Chapters IV and V.

Although separation science in general and chromatography in particular have contributed extensively to advancing the field of proteomics, new approaches for the selective capturing of complex sub-glycoproteomics such as sialylated glycoproteins that are altered in cancers are badly needed. In this regards, a multi column liquid phase based platform was introduced for the online depletion of high abundance proteins and capturing of sialoglycoproteins. Thus, Chapters IV and V involved the development of monolithic columns with immobilized lectins for lectin affinity chromatography (LAC) enrichment of human serum sialoglycoproteins. To achieve this objective, *Sambucus Nigra* lectin (SNA) and *Maakia amurensis* lectin (MAL-II) were immobilized onto GMM/PETA monolithic columns for use in a multi column liquid phase based platform to capture sialoglycoproteins from disease free-human serum and from breast cancer serum for the identification of differentially expressed sialylated glycoproteins in breast cancer by liquid chromatography (LC) coupled to tandem mass spectrometry (LC-MS/MS).

Conclusions

This introductory chapter summarized the progress made in monolithic columns for HPLC. The overviewed monoliths included organic, inorganic, hybrid and nanoparticle incorporated monoliths. Also, the progress made so far in proteomics sample preparation approaches have been highlighted. This involved the description of the

methodological approaches developed so far for reducing the complexity of proteomics samples including the depletion of high abundance proteins from serum, the enrichment of specific subproteomes in serum and the fractionation of the various subproteomes by different chromatographic techniques. Finally, the rationale and scope of the dissertation have been summarized.

References

1. Liao, J.-L., R. Zhang, and S. Hjertén, *Continuous beds for standard and micro high-performance liquid chromatography.* J. Chromatogr. A, 1991. **586**: p. 21-26.
2. Minakuchi, H., K. Nakanishi, N. Soga, N. Ishizuka, and N. Tanaka, *Octadecylsilylated Porous Silica Rods as Separation Media for Reversed-Phase Liquid Chromatography.* Anal. Chem., 1996. **68**(19): p. 3498-3501.
3. Niu, W., L. Wang, L. Bai, and G. Yang, *The fabrication of monolithic capillary column based on poly (bisphenol A epoxy vinyl ester resin-co-ethylene glycol dimethacrylate) and its applications for the separation of small molecules in high performance liquid chromatography.* J. Chromatogr. A, 2013. **1297** p. 131-137.
4. Ikegami, T. and N. Tanaka, *Monolithic columns for high-efficiency HPLC separations.* Curr. Opin. Clin. Bio., 2004. **8**(5): p. 527-533.
5. Kalashnikova, I., N. Ivanova, and T. Tennikova, *Development of a Strategy of Influenza Virus Separation Based on Pseudoaffinity Chromatography on Short Monolithic Columns.* Anal. Chem., 2008. **80**(6): p. 2188-2198.
6. Deverell, J.A., T. Rodemann, J.A. Smith, A.J. Canty, and R.M. Guijt, *UV initiated formation of polymer monoliths in glass and polymer microreactors.* Sens. Actuators B: , 2011. **155**(1): p. 388-396.
7. Urban, J. and P. Jandera, *Polymethacrylate monolithic columns for capillary liquid chromatography.* J. Sep. Sci., 2008. **31**(14): p. 2521-2540.

8. Svec, F. and C.G. Huber, *Monolithic Materials: Promises, Challenges, Achievements.* Anal. Chem., 2006. **78**(7): p. 2100-2107.

9. Urban, J. and P. Jandera, *Recent advances in the design of organic polymer for reversed-phase and hydrophilic interaction chromatography separations of small molecules.* Anal. Bioanal. Chem., 2013. **405**(7): p. 2123-2131.

10. Altmaier, S. and K. Cabrera, *Structure and performance of silica-based monolithic HPLC columns.* J. Sep. Sci., 2008. **31**(14): p. 2551-2559.

11. André, C. and Y.C. Guillaume, *Boron nitride nanotubes and their functionalization via quinuclidine-3-thiol with gold nanoparticles for the development and enhancement of the HPLC performance of HPLC monolithic columns.* Talanta, 2012. **93**(0): p. 274-278.

12. Aggarwal, P., H.D. Tolley, and M.L. Lee, *Monolithic bed structure for capillary liquid chromatography*. J. Chromatogr. A, 2012. **1219**(0): p. 1-14.

13. Bunch, D.R. and S. Wang, *Applications of monolithic columns in liquid chromatography-based clinical chemistry assays.* J. Sep. Sci., 2011. **34**(16-17): p. 2003-2012.

14. Siouffi, A.M., *About the C term in the van Deemter's equation of plate height in monoliths.* J. Chromatogr. A, 2006. **1126**(1–2): p. 86-94.

15. Meyers, J.J. and A.I. Liapis, *Network modeling of the convective flow and diffusion of molecules adsorbing in monoliths and in porous particles packed in a chromatographic column.* J. Chromatogr. A, 1999. **852**(1): p. 3-23.

16. Ericson, C., J.-L. Liao, K.i. Nakazato, and S. Hjertén, *Preparation of continuous beds for electrochromatography and reversed-phase liquid chromatography of low-molecular-mass compounds.* J. Chromatogr. A, 1997. **767**(1–2): p. 33-41.

17. Dong, M., M. Wu, F. Wang, M. Ye, Z. Liu, and H. Zou, *Coupling Strong Anion-Exchange Monolithic Capillary with MALDI-TOF MS for Sensitive Detection of Phosphopeptides in Protein Digest.* Anal. Chem., 2010. **82**(7): p. 2907-2915.

18. Nischang, I. and O. Brüggemann, *On the separation of small molecules by means of nano-liquid chromatography with methacrylate-based macroporous polymer monoliths.* J. Chromatogr. A, 2010. **1217**(33): p. 5389-5397.

19. Svec, F., *Porous polymer monoliths: Amazingly wide variety of techniques enabling their preparation.* J. Chromatogr. A, 2010. **1217**(6): p. 902-924.

20. Svec, F. and J.M.J. Frechet, *Kinetic Control of Pore Formation in Macroporous Polymers. Formation of "Molded" Porous Materials with High Flow Characteristics for Separations or Catalysis.* Chem. Mater., 1995. p. 707-715.

21. Urban, J., P. Jandera, and P. Schoenmakers, *Preparation of monolithic columns with target mesopore-size distribution for potential use in size-exclusion chromatography.* J. Chromatogr. A, 2007. **1150**(1–2): p. 279-289.

22. Svec, F., *Preparation and HPLC applications of rigid macroporous organic polymer monoliths.* J. Sep. Sci., 2004. **27**(10-11): p. 747-766.

23. Bandari, R., W. Knolle, and M.R. Buchmeiser, *Comparative study on the separation behavior of monolithic columns prepared via ring-opening metathesis polymerization and via electron beam irradiation triggered free radical polymerization for proteins.* J. Chromtogr. A, 2008. **1191**. 268-273.

24. Ueki, Y., T. Umemura, Y. Iwashita, T. Odake, H. Haraguchi, and K.-i. Tsunoda, *Preparation of low flow-resistant methacrylate-based monolithic stationary phases of different hydrophobicity and the application to rapid reversed-phase liquid chromatographic separation of alkylbenzenes at high flow rate and elevated temperature.* J. Chromatogr. A, 2006. **1106**(1–2): p. 106-111.

25. Moravcová, D., P. Jandera, J. Urban, and J. Planeta, *Characterization of polymer monolithic stationary phases for capillary HPLC.* J. Sep. Sci., 2003. **26**(11): p. 1005-1016.

26. Matusova, S.M., K.I. Ivanova, I.A. D'yachkov, A.D. Smolenkov, A.V. Pirogov, and O.A. Shpigun, *Poly(alkyl methacrylate) monolithic columns for HPLC.* Russ. Chem. Bull., 2008. **57**(12): p. 2554-2560.

27. Podgornik, A., M. Barut, A. Štrancar, D. Josić, and T. Koloini, *Construction of Large-Volume Monolithic Columns.* Anal. Chem., 2000. **72**(22): p. 5693-5699.

28. Premstaller, A., H. Oberacher, W. Walcher, A.M. Timperio, L. Zolla, J.-P. Chervet, N. Cavusoglu, A. van Dorsselaer, and C.G. Huber, *High-Performance Liquid Chromatography−Electrospray Ionization Mass Spectrometry Using Monolithic Capillary Columns for Proteomic Studies.* Anal. Chem., 2001. **73**(11): p. 2390-2396.

29. Gatschelhofer, C., A. Mautner, F. Reiter, T.R. Pieber, M.R. Buchmeiser, and F.M. Sinner, *Ring-opening metathesis polymerization for the preparation of norbornene-based weak cation-exchange monolithic capillary columns.* J. Chromatogr. A, 2009. **1216**(13): p. 2651-2657.

30. Hosoya, K., N. Hira, K. Yamamoto, M. Nishimura, and N. Tanaka, *High-Performance Polymer-Based Monolithic Capillary Column.* Anal. Chem., 2006. **78**(16): p. 5729-5735.

31. Maruška, A., C. Ericson, Á. Végvári, and S. Hjertén, *(Normal-phase) capillary chromatography using acrylic polymer-based continuous beds.* J. Chromatogr. A, 1999. **837**(1–2): p. 25-33.

32. Foo, H.C., J. Heaton, N.W. Smith, and S. Stanley, *Monolithic poly (SPE-co-BVPE) capillary columns as a novel hydrophilic interaction liquid chromatography stationary phase for the separation of polar analytes.* Talanta, 2012. **100**(0): p. 344-348.

33. Wang, Q.C., F. Svec, and J.M.J. Frechet, *Hydrophilization of Porous Polystyrene-Based Continuous Rod Column.* Anal. Chem., 1995. **67**(3): p. 670-674.

34. Jiang, Z., N.W. Smith, P.D. Ferguson, and M.R. Taylor, *Novel highly hydrophilic zwitterionic monolithic column for hydrophilic interaction chromatography.* J. Sep. Sci., 2009. **32**(15-16): p. 2544-2555.

35. Causon, T.J., A. Nordborg, R.A. Shellie, and E.F. Hilder, *High temperature liquid chromatography of intact proteins using organic polymer monoliths and alternative solvent systems.* J. Chromatogr. A, 2010. **1217**(21): p. 3519-3524.

36. Jandera, P., *Advances in the development of organic polymer monolithic columns and their applications in food analysis—A review.* J. Chromatogr. A, 2013(0).

37. Wang, N., S. He, and Y. Zhu, *Low-level bromate analysis by ion chromatography on a polymethacrylate-based monolithic column followed by a post-column reaction.* Eur. Food. Res. Technol., 2012. **235**(4): p. 685-692.

38. Randon, J., S. Huguet, A. Piram, G. Puy, C. Demesmay, and J.-L. Rocca, *Synthesis of zirconia monoliths for chromatographic separations.* J. Chromatogr. A, 2006. **1109**(1): p. 19-25.

39. Wei, J., Z.-T. Jiang, R. Li, and J. Tan, *Use of the Synthesized Titania Monolith to Determine Benzoic Acid and Vanillin in Foodstuffs by HPLC.* Anal. Lett., 2012. **45**(12): p. 1724-1735.

40. Nakanishi, K., *Pore Structure Control of Silica Gels Based on Phase Separation.* J. Porous Mat., 1997. **4**(2): p. 67-112.

41. Qu, Q., Q. Gu, L. Shi, Z. Gu, and X. Hu, *Porous silica microspheres obtained by grinding monolithic columns as stationary phase for high performance liquid chromatography.* Anal. Methods, 2012. **4**(10): p. 3200-3205.

42. Ahmed, A., P. Myers, and H. Zhang, *Preparation of aligned porous silica monolithic capillary columns and their evaluation for HPLC.* Anal. Methods, 2012. **4**(12): p. 3942-3947.

43. Tanaka, N., H. Kimura, D. Tokuda, H. Minakuchi, K. Nakanishi, Y. Shintani, M. Furuno, and K. Cabrera, *Simple and Comprehensive Two-Dimensional Reversed-Phase HPLC Using Monolithic Silica Columns.* Anal. Chem., 2004. **76**(5): p. 1273-1281.

44. Miyazaki, S., M. Takahashi, M. Ohira, H. Terashima, K. Morisato, K. Nakanishi, T. Ikegami, K. Miyabe, and N. Tanaka, *Monolithic silica rod columns for high-efficiency reversed-phase liquid chromatography.* J. Chromatogr. A, 2011. **1218**(15): p. 1988-1994.

45. Jandera, P., *Stationary and mobile phases in hydrophilic interaction chromatography: a review*. Anal. Chim. Acta, 2011. **692**(1–2): p. 1-25.

46. Randon, J., J.-F. Guerrin, and J.-L. Rocca, *Synthesis of titania monoliths for chromatographic separations.* J. Chromatogr. A, 2008. **1214**(1–2): p. 183-186.

47. Randon, J., S. Huguet, C. Demesmay, and A. Berthod, *Zirconia based monoliths used in hydrophilic-interaction chromatography for original selectivity of xanthines.* J. Chromatogr. A, 2010. **1217**(9): p. 1496-1500.

48. Song, Y., T. Funatsu, and M. Tsunoda, *Rapid determination of amino acids in biological samples using a monolithic silica column.* Amino Acids, 2012. **42**(5): p. 1897-1902.

49. Bamba, T., E.-i. Fukusaki, Y. Nakazawa, and A. Kobayashi, *Rapid and high-resolution analysis of geometric polyprenol homologues by connected octadecylsilylated monolithic silica columns in high-performance liquid chromatography.* J. Sep. Sci., 2004. **27**(4): p. 293-296.

50. Bamba, T., E. Fukusaki, H. Minakuchi, Y. Nakazawa, and A. Kobayashi, *Separation of polyprenol and dolichol by monolithic silica capillary column chromatography.* J. Lipid Res., 2005. **46**(10): p. 2295-2298.

51. Ou, J., H. Lin, Z. Zhang, G. Huang, J. Dong, and H. Zou, *Recent advances in preparation and application of hybrid organic-silica monolithic capillary columns.* Electrophoresis, 2013. **34**(1): p. 126-140.

52. Nicole, L., C. Boissiere, D. Grosso, A. Quach, and C. Sanchez, *Mesostructured hybrid organic-inorganic thin films.* J. Mater. Chem., 2005. **15**(35-36):3598-3627.

53. Walcarius, A. and M.M. Collinson, *Analytical Chemistry with Silica Sol-Gels: Traditional Routes to New Materials for Chemical Analysis.* Annu. Rev. Anal. Chem., 2009. **2**(1): p. 121-143.

54. Ma, J., G. Yang, C. Yan, Y. Gu, L. Bai, Y. Duan, and J. Li, *The preparation of a novel organic-inorganic hybrid monolithic column with sonication-assist and its application.* Anal. Methods, 2012. **4**(1): p. 247-253.

55. Zhang, Z., M. Wu, R.a. Wu, J. Dong, J. Ou, and H. Zou, *Preparation of Perphenylcarbamoylated β-Cyclodextrin-silica Hybrid Monolithic Column with "One-Pot" Approach for Enantioseparation by Capillary Liquid Chromatography.* Anal. Chem., 2011. **83**(9): p. 3616-3622.

56. Zhang, Y., H. Liu, X. Zhang, H. Lei, L. Bai, and G. Yang, *On-line solid phase extraction using organic–inorganic hybrid monolithic columns for the determination of trace β-lactam antibiotics in milk and water samples.* Talanta, 2013. **104**(0): p. 17-21.

57. Roux, R., M.A. Jaoudé, C. Demesmay, and J.L. Rocca, *Optimization of the single-step synthesis of hybrid C8 silica monoliths dedicated to nano-liquid chromatography and capillary electrochromatography.* J. Chromatogr. A, 2008. **1209**(1–2): p. 120-127.

58. Lin, H., J. Ou, Z. Zhang, J. Dong, M. Wu, and H. Zou, *Facile Preparation of Zwitterionic Organic-Silica Hybrid Monolithic Capillary Column with an Improved "One-Pot" Approach for Hydrophilic-Interaction Liquid Chromatography (HILIC).* Anal. Chem., 2012. **84**(6): p. 2721-2728.

59. Pfaunmiller, E., M. Paulemond, C. Dupper, and D. Hage, *Affinity monolith chromatography: a review of principles and recent analytical applications.* Anal. Bioanal. Chem., 2013. **405**(7): p. 2133-2145.

60. Mallik, R. and D.S. Hage, *Affinity monolith chromatography.* J. Sep. Sci., 2006. **29**(12): p. 1686-1704.

61. Oxley, D., N. Ktistakis, and T. Farmaki, *Differential isolation and identification of PI(3)P and PI(3,5)P2 binding proteins from Arabidopsis thaliana using an agarose-phosphatidylinositol-phosphate affinity chromatography.* J. Proteomics, 2013(0).

62. Zeng, Z., M. Hincapie, S.J. Pitteri, S. Hanash, J. Schalkwijk, J.M. Hogan, H. Wang, and W.S. Hancock, *A Proteomics Platform Combining Depletion, Multi-lectin Affinity Chromatography (M-LAC), and Isoelectric Focusing to Study the Breast Cancer Proteome.* Anal. Chem., 2011. **83**(12): p. 4845-4854.

63. Leitner, A., *Phosphopeptide enrichment using metal oxide affinity chromatography.* TrAC 2010. **29**(2): p. 177-185.

64. Duong-Thi, M.-D., M. Bergström, T. Fex, S. Svensson, S. Ohlson, and R. Isaksson, *Weak Affinity Chromatography for Evaluation of Stereoisomers in Early Drug Discovery.* J. Biomol. Screen., 2013.

65. Olesen, K., R. Karlsson, U. Lind, M. Davidson, A. Blomberg, and A. Karlsson, *Detection of ligand–receptor binding using microfluidic frontal affinity chromatography on proteoliposomes derived directly from native cell membranes.* J. Chromatogr. B., 2013. **931**(0): p. 84-89.

66. Jiang, T., R. Mallik, and D.S. Hage, *Affinity Monoliths for Ultrafast Immunoextraction.* Anal. Chem., 2005. **77**(8): p. 2362-2372.

67. Selvaraju, S. and Z.E. Rassi, *Targeting human serum fucome by an integrated liquid-phase multicolumn platform operating in "cascade" to facilitate comparative mass spectrometric analysis of disease-free and breast cancer sera.* Proteomics, 2013. **13**(10-11): p. 1701-1713.

68. Jmeian, Y. and Z. El Rassi, *Tandem Affinity Monolithic Microcolumns with Immobilized Protein A, Protein G', and Antibodies for Depletion of High Abundance Proteins from Serum Samples: Integrated Microcolumn-Based Fluidic System for Simultaneous Depletion and Tryptic Digestion.* J. Proteome Res., 2007. **6**(3): p. 947-954.

69. Jmeian, Y. and Z. El Rassi, *Multicolumn Separation Platform for Simultaneous Depletion and Prefractionation Prior to 2-DE for Facilitating In-Depth Serum Proteomics Profiling.* J. Proteome Res., 2009. **8**(10): p. 4592-4603.

70. Dainiak, M.B., I.Y. Galaev, and B. Mattiasson, *Affinity cryogel monoliths for screening for optimal separation conditions and chromatographic separation of cells.* J. Chromatogr. A, 2006. **1123**(2): p. 145-150.

71. Dainiak, M.B., A. Kumar, I.Y. Galaev, and B. Mattiasson, *Detachment of affinity-captured bioparticles by elastic deformation of a macroporous hydrogel.* Proc. Nat. Acad. Sci. U.S. A., 2006. **103**(4): p. 849-854.

72. Chambers, S.D., F. Svec, and J.M.J. Fréchet, *Incorporation of carbon nanotubes in porous polymer monolithic capillary columns to enhance the chromatographic separation of small molecules.* J. Chromatogr. A, 2011. **1218**(18): p. 2546-2552.

73. Aqel, A., K. Yusuf, Z.A. Al-Othman, A.Y. Badjah-Hadj-Ahmed, and A.A. Alwarthan, *Effect of multi-walled carbon nanotubes incorporation into benzyl methacrylate monolithic columns in capillary liquid chromatography.* Analyst, 2012. **137**(18): p. 4309-4317.

74. Claude Guillaume, Y. and C. André, *Fast enantioseparation by HPLC on a modified carbon nanotube monolithic stationary phase with a pyrenyl aminoglycoside derivative.* Talanta, 2013. **115**(0): p. 418-421.

75. Anderson, N.L. and N.G. Anderson, *Proteome and proteomics: New technologies, new concepts, and new words.* Electrophoresis, 1998. **19**(11): p. 1853-1861.

76. Zhang, A.-h., H. Sun, G.-l. Yan, Y. Han, and X.-j. Wang, *Serum Proteomics in Biomedical Research: A Systematic Review.* Appl. Biochem. Biotechnol., 2013. **170**(4): p. 774-786.

77. Calvete, J.J., E. Fasoli, L. Sanz, E. Boschetti, and P.G. Righetti, *Exploring the Venom Proteome of the Western Diamondback Rattlesnake, Crotalus atrox, via Snake Venomics and Combinatorial Peptide Ligand Library Approaches.* J.Proteome Res., 2009. **8**(6): p. 3055-3067.

78. Hartwig, S. and S. Lehr, *Combination of Highly Efficient Hexapeptide Ligand Library-Based Sample Preparation with 2D DIGE for the Analysis of the Hidden Human Serum/Plasma Proteome*, in *Difference Gel Electrophoresis (DIGE)*, R. Cramer and R. Westermeier, Editors. 2012, Humana Press. p. 169-180.

79. Anderson, N.L., N.G. Anderson, L.R. Haines, D.B. Hardie, R.W. Olafson, and T.W. Pearson, *Mass Spectrometric Quantitation of Peptides and Proteins Using*

Stable Isotope Standards and Capture by Anti-Peptide Antibodies (SISCAPA). J. Proteome Res., 2004. **3**(2): p. 235-244.

80. Kawashima, Y., T. Fukutomi, T. Tomonaga, H. Takahashi, F. Nomura, T. Maeda, and Y. Kodera, *High-Yield Peptide-Extraction Method for the Discovery of Subnanomolar Biomarkers from Small Serum Samples.* J. Proteome Res., 2010. **9**(4): p. 1694-1705.

81. Roche, S., L. Tiers, M. Provansal, M. Seveno, M. Piva, P. Jouin, and S. Lehmann, *Depletion of one, six, twelve or twenty major blood proteins before proteomic analysis: the more the better?* J. Proteomics, 2009. **72**: p. 945 - 951.

82. Ekaterina, M., H.C. Scott, K. Oleg, D. Hans, A.M. Deelder, and P. Magnus, *Protein Fractionation for Quantitative Plasma Proteomics by Semi-Selective Precipitation., J. Proteome Bioinfor.,* 2012.

83. Fernandez-Costa, C., V. Calamia, P. Fernandez-Puente, J.-L. Capelo-Martinez, C. Ruiz-Romero, and F. Blanco, *Sequential depletion of human serum for the search of osteoarthritis biomarkers.* Proteome Sci., 2012. **10**(1): p. 55.

84. Holewinski, R.J., Z. Jin, M.J. Powell, M.D. Maust, and J.E. Van Eyk, *A fast and reproducible method for albumin isolation and depletion from serum and cerebrospinal fluid.* Proteomics, 2013. **13**(5): p. 743-750.

85. Janecki, D.J., S.C. Pomerantz, E.J. Beil, and J.F. Nemeth, *A fully integrated multi-column system for abundant protein depletion from serum/plasma.* J. Chromatogr. B., 2012. **902**(0): p. 35-41.

86. Mortezai, N., C. Wagener, and F. Buck, *Combining lectin affinity chromatography and immunodepletion – A novel method for the enrichment of disease-specific glycoproteins in human plasma.* Methods, 2012. **56** p. 254-259.

87. Yang, H.-H., K.-H. Lu, Y.-F. Lin, S.-H. Tsai, S. Chakraborty, W.-J. Zhai, and D.-F. Tai, *Depletion of albumin and immunoglobulin G from human serum using epitope-imprinted polymers as artificial antibodies.* J. Biomed. Mater. Res., A, 2013. **101A**(7): p. 1935-1942.

88. Malinovska, L., S. Kroschwald, M.C. Munder, D. Richter, and S. Alberti, *Molecular chaperones and stress-inducible protein-sorting factors coordinate the spatiotemporal distribution of protein aggregates.* Mol. Biol. Cell, 2012. **23**(16): p. 3041-3056.

89. Fattahi, S., N. Kazemipour, J. Valizadeh, M. Hashemi, and H. Ghazizade, *Comparison of Different Albumin Removal Methods for Evaluation of Human Serum Proteome.* J. Proteome Res., 2, 2012. **14**(4): p. 1-5.

90. Fischer, R., D.C. Trudgian, C. Wright, L.A. Bradbury, M.A. Brown, P. Bowness, and B.M. Kessler, *Discovery of Candidate Serum Proteomic and Metabolomic Biomarkers in Ankylosing Spondylitis.* Mol. Cell. Proteomics, 2012. **11**(2).

91. Selvaraju, S. and Z. El Rassi, *Liquid-phase-based separation systems for depletion, prefractionation and enrichment of proteins in biological fluids and matrices for in-depth proteomics analysis – An update covering the period 2008–2011.* Electrophoresis, 2012. **33**(1): p. 74-88.

92. Tan, S.H., A. Kapur, and M.S. Baker, *Chicken Immune Responses to Variations in Human Plasma Protein Ratios: A Rationale for Polyclonal IgY Ultraimmunodepletion.* J. Proteome Res., 2012. **11**(12): p. 6291-6294.

93. Yu, Y., J. Xu, Y. Liu, and Y. Chen, *Quantification of human serum transferrin using liquid chromatography–tandem mass spectrometry based targeted proteomics.* J. Chromatogr. B., 2012. **902**(0): p. 10-15.

94. Huillet, C., et al., *Accurate Quantification of Cardiovascular Biomarkers in Serum Using Protein Standard Absolute Quantification (PSAQ™) and Selected Reaction Monitoring.* Mol. Cell. Proteomics, 2012. **11**(2).

95. Scholl, P.F., et al., *Maternal serum proteome changes between the first and third trimester of pregnancy in rural Southern Nepal.* Placenta, 2012. **33**(5): p. 424-432.

96. Andac, M., I.Y. Galaev, and A. Denizli, *Molecularly imprinted poly(hydroxyethyl methacrylate) based cryogel for albumin depletion from human serum.* Colloids surf., B, 2013. **109**(0): p. 259-265.

97. Liu, T., et al., *Analysis of serum total and free PSA using immunoaffinity depletion coupled to SRM: correlation with clinical immunoassay tests.* J. Proteomics, 2012. **75**(15): p. 4747-4757.

98. Zhu, G., P. Zhao, N. Deng, D. Tao, L. Sun, Z. Liang, L. Zhang, and Y. Zhang, *Single Chain Variable Fragment Displaying M13 Phage Library Functionalized Magnetic Microsphere-Based Protein Equalizer for Human Serum Protein Analysis.* Anal. Chem., 2012. **84**(18): p. 7633-7637.

99. Di Girolamo, F., P.G. Righetti, M. Soste, Y. Feng, and P. Picotti, *Reproducibility of combinatorial peptide ligand libraries for proteome capture evaluated by selected reaction monitoring.* J. Proteomics, 2013. **89**(0): p. 215-226.

100. Fasoli, E., M. Colzani, G. Aldini, A. Citterio, and P.G. Righetti, *Lemon peel and Limoncello liqueur: A proteomic duet.* Biochim Biophys. Acta., 2013. **1834**(8): p. 1484-1491.

101. Esteve, C., A. D'Amato, M.L. Marina, M.C. García, and P.G. Righetti, *In-depth proteomic analysis of banana (Musa spp.) fruit with combinatorial peptide ligand libraries.* Electrophoresis, 2013. **34**(2): p. 207-214.

102. Righetti, P. and E. Boschetti, *Combinatorial peptide libraries to overcome the classical affinity-enrichment methods in proteomics.* Amino Acids, 2013. **45**(2): p. 219-229.

103. Righetti, P.G., E. Boschetti, and G. Candiano, *Mark Twain: How to fathom the depth of your pet proteome.* J. Proteomics, 2012. **75**(15): p. 4783-4791.

104. Saez, V., E. Fasoli, A. D'Amato, E. Simó-Alfonso, and P.G. Righetti, *Artichoke and Cynar liqueur: Two (not quite) entangled proteomes.* Biochim. biophys. Acta, 2013. **1834**(1): p. 119-126.

105. D'Amato, A., C. Esteve, E. Fasoli, A. Citterio, and P.G. Righetti, *Proteomic analysis of Lycium barbarum (Goji) fruit via combinatorial peptide ligand libraries.* Electrophoresis, 2013. **34**(12): p. 1729-1736.

106. Fasoli, E., A. D'Amato, A. Citterio, and P.G. Righetti, *Anyone for an aperitif? Yes, but only a Braulio DOC with its certified proteome.* J. Proteomics, 2012. **75**(11): p. 3374-3379.

107. Fasoli, E., A. D'Amato, P.G. Righetti, R. Barbieri, and D. Bellavia, *Exploration of the Sea Urchin Coelomic Fluid via Combinatorial Peptide Ligand Libraries.* The Biol. Bull., 2012. **222**(2): p. 93-104.

108. D'Amato, A., E. Fasoli, A.V. Kravchuk, and P.G. Righetti, *Mehercules, adhuc Bacchus! The Debate on Wine Proteomics Continues.* J. Proteome Res., 2011. **10**(8): p. 3789-3801.

109. Santucci, L., G. Candiano, A. Petretto, C. Lavarello, M. Bruschi, G.M. Ghiggeri, A. Citterio, and P.G. Righetti, *Combinatorial ligand libraries as a two-dimensional method for proteome analysis.* J. Chromatogr. A, 2013. **1297**(0): p. 106-112.

110. Tu, C., J. Li, R. Young, B.J. Page, F. Engler, M.S. Halfon, J.M. Canty, and J. Qu, *Combinatorial Peptide Ligand Library Treatment Followed by a Dual-Enzyme, Dual-Activation Approach on a Nanoflow Liquid Chromatography/Orbitrap/Electron Transfer Dissociation System for Comprehensive Analysis of Swine Plasma Proteome.* Anal. Chem., 2011. **83**(12): p. 4802-4813.

111. Liu, Y., N. Qiu, and M. Ma, *Comparative proteomic analysis of hen egg white proteins during early phase of embryonic development by combinatorial peptide ligand library and matrix-assisted laser desorption ionization-time of flight.* Poultry Science, 2013. **92**(7): p. 1897-1904.

112. Lorkova, L., J. Pospisilova, J. Lacheta, S. Leahomschi, J. Zivny, D. Cibula, J. Zivny, and J. Petrak, *Decreased concentrations of retinol-binding protein 4 in*

sera of epithelial ovarian cancer patients: A potential biomarker identified by proteomics. Oncology Reports, 2012. **27**(2): p. 318-324.

113. Gomes, C., et al., *Glycoproteomic Analysis of Serum from Patients with Gastric Precancerous Lesions.* J. Proteome Res., 2013. **12**(3): p. 1454-1466.

114. Cheung, R., J. Wong, and T. Ng, *Immobilized metal ion affinity chromatography: a review on its applications.* Appl. Microbiol. Biot., 2012. **96**(6): p. 1411-1420.

115. Yue, X.-S. and A.B. Hummon, *Combination of Multistep IMAC Enrichment with High-pH Reverse Phase Separation for In-Depth Phosphoproteomic Profiling.* J. Proteome Res., 2013. **12**(9): p. 4176-4186.

116. Yan, Y., Z. Zheng, C. Deng, Y. Li, X. Zhang, and P. Yang, *Hydrophilic Polydopamine-Coated Graphene for Metal Ion Immobilization as a Novel Immobilized Metal Ion Affinity Chromatography Platform for Phosphoproteome Analysis.* Anal Chem., 2013. **85**(18): p. 8483-8487.

117. Sun, Z., K.L. Hamilton, and K.F. Reardon, *Evaluation of Quantitative Performance of Sequential Immobilized Metal Affinity Chromatographic Enrichment for Phosphopeptides.* Anal. Biochem., 2013, 445.

118. Zeng, Y.Y., H.-J. Chen, K.J. Shiau, S.-U. Hung, Y.-S. Wang, and C.-C. Wu, *Efficient enrichment of phosphopeptides by magnetic TiO2-coated carbon-encapsulated iron nanoparticles.* Proteomics, 2012. **12**(3): p. 380-390.

119. Zhou, H., M. Ye, J. Dong, G. Han, X. Jiang, R. Wu, and H. Zou, *Specific Phosphopeptide Enrichment with Immobilized Titanium Ion Affinity Chromatography Adsorbent for Phosphoproteome Analysis.* J. Proteome Res., 2008. **7**(9): p. 3957-3967.

120. Liu, Z., M. Li, Z. Li, F. Pu, J. Ren, and X. Qu, *Easy access to selective binding and recyclable separation of histidine-tagged proteins using Ni2+-decorated superparamagnetic nanoparticles.* Nano Research, 2012. **5**(7): p. 450-459.

121. Lee, J., S.Y. Lee, S.H. Park, H.S. Lee, J.H. Lee, B.-Y. Jeong, S.-E. Park, and J.H. Chang, *High throughput detection and selective enrichment of histidine-tagged enzymes with Ni-doped magnetic mesoporous silica.* J. Mater. Chem., B, 2013. **1**(5): p. 610-616.

122. Coffinier, Y., N. Nguyen, H. Drobecq, O. Melnyk, V. Thomy, and R. Boukherroub, *Affinity surface-assisted laser desorption/ionization mass spectrometry for peptide enrichment.* Analyst, 2012. **137**(23): p. 5527-5532.

123. Wang, F., C. Chmil, F. Pierce, K. Ganapathy, B.B. Gump, J.A. MacKenzie, Y. Mechref, and K. Bendinskas, *Immobilized metal affinity chromatography and human serum proteomics.* J. Chromatogr. B, 2013. **934**(0): p. 26-33.

124. Li, H. and Z. Liu, *Recent advances in monolithic column-based boronate-affinity chromatography.* TrAC, 2012. **37**(0): p. 148-161.

125. Shi, T., et al., *Antibody-free, targeted mass-spectrometric approach for quantification of proteins at low picogram per milliliter levels in human plasma/serum.* Proc. Nat. Acad. Sci., 2012. **109**(38): p. 15395-15400.

126. Kuo, C.-W., I.L. Wu, H.-H. Hsiao, and K.-H. Khoo, *Rapid glycopeptide enrichment and N-glycosylation site mapping strategies based on amine-functionalized magnetic nanoparticles.* Anal. Bioanal. Chem., 2012. **402**(9): p. 2765-2776.

127. Palandra, J., A. Finelli, M. Zhu, J. Masferrer, and H. Neubert, *Highly Specific and Sensitive Measurements of Human and Monkey Interleukin 21 Using Sequential Protein and Tryptic Peptide Immunoaffinity LC-MS/MS.* Anal. Chem., 2013. **85**(11): p. 5522-5529.

128. Kuhn, E., et al., *Interlaboratory Evaluation of Automated, Multiplexed Peptide Immunoaffinity Enrichment Coupled to Multiple Reaction Monitoring Mass Spectrometry for Quantifying Proteins in Plasma.* Mol. Cell. Proteome, 2012. **11**(6).

129. Zhu, S., X. Zhang, M. Gao, G. Hong, G. Yan, and X. Zhang, *Developing a strong anion exchange/RP (SAX/RP) 2D LC system for high-abundance proteins depletion in human plasma.* Proteomics, 2012. **12**(23-24): p. 3451-3463.

130. Kimura, A., K. Sogawa, M. Satoh, Y. Kodera, O. Yokosuka, T. Tomonaga, and F. Nomura, *The application of a three-step serum proteome analysis for the discovery and identification of novel biomarkers of hepatocellular carcinoma.* Int. J Proteomics, 2012. **2012**: p. 623190.

131. Stobaugh, J.T., K.M. Fague, and J.W. Jorgenson, *Prefractionation of Intact Proteins by Reversed-Phase and Anion-Exchange Chromatography for the Differential Proteomic Analysis of Saccharomyces cerevisiae.* J. Proteome Res., 2012. **12**(2): p. 626-636.

132. Ma, C., et al., *N-linked glycoproteome profiling of human serum using tandem enrichment and multiple fraction concatenation.* Electrophoresis, 2013. **34**(16): p. 2440-2450.

133. Boichenko, A.P., N. Govorukhina, A.G.J. van der Zee, and R. Bischoff, *Multidimensional separation of tryptic peptides from human serum proteins using reversed-phase, strong cation exchange, weak anion exchange, and fused-core fluorinated stationary phases.* J. Sep. Sci., 2013: p. n/a-n/a.

134. Shi, T., et al., *Targeted Quantification of Low ng/mL Level Proteins in Human Serum without Immunoaffinity Depletion.* J. Proteome Res., 2013. **12**(7): p. 3353-3361.

135. Kuzmanov, U., C.R. Smith, I. Batruch, A. Soosaipillai, A. Diamandis, and E.P. Diamandis, *Separation of kallikrein 6 glycoprotein subpopulations in biological fluids by anion-exchange chromatography coupled to ELISA and identification by mass spectrometry*. Proteomics, 2012. **12**(6): p. 799-809.

136. Opstal-van Winden, A.W.J., J.H. Beijnen, A. Loof, W.L. van Heerde, R. Vermeulen, P.H.M. Peeters, and C.H. van Gils, *Search for Breast Cancer Biomarkers in Fractionated Serum Samples by Protein Profiling With SELDI-TOF MS.* J. Clin. Lab. Anal., 2012. **26**(1): p. 1-9.

137. Lee, L.Y., M. Hincapie, N. Packer, M.S. Baker, W.S. Hancock, and S. Fanayan, *An optimized approach for enrichment of glycoproteins from cell culture lysates using native multi-lectin affinity chromatography.* J. Sep. Sci., 2012. **35**(18): p. 2445-2452.

138. Yang, Z., L.E. Harris, D.E. Palmer-Toy, and W.S. Hancock, *Multilectin Affinity Chromatography for Characterization of Multiple Glycoprotein Biomarker Candidates in Serum from Breast Cancer Patients.* Clin. Chem., 2006. **52**(10): p. 1897-1905.

139. Fanayan, S., M. Hincapie, and W.S. Hancock, *Using lectins to harvest the plasma/serum glycoproteome.* Electrophoresis, 2012. **33**(12): p. 1746-1754.

140. Selvaraju, S. and Z. El Rassi, *Tandem lectin affinity chromatography monolithic columns with surface immobilised concanavalin A, wheat germ agglutinin and Ricinus communis agglutinin-I for capturing sub-glycoproteomics from breast cancer and disease-free human sera.* J. Sep. Sci., 2012. **35**(14): p. 1785-1795.

141. Baranauskiene, J., J. Kazlauske, S. Gustaite, B. Niemeyer, and J. Liesiene, *comparative study of macroporous silica- and cellulose-based sorbents for lectin affinity chromatography*. J. Liq. Chromatogr. Relt.Technol., 2013.

142. Bergström, M., E. Åström, P. Påhlsson, and S. Ohlson, *Elucidating the selectivity of recombinant forms of Aleuria aurantia lectin using weak affinity chromatography.* J. Chromatogr. B., 2012. **885–886**(0): p. 66-72.

143. Jung, K. and W. Cho, *Serial Affinity Chromatography as a Selection Tool in Glycoproteomics.* Anal. Chem., 2013. **85**(15): p. 7125-7132.

144. Gonzalez-Begne, M., B. Lu, L. Liao, T. Xu, G. Bedi, J.E. Melvin, and J.R. Yates, *Characterization of the Human Submandibular/Sublingual Saliva Glycoproteome Using Lectin Affinity Chromatography Coupled to Multidimensional Protein Identification Technology.* J. Proteome Res., 2011. **10**(11): p. 5031-5046.

145. Mann, B.F., A.K.P. Mann, S.E. Skrabalak, and M.V. Novotny, *Sub 2-μm Macroporous Silica Particles Derivatized for Enhanced Lectin Affinity Enrichment of Glycoproteins.* Anal. Chem., 2013. **85**(3): p. 1905-1912.

146. Bell, C., G.T. Smith, M.J. Sweredoski, and S. Hess, *Characterization of the Mycobacterium tuberculosis Proteome by Liquid Chromatography Mass*

Spectrometry-based Proteomics Techniques: A Comprehensive Resource for Tuberculosis Research. J. Proteome Res., 2012. **11**(1): p. 119-130.

147. Yao, L., W. Lao, Y. Zhang, X. Tang, X. Hu, C. He, X. Hu, and L.X. Xu, *Identification of EFEMP2 as a Serum Biomarker for the Early Detection of Colorectal Cancer with Lectin Affinity Capture Assisted Secretome Analysis of Cultured Fresh Tissues.* J. Proteome. Res., 2012. **11**(6): p. 3281-3294.

148. Benkovska, D., D. Flodrova, and J. Bobalova, *Application of monolithic affinity hplc column for rapid determination of malt glycoproteins.* J. Liq. Chromtogr. Rel. Technol., 2012. **36**(5): p. 561-572.

CHAPTER II

POLY (GLYCERYL METHACRYLATE – ETHYLENE GLYCOL DIMETHACRYLATE) COPOLYMER MONOLITH SUPPORTED MULTIWALL NANOTUBES FOR REVERSED PHASE CHROMATOGRAPHY

Introduction

Monolithic stationary phases have been used in CE, CEC, and HPLC. Monolithic stationary phases allow tailoring the surface of the material that best suits the separation of the solutes of interest since in many instances different kind of interactions could be used in the separation of compounds. Recently, great attention has been paid for using nanomaterials as chromatographic stationary phases. In this regard, nanotubes are emerging as chromatographic stationary phases due to their unique characteristics [1].

Nanoparticles, nanotubes, fullerenes and nano sized diamonds are widely used in research due to their unique properties, such as availability of large surface area for

chemical interactions, thermal conductivity, chemical and thermal stability and tensile strength. Some of these properties have contributed to their rapid growth in separation sciences [2-4]. Nanotubes in general started emerging in nanostructures since 1980, and carbon nanotubes in particular gained popularity in research due to their unique chemical and physical properties [5]. Carbon possesses the ability to bind with various chemical compounds and create materials having diverse characteristics [6]. Carbon nanotubes belong to the fullerene family of carbon allotropes. It is tubular in shape and consists of covalently bonded carbon atoms [7]. A single-walled carbon nanotube (SWNT) can be described as a sheet of graphene rolled into a seamless cylinder and the ends capped with the hemispherical, fullerene like structures [5]. Multi-walled carbon nanotubes (MWCNTs) have relatively complex structure consisting of additional concentric cylindrical shells of graphene sheets coaxially arranged around the central core of the SWNT [4].

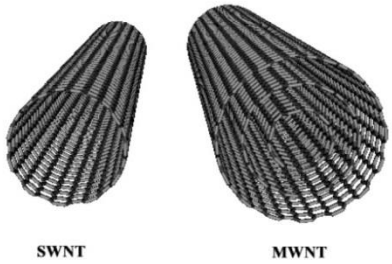

Figure 1. *Schematic illustration of SWNT and MWNT (Adapted from Chem draw).*

The application of carbon nanotubes (CNT) as a chromatographic separation media has increased due to the fact that they show high resemblance to graphitic carbon,

which is a well-known stationary phase in chromatography [8-10]. MWCNTs have been used as adsorbents for solid-phase extraction (SPE) of several compounds. The adsorptive potential of MWCNTs has been used in environmental analysis of several compounds e.g. pesticides and polyaromatic hydrocarbons [11-14]. Non-modified MWCNTs, activated carbon and graphitized carbon black (Carbopack B) have been used as column packing materials, and their separation ability has been shown in gas chromatography. It has been shown that MWCNTs are better packing material than activated charcoal and carbopack B for volatile compounds, especially with low boiling compounds [15]. In order to achieve high resolution and stability at high temperatures in gas chromatography CNTs have been immobilized onto the wall of GC capillary columns by chemical vapor deposition. By changing the thickness of CNT wall coatings different retention capabilities have been achieved [16, 17]. Covalently modified CNT also have been used in GC to enhance the dispersion of CNT and to increase the affinity of polar solutes [18]. Enhanced separation of alkanes and aromatic compounds was achieved by packing the GC column with MWCNT-COOH and MWCNT-$CONH_2$ [19].

Carbon nanotubes have also been tested as stationary phases for CEC. In CEC, open tubular columns as well as organic monolithic stationary phases incorporated with CNT have been used. In one investigation, a fused-silica capillary was silanized and a carboxyl modified MNCNT was immobilized onto the capillary walls. The columns thus obtained showed high resolution, high separation efficiency, good retention factors and reproducibility [13, 20]. In another study, acid treated SWCNTs immobilized on a

poly(diallydimethylammonium chloride)-modified fused silica surface showed improved baseline separation of a mixture of seven nitrogen-containing aromatic compounds compared to capillary zone electrophoresis [21]. An organic monolithic stationary phase consisting of vinylbenzyl chloride (VBC) and ethylene dimethacrylate (EDMA) incorporated with SWCNT and without SWCNT has been tested with a mixture of peptides. The organic monolith VBC-EDMA-SWCNT thus obtained showed better peak efficiency and good peak retention compared to the control column i.e. without SWCNTs [22]. More recently, a capillary column filled with carboxy functionalized nanotubes that were incorporated in the glycidyl methacrylate (GMA) and ethylene glycol dimethacrylate (EDMA) was used in the separation of small molecules in the reversed phase chromatography mode. Superior efficiency was achieved with a GMA/EDMA column with nanoparticles when compared to the control column, i.e. without SWCNT [23].

The use of CNT as stationary phases in HPLC is a recent promising trend in separation science. Baseline separation of polycyclic aromatic hydrocarbons (PAHs) was achieved in HPLC with MWCNTs assembled layer by layer onto silica microspheres to form MWCNTs/SiO_2 [8]. Other research reports have shown that silica HPLC columns incorporated with CNTs yielded high separation efficiency for peptides and small aromatic compounds [3, 24]. Although there have been studies conducted in the field of incorporating CNT into monolithic stationary phases for HPLC, the full potentials of nanotube-supported monoliths still need further studies to achieve monoliths with

improved characteristics to produce columns with the best performance for the separation of a wide range of solutes.

Thus, it is the aim of this study to develop MWCTs incorporated into a suitable organic polymer monolith for use as a novel stationary phase in HPLC. To achieve a column with best performance, several experiments were carried out by changing the amount and type of nanoparticles, the polymerization temperature of the monolith and the high power sonication time of nanotubes. As will be shown, the nanoparticle-incorporated monolith is hydrophobic in nature and also has π bonds. The optimized column was used for the reversed phase separation of small molecules, and offered good enantio-resolution for chiral molecules due to the unique characteristics of MWNTs.

Experimental

Instrumentation

The HPLC setup consisted of a quaternary solvent delivery system Model Q-grad pump from Lab Alliance (State College, PA, USA), a solvent delivery system model CM4000 and a model 3100 UV-Vis variable wavelength detector from Milton Roy, LDC division (Riviera Beach, FL, USA) and a Rheodyne injector model 7010 (Cotati, CA, USA) equipped with a 20 μL sample loop. A constant pressure air driven pump Model Shandon from Southern Products Limited (Cheshire, UK) was used for column packing. A Branson 1510 ultrasonic cleaner was from Emersion (Danbury, CT, USA). The water

bath model 2100 and high power sonicator model sonic dismembrator 50 were from Thermo Fischer Scientific (Waltham, MA, USA).

Reagents and Materials

Multi-walled carbon nanotubes (MWCNTs) were purchased from Sun Innovation Inc. (Fremont, CA). Alkyl benzenes (ABs), phenoxy acid herbicides, cyanobenzene derivatives, benzonitrile, aniline derivatives, trifluoroacetic acid (TFA), 2,2'-azobis(isobutyronitrile) (AIBN), pentaerithrytol triacrylate (PETA), butyl methacrylate (BMA), ethylene glycol dimethacrylate (EDMA), ethylenedimethacrylate (EMA), methyl methacrylate (MMA), chlorophenols, glycidyl methacrylate (GMA), 1-dodecanol, cyclohexanol, DL-dansyl (Dns) amino acids were purchased from Sigma Aldrich (Milwaukee, WI, USA). Glyceryl monomethacrylate (GMM) was from Monomer-Polymer and Dajac Labs (Trevose, PA, USA). HPLC grade acetonitrile and isopropyl alcohol were purchased from Pharmco Aaper (Brookfield, CT, USA). Stainless steel tubing of 4.6 mm id was obtained from Alltech Associates (Deerfield, IL, USA).

Preparation of monolithic columns

A polymerization mixture of 6g was prepared by weighing monomers and porogens according to the values listed in Table 1. All the mixtures were first vortexed for 1 min, sonicated at 40 $^{\circ}$C for 15 min, purged with nitrogen for 5 min and then introduced into a stainless steel column of dimensions 25 cm x 4.6 mm id that function as

a mold for the monolith. Both column ends were plugged tightly with column end fittings and thereafter heated at 50 ˚C - 60 ˚C in a water bath for 15 -20h. The monolithic columns thus obtained were washed with acetonitrile for 30 min followed by isopropyl alcohol for 30 min. The monolith was transferred from the 25 cm mold to a shorter column of 10 cm x 4.6 mm id by connecting the two columns by a ¼ "-union and passing isopropanol (IPA) using constant pressure pump at 6000 psi until the monolith was completely transferred. Thereafter, the column was washed with the running buffer and tested with standard solutes. A series of monolithic compositions were tested. The GMM/EDMA monolith was found as a suitable monolith to incorporate nanoparticles. SN3251 was incorporated in different amounts in the GMM/EDMA monolith and 3 mg quantity was found as the best amount. In order to homogenize and break the nanotubes into smaller ones, the MWCNTs was dissolved in 1-dodecanol and subjected to high power sonication for 1 min, 15 min and 30 min while keeping the vial in ice to prevent evaporation and then added the monomer and the rest of the material. Once the polymerization solution was sonicated, the column was prepared similarly as above.

Chromatographic conditions

To achieve a good retention of small molecules, the polarity of the mobile phase must be adjusted. Different compositions of ACN/H_2O with 0.1% of TFA were used as the mobile phases. For the chiral separation of D and L Dns-amino acids, a mobile phase consisting of 25 mM sodium acetate, 35% v/v ACN, pH 4.1 was used. All samples were

prepared by dissolving the solutes in the mobile phase and injected *via* a 20 μL injection loop. Isocratic separation of small molecules and chiral compounds were carried out at a flow rate of 1 mL/min.

Results and discussion

Column optimization incorporating MWCNTs

In order to find the monolithic stationary phase best suited to incorporate MWCNTs, a series of monolithic columns incorporating different nanotubes and monomer compositions were tested, see Table 1. These were compared with a blank monolith that would have the least hydrophobic character.

The MN1 monolith (see Table 1 for composition) did not meet the criteria as a blank monolith, since it showed some retention toward alkyl benzenes and proteins. In other words, MN1 possessed RPC properties. The addition of 12.5 mg of MWCNTs to MN1 yielded the MN1a monolith, which resulted in a moderate enhancement of protein retention as shown in Table 2, but the protein bands were broad. Since the aim was to achieve separation and retention solely *via* the incorporated MWCNTs, the search for an ideal blank monolith continued. In this regard, MMA has a smaller alkyl chain than BMA, and therefore, it might generate a less hydrophobic monolith (designated as MN2) than BMA. As expected, MN2 yielded less retention time than MN1, but it gave higher backpressure (~ 5000 psi at 1 mL/min). In order to produce a monolith with a more

porous structure, the concentration of the crosslinker was increased. The resulting monolith (MN2) did show more permeability and in turn lower pressure (~2000 psi at 1 mL/min). To further improve the monolith, a new cross linker e.g., TRIM, was evaluated. The resulting MN3 monolith did not separate alkyl benzenes and proteins indicating a suitable blank monolith. Then, 37.5 mg SN6957838 MWCNTs were incorporated into MN3 to increase the hydrophobic character of the stationary phase (denoted as MN3a) and in turn yield good separation and retention. However, the monolith MN3a, gave a high pressure and MWCNTs did not show a homogeneous dispersion in the monolith. This led to a monolith with low performance even after decreasing the amount of MWCNTs to 12.5 mg (MN3b). The monolith designated as MN4 was developed using GMM/PETA, see Table 1. This monolith (MN4) was not suitable as a blank because it produced high pressure. All of the above monoliths were unsatisfactory because they showed residual hydrophobicity or exhibited low permeability. Finally, the suitable blank monolith was achieved using the monomers GMM/EDMA and designated as MN5. As expected, MN5 yielded no retention towards AB as shown in Fig. 1

TABLE 1

COMPOSITION OF MONOLITHS INTRODUCED AND EVALUATED IN THIS STUDY

Monolith #	Monolithic composition			
	Monomer (% w/w) / Cross-linker (% w/w)	Porogen (% w/w)	MWCNTs (mg)	Temp. and time
MN1	BMA (30%) / EDMA (20%)	1-propanol (30%)/ water (5%)/1,4-Butanediol(15%)	0	60 ^{o}C for 20 h
MN 1a			SN6957838 12.5 mg	60 ^{o}C for 15 h
MN 2	MMA (19%)/EDMA (21%)	1-propanol (36%)/ water (6 %)/1,4-Butanediol (18%)	0	
MN 2 a	MMA (16%)/EDMA (24%)			
MN 3	MMA(12%) / TRIM (28%)			
MN 3 a			SN6957838 37.5 mg	
MN 3 b			SN6957838 12.5 mg	
MN 4	GMM (7.6%)/ PETA (7%)	Cyclohexanol (59%)/ Dodecanol (23%), Water (3.4)%	SN6957838 25 mg	

MN 5	GMM (18%)/ EDMA (12%)	Cyclohexanol (35%)/ Dodecanol (35%)	0	50 °C for 15 h
MN 5 a			SN6957838 12.5 mg	
MN 5 b				55 °C for 15 h
MN 5 c		Cyclohexanol (35%)/ Dodecanol (35%)	SN6957838 12.5 mg	58 °C for 15 h
MN 5 d			SN2302 12.5 mg	55 °C for 15 h
MN 5 e			SN32547 12.5 mg	
MN 5 f			SN32547 6 mg	
MN 5 g			SN32547 3 mg	
MN 5 h			SN32541 1 mg	

Incorporating MWCNTs into the MN5 monolith.

Nanotubes are inert, hydrophobic in nature and may undergo strong van der Walls and π–π interactions with the solutes. Due to these characteristics, the MWCNTs are

expected to achieve the desired retention for solutes under RPC mobile phase conditions; that is hydro-organic mobile phases.

TABLE 2

COMPARISON OF THE RETENTION TIMES OBTAINED WITH MN1 AND MN1a WITH AND WITHOUT NANOPARTICLES

Protein	Retention time (min)			
	MN1	MN1a		
	75% ACN	75% ACN	70% ACN	65% ACN
Ribonuclease A	5.51	5.78	6.06	6.16
Cytochrome C	6.3	6.62	7.04	7.25
Lysozyme	6.86	7.27	7.78	7.85
BSA, Transferrin	7.39	7.93	8.42	8.53
Carbonic anhydrase	8.05	8.6	9.04	9.15
Ovalbumin	8.82	9.32	9.82	9.96

MN5 monolith with SN 6957838. First, MWCNTs batch # SN 6957838 were selected and incorporated into the MN5 blank monolith. These nanotubes have an outer diameter of 20-30 nm, an internal diameter of 5-10 nm, and a length of 1-2 μm. With the addition of 12.5 mg of SN6957838 to the MN5 monolith to yield the monolith MN5a, which showed some retention towards ABs, see Fig. 3a. In order to enhance the separation and retention of ABs, the polymerization temperature was changed to 55 ^{o}C and 58 ^{o}C and the corresponding monoliths were designated as MN5b, and MN5c, respectively. The

chromatograms of AB separations using MN5b and MN5c are shown in Fig. 3B and C. As shown in these Figures, an improved separation was achieved on MN5b at a polymerization temperature of 55˚C. The retention values of ABs are reported in Table 3. From these data, it is clear that the 55 ^{o}C was the best temperature and was used as the polymerization temperature in the rest of the study.

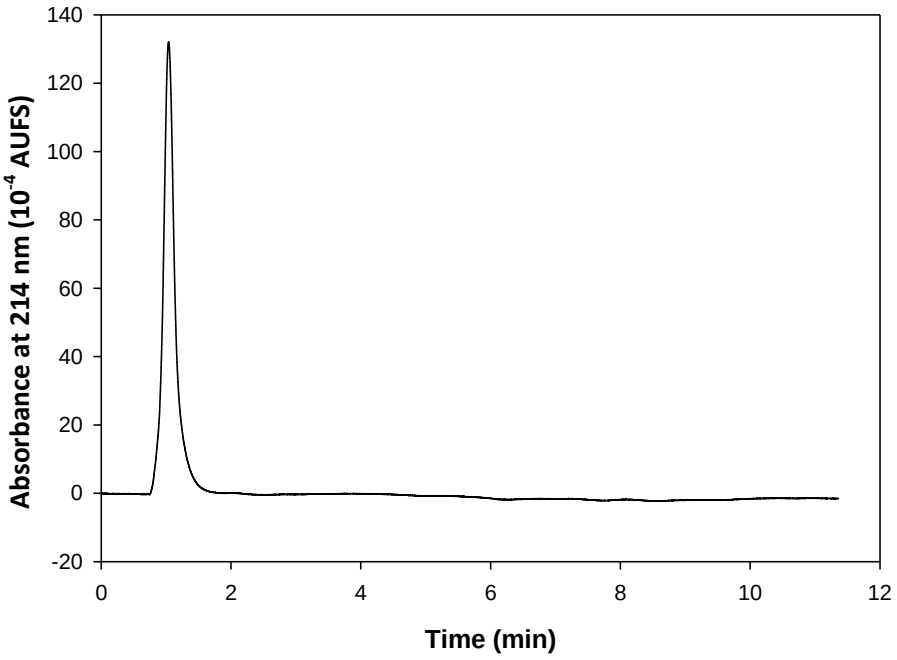

Figure 2. *Chromatogram of a mixture of 7 ABs (toluene, ethyl benzene, propyl benzene, butyl benzene, amyl benzene, hexyl benzene and heptyl benzene) using MN5 monolith. Mobile phase, ACN: H_2O (35:65 v/v) containing 0.1% TFA; column dimensions, 10 cm x 4.6 mm I.D.; flow rate, 1 mL/min.*

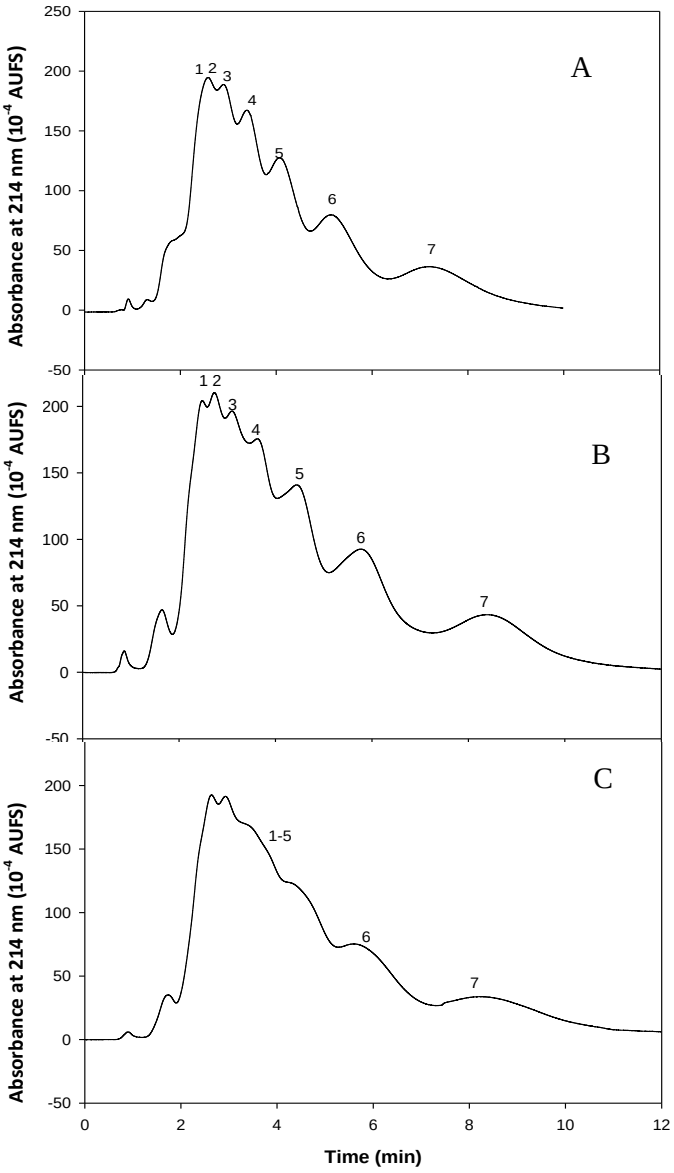

Figure 3. *Chromatograms of ABs using (A) MN5a (50 ^{o}C) (B) MN5b (55 ^{o}C) and (C) MN5c (58 ^{o}C) monolithic columns prepared at different polymerization temperatures. Mobile phase, ACN: H_2O (35:65 v/v) containing 0.1% TFA. Other conditions are as in Fig.2. Solutes: 1, toluene; 2, ethyl benzene; 3, propyl benzene; 4, butyl benzene; 5, amyl benzene; 6,hexylbenzene; 7,heptylbenzene.*

TABLE 3

RETENTION TIMES OF ABS OBTAINED ON GMM/EDMA MONOLITH INCORPORATING MWCNTS PREPARED AT DIFFERENT POLYMERIZATION TEMPERATURES

Alkyl Benzene	50 ^{o}C			55 ^{o}C			58 ^{o}C		
	t_R	k'	log k'	t_R	k'	log k'	t_R	k'	log k'
Toluene	2.36	1.8	0.255	2.48	1.62	0.21	2.64	1.93	0.28
Ethyl benzene	2.56	2.04	0.31	2.74	1.87	0.27	2.92	2.24	0.35
Propyl benzene	2.88	2.43	0.38	3.1	2.59	0.41	3.32	2.68	0.43
Butyl benzene	3.55	3.22	0.51	3.62	3.21	0.51	3.74	3.15	0.5
Amyl benzene	4.12	3.9	0.58	4.44	4.16	0.62	4.33	3.81	0.58
Phenyl hexane	5.25	5.25	0.72	5.76	5.67	0.75	5.6	5.22	0.72
Phenyl heptane	7.29	7.67	0.88	8.4	8.76	0.94	8.25	7.25	0.86

TABLE 4

RETENTION TIMES OF ALKYL BENZENES AT DIFFERENT ACETONITRILE CONCENTRATIONS ON MN5e MONOLITH

	35% ACN			40% ACN			45 % ACN		
	t_R	k'	log k'	t_R	k'	log k'	t_R	k'	log k'
Toluene	2.67	2.81	0.44	1.92	1.74	0.24	1.56	1.6	0.12
Ethyl benzene	3.08	3.28	0.52	2.08	1.97	0.29	1.61	1.69	0.14
Propyl benzene	3.7	4.14	0.62	2.3	2.28	0.35	1.73	1.79	0.19
Butyl benzene	4.55	5.32	0.73	2.65	2.78	0.44	1.84	2.19	0.24
Amyl benzene	5.54	6.69	0.82	2.98	3.25	0.52	1.94	2.5	0.28
Phenyl hexane	6.78	8.41	0.92	3.67	4.24	0.62	2.08	2.71	0.32
Phenyl heptane	8.31	10.54	1.02	3.73	4.32	0.63	2.28	1.6	0.38

MN5 monolith with SN 32547. SN 32547 is OH-MWCNTs and has the following specifications: 10-20 nm OD, 5-10 nm ID, and 10-30 μm length. The monolithic column prepared with OH-MWCNT (MN5e) showed good separation and retention, see Fig. 4.

The monolith MN5e (see Table 1 for the composition) was further tested with the ABs test mixture while changing the composition of the mobile phase. The retention of ABs at different ACN concentration is shown in Table 4. At 35% ACN concentration, the column shows the best retention. To obtain a column with optimized retention characteristics, the amount of OH-MWCNTs added to the polymerization mixture was varied. The ABs test mixture was injected onto all the columns (i.e., MN5d –MN5h columns) at different ACN concentrations. With increasing the ACN concentration the k' values of ABs decreased, see Fig. 5. The monolithic composition and the amounts of nanotubes incorporated into MN5d-MN5h columns are shown in Table 1. Out of these monoliths MN5g with 3 mg of OH-MWCNTs showed the best retention and separation for ABs, see Fig. 4. The column made with 1 mg of OH-MWCNTs, (MN5h) poorly separated ABs, a fact that indicates that the MWCNTs help in the separation of ABs. The k' values of the solutes are linearly proportional to the amount of MWCNTs incorporated into the monolith. The hydrophobic character and π–π interactions of the column increased with an increased amount of OH-MWCNTs in the polymerization mixture. Fig. 5 shows the linear relationship of k' values of ABs obtained on the monolithic columns vs. the amount of nanotubes incorporated in the columns MN5d –MN5h at different acetonitrile concentrations.

Effect of high power sonication. Even though the above monolith gave better performance with ABs, it did not show improvement for protein, peptide or amino acid separations. In order to achieve a better dispersion of the MWCNTs , the MWCNTs were

subjected to a high power sonication [25, 26] before incorporating the nanotubes in the monolith, and columns were prepared at varying time of the high power sonication. Both the 1 min and 15 min sonication times resulted better peak shapes with latter resulted much better peak efficiency. The column made using OH-MWCNTs at 30 min sonication did not show any improvement (see Fig. 6). This may be due to the fact that OH-MWCNTs may change their properties while subjecting them to high power sonication. Therefore, for the rest of the investigation, the 15 min sonicated column was used, and the MN5g column whose nanotubes were sonicated for 15 min was designated as MN5g-15.

Chromatographic evaluation of the optimized MN5g-15 columns

Based on the series of monolithic columns evaluated above, which involved optimizing different parameters such as polymerization temperatures, nature of the monolith, the amount and type of MWCNT and sonication time, the MN5g-15 column was identified as the best column. On this basis, the column was evaluated with different types of solutes.

Aromatic compounds with different functional groups. Aromatic compounds with different substituents on the benzene ring were used as model solutes to characterize the chromatographic properties of the MN5g-15 column. With the addition of OH-MWCNTs to the monolith, it is expected that the column would exhibit π–π interaction in addition to hydrophobic interaction. To analyze the hydrophobic and π–π interactions exhibited by the MN5g-15 stationary phase, aromatic compounds having different electron donating/withdrawing groups on the aromatic ring(s) were chromatographed on the column.

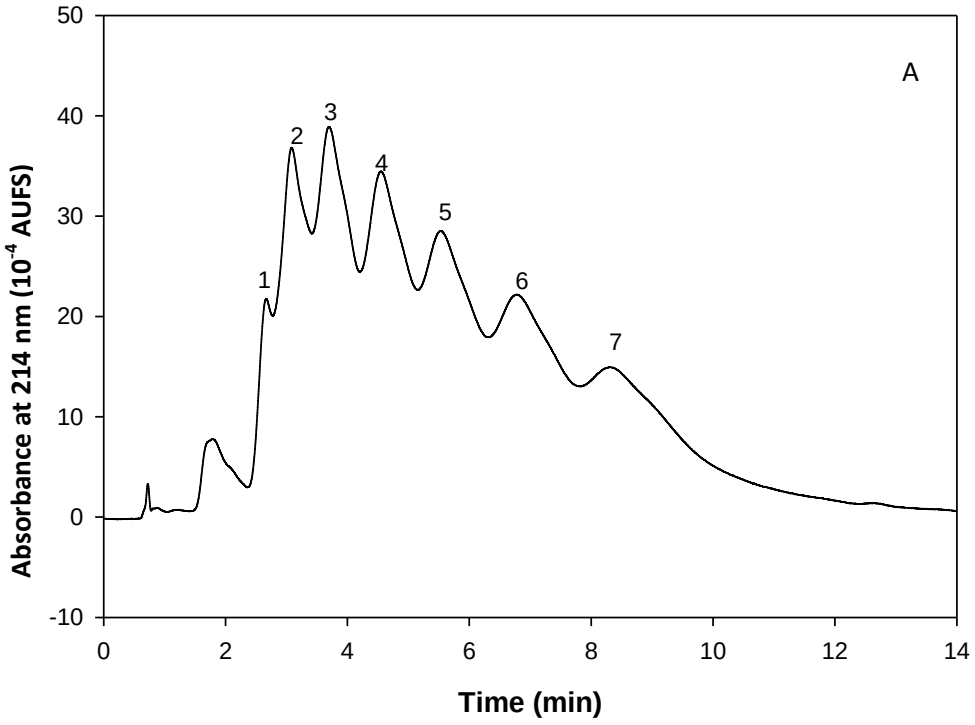
A
Absorbance at 214 nm (10-4 AUFS)
Time (min)
1
2
3
4
5
6
7

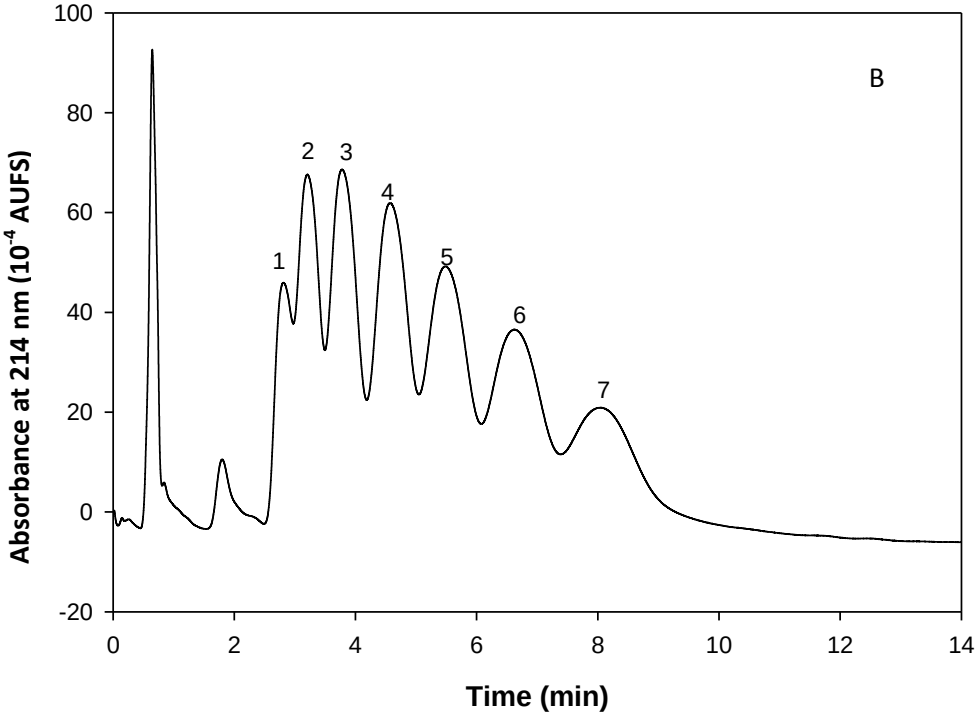
B
Absorbance at 214 nm (10-4 AUFS)
Time (min)
1
2
3
4
5
6
7

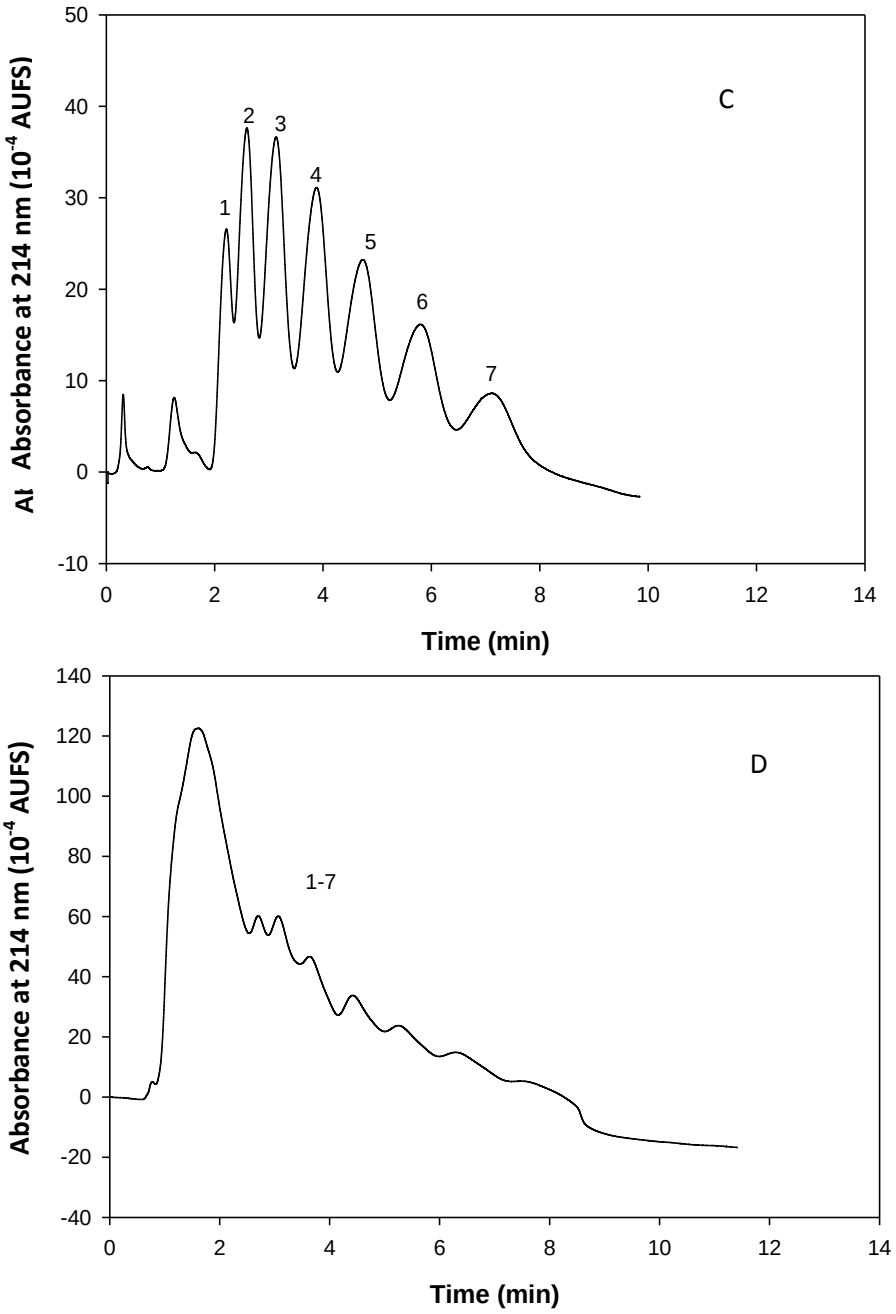

Figure 4: *Chromatograms of ABs obtained on GMM/EDMA columns with varying amounts of OH-MWCNTs. (A)MN5e, (B) MN5f, (C) MN5g, (D) MN5h. Mobile phase, ACN: H_2O (35:65 v/v) at 0.1% TFA. Other conditions as in Fig. 2. Solutes: 1, toluene; 2, ethylbenzene; 3, propy benzene; 4,butylbenzene; 5,amylbenzene; 6, hexylbenzene; 7, heptylbenzene.*

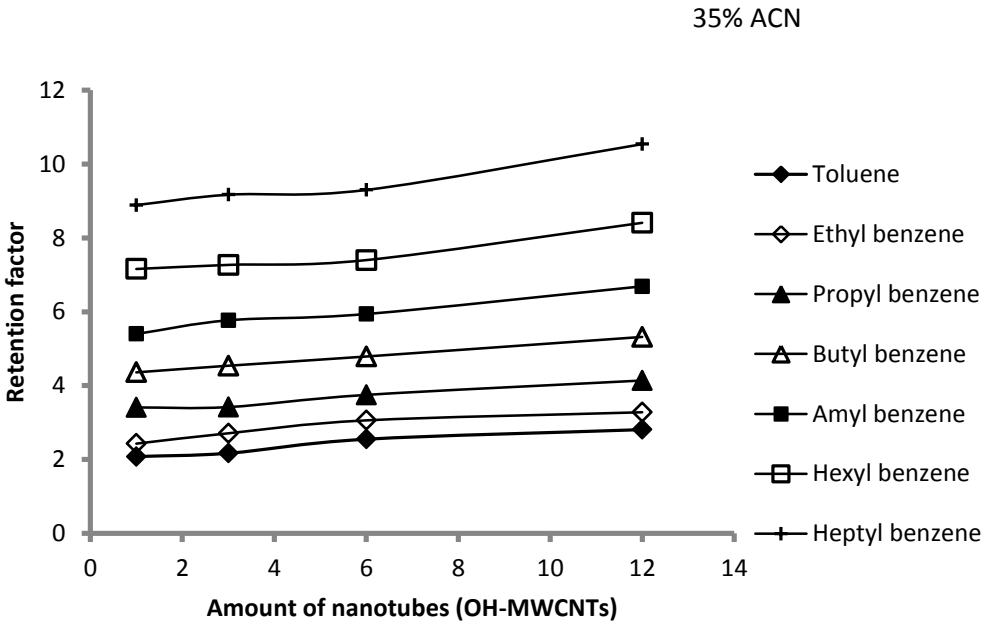
35% ACN
Retention factor
Amount of nanotubes (OH-MWCNTs)
Toluene
Ethyl benzene
Propyl benzene
Butyl benzene
Amyl benzene
Hexyl benzene
Heptyl benzene

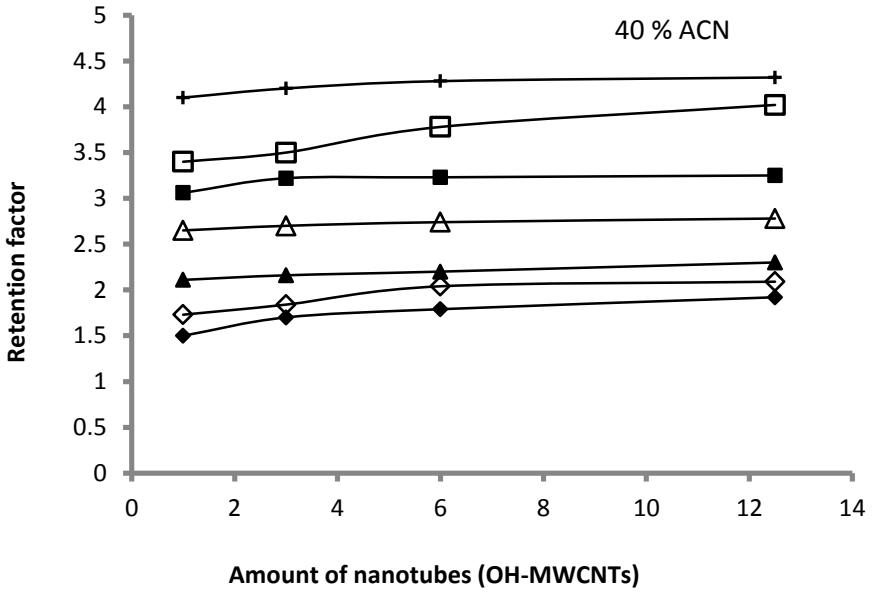
40 % ACN
Retention factor
Amount of nanotubes (OH-MWCNTs)

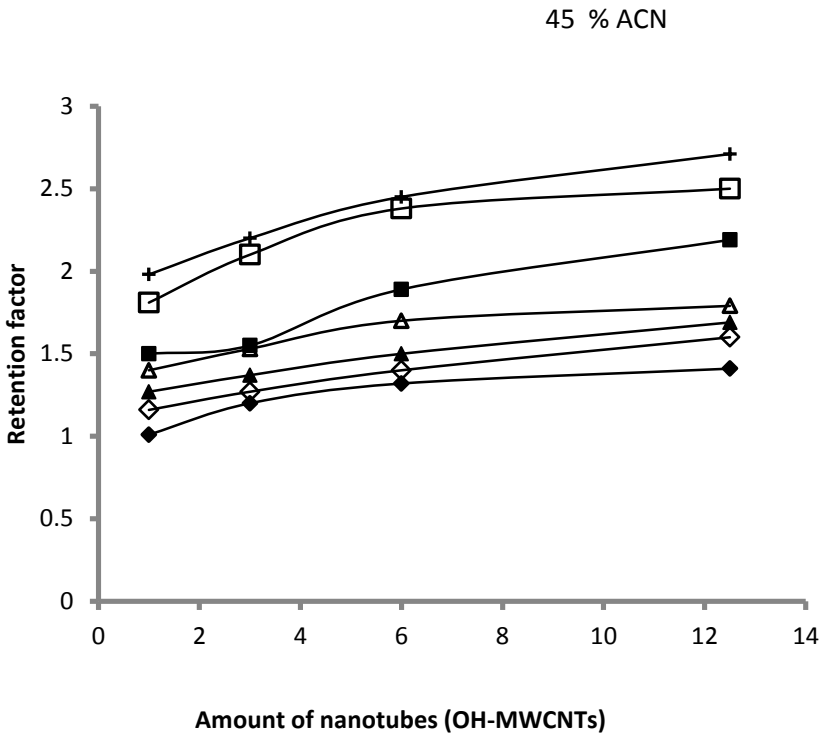

Figure 5. *Retention factors of ABs at different acetonitrile concentration obtained on GMM/EDMA monolithic columns incorporating various amounts of OH-MWCNTs.*

Aromatic compounds with different functional groups. Aromatic compounds with different substituents on the benzene ring were used as model solutes to characterize the chromatographic properties of the MN5g-15 column. With the addition of OH-MWCNTs to the monolith, it is expected that the column would exhibit π–π interaction in addition to hydrophobic interaction. To analyze the hydrophobic and π–π interactions exhibited by the MN5g-15 stationary phase, aromatic compounds having different electron donating/withdrawing groups on the aromatic ring(s) were chromatographed on the column.

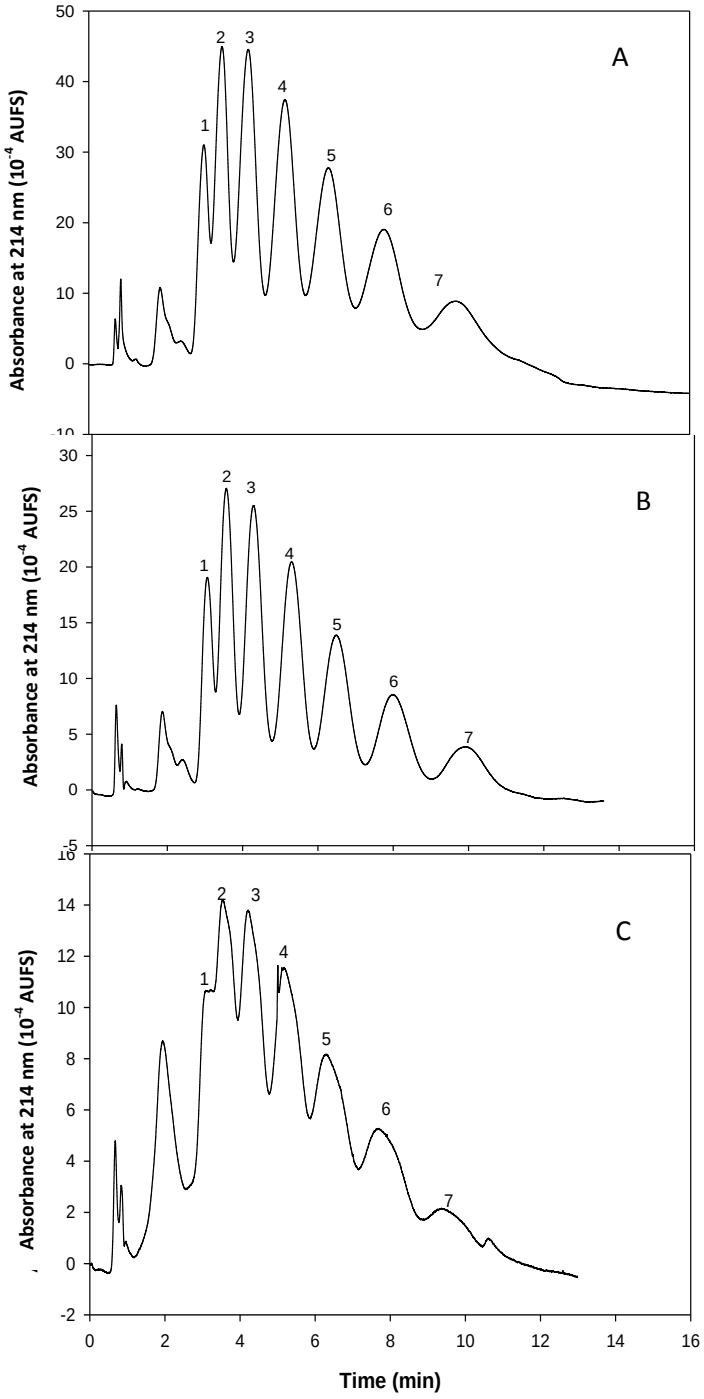

Figure 6. *Chromatograms of ABs obtained on the MN5g monolith with different times of high power sonication. A. 1 min, B. 15 min, C. 30 min. Mobile phase, ACN: H_2O (35:65 v/v)*

at 0.1% TFA. Other conditions as in Fig.2. Solutes 1, toluene; 2,ethylbenzene; 3, propyl benzene; 4, butylbenzene; 5, amylbenzene; 6, hexylbenzene; 7, heptylbenzene.

TABLE 5

COMPARISON OF THE k' VALUES OF ABS OBTAINED ON MN5g COLUMN AT VARIOUS HIGH POWER SONICATION TIME

	0 min	1 min	15 min	30 min
Toluene	2.17	3.38	3.78	3.65
Ethyl benzene	2.71	4.07	4.57	4.2
Propyl benzene	3.44	5.05	6.65	5.19
Butyl benzene	4.54	6.42	7.28	6.58
Amyl benzene	5.77	8.11	9.15	8.26
Phenyl hexane	7.3	10.22	11.46	10.29
Phenyl heptane	9.17	12.94	14.5	12.76

Electron-donating substituents on the benzene ring make the ring more π donating than benzene. These groups are called benzene ring activating groups [25]. They increase the electron density on the benzene ring. Typical examples of strongly activating groups are $–NH_2$, NHR, $-NR_2$, OH and O^-; while representative moderately activating groups are $–NHCOCH_3$, -NHCOR, $-OCH_3$ and –OR and weakly activating substituents are $–CH_3$, $-C_2H_5$, -R, and $–C_6H_5$. Electron-withdrawing groups decrease the electron density on the benzene ring by making the ring able to accept more π electrons. These are called deactivating groups

and are classified into (i) weakly deactivating groups such as –F, -Cl, -Br and -I; (ii) moderately deactivating substituents such as -CN, -SO_3H, -COOH, -COOR, -CHO and -COR; and (iii) strongly deactivating groups such as -NO_2, -NR_3, -CF_3, and CCl_3[26].

TABLE 6

CHROMATOGRAPHIC BEHAVIOR OF PARA SUBSTITUTED TOLUENE COMPOUNDS. MOBILE PHASE, ACN:H_2O (20:80 v/v) CONTAINING 0.1% TFA

Compound	t_R	k'	log k'
p-toluidine	1.11	0.44	-0.35
p-tolualdehyde	2.068	1.68	0.22
p-tolunitrie	2.24	1.91	0.28
toluene	3.78	3.9	0.59

Toluene derivatives. *p*-Toluidine, *p*-tolualdehyde, *p*-tolunitrile and toluene were used as model solutes. When the mixture of these solutes was injected onto the column, the observed elution order was *p*-toluidine, *p*-tolualdehyde, *p*-tolunitrile and toluene with the k' values of 0.44, 1.68, 1.91 and 3.9, respectively, see Table 6. Regarding hydrophobicity, toluene is more hydrophobic than the other 3 solutes. *p*-Toluidine, *p*-tolualdehyde and *p*-tolunitrile eluted in the order of increasing deactivation of the benzene ring by their respective substituents which indicate π-π interactions in addition to nonpolar interactions with the nanotubes on the surface of the monolith, while toluene being the most hydrophobic and carrying the weakly activating methyl group was the last eluting compound, a fact that indicates mainly nonpolar interactions of toluene with the surface carbon nanotubes.

A mixture of *m* substituted toluene compounds including *m*-toluidine, *m*-tolualdehyde, *m*-tolunitrile, toluene and *m*-nitrotoluene were separated on the column and the k'values for these compounds were 0.31, 2.42, 2.8, 3.9, 4.52 respectively, see Table 7. *m*-Nitrotoluene is more retained on the column than toluene. This gives the idea that the

TABLE 7

CHROMATOGRAPHIC BEHAVIOR OF META SUBSTITUTED TOLUENE COMPOUNDS. MOBILE PHASE, ACN:H_2O (20:80 v/v) CONTAINING 0.1% TFA

Compound	t_R	k'	log k'
m-toluidine	1.05	0.31	-0.51
m-tolualdehyde	2.74	2.42	0.38
m-tolunitrile	3.04	2.8	0.45
Toluene	3.78	3.9	0.59
m-nitrotoluene	4.42	4.52	0.65

retention mechanism is due to the hydrophobic interactions and π–π interactions. The strong electron withdrawing group on *m*-nitrotoluene decreases the π electron density on the aromatic ring, making it a soft Lewis acid that can accept π electrons from OH-MWCNTs which is having high π electron density resulting in π-donor-π-acceptor complexes. The π–π interactions make the nitrotoluene more retained on the column than other solutes.

Benzene derivatives. In addition to toluene derivatives, other compounds that show potential of π–π interactions were also analyzed on the MN5g-15 column. Benzene

derivatives such as benzonitrile, benzaldehyde, nitrobenzene and toluene were injected onto MN5g-15 monolith using the mobile phase, ACN:H_2O (30:70 v/v) containing 0.1% TFA. The elution order was observed as benzonitrile, benzaldehyde, nitrobenzene and toluene with the observed respective k' values as 2.08, 3.44, 3.44 and 4.05, see Table 8. Toluene has a weakly

TABLE 8

CHROMATOGRAPHIC BEHAVIOR OF BENZENE DERIVATIVES

Compound	t_R	k'	log k'
Benzonitrile	2.5	2.08	0.31
Benzaldehyde	3.6	3.44	0.53
Nitrobenzene	3.65	3.45	0.54
Toluene	4.05	4	0.602

activating methyl group which weakly increases the electron donating density of the benzene ring but it has a relatively high hydrophobic character. The other three compounds have deactivating substituents with the strongest deactivator being the nitro group followed by moderate nitrile and then aldehyde. Nitro-substituted benzene is expected to have greater retention on the column because nitrobenzene has low π electron density and it has the ability to accept π electrons from the π electrons of OH-MWCNTs resulting in π–π interactions that leads to π-donor-π-acceptor complexes [25, 27]. But in this case toluene shows the higher retention due to hydrophobic interaction with the stationary phase.

Anilines. The retentive character of the column was further studied using a mixture of anilines with ACN: H_2O (20:80 v/v) containing 0.1% TFA as the mobile phase, see Fig. 7. The order of elution was aniline, ethylaniline, bromoaniline and 2, 4- dichloroaniline.

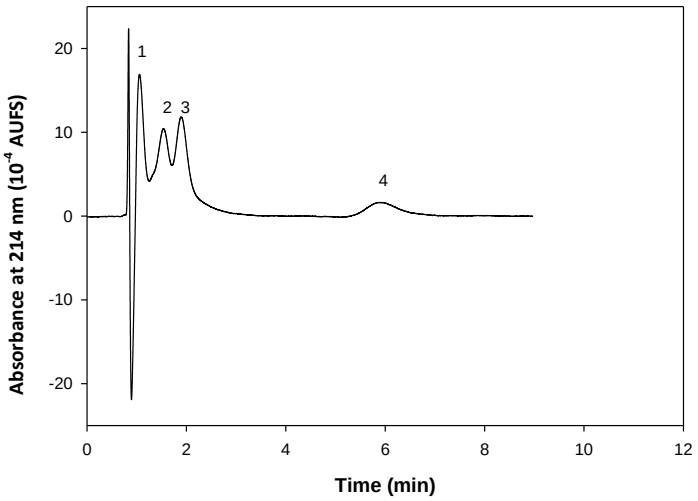

Figure 7. *Chromatogram of anilines obtained on MN5g-15 column. Solutes: (1), aniline; (2),4-ethylaniline; (3),4-bromoaniline; (4),2,4-dichloroaniline. Mobile phase, ACN:H_2O (20:80 v/v) containing 0.1% TFA, Other conditions as in Fig.2.*

The retention shows the typical RPC characteristics where halogenated anilines were more retained than ethyl substituted anilines. This demonstrates that hydrophobicity and π–π interactions play a major role in separating the anilines under investigation.

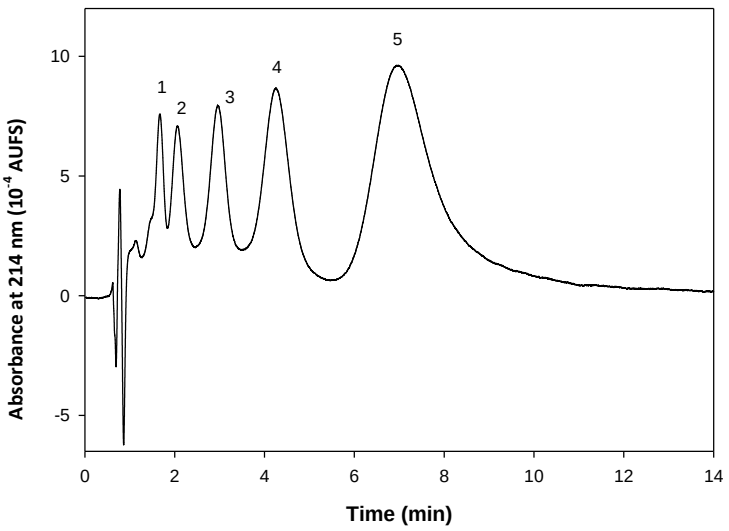

Figure 8. *Chromatogram of some phenolic compounds obtained on MN5g-15 column. Solutes: (1), phenol; (2), 2-chlorophenol; (3), 4-nitrophenol; (4), 2,4,5-trinitrophenol; (5), pentachlorophenol. Mobile phase, ACN:H_2O (40:60 v/v) containing 0.1% TFA, Other conditions as in Fig.2.*

Phenolic compounds. In this section, some phenols were analyzed on the MN5g-15 column using the mobile phase composed of ACN:H_2O (40:60 v/v) containing 0.1% TFA. Fig. 8 shows the separation of some phenolic compounds using the MN5g-15 stationary phase. The observed elution order was phenol, 2-chlorophenol, *4*-nitrophenol, 2, 4, 5-trichlorophenol and pentachlorophenol with the k' values of 1.14, 1.64, 2.76, 4.46, 7.78, respectively. Phenol eluted faster than the substituted phenols such as 2,4,5-trichlorophenol and pentachlorophenol, which yielded higher retention due to their hydrophobic and π–π interactions. It is observed that the degree of halogenation and the size of the solute control the retention. More halogenated phenols were retained for longer time on the stationary phase showing the RPC behavior for separation.

Herbicides. Herbicides are a group of highly toxic compounds that can accumulate in the environment or in drinking water resulting in serious damage to the human health. Therefore, it is important to develop a method to analyze for these compounds [28]. The chromatographic properties of the MN5g-15 column were further evaluated using phenoxy herbicides as model solutes, see Fig. 9. Since they are polar solutes they can be ionized easily, therefore, the pH of the mobile phase was adjusted to pH 2.12 using Na_2HPO_4. As

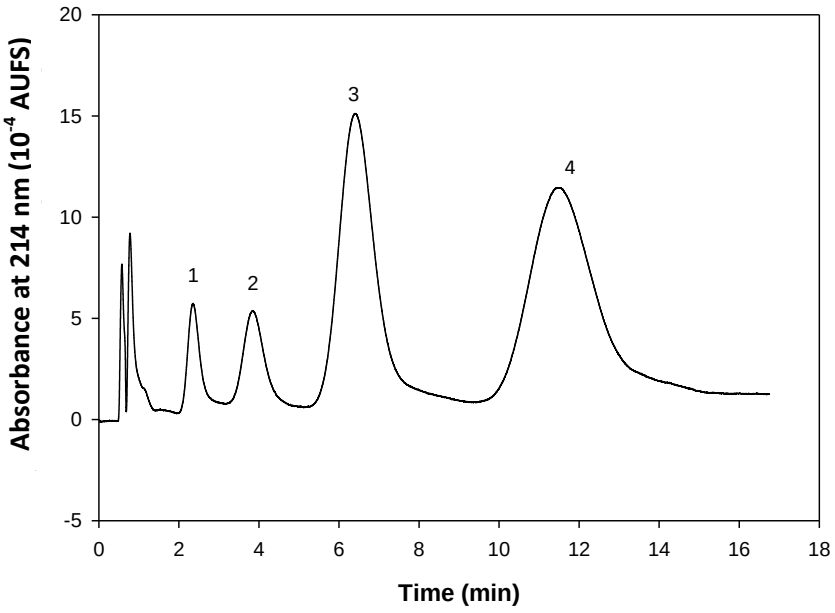

Figure 9. *Chromatogram of some phenoxy herbicides obtained on MN5g-15 column. Mobile phase, ACN:H_2O (40:60 v/v) at 0.1% TFA, Other conditions as in Fig.2. Solutes: (1), 2-phenoxypropionic acid; (2), 2-(2-chloro) propionic acid; (3), methylchlorophenoxypropionic acid; (4), 2-(2,4,5-trichloropenoxy)-propionic acid.*

can be seen in Fig. 9, the column was able to separate 2-phenoxypropionic acid, 2-(2-chloro)-propionic acid, methyl chloro phenoxy propionic acid, 2-(2,4,5- trichlorophenoxy)propionic acid with the k' values of 2.01, 3.93, 7.19, 11.74, respectively. These data illustrate the fact

that 2-(2,4,5-trichlorophenoxy)propionic acid with three chlorine atoms attached to the benzene ring exhibits a higher retention than 2-phenoxy propionic acid. Similarly, 2-(2-chloro) propionic acid is more retained on the column than 2-phenoxypropionic acid. This gives the idea that chloride substitution can induce $\pi-\pi$ interactions with the stationary phase and increase solute retention. In addition, phenoxy herbicides show other interactions due to the polar groups such as -COOH, -OH.

Separation of chiral compounds

The analysis of enantiomers is an area of increasing importance in separation science. In HPLC, chiral separation is carried out using chiral additives in the mobile phase or using a chiral stationary phase [29]. Enantiomers are isomeric forms of the same compound, which differ only in their spatial orientation and have identical physical properties. In order to separate racemic mixtures, the two enantiomers should interact differently with the OH-MWCNTs in the stationary phase. Due to their unique physical, chemical, and electrical properties, MWCNTs have been the subject of intense research as chiral selectors in CE but to a lesser extent in HPLC [7, 29-37]. The MWCNTs have large surface to volume, which in turn results in achieving a favorable mass transfer and thus enhanced chromatographic efficiency towards the separation of chiral compounds. The chirality of the MWCNTs arises from the arrangement of multiple walls around the central cylinder [38].

The MN5g-15 column was able to successfully separate five enantiomeric compounds including phenoxy herbicides such as phenoxypropionic acid, 2,4-dichloro-phenylpropionic acid, racemic derivatized amino acids such as dansylated (Dns)-methionine,

Dns-phenylalanine and the pharmaceutically important compound bupivacaine; for their structures see Fig. 10.

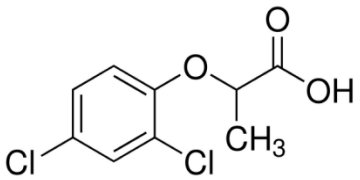

2,4-dichloro phenoxy propionic acid

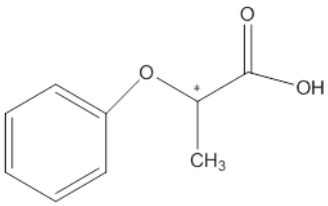

2-phenoxy propionic acid

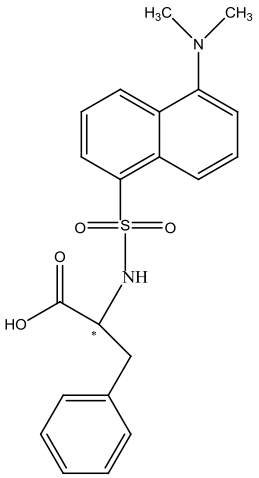

Dansyl phenylalanine

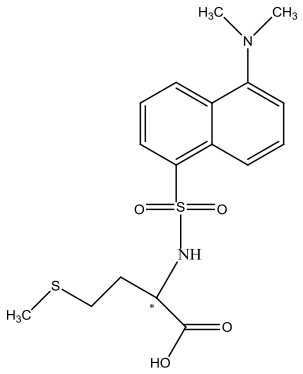

Dansyl methionine

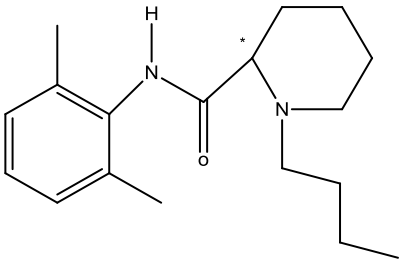

Bupivacaine

Figure 10. *Chiral compounds separated on the MN5g-15 column (* indicates the stereocenters).*

To achieve an optimal enantioseparation, the column loading in nanotubes needs to be optimized. This was carried out by varying the amount of OH-MWCNTs incorporated in the monolith. The results are shown in Table 10 where it can be see that 3 mg of OH-MWCNTs yielded enhanced performance for separating the chiral compounds under investigation. Enantiomeric phenoxypropionic acid and 2,4-dichlorophenylpropionic acid were separated using the mobile phase 50 mM sodium acetate 25% ACN, pH of 4.12, see Fig. 11. Since the pKa value of phenoxy herbicides is around 4.14, these compounds are partially ionized at the pH of the mobile phase, a condition that favored separation. Also, Dns- methionine and Dns-phenylalanine were separated using 25 mM acetate buffer, 35% ACN, pH 4.12. This shows that MWCNTs can function as a chiral stationary phase to separate enantiomeric compounds.

TABLE 9

ENATIOMERIC RESOLUTION SEPARATION OF COMPOUNDS USING

MN5g-15 COLUM

Compound Name	Resolution of chiral compounds with varying amount of nanotubes			
	2 mg	3 mg	4 mg	5 mg
DNS methionine	0.42	1.35	0.24	0
DNS Phenyl alanine	0.84	1.25	0.62	0
Bupivacaine	0.7	1.02	0.5	0
Phenoxy propionic acid	0	1.4 P.S.	0	0
2,4-Dichloro phenyl propionic acid	0	1.28	0	0

PS: Partially resolved, see Fig.9 a

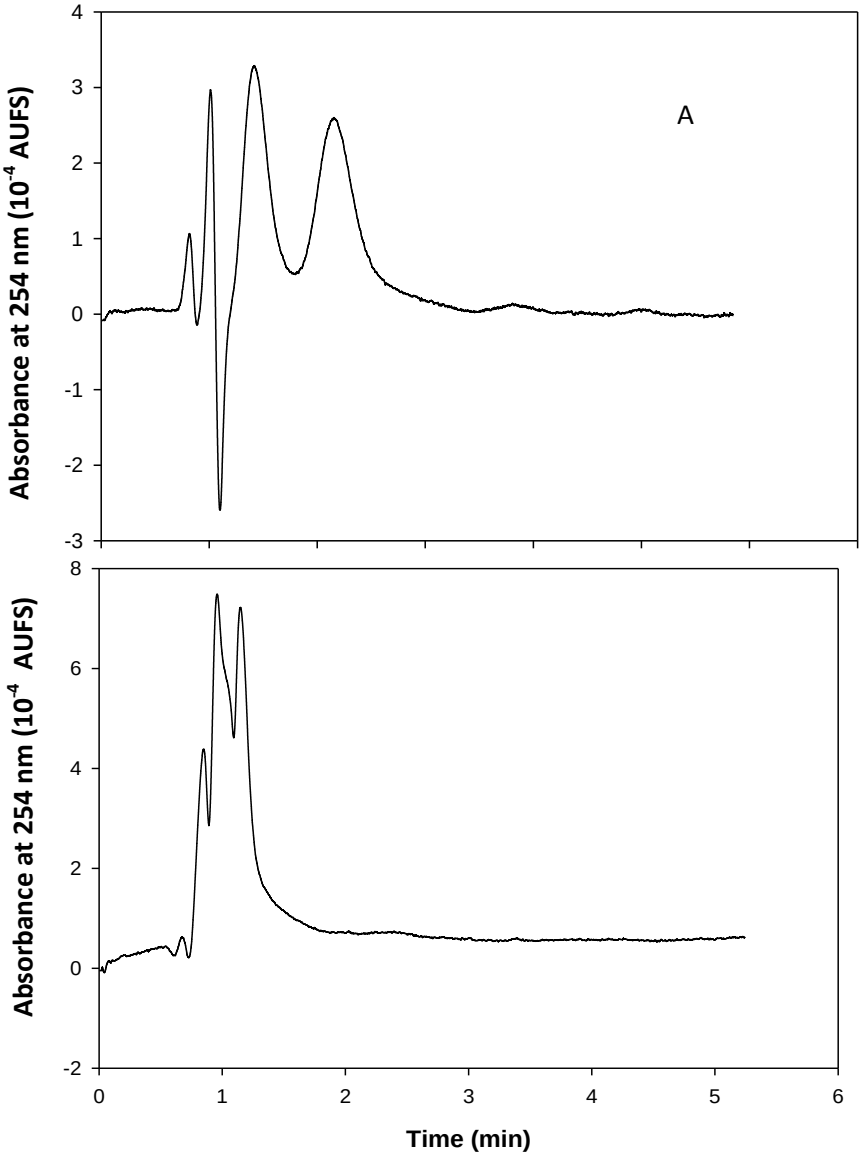

Figure 11. *Separation of raceimic phenoxy herbicides using MN5g-15 column. Mobile phase, ACN: H_2O (40:60 v/v) at 50 mM sodium acetate, pH 4.12, Other conditions as in Fig.2.Solutes; A, 2,4-dichlorophenoxy propionic acid; B, phenoxy propionic acid.*

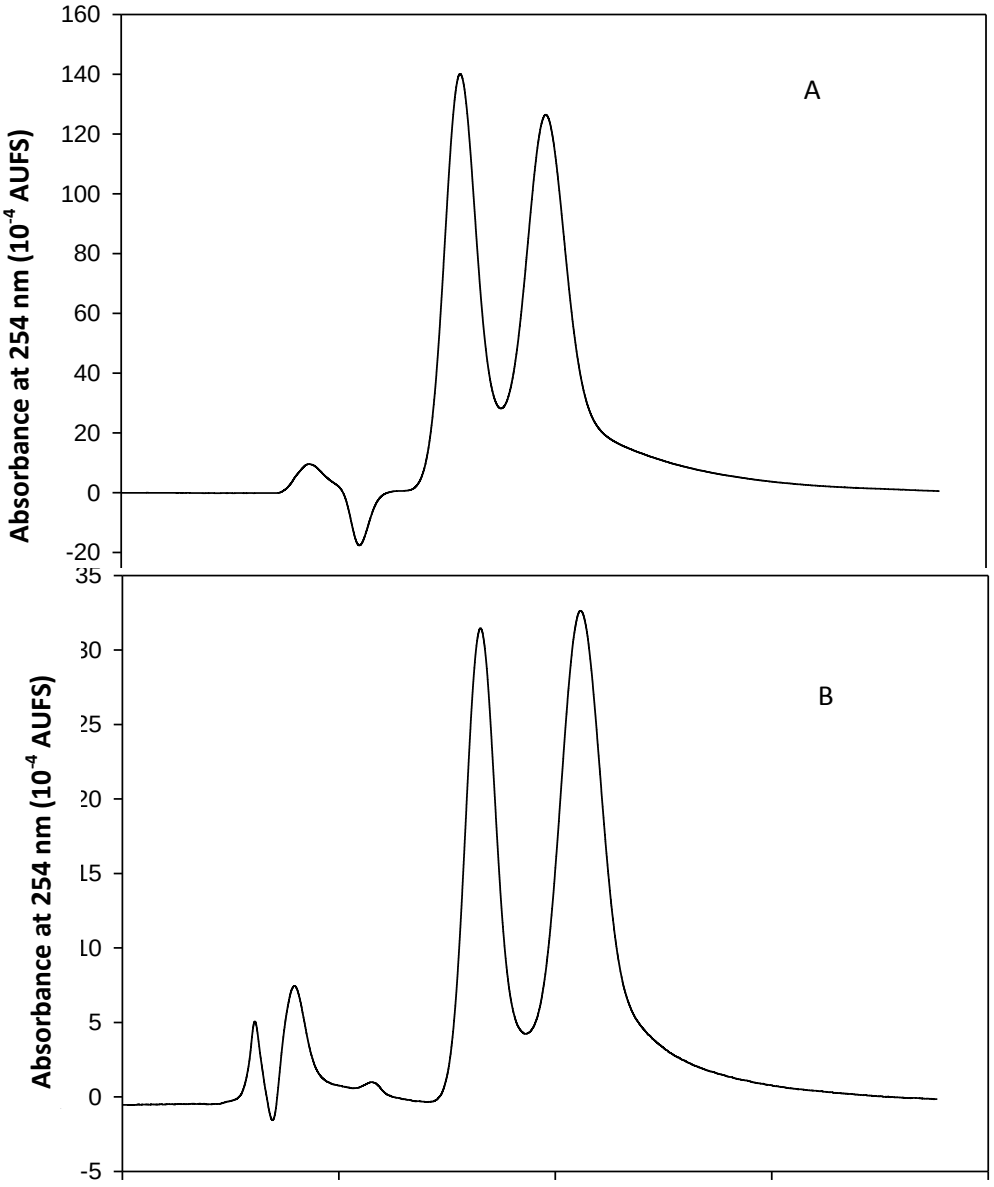

Figure 12. *Separation of Dns amino acids obtained on the MN5g-15 column. Mobile phase, ACN:H_2O (35:65v/v) containing 25 mm mM sodium acetate, pH 4.1, Other conditions as in Fig.2 Solutes; A, Dns-methionine; B, Dns -phenylalanine.*

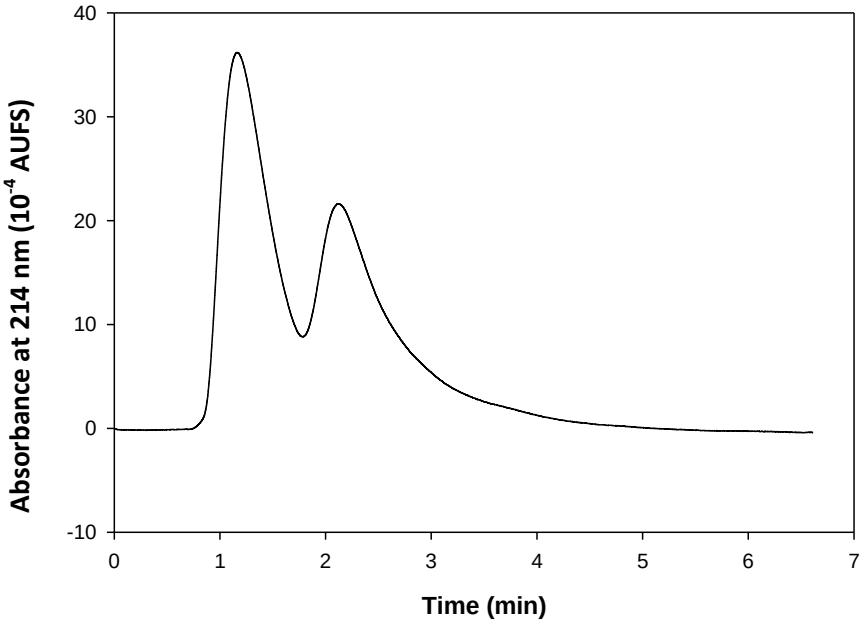

Figure 13. *Separation of racemic Bupivacaine obtained on the MN5g-15 column. Mobile phase, ACN:H_2O (55:45v/v) containing 0.1% TFA. Other conditions as in Fig.2.*

In this study, SN 32547 was identified as the optimum chiral selector. The chiral resolution is based on the inclusion complexation between the chiral selector e.g., OH-MWCNTs and the enantiomer, which causes the selective retardation of the enantiomer [39, 40]. When the racemic mixture is injected onto the column it forms an analyte–chiral selector complex. Two enantiomers have different affinity for the chiral selector and therefore the chromatographic retention of these enantiomers is different. By increasing the chiral selector concentration, resolution is increased up to a certain level. After the addition the 3 mg of MWCNTs there were no chiral separation is achieved. Here the chiral selector is OH-MWCNTs. Increasing OH-MWCNTs prevents the free movement of the analyte in the

stationary phase. Therefore, with the addition of 5 mg of OH-MWCNTs, zero resolution is achieved. To provide a maximum resolution there is an optimum OH-MWCNTs concentration. By observing the enantiomeric resolution of Table 9, it can be seen that 2 mg of OH-MWCNTs are not sufficient for the retention and consequently a good resolution of the racemic mixture. 3 mg OH-MWCNTs is the optimum chiral selector concentration. The columns made out of 4 mg and 5 mg of OH-MWCNTs show low resolution due to an increase in the retention time of the enantiomers causing increased band broadening and thereby decreasing the resolution of enantiomers.

Conclusions

This study introduced a novel monolithic stationary phase for RPC separation by HPLC. The monolith, which was designated as MN5g-15, allowed separation solely *via* differential interaction of the solutes with OH-MWCNTs (i.e., the carbon nanotubes). A wide range of aromatic compounds such as benzene derivatives, toluene derivatives, anilines and chlorophenols were resolved by the column. The separation of these compounds was mainly due to $\pi-\pi$ interactions and hydrophobic interactions. The column proved useful for the enantioseparations of some racemic compounds.

References

1. Wu, R.a., L. Hu, F. Wang, M. Ye, and H. Zou, *Recent development of monolithic stationary phases with emphasis on microscale chromatographic separation.* J. Chromatogr. A, 2008. **1184**(1–2): p. 369-392.
2. Speltini, A., D. Merli, and A. Profumo, *Analytical application of carbon nanotubes, fullerenes and nanodiamonds in nanomaterials-based chromatographic stationary phases: A review*. Anal. Chim. Acta, 2013. **783**(0): p. 1-16.
3. André, C., R. Aljhani, T. Gharbi, and Y.C. Guillaume, *Incorporation of carbon nanotubes in a silica HPLC column to enhance the chromatographic separation of peptides: Theoretical and practical aspects.* J. Sep. Sci., 2011. **34**(11): p. 1221-1227.
4. Trojanowicz, M., *Analytical applications of carbon nanotubes: a review.* TrAC Trends in Anal. Chem., 2006. **25**(5): p. 480-489.
5. Pauwels, J. and A. Schepdael, *Carbon nanotubes in capillary electrophoresis, capillary electrochromatography and microchip electrophoresis.* Cent. Eur. J. Chem., 2012. **10**(3): p. 785-801.
6. *Theme issue: carbon nanostructures.* J. Mater. Chem., 2008. **18**(13): p. 1415-1416.

7. Valcárcel, M., S. Cárdenas, and B.M. Simonet, *Role of Carbon Nanotubes in Analytical Science.* Anal. Chem., 2007. **79**(13): p. 4788-4797.

8. Liang, X., S. Liu, H. Liu, X. Liu, and S. Jiang, *Layer-by-layer self-assembled multi-walled carbon nanotubes/silica microsphere composites as stationary phase for high-performance liquid chromatography.* J. Sep. Sci., 2010. **33,** 3304-3312.

9. Knox, J.H., B. Kaur, G.R. Millward, *Structure and performance of porous graphitic carbon in liquid chromatography.* J.Chromatogr. A, 1986. **352**): p. 3-25.

10. Ting, E.-Y. and M.D. Porter, *Separations of benzodiazepines using electrochemically modulated liquid chromatography: Efficient separations from changes in the voltage applied to a porous graphitic carbon stationary phase.* J. Chromatogr. A, 1998. **793**(1): p. 204-208.

11. Cai, Y., G. Jiang, J. Liu, and Q. Zhou, *Multiwalled Carbon Nanotubes as a Solid-Phase Extraction Adsorbent for the Determination of Bisphenol A, 4-n-Nonylphenol, and 4-tert-Octylphenol.* Anal. Chem., 2003. **75**(10): p. 2517-2521.

12. Cai, Y.-q., Y.-e. Cai, S.-f. Mou, and Y.-q. Lu, *Multi-walled carbon nanotubes as a solid-phase extraction adsorbent for the determination of chlorophenols in environmental water samples.* J. Chromatogr. A, 2005. **1081**(2): p. 245-247.

13. Ravelo-Pérez, L.M., J. Hernández-Borges, and M.Á. Rodríguez-Delgado, *Multi-walled carbon nanotubes as efficient solid-phase extraction materials of organophosphorus pesticides from apple, grape, orange and pineapple fruit juices.* J. Chromatogr. A, 2008. **1211**(1–2): p. 33-42.

14. Li, L., Y. Huang, Y. Wang, and W. Wang, *Hemimicelle capped functionalized carbon nanotubes-based nanosized solid-phase extraction of arsenic from environmental water samples.* Anal. Chim. Acta, 2009. **631**(2): p. 182-188.

15. Li, Q. and D. Yuan, *Evaluation of multi-walled carbon nanotubes as gas chromatographic column packing.* J. Chromatogr. A, 2003. **1003**(1–2): p. 203-209.

16. Saridara, C. and S. Mitra, *Chromatography on Self-Assembled Carbon Nanotubes.* Anal. Chem., 2005. **77**(21): p. 7094-7097.

17. Sae-Khow, O. and S. Mitra, *Simultaneous Extraction and Concentration in Carbon Nanotube Immobilized Hollow Fiber Membranes.* Anal. Chem., 2010. **82**(13): p. 5561-5567.

18. Fagnoni, M., A. Profumo, D. Merli, D. Dondi, P. Mustarelli, and E. Quartarone, *Water-Miscible Liquid Multiwalled Carbon Nanotubes.* Adv. Mat., 2009. **21**(17): p. 1761-1765.

19. Speltini, A., D. Merli, E. Quartarone, and A. Profumo, *Separation of alkanes and aromatic compounds by packed column gas chromatography using functionalized Multi-Walled Carbon Nanotubes as stationary phases.* J. Chromatogr. A, 2010. **1217**(17): p. 2918-2924.

20. Chen, J.-L., *Multi-wall carbon nanotubes bonding on silica-hydride surfaces for open-tubular capillary electrochromatography.* J. Sep. Sci., 2010. **1217**p. 715-721.

21. Luong, J.H.T., P. Bouvrette, Y. Liu, and E. Sacher, *Electrophoretic separation of aniline derivatives using fused silica capillaries coated with acid treated single-walled carbon nanotubes.* J. Chromatogr. A, 2005. **1074**(1–2): p. 187-194.

22. Li, Y., Y. Chen, R. Xiang, D. Ciuparu, L.D. Pfefferle, C. Horváth, and J.A. Wilkins, *Incorporation of Single-Wall Carbon Nanotubes into an Organic Polymer Monolithic Stationary Phase for μ-HPLC and Capillary Electrochromatography.* Anal. Chem., 2005. **77**(5): p. 1398-1406.

23. Chambers, S.D., F. Svec, and J.M.J. Fréchet, *Incorporation of carbon nanotubes in porous polymer monolithic capillary columns to enhance the chromatographic separation of small molecules.* J. Chromatogr. A, 2011. **1218**(18): p. 2546-2552.

24. André, C., G. Lenancker, and Y.C. Guillaume, *Non-covalent functionalisation of monolithic silica for the development of carbon nanotube HPLC stationary phases.* Talanta, 2012. **99**(0): p. 580-585.

25. Karenga, S. and Z. El Rassi, *Naphthyl methacrylate-based monolithic column for RP-CEC via hydrophobic and π interactions.* Eletrophoresis, 2010. **31** p. 991-1002.

26. Carey, F.A. and R.J. Sundberg, *Advanced organic chemistry*. 5th ed. 2007, New York: Springer.

27. Brindle, R. and K. Albert, *Stationary phases with chemically bonded fluorene ligands: A new approach for environmental analysis of π-electron containing solutes.* J. Chromatogr. A, 1997. **757**(1–2): p. 3-20.

28. González-Curbelo, M.Á., A.V. Herrera-Herrera, J. Hernández-Borges, and M.Á. Rodríguez-Delgado, *Analysis of pesticides residues in environmental water*

samples using multiwalled carbon nanotubes dispersive solid-phase extraction. J. Sep. Sci., 2013. **36**(3): p. 556-563.

29. Sancho, R. and C. Minguillon, *The chromatographic separation of enantiomers through nanoscale design.* Chem. Soc. Rev., 2009. **38**(3): p. 797-805.

30. Na, N., Y. Hu, J. Ouyang, W.R.G. Baeyens, J.R. Delanghe, and T.D. Beer, *Use of polystyrene nanoparticles to enhance enantiomeric separation of propranolol by capillary electrophoresis with Hp-beta-CD as chiral selector.* Anal. Chim. Acta, 2004. **527**(2): p. 139-147.

31. Du, Y., S. Guo, H. Qin, S. Dong, and E. Wang, *Target-induced conjunction of split aptamer as new chiral selector for oligopeptide on graphene-mesoporous silica-gold nanoparticle hybrids modified sensing platform.* Chem. Comm., 2012. **48**(6): p. 799-801.

32. Nilsson, C. and S. Nilsson, *Nanoparticle-based pseudostationary phases in capillary electrochromatography.* Electrophoresis, 2006. **27**(1): p. 76-83.

33. Wang, Y., X. Yin, M. Shi, W. Li, L. Zhang, and J. Kong, *Probing chiral amino acids at sub-picomolar level based on bovine serum albumin enantioselective films coupled with silver-enhanced gold nanoparticles.* Talanta, 2006. **69**(5): p. 1240-1245.

34. Ward, T.J. and B.A. Baker, *Chiral Separations.* Anal. Chem., 2008. **80**(12): p. 4363-4372.

35. Suárez, B., B.M. Simonet, S. Cárdenas, and M. Valcárcel, *Surfactant-coated single-walled carbon nanotubes as a novel pseudostationary phase in capillary EKC.* Electrophoresis, 2007. **28**(11): p. 1714-1722.

36. Gübitz, G. and M.G. Schmid, *Chiral separation by capillary electromigration techniques.* J. Chromatogr. A, 2008. **1204**(2): p. 140-156.

37. Weng, X., H. Bi, B. Liu, and J. Kong, *On-chip chiral separation based on bovine serum albumin-conjugated carbon nanotubes as stationary phase in a microchannel.* Electrophoresis, 2006. **27**(15): p. 3129-3135.

38. Silva, R.A., M.C. Talío, M.O. Luconi, and L.P. Fernández, *Evaluation of carbon nanotubes as chiral selectors for continuous-flow enantiomeric separation of carvedilol with fluorescent detection.* J Pharm. Biomed Anal, 2012. **70**(0): p. 631-635.

39. Fanali, S. and Z. Aturki, *Use of cyclodextrins in capillary electrophoresis for the chiral resolution of some 2-arylpropionic acid non-steroidal anti-inflammatory drugs.* J. Chromatogr. A, 1995. **694**(1): p. 297-305.

40. Schmid, M. and G. Gübitz, *Enantioseparation by chromatographic and electromigration techniques using ligand-exchange as chiral separation principle.* Anal. Bioanal. Chem., 2011. **400**(8): p. 2305-2316.

CHAPTER III

OCTADECYL MONOLITHIC COLUMNS FOR PROTEIN SEPARATION

Introduction

High performance liquid chromatography is a high efficiency separation technique for quantitative and qualitative analysis of a wide range of compounds. In HPLC, the column is the heart of the separation process. Columns packed with micro particulates have several limitations for the efficient separation such as slow diffusional mass transfer and large void volume between the packed particles [1-4]. Monolithic columns evolved significantly in last decades and have proven a very good alternative to particle packed columns due to their ability to separate a wide range of compounds [5, 6]. Higher separation efficiency could be achieved due to the small sized skeletons and wide flow-through pores of the monolithic columns [7, 8]. The monolithic column is a continuous rigid skeleton with uniform pore size and if necessary, the surface can be functionalized to achieve the desired binding properties [9]. They can be developed using synthetic organic materials, natural polymers or inorganic materials and have specific hydrodynamic properties such as lower mass transfer resistance and pressure drop [10-14]. Reversed phase interaction can be achieved in HPLC using uncharged or

hydrophobic monoliths [15]. The advantages of monolithic columns are that they exhibit good flow profile, good permeability, withstand high pressure, allow tailor made surfaces and by selecting the appropriate monomers, one can control the interactions of the monolithic surface.

One of the challenges in proteomic research is the separation and identification of compounds with very similar physicochemical properties [16, 17]. In RPC, proteins are bound to hydrophobic matrices. When the organic solvent interacts with the protein and the monolithic stationary phase it displaces the protein. Reports have shown that RPC has good resolving power for proteins [18-20]. Proteins differ in their size and they have different polarities, therefore they have different interactions with the monolithic surface. There have been several attempts to separate proteins using monolithic columns. In the the first attempt, a single piece of cellulose sponge was used in separating proteins [21]. In another study, proteins were separated on polyacrylamide based monolithic columns [14]. Similarly, norbornene based monoliths were also used in separating proteins [22, 23]. In another study, macroporous poly(styrene–co-divinylbenzene) monolithic stationary phases have been prepared by free radical polymerization and were able to separate proteins and peptides in a relatively short time [24].

Additions of nanotubes to monolithic stationary phases are gaining popularity due to their unique characteristics [25-27]. Svec at al. introduced carbon nanotubes in the polymerization mixture and achieved 44000 plates/m for benzene with monolithic capillary columns [28]. Guillaume et al. added carbon nanotube (CNT) monolithic column coated with a pyrenyl derivative as the chiral selector. A solution of pyrenyl neomycine A was pumping through a monolithic CNT column. The column was used for

HPLC chiral separation of underivatized amino acids [29]. Multiwalled carbon nanotubes were incorporated into a polymethacrylate-based monolith made out of EDMA and GMA and used for separation of anions. The study analyzed the efficiency of separation with changing amounts of MWCNTs, and studied thermal stability and Raman characteristics of the polymer [30]. ODA/TRIM monolith (or ODM monolith) is an organic and neutral monolith showing RPC characteristics. Neutral monoliths, void of fixed charges, were introduced and tested in our laboratory. The first monolith was reported by Okanda and El Rassi [31] and another attempt was reported by Karenga and El Rassi [32]. In this investigation, the previously reported ODM monolith from our laboratory [32], originally for use in RP-CEC, was slightly altered to render it suitable for RPC separation by HPLC. The alteration was concerned with making the column operate at high mobile phase using flow velocity high precision HPLC pump. The original ODM monolith was ideal for CEC where the mobile phase was transported through the capillary column by electroosmotic flow (EOF). Therefore, it was necessary to optimize the composition of the monolith to yield a highly permeable column for use in HPLC, yet with good separation efficiency toward proteins. The monolith was further evaluated for proteins by adding multi walled carbon nanotubes (MWCNTs) to the monolith.

Experimental

Instrumentation

The HPLC setup consisted of a quaternary solvent delivery system Model Q-grad pump from Lab Alliance (State College, PA, USA), a solvent delivery system model

CM4000, and a Model SpectroMonitor 3100 UV-Vis variable wavelength detector from Milton Roy, LDC division (Riviera Beach, FL, USA) and a Rheodyne injector Model 7010 (Cotati, CA, USA) equipped with a 20 μL loop. A constant pressure air-driven pump Model Shandon from Southern Products Limited (Cheshire, UK) was used for column packing. An ultrasonic cleaner, Model 1510 Branson was purchased from Emersion (Danbury, CT, USA). The water bath Model 2100 was obtained from Thermo Fischer Scientific (Waltham, MA, USA).

Reagents and Materials

Multiwalled carbon nanotubes were purchased from Sun Innovation Inc. (Fremont, CA). Alkyl benzenes (ABs), trifluoroacetic acid (TFA), 2,2'-azobis(isobutyronitrile) (AIBN), octadecyl acrylate (ODA), trimethylolpropane trimethacrylate (TRIM), ethylene glycol dimethacrylate (EDMA), ethylene glycol and cyclohexane, were purchased from Sigma Aldrich (Milwaukee, WI, USA). Egg white lysozyme, bovine serum albumin, ribonuclease A, ovalbumin, horse heart cytochrome C, bovine erythrocytes carbonic anhydrase, bovine milk β–lactoglobulin A and B and bovine milk α-lactalbumin were purchased from Sigma (St. Louis, MO, USA). Chicken white lysozyme were from Promega (Madison, WI, USA). HPLC grade acetonitrile and isopropyl alcohol purchased from Pharmco Aaper (Brookfield, CT, USA). Stainless steel tubing of 4.6 mm id was obtained from Alltech Associates (Deerfield, IL, USA).

Preparation of monolithic columns

A polymerization mixture consisting of 5.5 g was prepared by weighing monomers and porogens according to the composition shown in Table 1. Cyclohexanol

composition was varied in the range of 50% - 54.2% and ethylene glycol was in the range of 20.9%-24.48%. All polymerization solutions for making the monoliths were vortexed for 1 min, sonicated at 40 ^{o}C for 15 min, purged with nitrogen for 5 min and introduced into stainless steel columns with dimensions of 25 cm x 4.6 mm id that function as a mold for the monolith. Both column ends were plugged tightly and heated at 60 ˚C in a water bath for 15 h. The monolithic column was washed with acetonitrile for 30 min followed by isopropyl alcohol. The monolith was transferred from the 25 cm mold to a shorter column of 10 cm x 4.6 mm id by connecting the two columns with a ¼ ‘‘-union and passing IPA using a constant pressure pump starting from the pressure of 6000 lb/ in^2 until the monolith was completely transferred. The column was washed with the running buffer and tested with standard solutes.

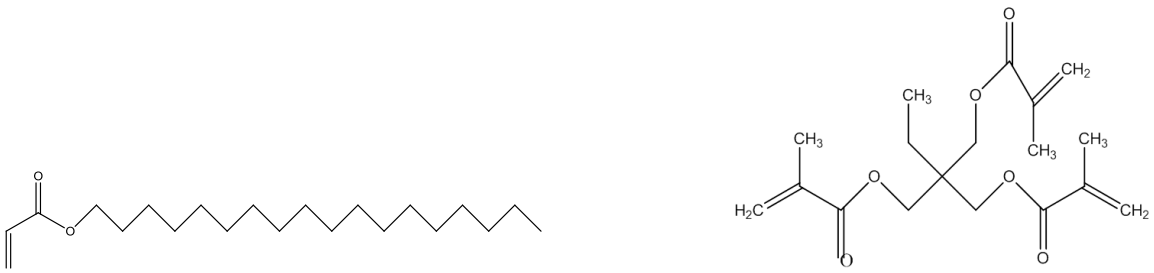

Figure 1. *Chemical structures of the monomer (A) ODA, and (B) the crosslinker TRIM.*

A series of ODA/TRIM monolithic compositions were tested and an optimized column suitable for the separation of alkyl benzene and proteins was identified. MWCNTs were added to the monolith which shows optimum performance for RPC of proteins. Different polymerization mixtures were prepared by changing the type and amount of nanotube added to the polymerization mixture. The monoliths were tested using mixture of standard proteins.

Chromatographic conditions

To achieve a good retention for small molecules, the polarity of the mobile phase must be adjusted by changing its composition. Different compositions of ACN/H_2O with 0.1% of TFA were used for the reversed phase separation. The proteins were analyzed using linear gradient of ACN from 0% - 75 % within 12 min. The alkylbenzenes were analyzed on the series of ODA/TRIM RPC columns using isocratic elution. All samples were prepared by dissolving the solutes in the mobile phase and were injected *via* a 20 μL sample loop. Isocratic separation of small molecules and linear gradient for proteins were carried out at flow rate of 1 mL/min.

TABLE 1

COMPOSITION OF MONOLITHS INTRODUCED AND EVALUATED IN THIS STUDY

Monolith #	Monolithic composition			
	Monomer (% w/w) / Cross-linker (% w/w)	Porogen (% w/w)	MWCNTs (mg)	Temp and Time
M1	ODA (7%) / TRIM (14.5 %)	Cyclohexanol (54.3%) Ethylene Glycol (21%) Water (3.2%)	0	60 ^{o}C for 15 h
M2		Cyclohexanol (53.58%) Ethylene Glycol (21.8%) Water (3.2%)		
M3		Cyclohexanol (52.4%) Ethylene Glycol (22.9%) Water (3.2%)		

M4	ODA (7%) / TRIM (14.5%)	Cyclohexanol (51.5%) Ethylene Glycol (23.8%) Water (3.2%)	0	60 °C for 15 h
M5		Cyclohexanol (50.5%) Ethylene Glycol (24.8%) Water (3.2%)		
M6	ODA (7.9%) /TRIM (13.6 %)	Cyclohexanol (52.4%) Ethylene Glycol (22.9%) Water (3.2%)		
M7	ODA (7%) /TRIM (14.5 %)		SN 2302 150 mg	
M8			SN 2302 25 mg	
M9			SN 2302 18 mg	
M10			SN 2302 12 mg	
M11			SN 2302 8 mg	
M12			SN 6957838 18 mg	
M13			SN 6957838 12mg	
M14			SN 6957838 8mg	

Results and discussion

Column fabrication and RPC characterization

Porogens and monomer composition. The monolithic RPC column was developed by optimizing previously developed and tested monolith in our laboratory for CEC [32]. This involved the adjustment of its characteristics to be suitable for use in HPLC. First, the original monolith was tested using the optimal composition described by Karenga and El Rassi [32]. This monolith was designated as M1column, see Table 1, which is the optimum column for CEC for the separation of proteins and alkyl benzenes, see Fig. 1. The M1 column which was fabricated in the presence of the porogens cyclohexanol and ethylene glycol at 54.2-wt % and 20.9-wt%, respectively, showed low permeability and in turn exhibited high pressure. The column did not show good separation efficiency for alkyl benzenes. This may be due to the high mass transfer resistance in small pores as it was manifested by the relatively high backpressure observed with the column. In order to increase the size of the pores, the porogen composition was changed as in M2, see Table 1. This composition did not show much improvement in terms of protein or alkyl benzene separations. Therefore, further decrease in the cyclohexanol concentration and increase in the concentration of ethylene glycol were necessary. The M3 column showed narrower peaks for proteins than all other columns investigated, but was not the optimum for the AB separation. It yielded higher retention time for alkyl benzenes but did not show efficient peaks. Similarly, we tested the M4 and M5 columns. Proteins were separated efficiently using the M3 column while the M4 column showed enhanced separation for

alkylbenzenes. Since for this series of columns, the porogen composition was changed while keeping that of the monomer constant, the only change would be the morphology of the resulting monoliths. As a result, the monolithic columns yielded similar retention times for proteins. The M3 column showed enhanced separation of proteins, which indicates that it has a relatively larger pore size thus providing easy accessibility for proteins and consequently greater separation efficiency. The other monoliths M1, M2, M4 and M5 were identified as not suitable for the separation of proteins as they showed lower separation efficiency. The M4 column was ideal for the separation of alkyl benzenes. These results indicate that M4 column has narrower channels or smaller pores, and therefore, it easily accessible for small molecules such as alkyl benzenes.

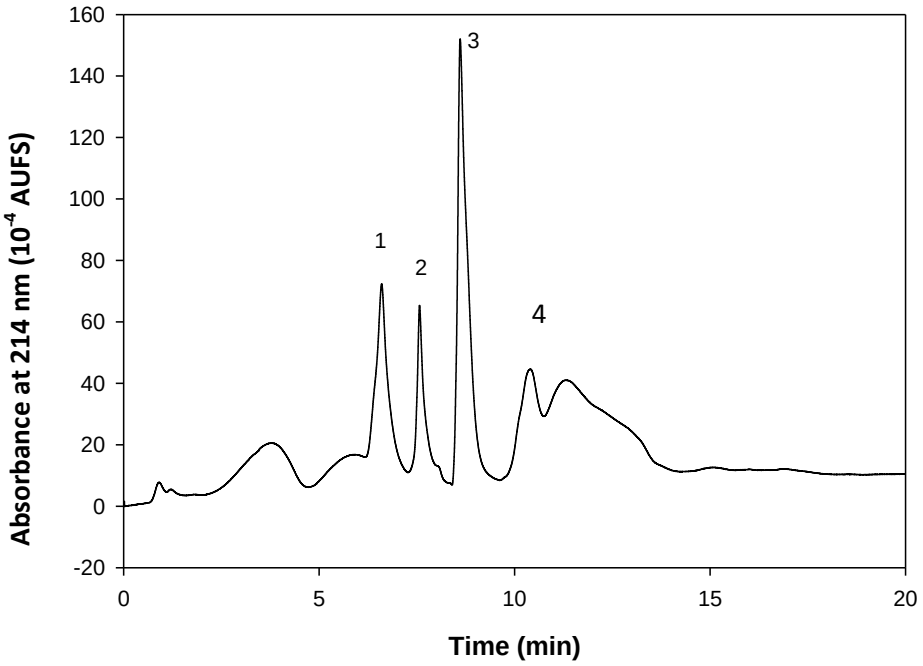

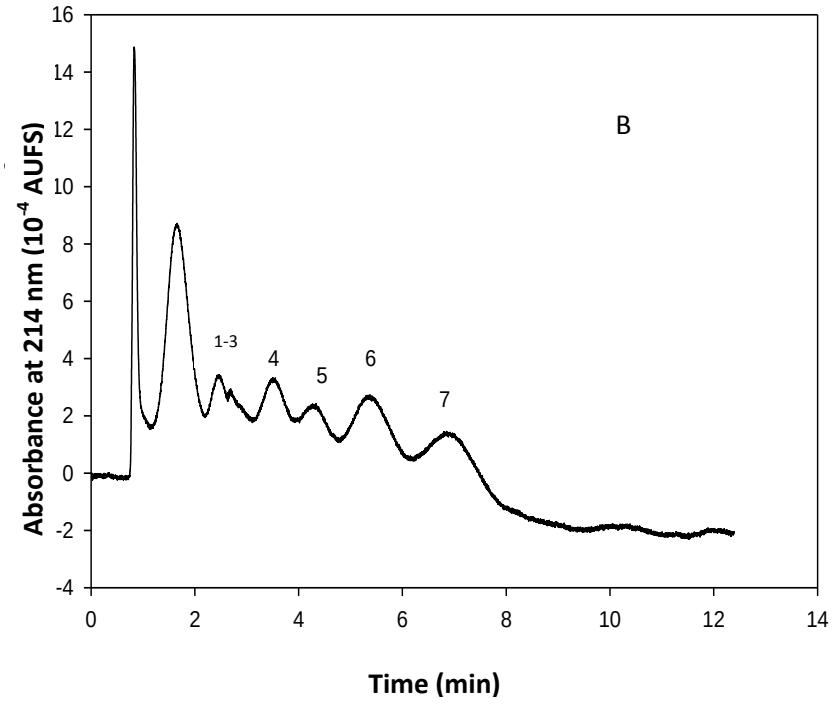

Figure 2. *Chromatograms of standard proteins (A) and alkyl benzenes (B) injected on the M1 column. Proteins were analyzed using a linear ACN gradient while alkyl benzenes were analyzed using isocratic elution. (A) Linear ACN gradient was carried out by increasing ACN from 0-75% of mobile phase B in 12 min. Mobile phase A consisted of H_2O/ ACN (95:5 v/v) containing 0.1% TFA and the mobile phase B consisted of ACN/H_20 (95:5 v/v) containing 0.1% TFA (B): Mobile phase, ACN: H_2O (65:35 v/v) containing 0.1% TFA. Solutes in A: (1), ribonuclease A; (2), cytochrome C; (3), bovine serum albumin; (4), ovalbumin; Solutes in B: (1), toluene; (2), ethylbenzene; (3), propylbenzene; (4), butylbenzene; (5), amylbenzene; (6), hexylbenzene; (7),heptylbenzene. Column dimensions 10 cm x 4.6 mm id; flow rate, 1 mL/min.*

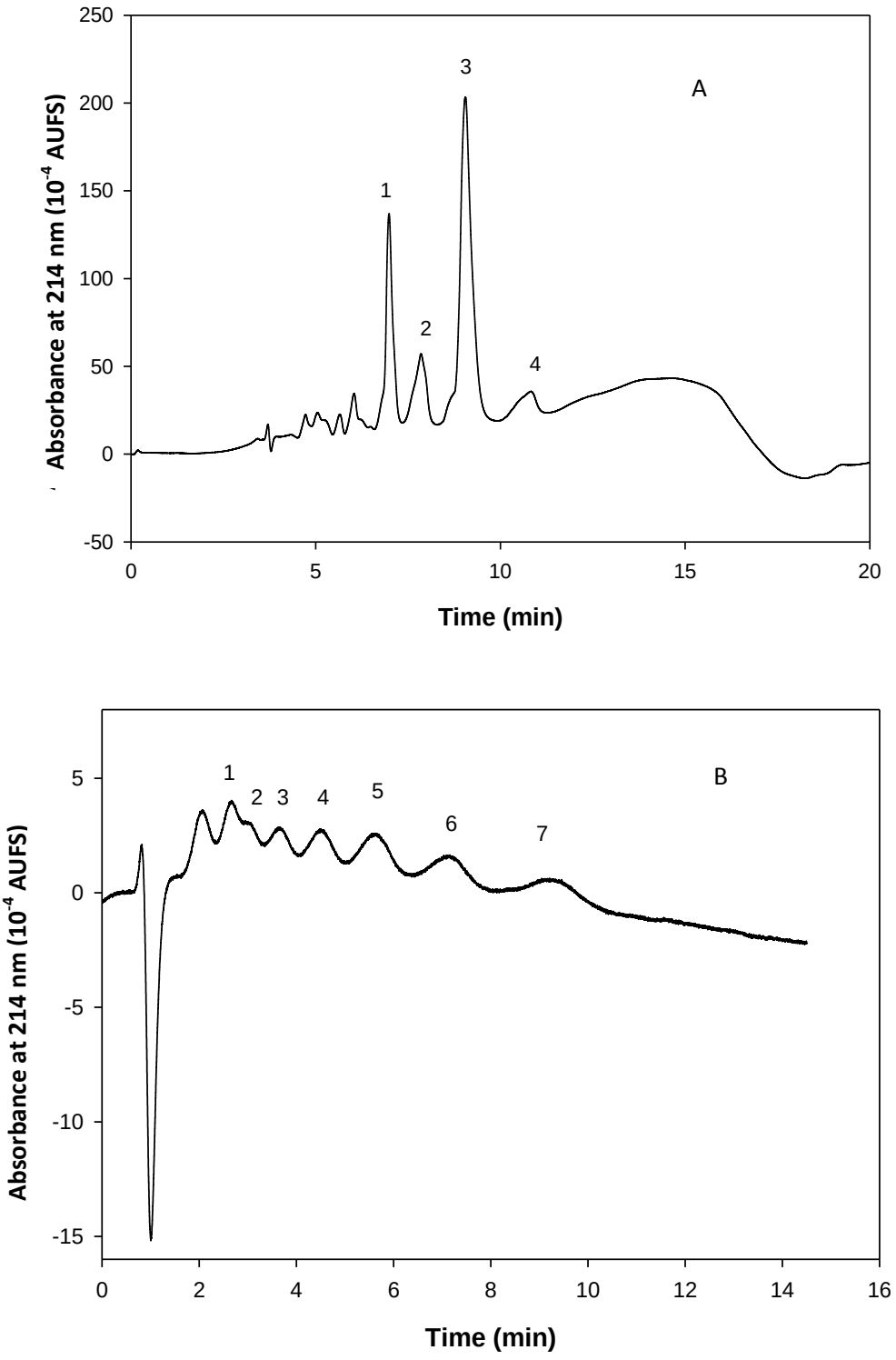

Figure 3. *Chromatograms of standard proteins (A) and alkyl benzenes (B) obtained on the M2 column. All other conditions are as in Fig. 2.*

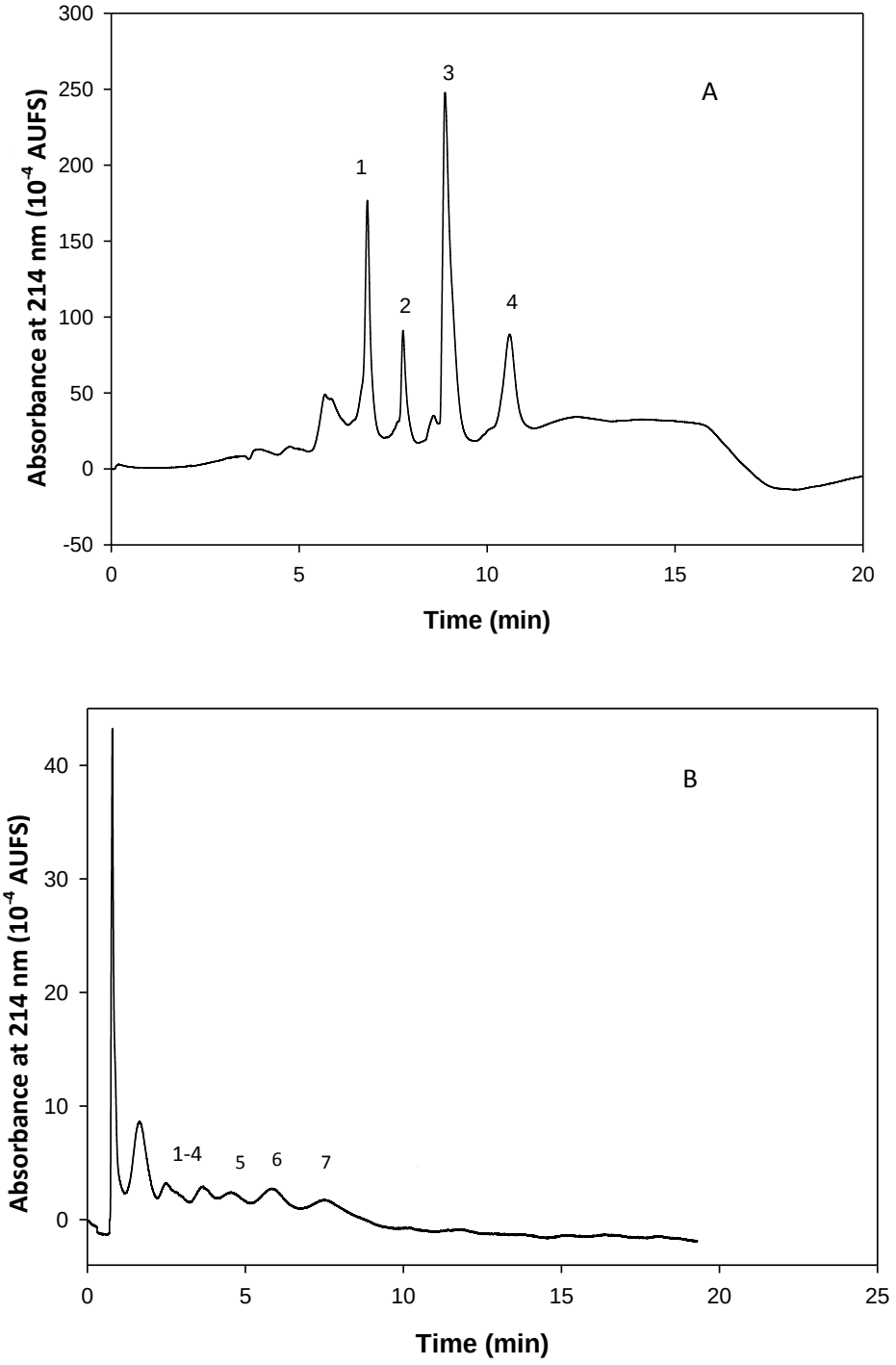

Figure 4. *Chromatograms of standard proteins (A) and alkylbenzenes (B) obtained on the M3 column. All other conditions are as in Fig. 2.*

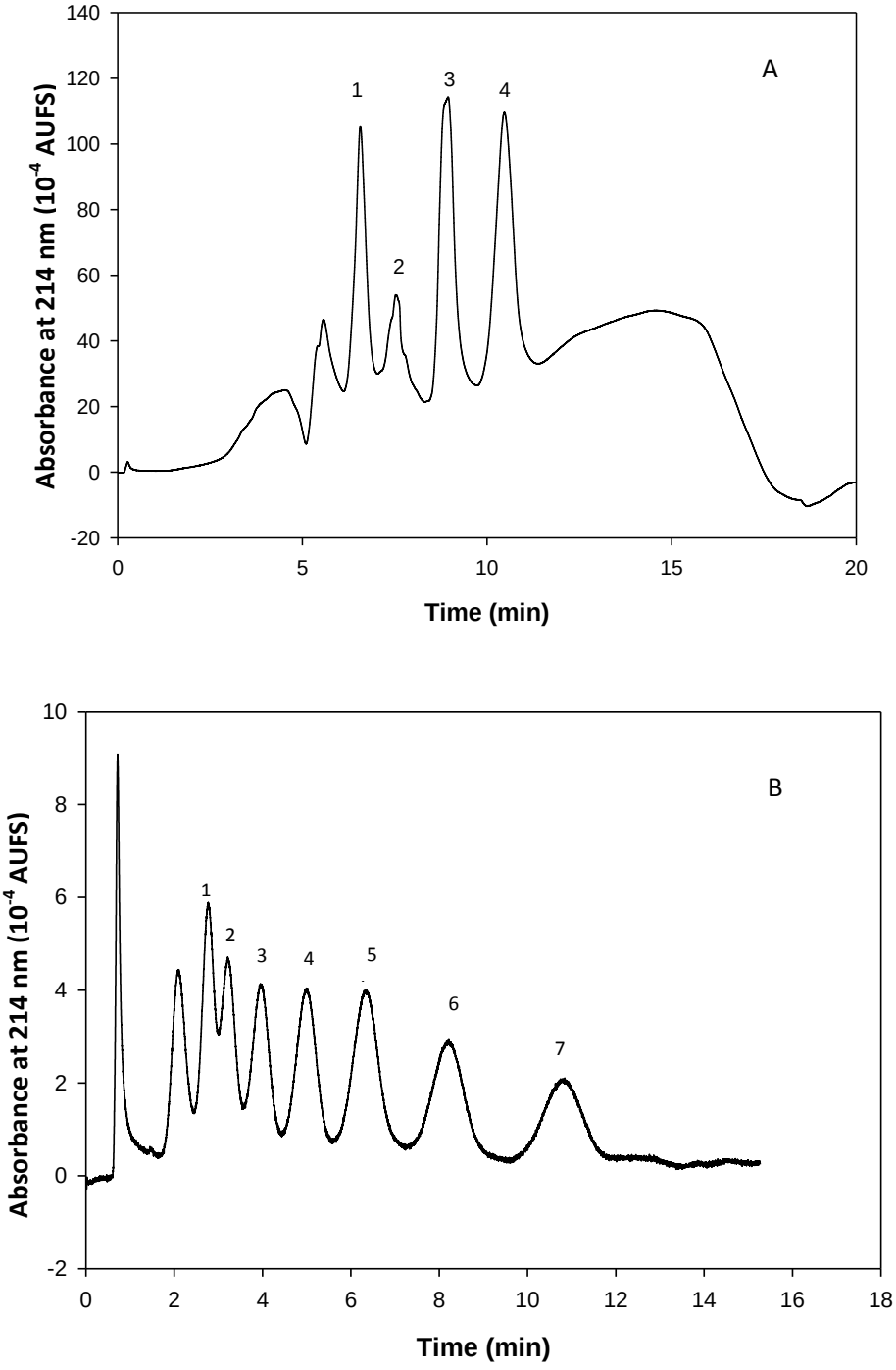

Figure 5. *Chromatograms of standard proteins (A) and alkylbenzenes (B) obtained on the M4 column. All other conditions are as in Fig. 2.*

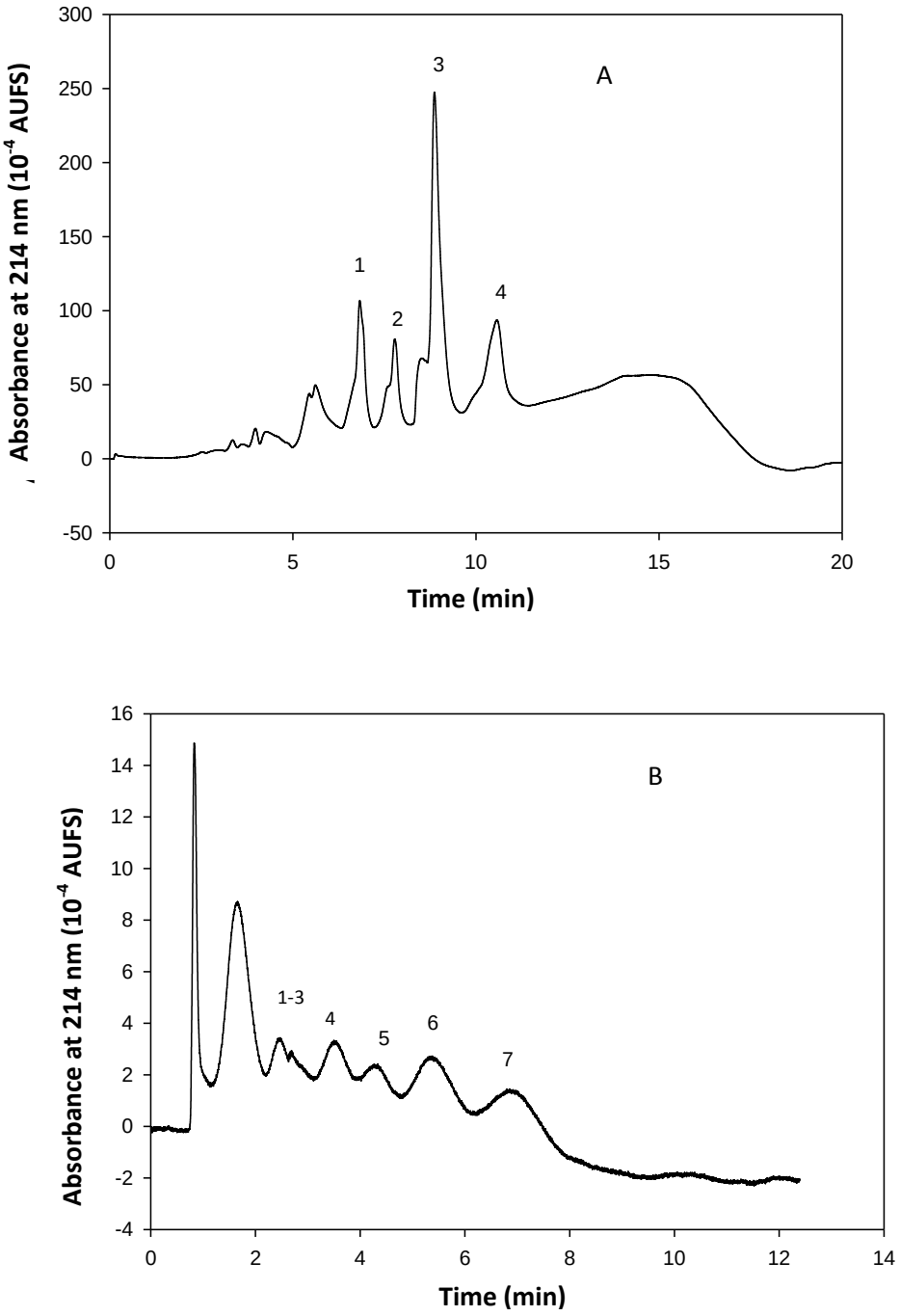

Figure 6. *Chromatograms of standard proteins (A) and alkylbenzenes (B) obtained on the M5 column. All other conditions are as in Fig. 2.*

Alkyl benzenes. Alkyl benzenes were chromatographed on the series of ODA/TRIM RPC columns, namely the M1-M5 monoliths, and the retention behavior was evaluated, see Table 2. It was observed that the k' values gradually increased from the M1 to the M4 column while decreasing the cyclohexanol content from 54.2-wt%-51.2-wt% and increasing the ethylene glycol from 20.9-wt%-23.6-wt% in the porogen. For the M4 column, the k' reached an optimum value and then decreased on the M5 column, see Fig. 7. This may indicate that the M4 column contains an ideal pore sizes for the separation of alkyl benzenes.

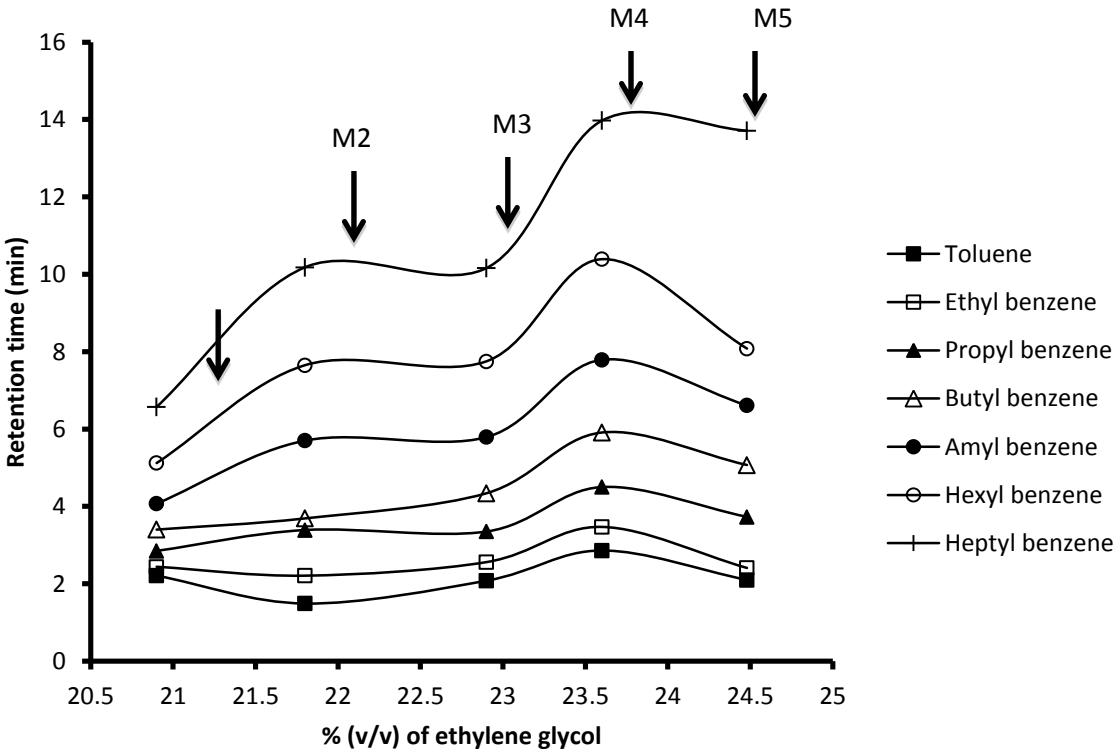

Figure 7. *Retention behavior of alkylbenzenes on the series of the RPC columns*

Since the M4 column showed the best performance for alkylbenzenes, the retention behavior of alkylbenzenes was evaluated on the M4 column while changing the ACN

concentration in the mobile phase from 65% - 80% (v/v), see Fig. 8. It can be seen that while increasing the organic content of the mobile phase, the log k' of ABs decreased. This indicates that upon decreasing the polarity of the mobile phase the k' values decreased which is the normal RPC behavior. This data indicate that the M4 column is suitable for RPC of small molecules.

Evaluation of ODA/TRIM RPC columns with proteins

A mixture of four standard proteins was injected onto the series of RPC columns and the retention times were measured, see Fig. 9. Each proteins show relatively similar retention times on this series of RPC columns using a linear ACN gradient.

TABLE 2

ANALYSIS OF ALKYL BENZENES THROUGH SERIES OF RP COLUMNS

Column		Thio urea	Toluene	Ethyl-benzene	Propyl - benzene	Butyl - benzene	Amyl - benzene	Hexyl-benzene	Heptyl benzene
M1	t_r	0.89	2.21	2.44	2.85	3.4	4.07	5.12	6.57
	k'		1.45	1.71	2.16	2.78	3.5	4.7	5.67
M2	t_r	0.83	2.07	2.67	3.67	4.52	5.62	7.18	9.28
	k'		1.49	2.21	3.39	3.69	5.7	7.65	10.18
M3	t_r	0.83	2.56	2.96	3.61	4.44	5.56	7.03	9.27
	k'		2.08	2.56	3.35	4.34	5.79	7.75	10.16
M4	t_r	0.71	2.78	3.22	3.96	4.98	6.33	8.2	10.78
	k'		2.86	3.47	4.5	5.91	7.79	10.39	13.97
M5	t_r	0.78	2.42	3.05	3.71	4.74	5.94	7.65	11.48
	k'		2.1	2.41	3.73	5.07	6.61	8.08	13.71

The columns were generated from the polymerization mixtures with constant monomer composition but at different porogen content. Therefore, it is believed that it will affect only the size of the channels thus generating relatively similar retention time for proteins.

Testing M3 column with proteins. The M3 column was further evaluated with several other standard proteins to explore its potentials in resolving complex protein mixtures using the linear ACN gradient.

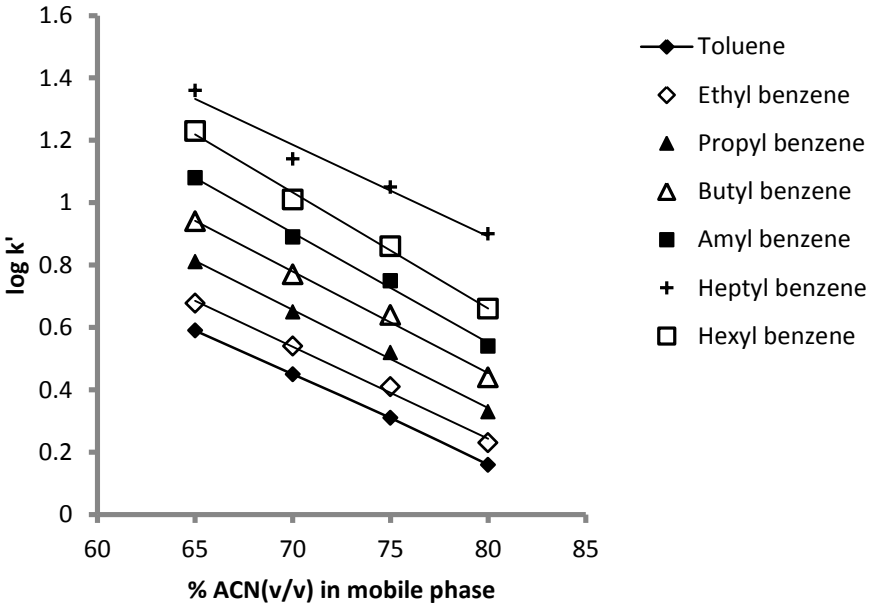

Figure 8. *Log k' of alkylbenzenes versus the % (v/v) ACN in the mobile phase.*

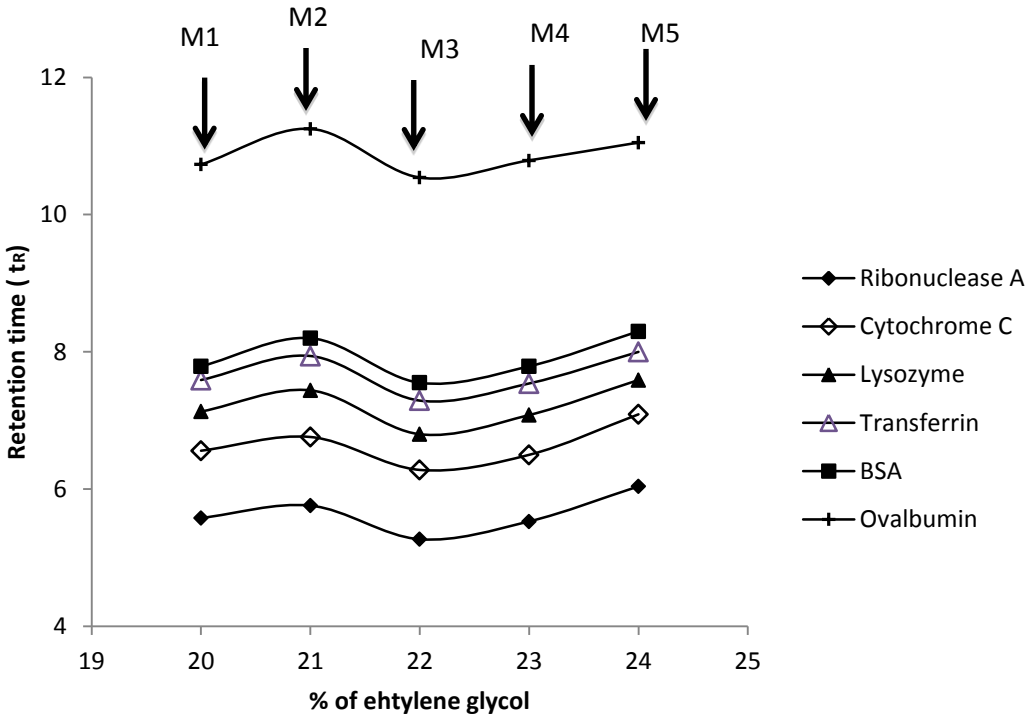

Figure 9. *Retention time of the standard proteins obtained on the RPC columns*

As shown in Fig. 10, the column was able to successfully separate 7 proteins including ribonuclease A, cytochrome C, lysozyme, transferrin, BSA, lactalbumin A and ovalbumin with the retention times of 6.8, 7.72, 8.14, 8.54, 8.82, 9.27 and 10.5 min, respectively. When comparing the elution order of the proteins in Fig. 10, the typical RPC behavior was obtained on the M3 column. Ribonuclease A and cytochrome C are hydrophilic proteins with relatively low molecular weights of 12, 200 and 13, 500, respectively, and therefore, they are expected to elute faster than other proteins. Other proteins having higher molecular weights such as BSA, β-lactoglobulin A, ovalbumin are hydrophobic proteins and consequently exhibit more hydrophobic interactions with the

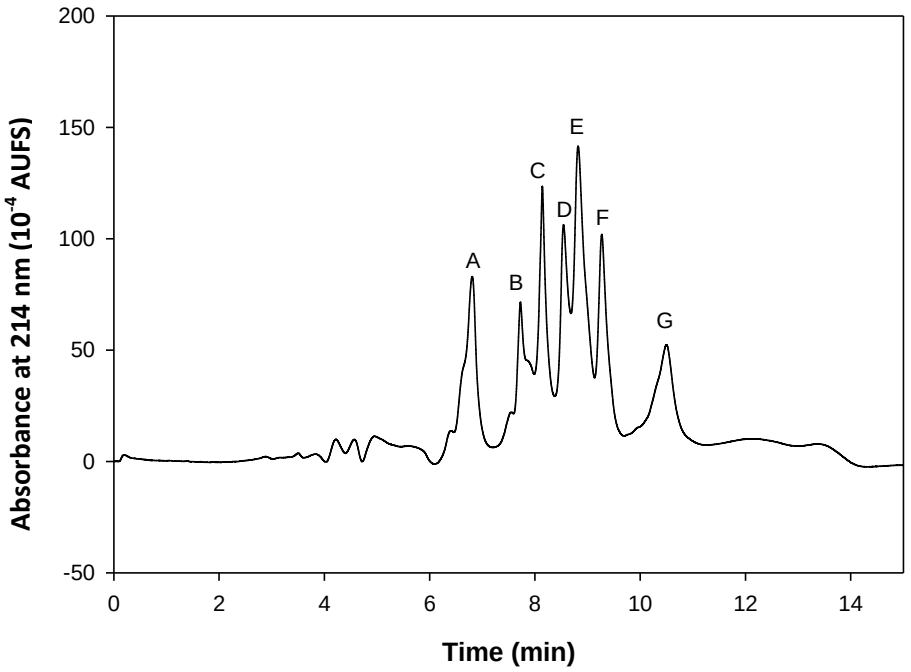

Figure 10. *Separation of standard proteins using linear ACN gradient on the M3 column. Solutes A, ribonuclease A; B, cytochrome C, lysozyme; D, transferrin; E, BSA; F, β-lactoglobulin A; D, ovalbumin. All the other conditions as in Fig. 2A.*

M3 monolithic stationary phase leading to more retention for these three proteins. Even though it has higher molecular weight than ovalbumin and β-lactoglobulin A, BSA eluted faster than these two proteins. Similarly, despite the fact that ribonuclease A has a higher molecular weight than cytochrome C it eluted faster. This observation for RPC retention indicates that the protein hydrophobicity or its size are not the only factors determining the retention of the solutes, since proteins can undergo denaturation in a hydro-organic mobile phase. The acid and organic solvent in the mobile phase partially denature the proteins, thereby exposing the more hydrophobic interiors. Therefore, the proteins with

more hydrophilic exteriors, such as cytochrome C exhibited a larger degree of hydrophobicity and interacted were strongly with the monolithic column [18, 20, 33].

Reproducibility of the M3 column using a mixture of standard proteins

Standard proteins were injected in triplicates onto the M3 column and the reproducibility of the retention time and peak areas were evaluated in terms of % RSD of solute retention and peak area, see Tables 2 and 3. The M3 column showed % RSD in terms of retention time of less than 1 for all 4 standard proteins studied, see Table 3. Regarding peak area, the % RSD for ribonuclease A, cytochrome C, BSA, ovalbumin were 20.48, 18.92, 3.62 and 5.82, respectively, see Table 4. The column showed good reproducibility in terms of retention time, but it showed deviation in peak area. This could be due to the minor fluctuations in sample preparation, such as sonication time amount weighted and storage.

TABLE 3

REPRODUCIBILITY OF RETENTION TIME (t_R) EXPRESSED IN %RSD

Protein	Retention time t_R (min)			Mean value of t_R	% RSD
	Trial 1	Trial 2	Trial 3		
Ribonuclease A	6.8	6.87	6.8	6.823	0.59
Cytochrome C	7.76	7.73	7.81	7.767	0.52
BSA	8.88	8.85	8.79	8.84	0.52
Ovalbumin	10.6	10.54	10.44	10.52	0.77

TABLE 4

REPRODUCIBILITY OF PEAK AREA ON M3 COLUMN EXPRESSED IN %RSD

	Area of the peak AP(mV)			Mean value of AP	
	Trial1	Trial 2	Trial 3		% RSD
Ribonuclease A	2346	2201	2873	2807	20.48
Cytochrome C	2058	3022	2699	2593	18.92
BSA	5034	4941	5296	5090	3.62
Ovalbumin	4431	4738	4979	4716	5.82

Incorporation of carbon nanotubes into the M3 monolithic column

The M3 column, which showed the best performance for the separation of proteins was further optimized by incorporating MWCNTs. The M3 monolith is a hydrophobic monolith and proved useful for RPC separation [32]. Carbon nanotubes are carbon allotropes with cylindrical structure and they are hydrophobic in nature [34]. The goal of adding MWCNTs to the monolith was to increase the hydrophobic nature of the monolith, thereby increasing the retention time of the solutes of interest. In addition to hydrophobic interactions, MWCNTs may establish π–π interactions with aromatic and π-bond rich solutes. On this basis, it was expected to enhance retention and in turn resolution of some solutes with the addition of MWCNTs to the M3 column.

In this section, a series of columns prepared by adding different types and amounts of MWCNTs, see Table 1. The M7 monolith was the first monolith fabricated with added MWCNTs, where 150 mg of SN3202 MWCNTs was added. The polymerization mix was very thick in appearance and the resulting monolith showed very high pressure. It did not yield any separation for proteins or alkyl benzenes. This may

indicate that, since the monolith contained a large amount of nanoparticles it blocked the pores, thereby decreasing the permeability of the monolith leading to poor flow and finally resulting in high pressure. From the M8 to the M11 monolith, we decreased the amount of SN3202 type of MWCNTs. The column performance improved in terms of pressure and also showed improved separation of proteins. Since by decreasing the amount of SN2302 MWCNTs some improvements were observed, the amount of MWCNTs was further decreased from 150 mg to 8 mg. For this series of monoliths, an enhanced performance was obtained for the M11 monolith, which was prepared by adding 8 mg of MWCNTs (see Fig 11A). By considering the physical properties of SN3202 MWCNTs, it had an outer diameter (OD) of 10-20 nm, inner diameter (ID) 5-10 nm with a length of 0.5-2 μm. Considering the characteristics of SN 6957838 MWCNTs, with the physical properties of an OD of 20-30 nm, an ID of 5-10 nm and a length of 1-2 μm, it was expected that the second MWCNTs having a larger OD expose more surface area to interact with the solute, thereby leading to an increase in retention. Monoliths were prepared by adding different amounts of 25 mg, 12.5 mg and 8 mg of SN6957838 MWCNTs, and the resulting monoliths were designated as M12, M13 and M14, respectively. It was observed that the optimum separation was achieved with the monolith containing 12.5 mg of MWCNTs, see Fig. 11B. The retention behavior of alkylbenzenes was evaluated on the series of monoliths, but a better separation than that obtained on the M4 column in terms of retention factor for alkylbenzenes could not be achieved. It is believed that M4 column has the ideal pore size for the separation of alkylbenzenes, see Table 5.

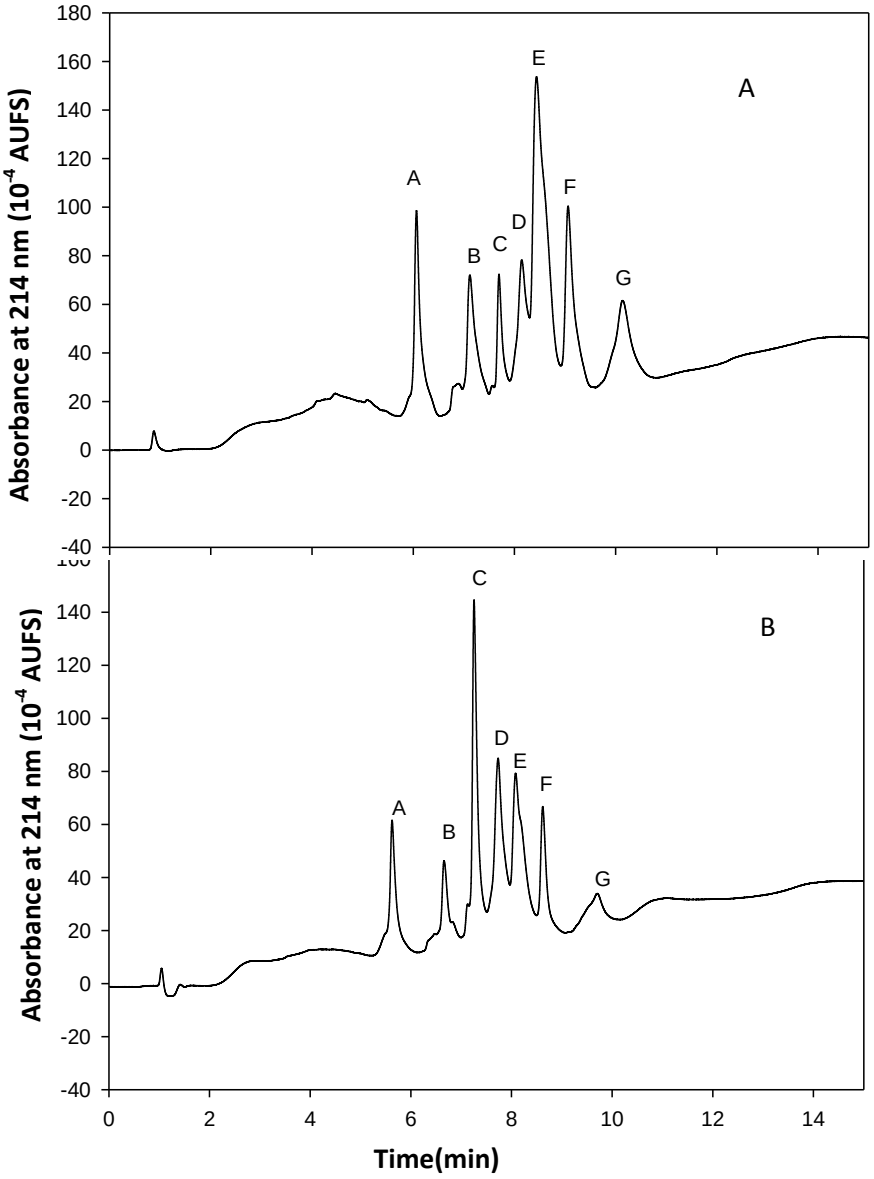

Figure 11. *Chromatograms of proteins obtained on (A) M11 and (B) M13 columns using a linear ACN gradient. Solutes (A), ribonuclease A; (B),cytochrome C; (C), lysozyme; (D),transferrin; €, BSA; F, lactoglobulin A; (G), ovalbumin. All other conditions as in Fig. 2A.*

Alkylbenzenes were less retained in the RPC column with the addition of MWCNTs. This may indicate that MWCNTs filled the pore structure to the point that the surface area available for alkyl benzenes interaction was reduced. Therefore, they eluted faster. On the other hand, the addition of MWCNTs to the monolith yielded enhanced performance for proteins mainly because MWCNTs have hydrophobic interactions and $\pi-\pi$ interactions with the proteins. Nanoparticles help to increase the retention time and also results in efficient separation with higher resolution, see Table 6.

TABLE 5

RETENTION FACTOR OF ALKYLBENZENES ON THE RPC COLUMNS

Alkyl benzenes	Retention factor of monolithic columns							
	M4	M8	M9	M10	M11	M12	M13	M14
Toluene	2.08	1.05	1.81	1.88	1.92	1.7	1.92	1.75
Ethyl benzene	2.56	1.26	1.95	1.91	2.0	1.81	2.0	1.92
Propyl benzene	3.35	1.69	2.45	2.57	3.05	2.4	3.05	2.4
Butyl benzene	4.34	2.11	2.91	3.18	3.97	2.8	3.97	3.1
Amyl benzene	5.79	2.83	3.25	4.425	5.22	3.12	5.22	3.97
Hexyl benzene	7.75	5.03	5.75	5.72	6.3	4.9	6.3	5.21
Heptyl benzene	10.16	5.21	7.27	7.63	7.9	7.1	7.9	7.5

TABLE 6

RETENTION FACTOR OF PROTEINS OBTAINED ON THE RPC COLUMNS

Proteins	Retention time of monolithic columns						
	M3	M9	M10	M11	M12	M13	M14
Ribonuclease A	5.85	5.92	5.97	6.06	6.14	5.63	6.05
Cytochrome C	6.82	7.02	7.0	7.12	6.9	6.66	7.07
Lysozyme	7.39	7.62	7.65	7.69	7.83	7.26	7.66
Transferrin	7.9	8.09	8.1	8.14	8.22	7.73	8.1
BSA	8.08	8.46	8.3	8.44	8.64	8.07	8.43
Carbonic anhydrase	8.51	8.93	8.7	9.06	9.06	8.6	9.02
ovalbumin	9.71	9.99	9.5	10.14	9.9	9.7	10.02

Conclusions

The ODA/TRIM column was successfully scaled up/optimized for use in RPC separations by HPLC. A series of monolithic columns was developed and the performance of each column was evaluated with alkylbenzenes and standard proteins. The M3 column showed optimum performance towards proteins while M4 column yielded better separation for alkylbenzenes. The addition of MWCNTs to the M3 monolith generally resulted in enhanced separation for proteins. The M13 column, which was prepared by adding 12.5 mg of SN 6957838 MWCNTs to the M3 monolith showed an optimum performance for the separation of a mixture of standard proteins. The enhanced separation of protein after addition of MWCNTs is believed to be due to the concurrence of both hydrophobic and $\pi-\pi$ interactions. Therefore, the M13 column was used in the RPC fractionation of complex proteomics samples in the subsequent chapters of this dissertation.

References

1. Núñez, O., T. Ikegami, W. Kajiwara, K. Miyamoto, K. Horie, and N. Tanaka, *Preparation of high efficiency and highly retentive monolithic silica capillary columns for reversed-phase chromatography by chemical modification by polymerization of octadecyl methacrylate.* J. Chromatogr. A, 2007. **1156**. 35-44.
2. Svec, F. and J.M.J. Fréchet, *Molded Rigid Monolithic Porous Polymers: An Inexpensive, Efficient, and Versatile Alternative to Beads for the Design of Materials for Numerous Applications.* Ind. Eng. Chem. Res., 1998. **38**(1): p. 34-48.
3. Guiochon, G., *Monolithic columns in high-performance liquid chromatography.* J. Chromatogr. A, 2007. **1168**(1–2): p. 101-168.
4. Hjertén, S., J.-L. Liao, and R. Zhang, *High-performance liquid chromatography on continuous polymer beds.* J. Chromatogr. A, 1989. **473**(0): p. 273-275.
5. Cabrera, K., *Applications of silica-based monolithic HPLC columns.* J. Sep. Sci., 2004. **27**(10-11): p. 843-852.
6. Núñez, O., K. Nakanishi, and N. Tanaka, *Preparation of monolithic silica columns for high-performance liquid chromatography.* J. Chromatogr. A, 2008. **1191**(1–2): p. 231-252.
7. Motokawa, M., H. Kobayashi, N. Ishizuka, H. Minakuchi, K. Nakanishi, H. Jinnai, K. Hosoya, T. Ikegami, and N. Tanaka, *Monolithic silica columns with various skeleton sizes and through-pore sizes for capillary liquid chromatography.* J. Chromatogr. A, 2002. **961**(1): p. 53-63.

8. Minakuchi, H., K. Nakanishi, N. Soga, N. Ishizuka, and N. Tanaka, *Effect of domain size on the performance of octadecylsilylated continuous porous silica columns in reversed-phase liquid chromatography.* J. Chromatogr. A, 1998. **797**(1–2): p. 121-131.

9. Gusev, I., X. Huang, and C. Horváth, *Capillary columns with in situ formed porous monolithic packing for micro high-performance liquid chromatography and capillary electrochromatography.* J. Chromatogr. A, 1999. **855**, 273-290.

10. Petro, M., F. Svec, and J.M.J. Fréchet, *Immobilization of trypsin onto "molded" macroporous poly(glycidyl methacrylate-co-ethylene dimethacrylate) rods and use of the conjugates as bioreactors and for affinity chromatography.* Biotechnol. Bioeng., 1996. **49**(4): p. 355-363.

11. Wang, Q.C., F. Svec, and J.M.J. Frechet, *Macroporous polymeric stationary-phase rod as continuous separation medium for reversed-phase chromatography.* Anal. Chem., 1993. **65**(17): p. 2243-2248.

12. Mohammad, J., B. Jäderlund, and H. Lindblom, *New polymer-based prepacked column for the reversed-phase liquid chromatographic separation of peptides over the pH range 2–12.* J. Chromatogr. A, 1999. **852**(1): p. 255-259.

13. Tisch, T.L., R. Frost, J.-L. Liao, W.-K. Lam, A. Remy, E. Scheinpflug, C. Siebert, H. Song, and A. Stapleton, *Biochemical separations by continuous-bed chromatography.* J. Chromatogr. A, 1998. **816**(1): p. 3-9.

14. Xie, S., F. Svec, and J.M.J. Fréchet, *Rigid porous polyacrylamide-based monolithic columns containing butyl methacrylate as a separation medium for the*

rapid hydrophobic interaction chromatography of proteins. J. Chromatogr. A, 1997. **775**(1–2): p. 65-72.

15. Oberacher, H. and C.G. Huber, *Capillary monoliths for the analysis of nucleic acids by high-performance liquid chromatography–electrospray ionization mass spectrometry*. TrAC., 2002. **21**(3): p. 166-174.
16. Rigobello-Masini, M., J. Penteado, and J. Masini, *Monolithic columns in plant proteomics and metabolomics.* Anal. Bioanal. Chem., 2013. **405**(7): p. 2107-2122.
17. Unger, K.K. and A.I. Liapis, *Adsorbents and columns in analytical high-performance liquid chromatography: A perspective with regard to development and understanding.* J. Sep. Sci., 2012. **35**(10-11): p. 1201-1212.
18. Goheen, S.C. and S.C. Engelhorn, *Hydrophobic interaction high-performance liquid chromatography of proteins.* J. Chromatogr. A, 1984. **317**(0): p. 55-65.
19. Glajch, J.L., J.J. Kirkland, and J. Köhler, *Effect of column degradation on the reversed-phase high-performance liquid chromatographic separation of peptides and proteins.* J. Chromatogr. A, 1987. **384**(0): p. 81-90.
20. Moore, R.M. and R.R. Walters, *Protein separations on reversed-phase high-performance liquid chromatography minicolumns.* J. Chromatogr. A, 1984. **317**(0): p. 119-128.
21. Kennedy, J.F., G.O. Phillips, P.A. Williams, T. Cellucon, and C. Cellucon, *Cellulosics: materials for selective separations and other technologies*. 1993, New York: Ellis Horwood.

22. Sinner, F. and M.R. Buchmeiser, *A New Class of Continuous Polymer Supports Prepared by Ring-Opening Metathesis Polymerization: A Straightforward Route to Functionalized Monoliths.* Macromolecules, 2000. **33**(16): p. 5777-5786.

23. Sinner, F.M. and M.R. Buchmeiser, *Ring-Opening Metathesis Polymerization: Access to a New Class of Functionalized, Monolithic Stationary Phases for Liquid Chromatography.* Angew. Chem int. Ed, 2000. **39**(8): p. 1433-1436.

24. Xie, S., R.W. Allington, F. Svec, and J.M.J. Fréchet, *Rapid reversed-phase separation of proteins and peptides using optimized 'moulded' monolithic poly(styrene–co-divinylbenzene) columns.* J. Chromatogr. A, 1999. **865**;169-174.

25. Sun, X., T. Chen, Z. Yang, and H. Peng, *The Alignment of Carbon Nanotubes: An Effective Route To Extend Their Excellent Properties to Macroscopic Scale.* Accounts Chem. Res., 2012. **46**(2): p. 539-549.

26. Svec, F., *Quest for organic polymer-based monolithic columns affording enhanced efficiency in high performance liquid chromatography separations of small molecules in isocratic mode.* J. Chromatogr. A, 2012. **1228**(0): p. 250-262.

27. Zhou, C., Z. Du, G. Li, Y. Zhang, and Z. Cai, *Oligomers matrix-assisted dispersion of high content of carbon nanotubes into monolithic column for online separation and enrichment of proteins from complex biological samples.* Analyst, 2013. **138**(19): p. 5783-5790.

28. Chambers, S.D., F. Svec, and J.M.J. Fréchet, *Incorporation of carbon nanotubes in porous polymer monolithic capillary columns to enhance the chromatographic separation of small molecules.* J. Chromatogr. A, 2011. **1218**(18): p. 2546-2552.

29. Claude Guillaume, Y. and C. André, *Fast enantioseparation by HPLC on a modified carbon nanotube monolithic stationary phase with a pyrenyl aminoglycoside derivative.* Talanta, 2013. **115**(0): p. 418-421.

30. Wang, N., S. He, W. Yan, and Y. Zhu, *Incorporation of multiwalled carbon nanotube into a polymethacrylate-based monolith for ion chromatography.* J. Appl. Poly. Sci., 2013. **128**(1): p. 741-749.

31. Okanda, F.M. and Z. El Rassi, *Capillary electrochromatography with monolithic stationary phases. 4. Preparation of neutral stearyl – acrylate monoliths and their evaluation in capillary electrochromatography of neutral and charged small species as well as peptides and proteins.* Electrophoresis, 2005. **26**(10): p. 1988-1995.

32. Karenga, S. and Z. El Rassi, *Neutral octadecyl monolith for reversed phase capillary electrochromatography of a wide range of solutes.* J. Sep. Sci., 2008. **31**(14): p. 2677-2685.

33. Fausnaugh, J.L., L.A. Kennedy, and F.E. Regnier, *Comparison of hydrophobic-interaction and reversed-phase chromatography of proteins.* J. Chromatogr. A, 1984. **317**(0): p. 141-155.

34. Li, S., H. Li, X. Wang, Y. Song, Y. Liu, L. Jiang, and D. Zhu, *Super-Hydrophobicity of Large-Area Honeycomb-Like Aligned Carbon Nanotubes.* J. Phys. Chem. B, 2002. **106**(36): p. 9274-9276.

CHAPTER IV

ONLINE DEPLETION OF HIGH ABUNDANCE PROTEINS AND CAPTURING OF SIAOGLYCOPROTEINS FROM HUMAN SERA *VIA* TANDEM IMMUNO-, PROTEIN A/G´ AND LECTIN AFFINITY COLUMNS AND SUBSEQUENT FRACTIONATION OF THE CAPTURED PROTEINS ON A REVERSED PHASE COLUMN

Introduction

Sialylation is an important post-translational modification (PTM) of proteins the level of which has been known for decades to be altered in diseases such as cancers. Therefore, the detection of aberrant sialylation of glycoproteins present in the serum should provide an insight into the pathological state of an individual. By measuring the level of this aberration over a time period one can have an idea of the progression of the disease [1]. Increased sialylation of tumor cell surfaces is well known and is due to either increased activity of the sialyltransferase or due to the increased branching of *N*-linked glycans leading to termini, which can be sialylated. Comparing the sialylation level before and after a given treatment one can predict the prognosis of cancer. The detection of sialoglycoproteins in cancer cells remains a major challenge for most qualitative and

quantitative analytical methods of analysis [2]. Sialic acids are found attached at the non-reducing terminus of the glycan moieties of glycoproteins *via* an α-2,3 or α-2,6 linkage to galactosyl residue and Hex-NAc (Hexose-N-acetyl glucosamine). Figure 1 shows the sialic acid moiety attached to the galactosyl residue with an α-2,3 linkage [3].

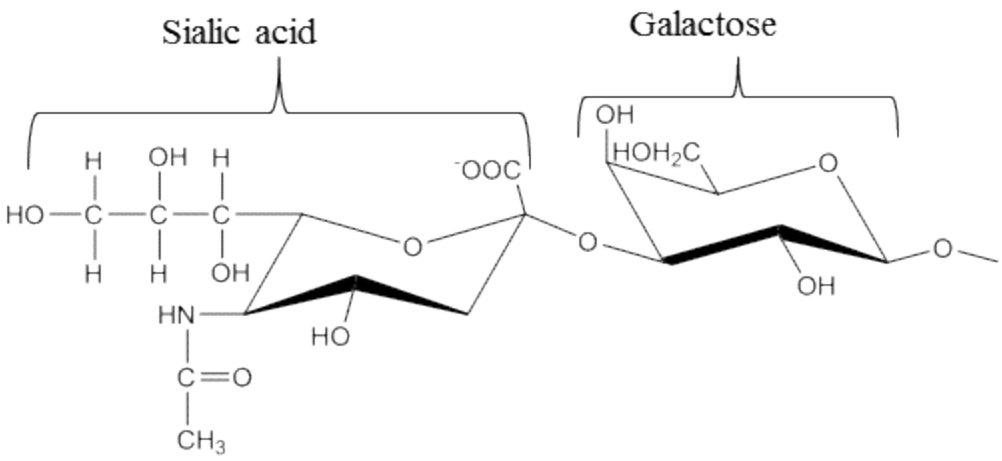

Figure 1. *Sialic acid moiety attached to a galactosyl residue with an α-(2, 3) linkage.*

In this chapter, the main goal is to specifically capture sialoglycoproteins from disease free and breast cancer sera with the aim of identifying their differential expressions in breast cancer serum with respect to disease free serum via liquid chromatography (LC) coupled to tandem mass spectrometry (MS/MS). The selective capturing of sialoglycoproteins has been achieved *via* lectin affinity chromatography (LAC), which involved the development of monolithic columns with surface immobilized lectins specific for sialic acids. Lectins are sugar-binding proteins, which are widely distributed in nature having the ability to recognize carbohydrates on the surface of proteins. In general, LAC has found increased use for capturing glycoproteins from human plasma [4-6] and cell culture lysates [7]. In our current investigation, *Sambucus*

nigra agglutinin (SNA) and *Maackia amurensis* (II) lectin (MAL-II), with complementary specificity to sialic acid bearing glycoproteins [8-10] were immobilized on a novel monolithic stationary phase that was originally introduced in our laboratory for immunoaffinity chromatography at reduced nonspecific interactions [11]. SNA lectin has been reported to show specificity towards sialic acids (Sia) in α–(2,6) linkages to galactose (Gal) or *N*-acetylgalactosamine (GalNAc), e.g., Sia-α2,6-Gal/GalNAc [12]. Figure 2 shows the three *N*-glycans types and the possible binding of SNA lectin to the sialic acid linked by α–(2,6)- linkages to galactose. The preference of the SNA lectin to binding with the α–(2,6) linkage can be attributed to the free hydroxyl group at C-3, which may play an important role in the binding of galactosyl residues to SNA and there is a significant difference between the three-dimensional arrangement of the sialic acid and galactosyl residues in the oligosaccharides containing 2,3- or 2,6-linkages. It is possible that the 2,6-linked isomers can assume a conformation which facilitates better contact with the binding sites of SNA as reported in NMR spectroscopy studies [8].

MAL-II lectin binds with sialic acid (e.g., *N*-acetylneuraminic acid) linked by α–2,3 linkages to galactose with high affinity and shows weak affinity to the *N*-acetylglucosamine (GlcNAc) and *N*-acetylgalactosamine (GalNAc) [9, 10]. Narrow specificity lectins such as SNA and MAL-II recognize and capture disease related glycoproteins and capture fewer plasma proteins than those with broader specificities. Therefore, narrow specificity lectins are attractive selectors for isolating disease specific glycosylated biomarkers [13]. The SNA and MAL-II columns should in principle be useful for the identification of differentially expressed sialoglycoproteins having sialic

acids linked to galactosyl residues with α–(2,6) and α–(2,3) linkages in breast cancer serum with respect to disease free serum.

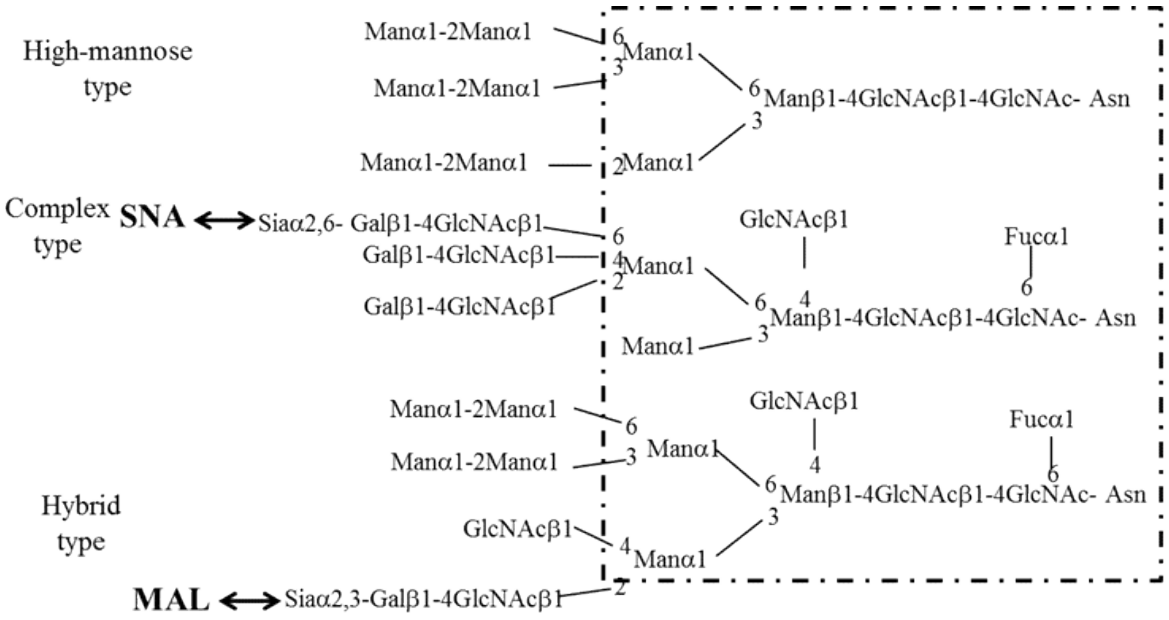

Figure 2. *Typical N-glycans. The structures within the dashed box is the trimannosyl core which is common to all glycan structures. Sialic acid residues linked to galactose in α–(2,6) linkages are shown to bind with SNA lectin.*

Several approaches have been used for the fractionation of complex glycoproteins. For instance, while single LAC is able to capturing a limited number of glycoproteins since most lectins show specificity towards a particular type of glycoproteins, serial LAC (serial-LAC) has been used to identify many types of glycoproteins in human serum [14-16]. However, in serial-LAC, serum fraction that pass through one lectin column as collected, dialyzed, dried and reconstituted and then transferred to the second lectin column, and so on. Although this column arrangement

allows collecting a large number of glycoproteins, it leads to sample loss due to excessive discontinues sample manipulation and experimental biases from column to column. To remedy this situation, multi LAC (M-LAC) has been suggested. M-LAC uses a mixture of lectins having specificities for different glycoproteins immobilized in a given column (i.e., a mixed bed column) and each lectin is eluted using a given haptenic sugar [4, 17]. However, this approach has a limitation due to the fact that the eluted glycoproteins from one lectin may bind again to another lectin in the mixed bed column, a fact that may require much harsher elution conditions such as lowering the pH of the eluting mobile phase. An elegant and effective column arrangement was demonstrated recently by Selvaraju and El Rassi that involved the use of tandem LAC columns with surface immobilized lectins of different selectivities to capture a wide range of glycoproteins form human serum [18, 19].

In this Chapter, tandem LAC consisting of immobilized SNA and MAL-II columns were incorporating into a recently introduced multicolumn platform in our laboratory [6] for the capturing of sialoglycoproteins from disease free and breast cancer sera. The platform was also equipped with an RPC column developed in Chapter III for the on-line fractionation of the sialoglycoproteins captured by the two-lectin columns. Two sets of approaches were examined. In one approach, 3-fold diluted serum was injected into the multicolumn platform without depleting the high abundance proteins (e.g., albumin and immunoglobulins (Ig's)) and in another approach the 3-fold diluted serum was depleted on-line from albumin and Ig's prior to capturing the sialoglycoproteins by the two-lectin columns. The depletion columns consisted of a monolithic stationary phase with surface immobilized anti-human serum albumin

antibody (anti-HSA), Protein A and Protein G´. While the anti-HSA column was for removing albumin, the Protein A and Protein G´ columns were for depleting the Ig's. Captured glycoproteins by SNA and MAL-II columns were fractionated on the RPC column using a linear ACN gradient. Fractions were collected and submitted to LTQ Orbitrap MS for the identification of captured sialoglycoproteins. The multicolumn platform was operated *via* switching valves and high precision HPLC pumps to control and direct the mobile phase through the multi column system and to move the serum from column to column while staying in the liquid phase thus avoiding sample manipulation and sample loss.

Experimental

Instrumentation

A Model 105 IsoTemp water bath from Fischer Scientific (Waltham, MA, USA) was used for the polymerization of monoliths. The liquid chromatography platform consisted of a quaternary solvent delivery system model Q-grad pump from Lab Alliance (State Collage, PA, USA), a solvent delivery system Model CM4000, and a Model 3100 UV-Vis variable wavelength detector from Milton Roy, LDC division (Riviera Beach, FL, USA) and a Rheodyne injector Model 7010 (Cotati, CA, USA) equipped with a 20 μL injection loop. Five Rheodyne switching valves and one 3-way valve was from SSI (State Collage, PA, USA) were used to control the direction of solvent flow. The fraction collector was from Spectra/Chrom CF-1 (Houston, TX, USA). Mass spectrometric analysis was performed using a hybrid LTQ-Orbitrap mass spectrometer from Thermo

Fisher Scientific (Waltham, MA, USA). Sample evaporation was done on a Savant SpeedVac Model AC 110 from Savant Instruments Inc. (Holbrook, NY, USA).

Reagents and Materials

The unconjugated lectins, namely SNA and MAL-II were obtained from Vector Laboratories (Burlingame, CA, USA). Pooled breast cancer serum from five donors and also pooled disease free human serum from five donors (same age group and race as the cancer serum) were purchased from Bioreclamation (Westbury, NY, USA). Stainless steel tubing of 4.6 mm id was obtained from Alltech Associates (Deerfield, IL, USA). TRIM, ODA, GMM, PETA, 1-dodecanol, sodium acetate, sodium periodate, sodium cyanoborohydride, lactose and AIBN were from Aldrich Chemical Co. (Milwaukee, WI, USA). Cyclohexanol was purchased from J.T. Baker (Phillipsburg, NJ, USA). Ethylene glycol was purchased from Fischer Scientific (Waltham, MA, USA). HPLC grade acetonitrile was purchased from Pharmco-Aaper (Farmers Branch, TX, USA).

Monolithic Affinity Columns

A 10 g polymerization mixture was made as follows: 7.6% w/w GMM and 7% PETA were mixed with a ternary porogenic solvent made of 59.1% w/w cyclohexanol, 22.9% w/w dodecanol, and 3.4% w/w water. AIBN at 1% w/w with respect to monomers was added to the polymerization mixture as the radical free initiator [17]. The polymerization mixture was sonicated for 15 min, purged with nitrogen for 5 min and then introduced into a 25 cm x 4.6 mm stainless steel column that functions as a mold

and heated in the water bath at 60 ^{o}C for 15 h. The mold was washed extensively with ACN followed by water. The monolith thus obtained was transferred from the 25 cm mold to two columns of 3 cm x 4.6 mm id each by connecting the mold column to the shorter column with a ¼" union and then pump water at a flow rate of 3 mL/min continuously until the unmodified monolithic support is completely transferred.

Depletion columns were homemade and were prepared according to Selvaraju and El Rassi [6] with the dimensions of anti-HSA column 5 cm and protein G' and protein A columns were 3 cm each with an internal diameter of 4.6 mm.

Immobilization of lectin

The SNA and MAL-II lectins were immobilized on the GMM/PETA monolithic column as follows. The 3 cm columns were allowed to react with a freshly prepared 0.1 M $NaIO_4$ for 2 h at room temperature to convert the diol groups into aldehyde groups followed by 10 min water wash. For MAL-II lectin, 0.5 mL volume was taken from the original vial and evaporated using a SpeedVac to remove all the solvent. The immobilization of lectin was done by passing through the column 1 mg of SNA lectin or concentrated MAL-II lectin described above in 0.5 mL of sodium acetate pH 6.4 containing 0.1 M lactose and 50 mM sodium cyanoborohydride. After passing the immobilization solution overnight any unreacted aldehyde was scavenged by passing a solution of 0.4 M Tris-HCl, pH 7.2 containing 50 mM sodium cyanoborohydride for 3 h at room temperature. The lectin columns were stored with the 20 mM Tris-HCl, pH 7.4 buffer containing 0.08% NaN_3 at 4 ˚C until further use.

Testing the lectin columns

Lectin columns were tested with standard proteins including α1-acid glycoprotein, fetuin, transferrin, healthy human serum and cancer serum at room temperature at a flow rate of 1 mL/min and the signal was monitored at λ=214 nm. The columns were first equilibrated with 10 column volumes of the binding mobile phase consisting of 20 mM Tris, 0.3 M NaCl, pH 7.4. Each standard protein was injected while passing the binding mobile phase, and was eluted by passing the eluting mobile phase consisting of 0.1 M lactose in 20 mM Tris-HCl, pH 7.4. Once the peak has eluted, the column was re-equilibrated with the binding mobile phase for readying it for another injection.

Chromatographic platform for the depletion of high abundance proteins (albumin and Igs) followed by capturing of sialoglycoproteins from serum

The multicolumn platform used for the simultaneous depletion of high abundance proteins such as albumin and immunoglobulins (Igs) followed by enrichment/capturing of sialoglycoproteins and subsequent fractionation of the captured proteins by RPC is shown in Fig. 3. The columns were connected in a predetermined order, and the flow direction for each column was controlled using independent switching valves. When the serum sample was injected into the platform, it entered the depletion columns first, namely anti human serum albumin column, protein G´ and protein A to deplete the high abundance proteins from the injected serum sample. Thereafter, the depleted serum entered the two

lectin columns connected in the order SNA column→MAL-II column. Finally, each lectin column was eluted independently, and the captured proteins were moved by the eluting mobile phase to the RPC column. This was followed by RPC fractionation using a linear gradient at increasing acetonitrile concentration in the mobile phase. The dimensions of the columns and their connection order were as follows: Anti HSA column (5 cm x 4.6 mm id) → protein G' column (3 cm x 4.6 mm id) → protein A column (3 cm x 4.6 mm id) → SNA column (3 cm x 4.6 mm id) → MAL-II column (3 cm x 4.6 mm id) → RPC column (10 cm x 4.6 mm id). The fabrication of the RPC column was described in Chapter III and it was designated as M3 column.

The RPC column, which was initially stored in ACN was washed with 20 column volumes of water to remove the ACN. The binding mobile phase consisted of 20 mM Tris, pH 7.4, containing 0.3 M NaCl. The eluting mobile phase for depletion column was 50 mM NaH_2PO_4, pH 2.2. The eluting mobile phase for lectin columns was 5 mM lactose in 20 mM Tris, pH 7.4. The aqueous rich mobile phase (mobile phase A) for the RPC column consisted of H_2O/ACN (95:5 v/v) containing 0.1% TFA and the organic-rich mobile phase (mobile phase B) consisted of ACN/ H_2O (95:5 v/v) containing 0.1% TFA. Three-fold diluted serum (20 μL) was injected while passing the binding mobile phase through the three depletion columns and the two-lectin columns while bypassing the RPC column. After 20 min of washing with the binding mobile phase, the depletion columns were eluted at a flow rate of 0.8 mL/min, followed by equilibration of the depletion columns. Another 20 μL of the same threefold diluted serum were injected onto the depletion and lectin columns.

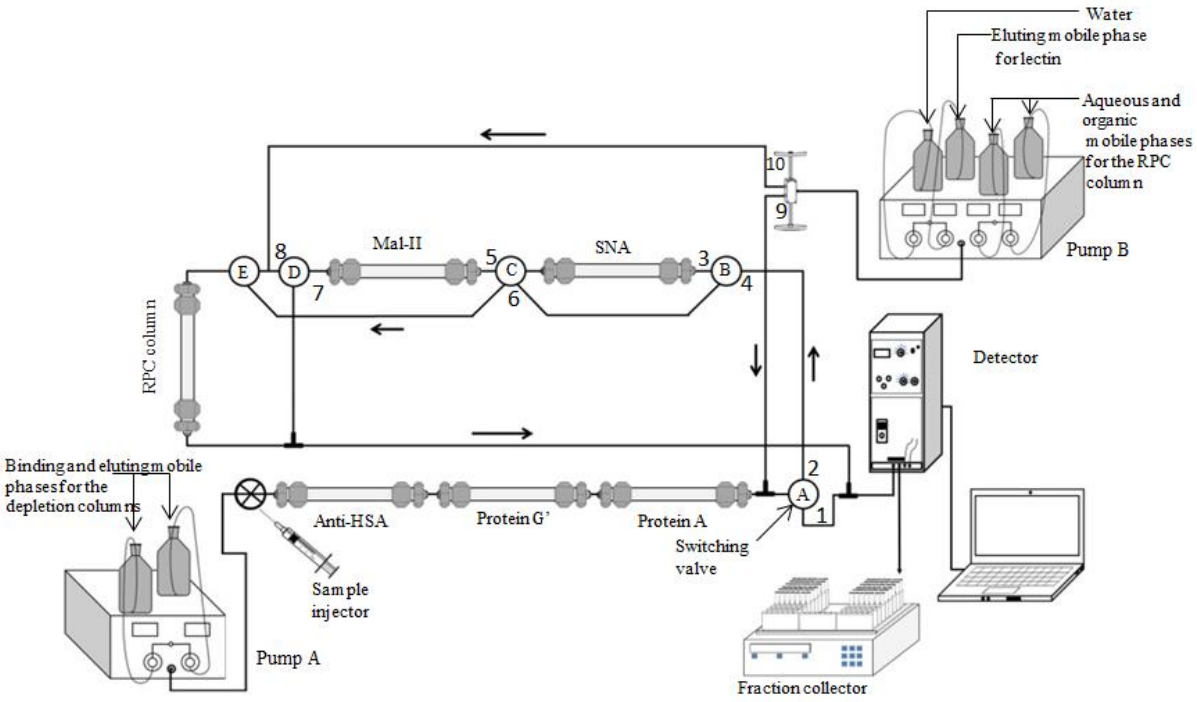

Figure 3. *An integrated platform for the simultaneous depletion of albumin and Igs, the enrichment of sialoglycoproteins, and subsequent RPC fractionation of the captured proteins by SNA and MAL-II lectin columns. When the switching valves A, B, C, and D were in 2, 3, 5, and 7 positions, respectively, the threefold diluted serum was injected onto the depletion and the lectin columns, followed by washing with the binding mobile phase (BMP) using pump A. Then, the eluting mobile phase for the depletion columns was passed by changing the valve A position to 1, thus by-passing the lectin and the RPC columns. The depletion columns were re-equilibrated again with the BMP, after which the valve A was changed back to position 2. Then, the SNA column was eluted using pump B, while the 3-way valve was in position 9, valve B in position 3 and valve C in position 6, thus by-passing the MAL-II column and passing through the RPC column. This was followed by washing, eluting, and re-equilibrating the RPC column using the*

mobile phase from pump B, while the 3-way valve is in position 10. Then, the MAL-II column was eluted by changing the 3-way valve position back to 9, valve B position to 4, valve C position to 5 and valve D position to 8. This was again followed by washing, eluting, and re-equilibrating the RPC column by keeping the 3-way-valve in the 10-position.

Serum proteins from a total of 40 μL (20 μL+20 μL) of three fold-diluted serum were accumulated onto the lectin columns. Using the eluting mobile phase, the proteins captured by the SNA column were transferred to the RPC column. RPC column was washed with mobile phase A to remove the salts for 20 min. This was followed by a linear gradient elution of increasing acetonitrile from 0 to 75% v/v mobile phase B in mobile phase A for 12 min and then 2 min of isocratic elution at 75% of mobile phase B. The column was returned to initial conditions within 1 min. After running the gradient elution, the RPC column was washed with water for 15 min. The second lectin MAL-II was eluted to the RPC column while maintaining the linear gradient elution the same as described above. The eluted protein fractions were collected every 30 sec using fraction collector and evaporated to dryness using SpeedVac. These samples were subjected to LC-MS/MS Orbitrap analysis.

Another set of data was obtained by injecting the 3-fold diluted non-depleted serum directly into the lectin columns and each lectin column was eluted to the RPC column for further fractionation as described above.

Results and discussion

As mentioned in the experimental section (see above), one set of data was collected by depleting the high abundance proteins from serum while another set of data was collected by omitting the depletion columns. Total number of captured proteins, including the number of glycoproteins, sialoglycoproteins and differentially expressed proteins was analyzed with the two data sets. Anti HSA, protein G´ and protein A columns were originally prepared and tested in our laboratory [18] .

Testing the lectin columns

The two-lectin columns were evaluated with standard sialoglycoproteins and serum to ensure whether the two lectins were properly immobilized and they showed specificity toward sialoglycoproteins. Three standard glycoproteins including α_1-acid glycoprotein, fetuin and transferrin, which are known for their sialic acid content [18-20] were analyzed on both the SNA and MALII columns. In the case of the SNA column, and with the exception of myoglobin, the other sialoglycoproteins (α_1-acid glycoprotein, fetuin and transferrin) exhibited partial retention as was manifested by a large flow through fraction (unretained fraction) that eluted with the binding mobile phase that consisted of 20 mM Tris, 0.3 M NaCl, pH 7.4, and a small fraction retained on the column that eluted when applying the eluting mobile phase that was made of 20 mM Tris, pH 7.4, containing 0.1 M lactose as the haptenic sugar, see Fig. 4 A, B and C. The large overflow (i.e., pass through fraction) observed in the case of transferrin and α_1-acid

glycoprotein is primarily due to the many glycoform constituents for each sialoglycoproteins with no affinity to the immobilized lectin and probably to surpassing the binding capacity of the column. In the case of MAL II column, fetuin and to a lesser extent α_1-acid glycoprotein showed some retention toward the immobilized lectin, see Fig. 4 A and B. This is due to the fact that MAL II lectin possesses more specific binding toward sialic acids with α-2, 3 linkages while SNA possesses affinity toward sialic acids with α-2,6 linkages. These sialoglycoproteins may contain higher number of α-2,6 linkages. For both lectins, myoglobin which is a non-glycoprotein was not captured and retained by the SNA or MAL columns, see Figs. 4D and 5C. Concerning the retained fractions of diseased free and breast cancer sera captured by the SNA column one can see by quick visual comparison of the two corresponding chromatograms that the retained signal corresponding to the retained fraction in cancer serum Fig. 4F is higher than that of the disease free serum, Fig 4E. Similar statement can be made for the MAL-II columns based on the visual comparison of the corresponding chromatograms of the retained signal for cancer serum, see Fig. 5E. This gives the idea that the breast cancer serum contains more sialoglycoproteins than the disease free serum, see Fig 5D.

Processing of serum *via* the multi column platform

Three fold diluted human serum (20 μL) were injected onto the depletion columns and the lectin columns while passing the binding mobile phase. In the anti-albumin column serum albumin was depleted and the serum passed to the protein A column and then to the G´ column to remove the highly abundance immunoglobulins from the serum.

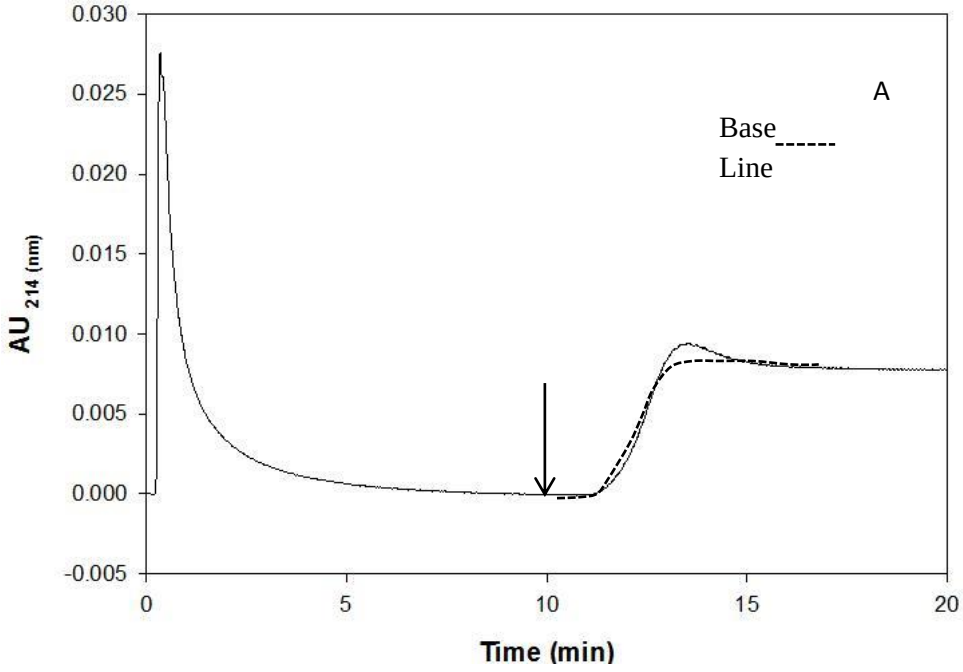
A
Base------
Line
AU 214 (nm)
Time (min)

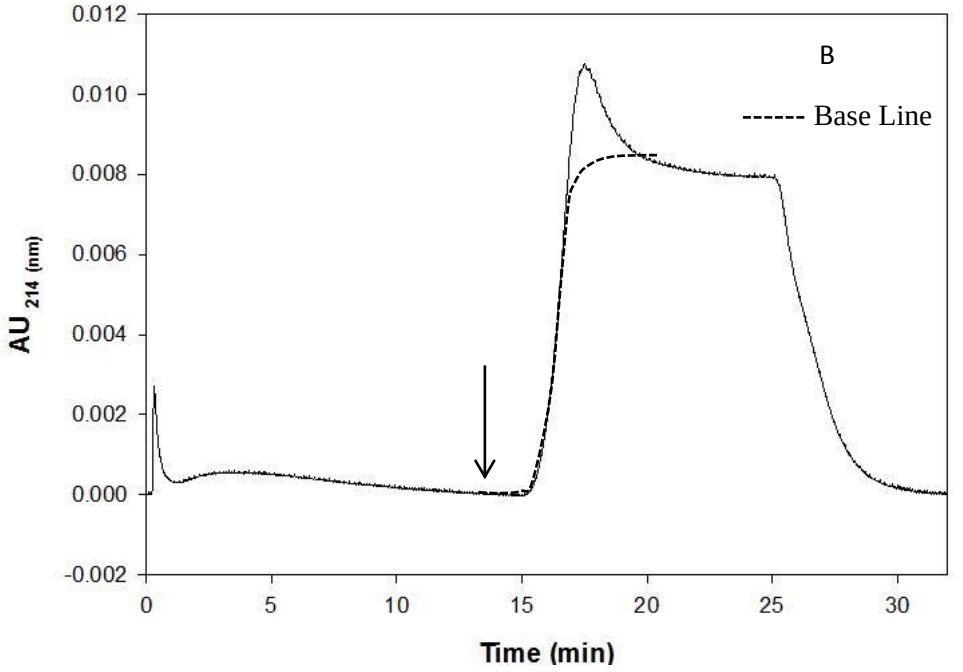
B
------ Base Line
AU 214 (nm)
Time (min)

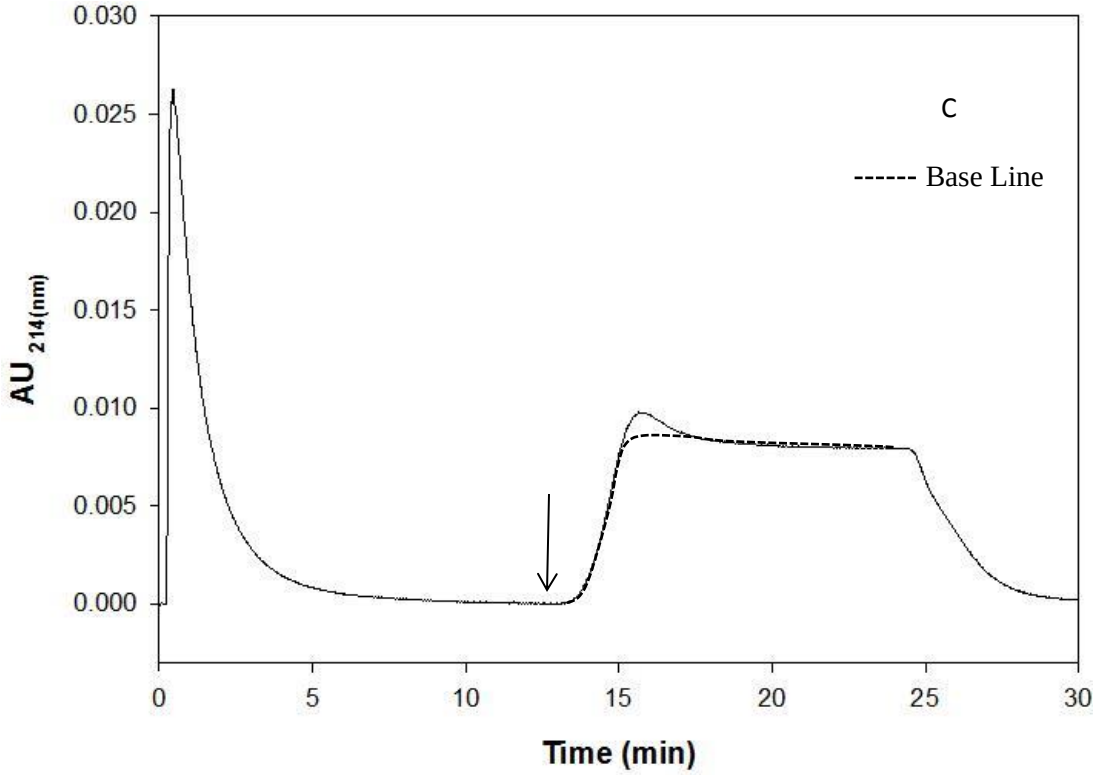
C
------ Base Line
AU 214(nm)
0.030
0.025
0.020
0.015
0.010
0.005
0.000
0
5
10
15
20
25
30
Time (min)

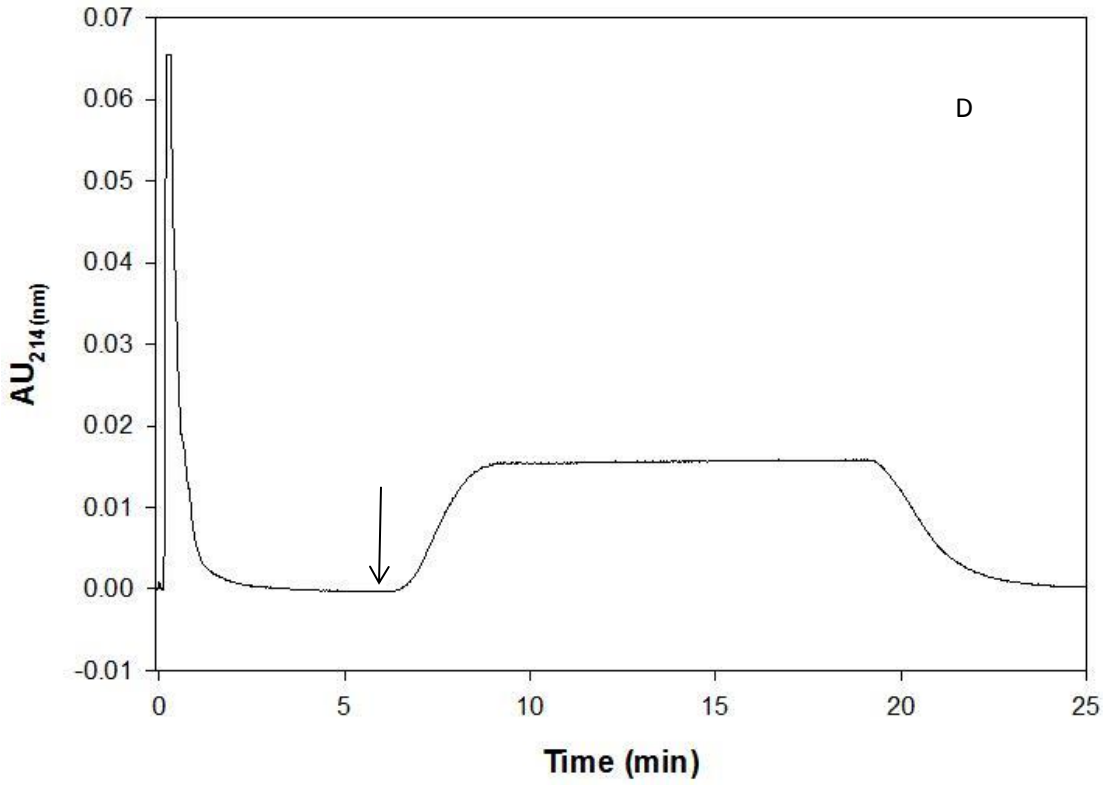
D
AU214(nm)
0.07
0.06
0.05
0.04
0.03
0.02
0.01
0.00
-0.01
0
5
10
15
20
25
Time (min)

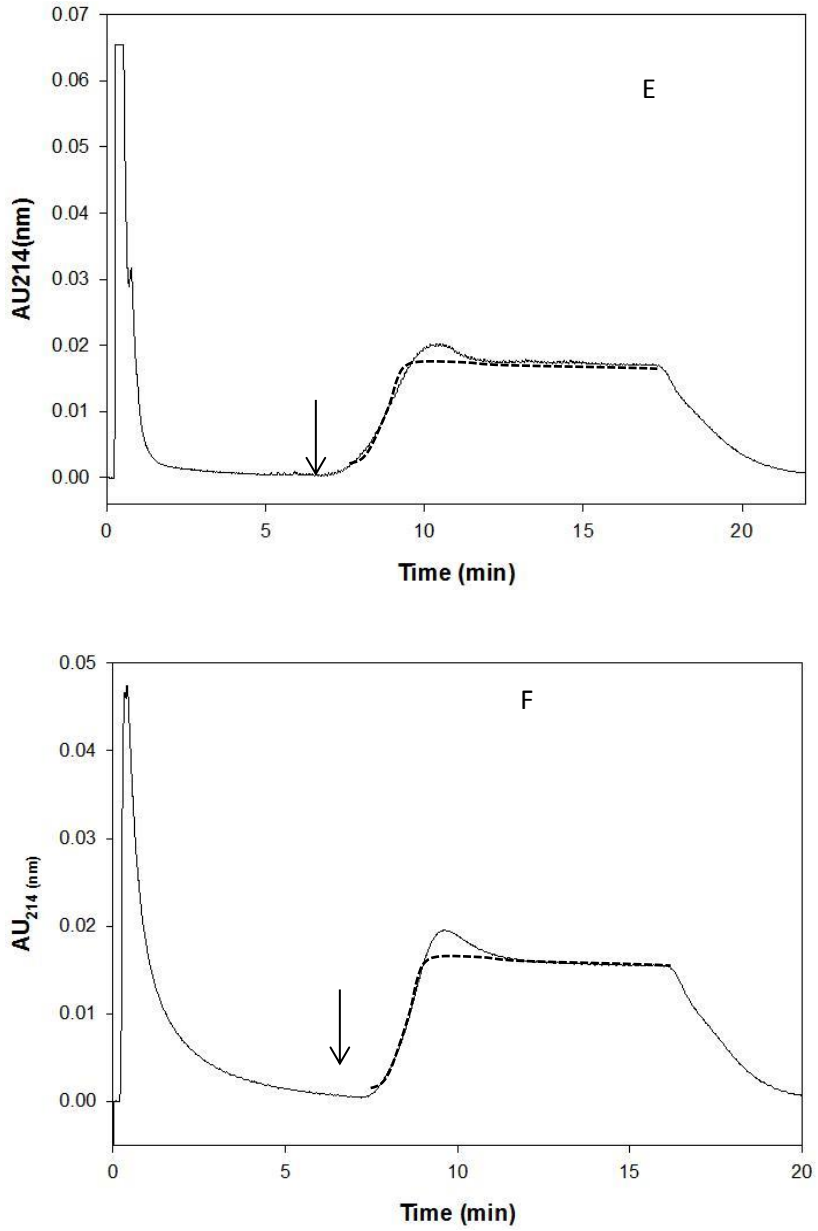

Figure 4. *Chromatograms of (A) α-1-acid glycoprotein, (B) fetuin, (C) transferrin, (D) myoglobin, (E) disease free serum and (F) breast cancer serum injected onto the SNA lectin column (3 cm x 4.6 mm id). Binding mobile phase, 20 mM Tris, pH 7.4, 0.3 M NaCl; eluting mobile phase, 20 mM Tris, pH 7.4, 0.1 M lactose; flow rate, 1 mL/min; wavelength, 214 nm. The arrow indicates the changes to eluting mobile phase.*

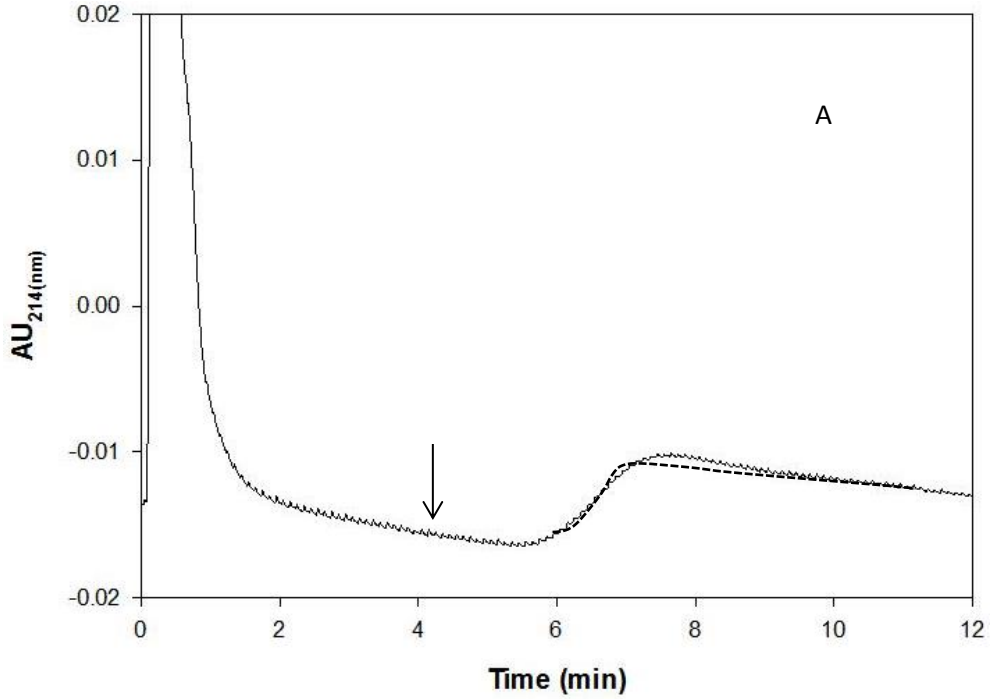
A
0.02
0.01
0.00
-0.01
-0.02
AU214(nm)
0
2
4
6
8
10
12
Time (min)

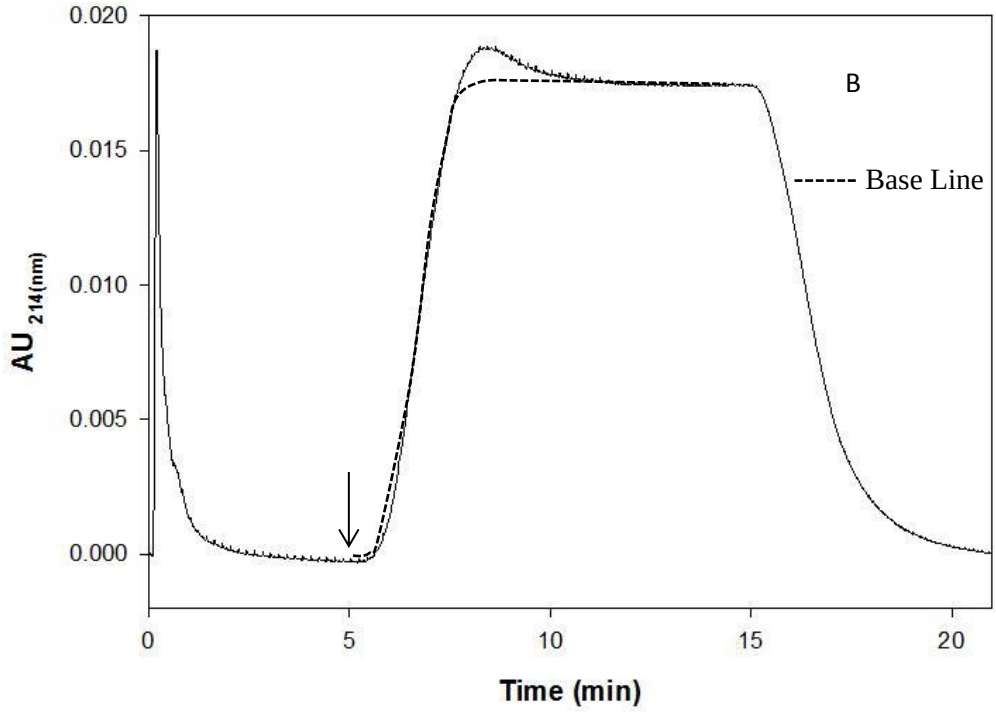
B
------ Base Line
0.020
0.015
0.010
0.005
0.000
AU 214(nm)
0
5
10
15
20
Time (min)

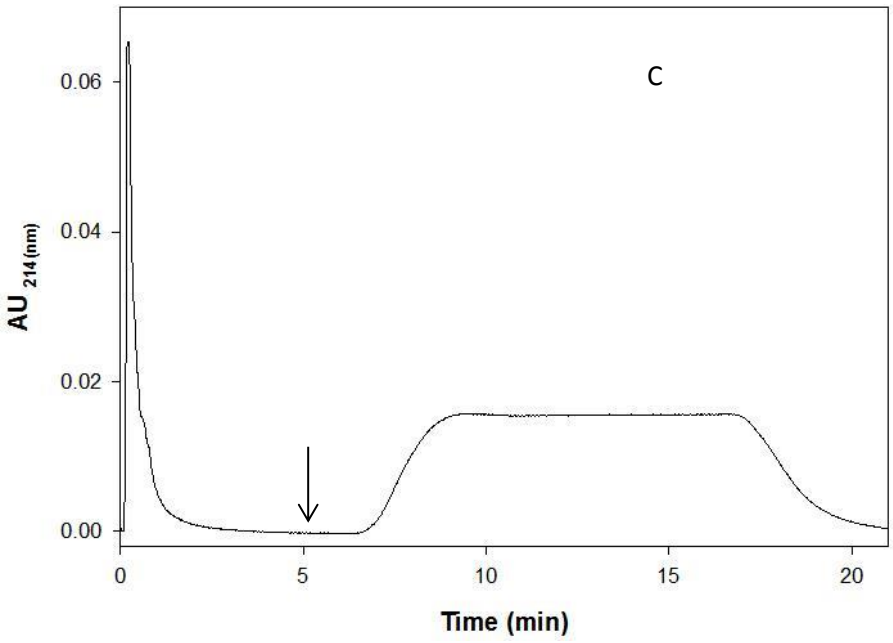
C
0.06
0.04
0.02
0.00
AU 214 (nm)
0
5
10
15
20
Time (min)

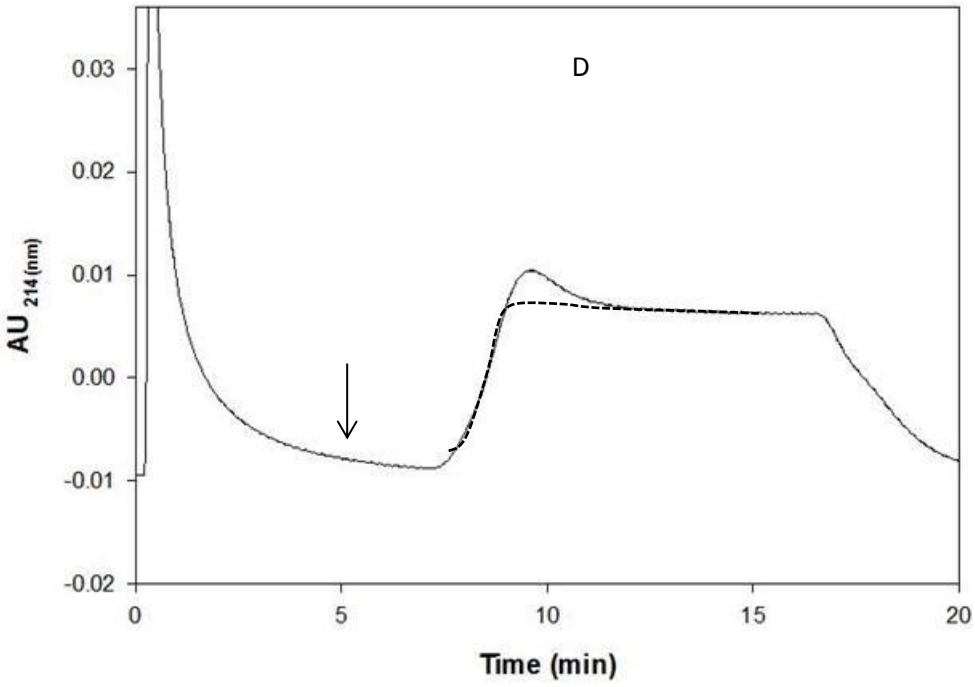
D
0.03
0.02
0.01
0.00
-0.01
-0.02
AU 214 (nm)
0
5
10
15
20
Time (min)

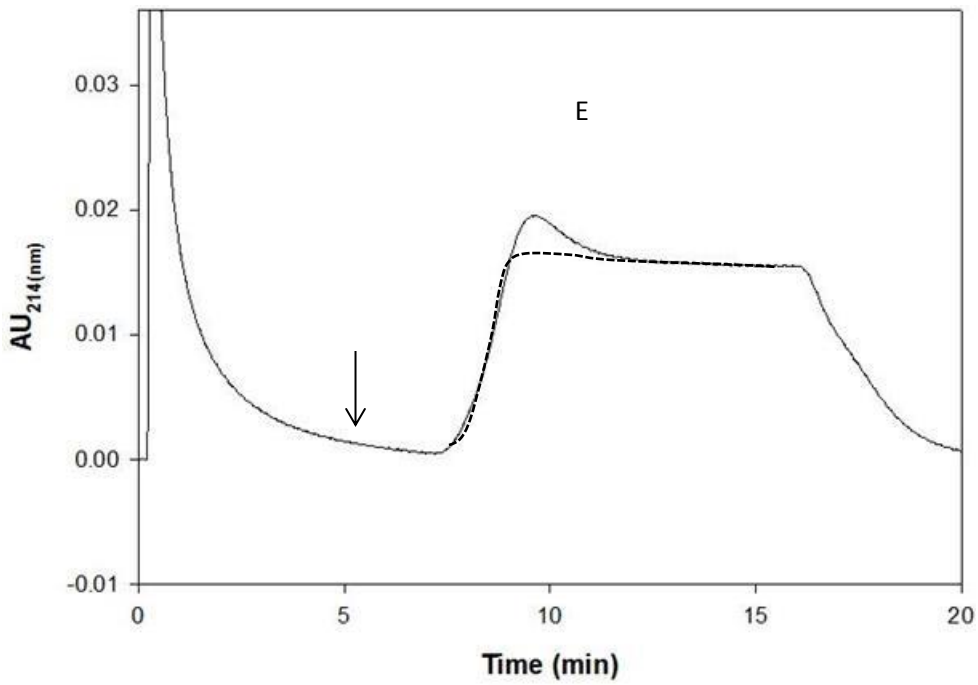

Figure 5. *Chromatograms of (A) α-1-acid glycoprotein, (B) fetuin, (C) myoglobin, (D) disease free serum, and (E) breast cancer serum injected onto the MAL-II lectin column (3cm x 4.6 mm id). All other conditions as in Fig. 4.*

Protein A and protein G´ are immunoglobulin binding proteins. These proteins are known to bind to the Fc region of antibodies from various species [18].

Protein G´ has a strong affinity to all Iggy's [19] while protein A binds with high affinity to IgG_1, IgG_2 and IgG_4 and has moderate affinity to IgG_3, IgA, IgD, IgE and IgM [20]. The columns were combined in the order of Protein G´ column and protein A column to remove high abundance immunoglobulins from the serum as much as possible. *Sambucus nigra* lectin binds preferentially to sialic acid attached to terminal galactose in α-2, 6 and to a lesser degree to α-2, 3 linkages. Binding is also inhibited to some extent

by lactose or galactose. This lectin does not appear to bind sialic acid linked to *N*-acetylgalactosamine. MAL-II lectin binds with the sialic acid in α-2,3 linkage. To capture maximum number of glycoproteins, serum was passed first to the SNA column and then to the MAL-II column. After passing the serum sample *via* lectin columns each lectin was eluted individually to the RPC column. RPC fractionation was carried out with a linear ACN gradient and 12 fractions were collected in 30 sec intervals from 8 min to 14 min. The chromatographic platform is shown in Fig. 3.

To assess the need for depletion, the same amount of serum sample was injected on the system with and without depletion columns. Fig. 8 shows the injection of disease free serum into the SNA and MAL columns in the absence of the depletion columns in the platform. Fig. 8A and B shows the injection of disease free and breast cancer sera into the multi column platform in the presence of depletion columns. When the serum is injected into the system without the depletion columns, high abundance proteins such as albumin, IgG's (IgG1, IgG2, IgG3, IgG4), IgA, IgM and IgD prevent the binding of sialylated proteins to the lectin columns. On the other hand, when the high abundance proteins are removed from the serum, sialoglycoproteins in the serum will have more access to the binding sites of the lectin columns. In fact, the lectin columns captured higher amount of proteins in the presence of albumin and Ig depletion columns. The number of proteins identified without depletion columns is relatively lower than in the presence of depletion columns, see the upcoming section below.

Importance of depleting high abundance proteins

A higher number of proteins were captured when the serum was depleted from high abundance proteins such as albumin and Ig's than from serum injected without depletion columns. This is due to the fact that when the serum was injected without depletion columns, the high abundance proteins bind nonspecifically with the lectin columns and saturate the binding sites. This is confirmed by the fact that the spectral count of albumin and Ig's are significantly higher in the fractions captured by the SNA and MAL-II lectin columns from non-depleted disease free serum, see Tables 1 and 2. As can be seen in these Tables, the average spectral count of albumin in non depleted serum was 103 in the SNA fractions and 43 in MAL-II fractions, while in depleted serum 77 spectral counts were detected for albumin in SNA fractions and 40 spectral counts in MAL-II fractions. In all cases, in SNA fractions high abundance proteins are in much higher number spectral counts than in MAL-II fractions, since the SNA column is placed as the first column in the tandem column format.

To further evaluate the importance of depleting high abundance proteins on the capturing capacity of the tandem lectin affinity columns, attention was paid to the number of sialoglycoproteins and low abundance proteins captured by the lectin columns in the presence and absence of depletion columns while keeping everything else the same including the amount of serum injected that was kept at 40 μL of three fold diluted disease free serum, see Fig. 6 and 8, respectively.

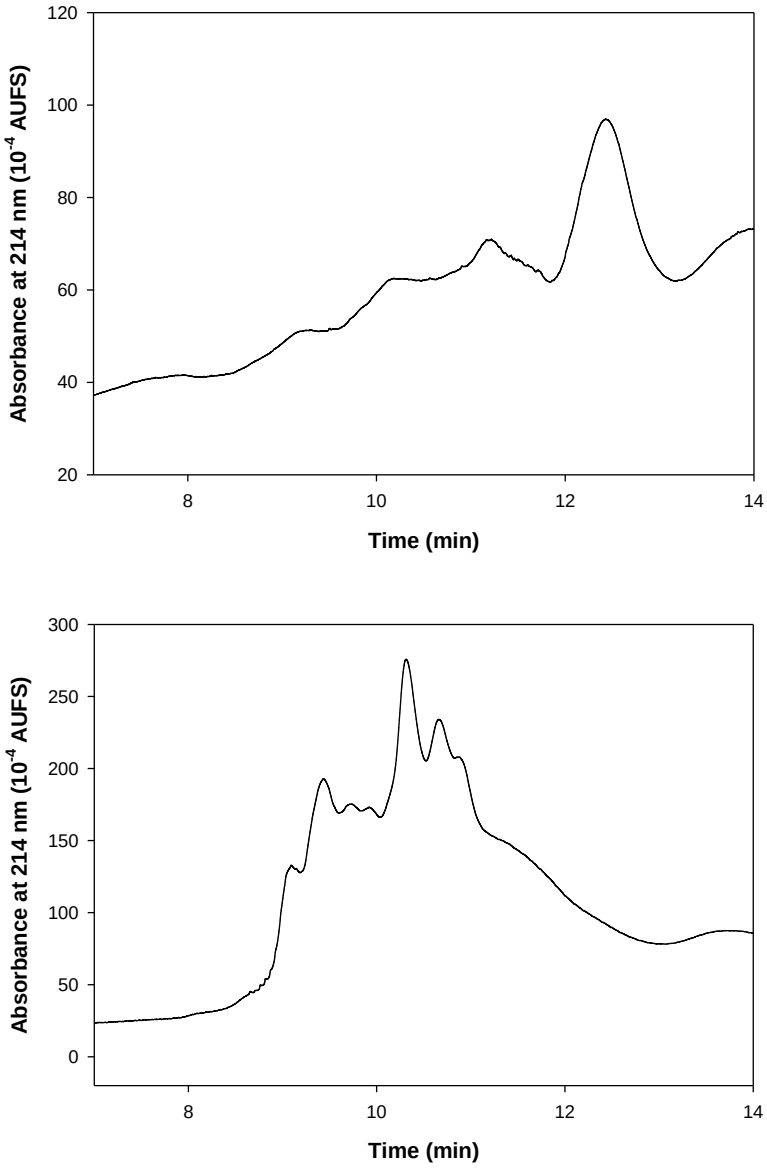

Figure 6. *Chromatograms of (A) RPC fractionation of the SNA captured proteins and (B) RPC fractionation of the MAL-II captured proteins without depletion. The RPC fractionation was carried out by a linear gradient elution at increasing ACN concentration in the mobile phase by going from 0 to 75% of mobile phase B in 12 min. Mobile phase A consisted of H_2O/ACN (95:5 v/v) containing 0.1% TFA and mobile phase*

B consisted of ACN/H_2O (95:5 v/v) containing 0.1% TFA. Flow rate, 1 mL/min; UV detection, 214 nm.

SNA and MAL-II columns captured significantly higher number of unique proteins in the presence of depletion columns than in their absence. Among these unique proteins there were sialoglycoproteins as well as low abundance proteins. For the SNA column, 88 unique proteins were captured from the depleted disease free serum while 48 unique proteins were captured from the non-depleted serum. In the presence of depletion columns, 21 low abundance proteins were identified while in the absence of depletion columns only 9 low abundance proteins were identified, see Table 3. The 21 low abundance proteins identified in the presence of depletion columns were annexin A2, calmodulin-like protein 5, carboxypeptidase B2, cathelicidin antimicrobial peptide, cholinesterase, coagulation factor V, dermcidin, desmoplakin, extracellular matrix protein 1,extracellular superoxide dismutase [Cu-Zn], galectin-7 gelsolin, intercellular adhesion molecule 2, lysozyme C, mannan-binding lectin serine protease 2, N-acetylglucosamine-1-phosphotransferase subunit gamma, phosphatidylcholine-sterol acyltransferase, phosphatidylinositol-glycan-specific phospholipase D, protein Z-dependent protease inhibitor, trypsin, transforming growth factor-beta-induced protein, and secreted phosphoprotein. The 9 low abundance proteins identified in the presence of depletion columns were catalase, cystatin-A, desmocollin-1, desmoglein-1, desmoplakin, extracellular matrix protein 1, filaggrin-2, glyceraldehyde-3-phosphate dehydrogenase, suprabasin and triosephosphate isomerase.

The number of unique proteins captured by MAL-II column in the presence and absence of depletion columns were 80 and 35, respectively, as measured in the collected RPC fractions by LC-MS/MS analysis. In the presence of depletion columns 16 low abundance proteins were identified while in the absence of depletion columns only 8 low abundance proteins were identified. The 16 low abundance proteins identified with the online depletion were annexin A2, carboxypeptidase B2, cartilage oligomeric matrix protein, cathelicidin antimicrobial peptide, cholinesterase, dermcidin, extracellular matrix protein 1, filaggrin, galectin-3-binding protein, histone H4, mannan-binding lectin serine protease, phosphatidylcholine-sterol acyltransferase, phosphatidylinositol-glycan-specific phospholipase D, protein S100-A7, protein S100-A8, sulfhydryl oxidase 1, transferrin receptor protein 1, and trypsin. In the absence of depletion columns, 8 low abundance proteins were identified namely attractin, cadherin-5, catalase, coagulation factor XIII B chain, complement factor H-related protein 4, cystatin-A, mannan-binding lectin serine protease 1, and vitamin K-dependent protein C.

The number of low abundance proteins captured by the SNA column was 21 in the presence of depletion columns and 9 in the absence of depletion columns. For MAL-II column, 18 and 8 low abundance proteins were identified in the presence and absence of depletion columns, respectively. Considering the amount of Igs captured, SNA lectin captured 12 Igs without depletion column while with the depletion columns it captured only 3 Igs. Considering MAL-II column, 6 Igs chains were captured without depletion columns and only 2 Ig's were captured when the depletion columns were present. Considering the spectral count for serum albumin, the captured SNA fractions exhibited 811 spectral counts in the absence of depletion column versus 369 spectral counts in the

presence of depletion columns. In the case of MAL-II column, the captured fractions yielded 160 spectral counts for serum albumin in the absence of depletion columns versus only 28 spectral counts for the same protein in the presence of depletion columns. Online depletion always favored the capture of higher number of unique proteins and low abundance proteins while the depletion minimized the spectral counts for albumin and the number of captured chains of Ig's. These data show that the online depletion is necessary for capturing a higher number of low abundance proteins.

The presence of serum albumin and Ig's in the LC-MS/MS fractions obtained with online tandem format may be due to protein-protein interactions that are frequently observed in complex proteomic samples and protein based affinity assays [6, 20, 21].

Reproducibility of the integrated multi column platform.

The day-to-day reproducibility of the multi column platform was evaluated in terms of the RPC fractionation chromatograms obtained by linear gradient elution of the SNA and MAL-II captured proteins from the depleted serum. The RPC chromatograms were readily reproducible. The day-to-day reproducibility was further assessed by calculating the percent RSD (%RSD) of the retention time and peak area. The average % RSD (n=2) for the retention times and the peak areas of the peaks for the SNA captured proteins were 0.11 and 12.2%, respectively, and for MAL-II the %RSD for the retention times and peak areas were 0.41 and 8.2%, respectively. In terms of reproducibility, it was observed that spectral counts of most proteins were similar in both day 1 and day 2. The proteins were identified with the spectral counts of the proteins with the 99.9% protein

identification probability, 95% peptide identification probability with minimum five unique peptides. As an example, galectin, which is a low abundance protein shows the spectral counts of 15 and 16 in day 1 and day 2, respectively.

Q-Q plots were determined for normal serum fractions 4 and 5, see Fig. 7. Q-Q plot or scatterplot is the representation of normalized spectral counts for each protein found in a given fraction on a certain day versus the normalized spectral count of the same protein found in that same fraction on another day. In the Q-Q plot for fraction 4 for day 1 and day 2, only 7 proteins were 2 standard deviations away of being the same in both categories while more than 40 proteins laid near the 45˚ line and are considered to have the same spectral counts. Proteins that were outside two standard deviation were afamin, antithrombin III, complement C3, α–1-antitrypsin, apolipoprotein A-1, extracellular matrix protein and inter alpha trypsin heavy chain H4. Also, in fraction 5, only 7 proteins were two standard deviations away from being the same. These 7 proteins were alpha-1-antitrypsin, apolipoprotein A-1, extracellular matrix protein, hemoglobin subunit beta, hemopexin, kininogen and plasminogen.

LC-MS/MS identification of proteins captured by the lectin columns

Identification of the proteins captured by the SNA columns. *Sambucus nigra* lectin (SNA) binds specifically to sialic acid linked with α-2, 6-galactose containing structures [11]. The captured proteins by the SNA column were eluted stepwise with the haptenic sugar lactose to the RPC column. The subsequent fractionation of the RPC column was performed with a 12 min linear gradient at increasing ACN concentration in the mobile phase by going from 0-75% v/v mobile phase B in mobile phase A. The

fractions were collected using a fraction collector that started the collection at 7.5 min of the gradient and ended at 12 min, which is the end of the gradient. Fractions of 0.5 mL were collected at 50 s intervals in Eppendorf tubes washed previously with ACN. Chromatograms of the RPC fractionation of SNA captured proteins are shown in Fig. 8a. These fractions were evaporated to dryness using RotorVap and submitted to the LC-MS/MS analysis. In the LC-MS/MS scaffold report, the proteins reported were those possessing protein identification probability greater than 99% with peptide identification probability greater than 95% and containing at least two unique peptides. The proteins identified from disease free and cancer sera are listed in Table 3.

The numbers of proteins identified from the disease free serum and breast cancer serum were 180 and 184, respectively. Fig. 9 shows the number of unique proteins to breast cancer and disease free serum samples. In the SNA fractions, the number of unique proteins identified from disease free and cancer serum were 20 and 24, respectively, while 160 proteins were common to both sera.

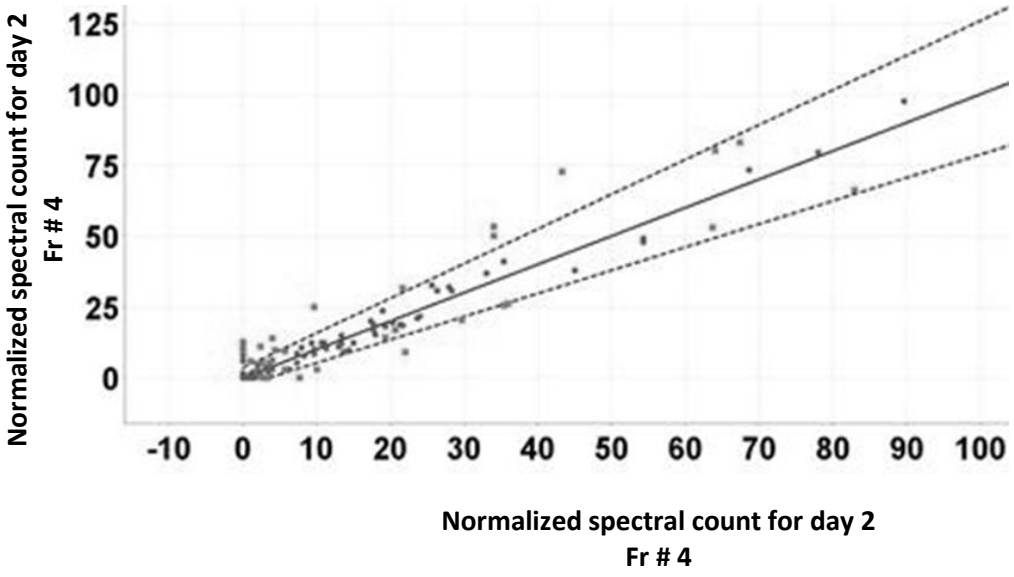

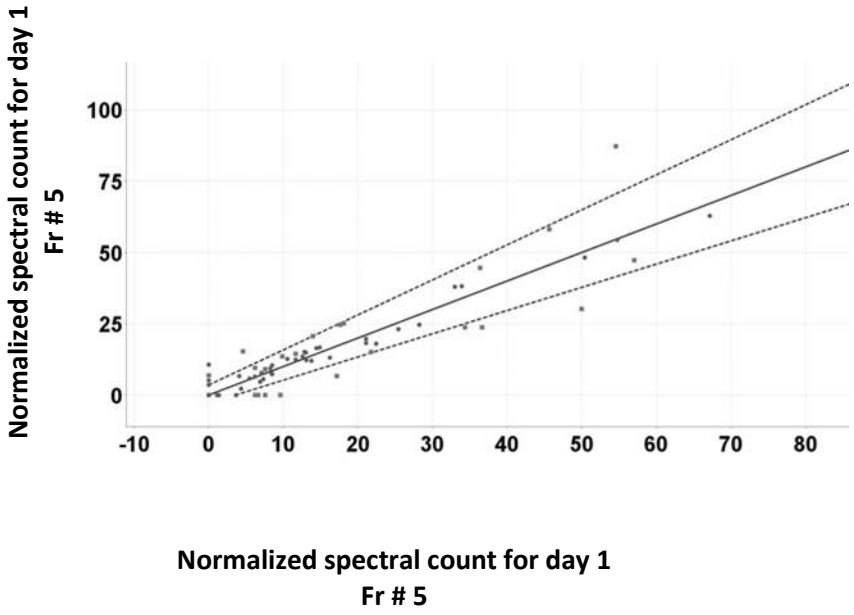

Figure 7. *Q-Q scatterplots for the day-to-day reproducibility of MS normalized spectral counts. The dots laid outside from the dotted lines were two-standard deviation away from being the same in both categories.*

The false discovery rate for peptide identification was 0.1% for both SNA and MAL-II captured proteins. The SNA column captured 184 proteins among them 83 have been reported to be sialoglycoproteins and 43 have been identified as low abundance proteins [3, 15, 16, 20, 22-32]. Concentration limits for low abundance of proteins in plasma range from ng level to $\leq$ 1 μg level. Low abundance proteins were assigned according to the human plasma proteome reference set that contains 1929 non redundant proteins [31]. Concentrations of some representative low abundance proteins are fillagrin

(0.82 ng/mL), annexin-1 (6.2 ng/mL), desmolegein (2.7 ng/mL), and calmodulin like protein 5 (8.1 ng/mL).

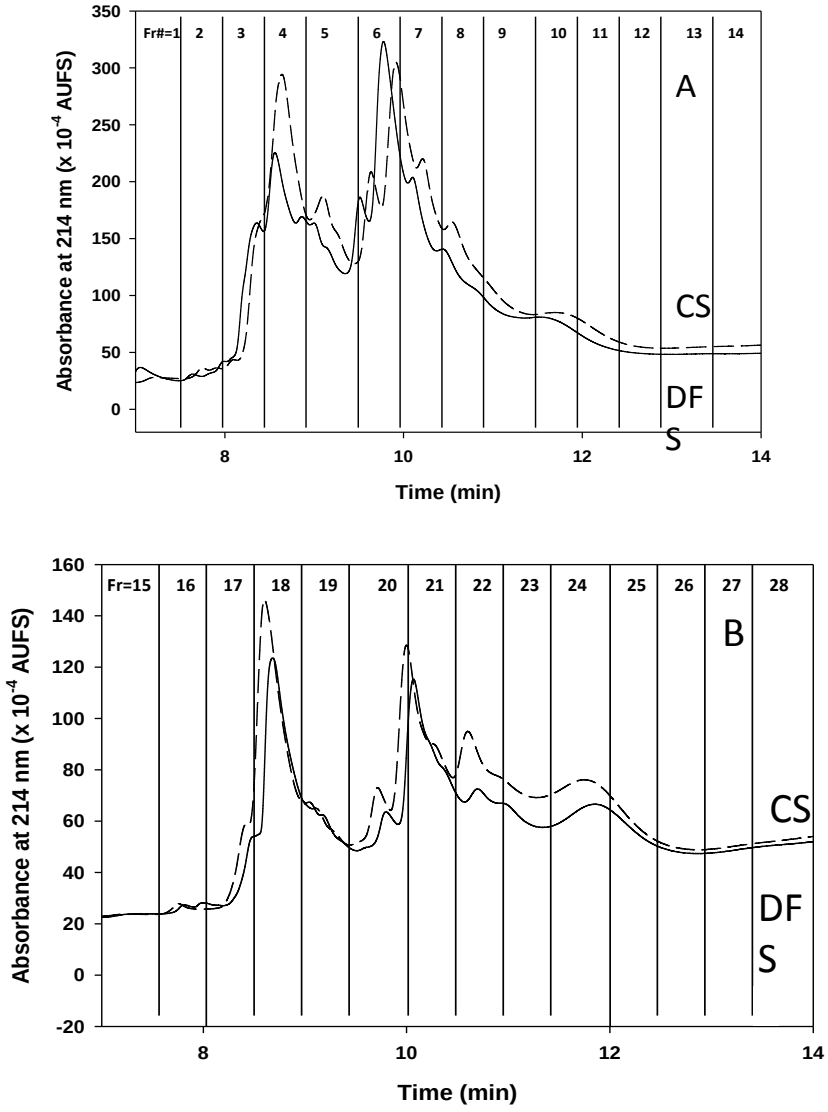

8. *Comparison of chromatograms of the RPC fractionation of proteins captured by the SNA column (A) and the MAL-II column (B) from disease free serum (DFS) and breast cancer serum (CS). All other conditions as in Fig. 4.*

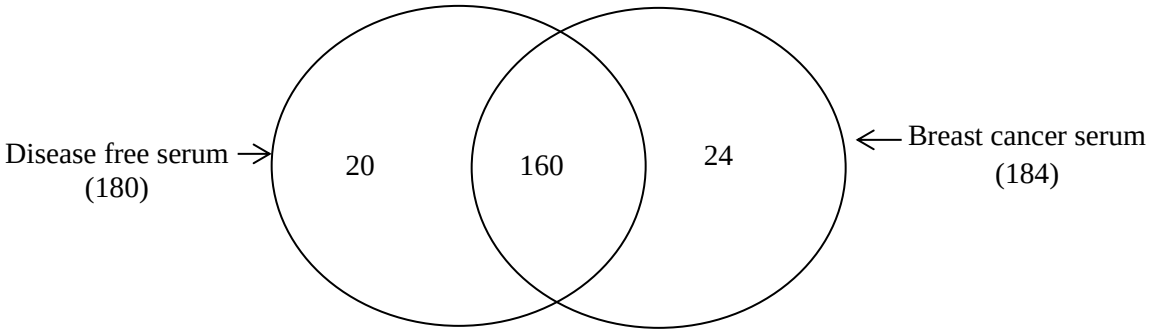

Figure 9. *Venn diagram for the LC-MS/MS identified proteins captured by the SNA column.*

Proteins such as apolipoportein C-1, serum paraoxonase/aryleserase were identified as cancer biomarker candidates [33]. Galectin-3-binding protein which is a low abundance protein and clusterin were reported as tumor glycoprotein biomarkers. They are present in both disease free and breast cancer sera [34]. Histidine rich glycoprotein, complement C3, and kininogen 1 were identified as sialylated biomarkers for ovarian cancer and these were present in normal serum as well as breast cancer serum. These proteins are present in both disease free serum as well as cancer serum while histidine rich glycoprotein and kininogen 1 are elevated in breast cancer serum [35]. Plasminogen, coagulation factor XII, complement C3, kininogen-1, Ig mu chain c region, Ig alpha-2 chain C, apolipoprotein A-I, apolipoprotein E (apo-E), apolipoprotein C-III, fibrinogen alpha chain, fibrinogen beta chain, complement C1q subcomponent subunit C, fibronectin, AMBP protein, vitronectin, histidine-rich glycoprotein, apolipoprotein D, complement factor H, clusterin, galectin-3-binding protein, interalpha-trypsin inhibitor heavy chain H4, complement factor h-related protein 5 were identified as sialylated glycoproteins bearing sialylated lewis x antigen in breast cancer serum, while interalpha-

trypsin inhibitor heavy chain H4, plasminogen, Ig gamma-2 chain c region, Ig mu chain C region, apolipoprotein A-I, apolipoprotein E, AMBP protein, vitronectin, clusterin, were identified as altered in their concentration by 3-fold or more in breast cancer serum compared to disease free serum [36].

Identification of proteins captured by MAL-II column. 153 and 157 non-redundant proteins were identified in the fractions captured by the MAL-II column from disease free and cancer sera using the multi column platform shown in Fig. 3. See Table 3 for the list of identified proteins and Fig. 10 for the Venn diagram. In the proteins captured by the MAL II column, 94 are known to be glycoproteins. Among the 94 glycoproteins 62 proteins are reported to be sialoglycoproteins and among them 37 are reported as low abundance proteins [31]. In the MAL-II captured proteins, 20 and 24 unique proteins were identified from disease free and cancer sera, respectively, while 133 proteins were common to both sera. Pregnancy zone protein, Phosphatidylinositol-glycan-specific phospholipase D, fetuin B, ficolin -3, galectin-3- binding protein, galectin 7 were identified as low abundance sialoglycoproteins [30, 37]. MAL-II column was able to capture 37 low abundance proteins. Concentrations of low abundance proteins identified were filaggrin (4.6 ng/mL), annexin A3 (1.6 ng/mL), serpin B3 (6.1 ng/mL), galectin 7(6.9 ng/mL), Plexin domain-containing protein (1.6 ng/mL), plectin 1(2.8 ng/mL) and calmodulin like protein 5(8.1 ng/mL) [31].

Leucine-rich alpha-2-glycoprotein was identified in the set of MAL-11 lectin captured proteins in both disease free and cancer serum as a novel serum biomarker for monitoring disease activity during therapy in autoimmune patients,

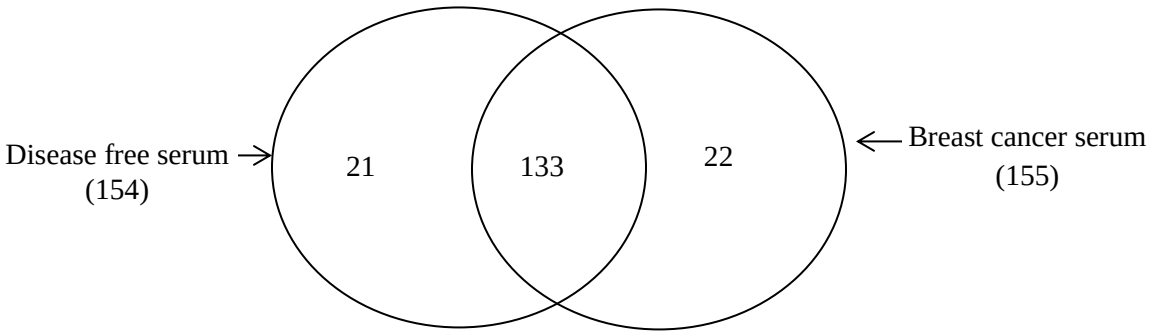

Figure 10. *Venn diagram for the LC-MS/MS identified proteins captured by MAL-II column.*

particularly useful in patients with active disease but normal c-reactive protein levels, which increase in the time of inflammation [38]. Previously reported cancer biomarkers such as complement C3, histidine-rich glycoprotein, and kininogen-1 were also identified among the captured proteins [39]. Low abundance protein junction plakoglobin was also identified and it is reported as a hepatic fibrosis biomarker [40]. In our work, by injecting disease free and breast cancer sera, other disease biomarkers were detected. This may due to the fact that these volunteers may suffer from other diseases, which have not been diagnosed yet. Therefore, proteomic analysis of serum is an important tool to diagnose various pathological conditions.

Raw LC-MS/MS data were analyzed in scaffold 5 software using IPI human database. NetGly predictor and Uniprot software were utilized to predict N-glycosylation sites of the identified proteins for both SNA and MAL-II captured proteins from disease free and breast cancer sera. From the set of SNA captured proteins 73% are glycoproteins

and 27% are non-glycoproteins for the disease free serum while for the cancer serum 79% are glycoproteins and 21% are non-glycoproteins. For MAL-II lectin for the normal serum 74% were glycoproteins and 26% were non-glycoproteins. For cancer serum 74% were glycoproteins while 22 % of proteins were non-glycoproteins. Capturing non glycoproteins by the lectin columns may be due to protein-protein interactions that are normally present in complex biological fluids such as serum and affinity based assays [6].

Differentially expressed proteins in SNA and MAL-II lectin fractions.

The RPC chromatograms of proteins captured by SNA and MAL-II columns from disease free and cancer sera are shown in Fig. 8 A and B. The two overlapping chromatograms exhibit differences such as peak intensity, retention time and peak shouldering. Differentially expressed proteins (DEP) from cancer serum were found relative to the disease free serum with 99.9% protein identification probability, 95% peptide identification probability and a minimum of five unique peptides. The DEP from breast cancer serum relative to disease free serum were identified using the quantitative Q-Q scatterplot, by plotting the normalized spectral count of proteins of breast cancer serum and disease free serum of the same fraction. The proteins that are more than two standard deviations away of being the same in both categories are considered as DEP. In addition, all these proteins had a p-value < 0.05 using the t-test. The DEP of cancer serum relative to disease free serum were conducted according to the approach by Selvaraju and El Rassi using the scatter plots [6, 18].

In the SNA captured proteins, 34 proteins were identified as DEP, and they are either up regulated or down regulated, see Table 7. Among them, 24 proteins were sialoglycoproteins [2, 41-43]. These DEP proteins showed differential expression in other types of malignancies than breast cancer. For instance, the level of clusterin was found to be significantly higher in patients with hepatocellular carcinoma (HCC) and it served as a candidate biomarker for the HCC [44]. Alpha-1-antitrypsin, apolipoprotein A-IV, complement C3, fibronectin were down regulated in SNA cancer serum relative to the normal serum. Apolipoprotein A-I, complement factor H, hemoglobin subunit beta and inter alpha trypsin inhibitor heavy chain H4 were up regulated in more than 3 serum fraction. Again, afamin which was up-regulated in fraction 5, has been reported to increase in expression in pre-diagnostic breast cancer serum [45].

In the MAL-II captured proteins, 24 proteins were identified as DEP. These proteins are listed in Table 8. Five low abundance proteins were differentially expressed in the MAL-II column captured fractions. Desmoplakin, junction plakoglobin, glyceraldehyde-3-phosphate dehydrogenase, and hornerin were down regulated, while extracellular matrix protein was up regulated in breast cancer serum relative to the disease free serum. 14 sialoglycoproteins were identified in MAL-II lectin fractions. Alpha-1-antitrypsin, apolipoprotein A-IV, haptoglobin and plasminogen were down regulated in two serum fractions. Kininogen-1 was up regulated in 3 fractions. During breast cancer, epidermal growth factor suppresses the level of protein desmoplakin [46], and it is also observed in our investigation that desmoplakin is down regulated in breast cancer serum. It has been reported that the level of serotransferrin is increased in breast cancer [47], which corroborate with our finding that serotransferrin is up regulated in

fraction 2. The up-regulated serotransferrin was reported as a candidate cancer biomarker for several other types of malignancies including lung cancer, brain cancer and ovarian cancer [48-50].

Conclusions

The integrated liquid phase multi column platform described here allowed the precise operation of various columns representing orthogonal modes of chromatography whereby each column accomplished its function in harmony with other columns. This was facilitated by incorporating in the platform high precision HPLC pumps and high pressure switching valves. In its maximum configuration the multi column platform consisted of six different columns including 3 depletion columns to remove the high abundance albumin and Ig's, 2 lectin columns to capture/enrich sialoglycoproteins, and one RPC column to fractionate the lectin captured proteins. The SNA column has captured 34 DEP while the MAL-II column captured 24 DEP with 11 DEP common to both lectins. Previously, reported breast cancer candidate biomarkers such as histidine rich glycoprotein, kininogen 1, afamin and clusterin were identified in the LC-MS/MS fractions. The integrated platform eliminated experimental bias and sample loss due to its integrated nature and cascading operation in the sense that the sample is transferred from column to column in the liquid phase avoiding sample manipulation.

TABLE 1

PROTEINS IDENTIFIED BY LC-MS/MS ANALYSIS OF SNA CAPTURED PROTEINS FROM NON DEPLETED DIESEASE FREE SERUM. DATA ON GS WERE FROM REFS. [2, 12, 15, 22-24, 35, 39, 45, 51, 52]

		Fr # 1	Fr # 2	Fr # 3	Fr # 4	Fr # 5	Fr # 6	Fr # 7
1	165 kDa protein	0	0	0	0	1	0	82
2	252 kDa protein	2	0	0	6	3	0	0
3	Alpha-1-acid glycoprotein 1 [GS]	0	0	0	6	4	4	0
4	Alpha-1-acid glycoprotein 2 [GS]	0	0	0	4	2	2	0
5	Alpha-1-antichymotrypsin [GS]	0	0	0	0	0	0	6
6	Alpha-1-antitrypsin [GS]	5	5	6	7	11	13	19
7	Alpha-1B-glycoprotein [GS]	0	0	1	5	10	1	0
8	Alpha-2-antiplasmin [GS]	0	0	0	2	1	0	5
9	Alpha-2-HS-glycoprotein [GS]	0	0	1	7	10	9	8
10	Angiotensinogen [GS]	0	0	0	0	0	0	5
11	Antithrombin-III [GS]	0	0	2	5	6	9	7
12	Apolipoprotein A-I [GS]	9	9	11	11	14	18	22
13	Apolipoprotein A-II*	3	0	1	3	3	5	2
14	Apolipoprotein A-IV*	6	1	8	7	8	14	15
15	Apolipoprotein B-100 [GS]	1	0	2	2	0	1	28
16	Apolipoprotein C-I*	1	0	0	3	4	2	3
17	Apolipoprotein C-II*	1	1	2	2	6	6	3
18	Apolipoprotein C-III [G]	0	1	2	4	5	4	0
19	Apolipoprotein D [GS]	0	0	3	7	7	7	4
20	Apolipoprotein E [G]	2	0	1	1	4	8	9
21	Apolipoprotein M [GS]	0	0	0	0	0	6	3
22	Attractin [1a]	0	0	0	0	0	9	2
23	Beta-2-glycoprotein 1 [GS]	0	0	9	9	6	6	3
24	Beta-Ala-His dipeptidase [1a]	0	0	0	0	0	0	5
25	C4b-binding protein alpha chain	0	0	0	0	5	2	0
26	Cadherin-5 [1a]	0	0	0	5	0	0	0
27	Carboxypeptidase N catalytic chain [1a]	0	0	0	0	0	4	0
28	Carboxypeptidase N subunit 2 [GS]	0	0	0	0	0	0	7

29	Catalase [1a]	0	5	0	0	0	0	0
30	CD5 antigen-like	0	0	0	0	0	3	4
31	Ceruloplasmin [GS]	0	0	0	3	11	30	18
32	Coagulation factor IX [1a]	0	0	0	0	0	4	2
33	Coagulation factor X [1a]	0	0	0	6	0	0	0
34	Coagulation factor XIII A chain [1a]	0	0	0	0	0	0	6
35	Coagulation factor XIII B chain [1a]	0	0	0	28	17	8	0
36	Complement C1r subcomponent	1	3	1	2	13	9	0
37	Complement C1r subcomponent-like protein [1a]	0	0	0	0	3	4	3
38	Complement C1s subcomponent	0	0	0	0	0	16	6
39	Complement C3 [GS]	5	3	3	5	6	6	48
40	Complement C5 [GS]	0	0	0	0	0	0	18
41	Complement component C6 precursor	0	0	0	1	26	23	0
42	Complement component C7	0	0	0	0	2	5	0
43	Complement factor B	0	0	1	4	3	15	5
44	Complement factor H [GS]	0	0	20	38	26	15	4
45	Complement factor H-related protein 1	0	0	3	4	0	0	0
46	complement factor H-related protein 4 [1a]	0	0	7	7	1	1	0
47	Complement factor I	0	0	3	1	20	14	10
48	Corneodesmosin [1a GS]	0	10	0	0	0	0	0
49	Cystatin-A [1a]	0	4	0	0	0	0	0
50	Desmocollin-1 [1a]	0	6	0	0	0	0	0
51	Desmoglein-1 [1a]	0	10	0	0	0	0	0
52	Extracellular matrix protein 1 [1a]	0	0	0	7	0	0	0
53	Fetuin-B [1a GS]	0	0	0	0	7	9	3
54	Fibrinogen beta chain	0	0	0	0	0	4	0
55	Fibronectin [GS]	0	9	15	16	7	10	28
56	Fibulin-1	1	0	1	0	3	6	5
57	Ficolin-3 [GS]	0	0	0	0	1	0	4
58	Filaggrin-2 [1a]	1	7	0	0	0	0	0
59	Galectin-3-binding protein [1aGS]	0	0	0	4	1	0	8
60	Gamma-B of Fibrinogen gamma chain	0	0	0	0	1	3	0
61	Glutathione peroxidase 3	0	0	0	0	0	1	4
62	Glyceraldehyde-3-phosphate dehydrogenase [1a]	0	5	0	0	0	0	0
63	Haptoglobin [GS]	0	0	2	22	23	24	21
64	Haptoglobin-related protein	0	0	0	0	2	4	5
65	Hemoglobin subunit alpha	0	0	0	0	0	5	0
66	Hemoglobin subunit beta	0	0	0	0	0	7	2
67	Hemopexin [GS]	0	0	0	2	20	14	6
68	Heparin cofactor 2 [GS]	0	0	0	0	0	0	4

69	Histidine-rich glycoprotein [GS]	0	0	0	8	12	10	8
70	Homo sapiens SNC73 protein (SNC73) mRNA	0	0	0	0	6	18	18
71	Hornerin [1a]	1	1	0	1	2	0	3
72	Hyaluronan-binding protein 2	0	0	0	0	6	4	0
73	IGK@ protein	0	0	4	8	7	10	10
74	IGL@ protein	0	0	0	0	0	1	3
75	Immunoglobulin J chain [GS]	2	3	4	2	1	2	6
76	Immunolgoobulin heavy chain	0	0	0	0	0	1	3
77	Inter-alpha (Globulin) inhibitor H2	1	0	5	4	3	4	17
78	Ig kappa chain V-IV region Len	4	5	8	15	13	3	7
80	Ig gamma chain-2 C region	12	15	22	13	31	2	4
81	Ig kappa chain V-III region WOL *	5	4	7	3	8	5	8
82	Ig lambda-2 chain C regions *	2	4	58	4	3	1	2
83	Ig mu chain C region	2	2	7	8	3	1	3
84	Ig alpha-2 chain C region G	4	5	3	2	3	5	6
85	Ig gamma-1 chain C region G							
86	Ig kappa chain V-III region WOL *	5	6	3	9	7	5	2
87	Ig heavy chain V-I region EU	15	16	23	25	25	26	2
88	Ig heavy chain V-I region HG3	12	23	34	34	23	56	14
84	Ig heavy chain V-III region GAL	11	32	21	12	14	26	14
85	Ig gamma-3 chain C region [G]	3	5	6	11	7	2	2
86	Inter-alpha-trypsin inhibitor heavy chain H1 [GS]	0	0	0	0	0	1	12
87	Inter-alpha-trypsin inhibitor heavy chain H4 [GS]	2	0	0	0	4	7	15
88	Keratin, type I cytoskeletal 10 [1a]	17	25	15	15	14	13	22
89	Keratin, type I cytoskeletal 13	0	5	0	0	0	0	0
90	Keratin, type I cytoskeletal 16 [1a]	0	0	0	0	1	0	5
91	Keratin, type I cytoskeletal 9	12	12	17	9	14	11	18
92	Keratin, type II cytoskeletal 1	18	26	19	18	18	12	20
03	Keratin, type II cytoskeletal 1b	0	11	0	0	0	0	0
94	Keratin, type II cytoskeletal 2 epidermal	13	25	10	15	9	8	16
95	Keratin, type II cytoskeletal 6A	8	9	11	0	3	2	19
96	Keratin, type II cytoskeletal 78	0	7	0	0	0	0	0
97	Kininogen-1 [GS]	3	4	12	32	31	27	20
98	Mannan-binding lectin serine protease 1 [1a]	0	0	0	0	0	3	0
99	Peroxiredoxin-2	0	5	0	0	0	0	0
100	Plasma kallikrein [GS]	0	0	0	0	0	1	12
101	Plasma protease C1 inhibitor [GS]	0	0	0	0	0	0	8
102	Plasminogen [GSGS]	0	0	1	21	20	6	0

103	Pregnancy zone protein [1a]	0	0	0	0	0	0	20
104	Protein S100-A9	0	0	0	0	0	1	4
105	Protein-glutamine gamma-glutamyltransferase E	0	5	0	0	0	0	0
106	Prothrombin	1	1	7	8	11	11	6
107	Putative uncharacterized protein DKFZp686C11235	0	0	0	0	0	3	3
108	Putative uncharacterized protein DKFZp686G11190	0	0	0	0	0	7	3
109	Scavenger receptor cysteine-rich type 1 protein M130	0	0	0	8	2	0	0
110	Serum albumin	81	125	130	110	160	120	85
112	Serum paraoxonase/arylesterase 1 [GS]	0	0	0	1	0	0	11
113	suprabasin [1a]	0	4	0	0	0	0	0
114	Triosephosphate isomerase [1a]	0	6	0	0	0	0	0
115	Uncharacterized protein	1	1	2	3	2	2	0
116	Uncharacterized protein	0	0	0	0	0	0	0
117	Uncharacterized protein	3	4	9	16	13	19	32
118	Uncharacterized protein	0	0	7	4	0	0	0
119	Uncharacterized protein	0	3	0	3	0	0	4
120	Uncharacterized protein	1	3	1	1	0	0	0
121	Uncharacterized protein	0	0	0	0	0	0	3
122	vitamin D-binding protein isoform 1 precursor	0	0	0	0	10	9	0
123	Vitamin K-dependent protein C [1a]	0	0	0	0	3	9	0
124	Vitamin K-dependent protein S	0	0	0	0	0	0	13
125	Vitronectin [GS]	4	0	3	4	6	6	0
126	Zinc-alpha-2-glycoprotein [GS]	0	4	1	8	5	2	0

G, glycoprotein; GS, sialylated glycoprotein; 1a, low abundance protein (few ng to sub μg/mL level); *, non-glycoprotein.

TABLE 2

PROTEINS IDENTIFIED BY LC-MS/MS ANALYSIS OF MAL-II CAPTURED PROTEINS FROM NON DEPLETED DIESEASE FREE SERUM. DATA ON GS WERE FROM REFS. [2, 16, 22-24, 32, 35, 39, 45, 51-53]

		Fr # 1	Fr # 2	Fr # 3	Fr # 4	Fr # 5	Fr # 6	Fr # 7
1	165 kDa protein	0	0	0	24	46	3	42
5	Antithrombin-III [GS]	0	7	3	1	1	0	0
6	Apolipoprotein A-I [GS]	10	12	22	21	17	9	17
7	Apolipoprotein A-II	2	2	5	4	3	2	3
8	Apolipoprotein A-IV	3	3	11	11	11	4	7
9	Apolipoprotein B-100 [GS]	2	3	4	14	25	6	22
10	Apolipoprotein C-I	2	1	2	3	3	4	2
11	Apolipoprotein D [GS]	5	5	4	2	0	3	0
12	Apolipoprotein E G	4	4	7	7	6	0	4
13	Apolipoprotein M [GS]	4	4	1	0	2	0	0
14	cDNA FLJ14473 fis, clone MAMMA1001080	4	6	12	13	13	0	11
15	Kininogen-1 [GS]	17	13	10	8	7	13	3
16	Keratin, type II cytoskeletal 6A	3	1	3	29	6	17	8
17	Alpha-2-HS-glycoprotein [GS]	5	5	3	3	3	1	0
18	Ceruloplasmin [GS]	4	7	6	6	4	0	4
19	Complement C1s subcomponent	2	8	2	2	0	0	0
20	Complement C3 (Fragment) [GS]	0	0	9	23	27	0	16
21	Desmoglein-1 [GS]	0	0	0	0	0	3	0
22	Haptoglobin [GS]	11	13	13	10	11	7	8
23	Hemopexin [GS]	6	3	1	1	0	0	0
24	Histidine-rich glycoprotein [GS]	3	2	0	0	0	0	0
25	Hornerin [1a]	0	0	2	3	1	10	2
26	IGK@ protein	2	5	7	10	9	3	9
27	Inter-alpha inhibitor H2	3	0	5	12	4	2	0
28	Inter-alpha-trypsin inhibitor heavy chain H1	0	0	4	5	1	0	0
29	Alpha-1-antichymotrypsin [GS]	0	0	4	5	2	0	2
30	Alpha-1-antitrypsin [GS]	5	8	21	18	18	3	9
31	Complement factor H [GS]	14	6	2	0	0	6	0
32	Inter-alpha-trypsin inhibitor heavy chain H4 [GS]	3	0	5	4	5	0	4
33	Keratin, type I cytoskeletal 13	0	0	0	0	0	4	0
34	Pregnancy zone protein [1a GS]	0	0	0	0	5	0	5
35	Serum albumin	35	33	22	21	19	17	13

36	Apolipoprotein L1 G	3	2	1	1	1	0	0
37	Ig mu chain C region	0	3	8	9	10	1	8
38	Clusterin [GS]	11	12	11	6	5	0	3
39	Fibronectin [GS]	3	2	7	17	19	3	17
40	Desmoplakin[1a]	0	0	0	1	0	6	0
41	Keratin, type I cytoskeletal 10 [1a]	16	12	18	18	18	21	16
42	Keratin, type I cytoskeletal 14 [1a]	2	4	4	16	5	12	4
43	Keratin, type I cytoskeletal 16 [1a]	0	0	1	13	1	7	3
44	Keratin, type I cytoskeletal 17	0	0	0	7	0	3	0
45	Keratin, type I cytoskeletal 9	8	12	15	17	15	16	16
46	Keratin, type II cytoskeletal 1	13	14	17	23	20	25	18
47	Keratin, type II cytoskeletal 2 epidermal	8	6	10	16	15	22	13
48	Ig kappa chain V-I region EU *	8	9	7	10	11	8	10
49	Ig kappa chain V-III region WOL*	2	3	5	4	5	6	10
50	Ig kappa chain V-IV region *	1	4	6	7	5	7	6
51	Ig lambda chain V-I region WAH*	3	3	2	2	4	2	5
52	Ig lambda chain V-III region LOI *	5	2	6	5	6	6	7
53	Ig lambda chain V-III region SH *	3	2	6	7	4	6	3
54	Keratin, type II cytoskeletal 5 [1a]	1	1	4	13	7	12	5
55	Keratin, type II cytoskeletal6B	0	0	0	3	0	2	0
56	Plasma protease C1 inhibitor[GS]	0	0	4	6	3	0	1
57	Putative uncharacterized protein	2	4	6	6	6	4	6
58	Putative uncharacterized protein DKFZp686I15212	3	3	4	4	5	0	4
59	Putative uncharacterized protein DKFZp686P15220	6	9	12	13	14	5	12
60	SAA2-SAA2 protein	4	5	3	2	0	0	0
61	Serotransferrin [GS]	18	11	6	1	3	6	0
62	Serum amyloid P-component	3	2	0	0	0	0	0
63	Serum paraoxonase/arylesterase 1	0	0	7	6	4	0	2
64	Transthyretin	5	3	1	0	0	3	0
65	Uncharacterized protein	2	0	0	0	0	3	0
66	Uncharacterized protein	1	3	3	0	0	0	0
67	Uncharacterized protein	0	0	4	4	4	0	1
68	vitamin D-binding protein isoform 1 precursor	5	0	0	0	0	0	0
69	Vitamin K-dependent protein S	0	0	4	0	0	0	0
70	Vitronectin [GS]	4	3	3	3	1	0	0

G, glycoprotein; GS, sialylated glycoprotein; 1a, low abundance protein (few ng to sub μg/mL level); *, non-glycoprotein.

TABLE 3

PROTEINS IDENTIFIED BY LC-MS/MS ANALYSIS OF THE SNA CAPTURED PROTEINS FROM DISEASE-FREE AND CANCER SERA AND FRACTIONATED ON THE RPC COLUMN. DATA ON GS WERE FROM REFS. [2, 12, 15, 16, 22-25, 30, 32, 39, 43, 45, 51, 53-59]

		Disease free serum									Breast cancer serum								
#	Identified Proteins	Fr # 1	Fr # 2	Fr # 3	Fr # 4	Fr # 5	Fr # 6	Fr # 7	Fr # 8	Fr # 9	Fr # 1	Fr # 2	Fr # 3	Fr # 4	Fr # 5	Fr # 6	Fr # 7	Fr # 8	Fr # 9
1	Actin, cytoplasmic 1*	0	0	0	0	0	0	0	0	0	7	0	0	0	1	0	0	0	0
2	Afamin [GS]	0	0	0	0	4	47	20	3	0	0	0	0	0	0	42	15	0	0
3	Alpha-1-acid glycoprotein 1 [GS]	0	0	12	13	4	0	0	0	0	0	0	16	14	5	0	0	14	0
4	Alpha-1-acid glycoprotein 2 [GS]	0	0	12	11	8	8	0	4	0	0	0	17	10	6	1	2	10	0
5	Alpha-1-antichymotrypsin [GS]	0	0	0	0	0	23	36	30	26	0	0	0	0	0	8	27	0	20
6	Alpha-1-antitrypsin [GS]	2	9	15	18	42	101	180	124	65	3	7	7	3	5	52	120	3	49
7	Alpha-1B-glycoprotein [GS]	0	0	12	31	6	6	0	0	0	0	0	17	34	6	4	0	34	0
8	Alpha-2-antiplasmin [GS]	0	0	4	2	24	0	14	26	21	0	0	2	0	1	0	13	0	23
9	Alpha-2-HS-glycoprotein [GS]	0	0	22	30	0	20	15	15	18	0	0	23	34	8	20	16	34	12
10	Alpha-2-macroglobulin [GS]	0	0	2	0	0	0	15	132	169	0	2	0	0	1	0	23	0	185
11	Angiotensinogen [GS]	0	0	0	0	0	0	14	19	16	0	0	0	0	0	0	10	0	11
12	Annexin A3 [1a]	0	0	0	0	0	0	0	0	0	2	0	0	0	1	0	0	0	0
13	Antileukoproteinase	2	0	0	0	0	0	0	0	0	0	0	0	0	0	0	0	0	0
14	Antithrombin-III [GS]	0	0	12	13	33	48	20	22	16	0	0	4	11	1	33	6	11	12
15	Apolipoprotein A-I [GS]	1	4	18	15	15	88	121	90	67	0	3	15	23	6	157	138	23	92
16	Apolipoprotein A-II *	0	2	1	6	8	8	13	13	14	0	3	1	5	1	15	16	5	10
17	Apolipoprotein A-IV *	0	10	32	25	13	30	37	34	31	0	2	22	18	8	47	78	18	34
18	Apolipoprotein B-100 [GS]	0	2	11	2	0	0	0	19	156	0	2	6	2	3	0	1	2	112
19	Apolipoprotein C-I *	0	0	4	12	7	0	0	0	1	0	0	9	20	3	10	3	20	2

20	Apolipoprotein C-II *	0	0	0	4	7	7	1	0	4	0	2	2	3	1	13	4	3	0
21	Apolipoprotein C-III [G]	0	0	4	13	13	6	4	1	6	0	0	8	13	3	10	6	13	6
22	Apolipoprotein D [GS]	0	3	8	1	10	22	15	9	9	0	5	15	11	7	29	21	11	14
23	Apolipoprotein E [G]	0	5	4	5	4	1	10	34	40	0	0	2	4	1	8	25	4	54
24	Apolipoprotein L1 [G]	0	0	0	2	10	0	0	4	13	0	0	0	9	0	0	0	9	23
25	Apolipoprotein M [GS]	0	0	0	0	12	5	2	4	0	0	0	0	1	0	7	2	1	5
26	Attractin [1a]	0	0	0	1	28	6	0	0	0	0	0	0	13	0	2	0	13	0
27	Beta-2-glycoprotein 1 [GS]	0	22	31	11	7	0	0	1	4	0	25	27	10	17	4	2	10	3
28	Beta-2-microglobulin [GS]	0	4	0	0	0	0	0	0	0	0	5	0	0	2	0	0	0	0
29	Beta-Ala-His dipeptidase [1a]	0	0	0	0	0	0	0	8	20	0	0	0	0	0	0	0	0	14
30	Biotinidase [GS]	0	0	0	0	0	3	0	0	0	0	0	0	0	0	0	0	0	0
31	C4b-binding protein alpha chain [G]	0	0	0	0	0	0	0	0	0	0	0	5	2	2	0	0	2	0
32	Cadherin-5 [GS]	0	0	1	0	0	0	0	0	0	0	0	3	0	1	0	0	0	0
33	Calmodulin-like protein 5 [1a]	0	0	0	0	0	0	0	0	0	1	0	2	0	0	0	0	0	0
34	Carboxypeptidase B2 [GS 1a]	0	0	0	0	27	6	0	0	0	0	0	0	0	0	9	0	0	0
35	Carboxypeptidase N catalytic chain [GS1a]	0	0	0	0	0	24	2	1	1	0	0	0	0	0	20	0	0	0
36	Carboxypeptidase N subunit 2 [GS]	0	0	0	0	1	0	0	0	7	0	0	0	0	0	0	0	0	10
37	Cartilage acidic protein 1 [G]	0	0	0	0	0	0	0	0	0	0	0	0	1	0	2	0	1	0
38	Cathelicidinant-imicrobial peptide [1a]	0	0	0	0	3	0	0	0	0	0	0	0	0	0	0	0	0	0
39	CD5 antigen-like *	0	0	0	0	0	6	4	3	1	0	0	0	0	0	15	9	0	8
40	Ceruloplasmin [GS]	0	0	4	15	97	70	51	54	47	0	0	5	12	2	65	56	12	44
41	Cholinesterase [1a]	0	0	0	0	0	1	0	1	4	0	0	0	0	0	2	1	0	3
42	Clusterin [GS]	0	0	0	7	42	38	8	11	11	0	0	0	17	0	34	11	17	9
43	Coagulation factor IX [GS 1a]	0	0	3	6	6	0	0	2	4	0	0	0	7	0	4	0	7	6
44	Coagulation factor V [GS1a]	0	0	5	0	0	0	0	0	0	0	0	4	0	1	0	0	0	0
45	Coagulation factor VII [GS]	0	0	0	0	0	1	0	0	0	0	0	0	0	0	0	0	0	0
46	Coagulation factor X [GS]	0	0	0	0	0	0	0	0	0	0	0	8	0	3	0	0	0	0
47	Coagulation factor XII [GS]	0	0	0	15	3	0	0	8	5	0	0	0	15	0	0	0	15	0

48	Coagulation factor XIII B chain [GS 1a]	0	0	88	12	2	0	0	0	0	0	0	87	10	29	0	0	10	0
49	Complement C1r subcomponent	3	0	0	27	10	0	0	0	0	0	0	0	57	0	0	6	57	0
50	Complement C1r subcomponent-like protein [GS1a]	0	0	0	11	1	2	0	0	0	0	0	0	11	0	0	0	11	0
51	Complement C1s subcomponent [GS]	0	0	0	0	49	11	2	6	3	0	0	0	0	0	6	6	0	0
52	Complement C2 [G]	0	0	0	0	0	0	0	0	16	0	0	0	0	0	0	0	0	0
53	Complement C3 [GS]	5	3	1	19	17	143	81	303	220	2	0	0	1	1	62	84	1	229
54	Complement C4-A [GS]	0	0	0	0	0	0	0	64	0	0	0	0	0	0	0	63	0	0
55	Complement C4-B [GS]	0	0	0	0	6	54	56	67	51	0	0	0	0	0	52	96	0	78
56	Complement C5 [G]	0	0	0	0	0	0	9	54	51	0	0	0	0	0	0	6	0	50
57	Complement component C6 [G]	0	0	0	43	26	0	0	0	0	0	0	0	57	0	1	0	57	0
58	Complement component C7 [G]	0	0	0	1	4	0	0	0	0	0	0	0	11	0	0	0	11	0
59	Complement component C8 alpha chain [G]	0	0	0	0	10	0	0	0	0	0	0	0	0	0	0	0	0	0
60	Complement component C8 beta chain [G]	0	0	0	0	9	0	0	0	0	0	0	0	0	0	0	0	0	0
61	Complement component C8 gamma chain [G]	0	0	0	0	9	0	0	0	0	0	0	0	0	0	0	0	0	0
62	Complement component C9 [G]	0	0	0	0	0	16	1	1	0	0	0	0	0	0	12	0	0	0
63	Complement factor B [G]	0	0	8	4	56	34	9	21	14	0	0	10	4	3	24	5	4	13
64	Complement factor H [GS]	0	2	66	5	0	0	0	10	1	0	46	101	25	49	2	7	25	1
65	Complement factor H-related protein 1 [GS]	0	2	3	0	0	0	0	0	0	0	8	11	0	7	0	0	0	0
66	Complement factor H-related protein 2 [GS]	0	4	11	0	0	0	0	0	0	0	6	13	0	6	0	0	0	0
67	Complement factor H-related protein 3 [GS1a]	0	0	5	0	0	0	0	0	0	0	5	0	0	2	0	0	0	0
68	Complement factor H-related protein 4 [GS1a]	0	0	8	0	0	0	0	0	0	0	0	5	0	2	0	0	0	0

69	Complement factor H-related protein 5 [GS]	0	0	6	0	0	0	0	0	0	0	0	4	0	1	0	0	0	0
70	Complement factor I [G]	0	0	0	55	32	22	13	18	15	0	0	0	65	0	14	17	65	11
71	Corticosteroid-binding globulin	0	0	0	0	0	0	0	0	2	0	0	0	0	0	0	0	0	2
72	Cystatin-C [GS]	0	0	0	0	0	0	0	0	0	0	0	2	0	0	0	0	0	0
73	Cysteine-rich secretory protein 3 [GS]	0	0	3	0	0	0	0	0	0	0	0	0	0	0	0	0	0	0
74	Dermcidin [1a]	1	0	1	0	0	0	0	0	0	0	0	0	0	0	0	0	0	0
75	Desmoplakin *[1a]	0	0	0	0	0	0	0	0	0	3	0	0	0	1	0	0	0	0
76	Extracellular matrix protein 1 [G1a]	0	0	8	0	0	0	0	0	0	0	0	17	0	6	0	0	0	0
77	Extracellular superoxide dismutase [Cu-Zn] [GS1a]	0	0	2	0	0	0	0	0	0	0	0	0	0	0	0	0	0	0
78	Fetuin-B [GS1a]	0	0	0	17	13	2	0	2	0	0	0	0	19	0	4	1	19	0
79	Fibrinogen alpha chain [GS]	9	6	0	0	0	0	0	1	0	10	5	0	0	5	0	0	0	0
80	Fibrinogen beta chain [GS]	0	0	0	0	1	0	0	0	0	0	0	0	0	0	0	0	0	0
81	Fibronectin [GS]	2	3	10	0	0	36	27	36	33	0	5	3	0	3	35	27	0	26
82	Fibulin-1 [GS]	0	0	0	0	2	0	0	0	0	0	0	0	0	0	0	0	0	0
83	Ficolin-2 [GS]	0	0	0	2	0	0	0	0	0	0	0	0	0	0	1	0	0	0
84	Ficolin-3 [GS1a]	0	0	0	1	5	10	8	13	13	0	0	0	4	0	11	10	4	11
85	Galectin-3-binding protein [1a GS]	0	0	2	0	0	0	0	0	5	0	0	0	0	0	0	0	0	14
86	Galectin-7 [1a]	0	4	8	0	5	0	0	0	0	3	0	0	0	1	7	10	0	0
87	Gamma-A of Fibrinogen gamma chain [GS]	0	0	0	0	1	2	0	0	0	0	0	0	0	0	0	0	0	0
88	Gelsolin [1a]	0	0	0	0	0	5	0	0	0	0	0	0	0	0	2	0	0	0
89	Haptoglobin [GS]	6	8	78	100	92	88	79	83	81	4	8	90	106	34	79	65	106	68
90	Haptoglobin-related protein*	0	0	0	52	52	49	44	45	43	0	0	0	54	0	47	42	54	37
91	Hemoglobin subunit alpha [G]	0	0	0	0	20	5	0	0	0	0	4	0	7	1	25	9	7	9
92	Hemoglobin subunit beta [G]	0	0	0	0	21	11	0	4	2	0	0	0	10	0	22	12	10	15
93	Hemoglobin subunit delta [G]	0	0	0	0	0	0	2	0	0	0	0	0	0	0	0	1	0	0
94	Hemopexin [GS]	2	0	4	67	42	22	16	13	14	0	0	4	73	1	16	15	73	9
95	Heparin cofactor 2 [GS]	0	0	0	0	0	21	22	21	20	0	0	0	0	0	14	20	0	19

96	Hepatocyte growth factor-like protein [G]	0	0	8	0	0	0	0	0	0	0	0	3	0	1	0	0	0	0
97	Histidine-rich glycoprotein [GS]	0	0	23	28	10	5	1	4	3	0	0	39	32	13	5	5	32	5
98	Hornerin *1a	0	0	4	0	0	0	0	0	0	0	0	0	0	0	0	0	0	0
99	Hyaluronan-binding protein 2 *	0	0	0	15	6	0	0	0	0	0	0	0	19	0	1	0	19	0
100	Hydrocephalus-inducing protein homolog *	0	0	0	0	3	0	0	0	0	0	0	0	1	0	0	0	2	0
101	Ig alpha-1 chain C region [G]	0	0	0	3	39	39	41	35	31	0	0	0	12	0	46	40	12	36
102	Ig alpha-2 chain C region [G]	0	0	0	0	31	34	32	28	0	0	0	0	0	0	33	30	0	19
103	Ig gamma-1 chain C region [G]	0	2	3	8	11	13	9	10	10	1	1	0	8	1	9	7	8	11
105	Ig kappa chain C region *	0	2	17	12	24	24	20	24	22	0	6	19	14	8	22	22	14	24
106	Ig kappa chain V-III region WOL *	0	3	4	0	1	3	5	4	3	0	4	0	1	1	5	5	1	5
107	Ig lambda-2 chain C regions *	0	0	12	0	11	15	15	14	16	0	0	12	0	4	17	5	0	10
108	Ig mu chain C region [GS]	0	0	0	4	17	21	17	22	25	0	0	0	9	0	34	31	9	32
109	Immunoglobulin J chain [GS]	1	0	0	0	7	3	5	3	6	3	0	0	0	1	6	6	0	6
110	Immunoglobulin lambda-like polypeptide 5 *	0	1	8	8	14	15	11	11	11	0	2	7	9	3	15	14	9	13
111	Insulin-like growth factor-binding protein 3 [GS]	0	0	0	0	0	0	0	0	0	5	0	0	0	2	0	0	0	0
112	Insulin-like growth factor-binding protein complex acid labile subunit [GS]	0	2	4	0	0	0	0	8	0	0	0	0	0	0	0	0	0	1
113	Inter-alpha-trypsin inhibitor heavy chain H1 [GS]	0	0	0	4	2	50	80	64	28	0	0	0	0	0	36	92	0	32
114	Inter-alpha-trypsin inhibitor heavy chain H2 [GS]	0	7	7	7	9	30	86	69	42	0	3	9	4	4	11	112	4	52
115	Inter-alpha-trypsin inhibitor heavy chain H3 [GS]	0	0	0	0	0	19	6	0	0	0	0	0	0	0	15	5	0	0
116	Inter-alpha-trypsin inhibitor heavy chain H4 [GS]	0	0	0	8	14	23	66	43	39	0	0	0	18	0	47	88	18	64
117	Intercellular adhesion molecule 2 [1a]	0	0	0	0	0	0	0	0	0	0	0	1	0	0	0	0	0	0

118	Junction plakoglobin *[1a]	0	0	1	0	0	0	0	0	0	0	0	0	0	0	0	0	0	0
119	Kallistatin [GS]	0	0	0	0	0	0	12	18	8	0	0	0	0	0	0	22	0	11
120	Keratin, type I cytoskeletal 10 [1a]	17	28	42	14	32	13	14	28	28	35	33	30	8	33	19	23	8	58
121	Keratin, type I cytoskeletal 14 [1a*]	12	13	36	0	0	0	0	0	11	37	14	16	0	23	0	0	0	21
122	Keratin, type I cytoskeletal 16 [1a]	0	0	30	0	0	0	0	0	0	30	12	0	0	14	0	0	0	0
123	Keratin, type I cytoskeletal 17 [1a]	0	0	14	0	0	0	0	0	0	45	0	0	0	15	0	0	0	0
124	Keratin, type I cytoskeletal 9*	25	33	44	7	18	11	15	22	48	27	25	25	16	26	16	10	16	38
125	Keratin, type II cytoskeletal 1*	30	39	58	18	34	25	20	26	46	39	33	45	22	39	20	15	22	59
126	Keratin, type II cytoskeletal 2 epidermal*	16	33	51	12	31	14	5	24	29	20	33	25	9	26	14	9	9	62
127	Keratin, type II cytoskeletal 5* [1a]	8	24	33	0	0	0	0	6	11	40	16	5	0	20	0	0	0	23
128	Keratin, type II cytoskeletal 6A *	10	12	30	0	0	1	0	0	5	44	16	13	0	24	0	0	0	18
129	Keratin, type II cytoskeletal 6B *	0	0	0	0	0	0	0	0	0	43	0	0	0	14	0	0	0	0
130	Keratin, type II cytoskeletal 6C*	0	0	0	0	0	0	0	0	0	44	0	0	0	15	0	0	0	0
131	Keratinocyte proline-rich protein	0	0	0	0	1	0	0	0	0	0	0	0	0	0	0	0	0	0
132	Leucine-rich alpha-2-glycoprotein [GS]	0	0	0	0	0	12	0	0	0	0	0	0	0	0	8	0	0	0
134	Leukocyte immunoglobulin-like receptor subfamily A member 3 [G]	0	0	3	0	0	0	0	0	0	0	0	2	0	1	0	0	0	0
135	LMW of Kininogen-1 [GS]	2	6	75	75	48	43	34	33	30	0	7	93	89	33	48	43	89	36
136	immunoglobulin gamma Fc region receptor III-A [G]	0	0	0	0	0	0	0	0	0	0	0	5	0	2	0	0	0	0
137	Lumican [GS]	0	0	0	2	0	0	1	0	0	0	0	0	0	1	0	3	0	0
138	Lysozyme C [1a]	2	0	4	0	0	0	0	0	0	0	0	1	0	0	0	0	0	0
139	Mannan-binding lectin serine protease 1 *[1a]	0	0	0	0	6	4	0	0	4	0	0	0	1	0	5	0	1	3
140	Mannan-binding lectin serine protease 2 *	0	0	0	0	0	0	0	0	0	0	0	6	0	2	0	0	0	0
141	Mannose-binding protein C *	0	1	0	0	3	0	0	0	0	0	0	3	0	0	0	0	1	0
142	Monocyte differentiation antigen CD14 [G]	0	2	0	0	0	1	0	0	0	0	0	0	0	0	0	0	0	0

143	N-acetylglucosamine-1-phosphotransferase subunit gamma[GS 1a]	0	0	0	0	1	0	0	0	0	0	0	0	0	0	0	0	0	0
144	N-acetylmuramoyl-L-alanine amidase [GS]	0	0	0	0	0	11	0	2	1	0	0	0	0	0	11	0	0	0
145	Ovalbumin [GS]	0	7	15	12	19	26	37	35	27	0	7	12	4	6	25	29	4	24
146	Peroxiredoxin-2*	0	0	0	0	0	0	0	0	0	0	0	0	0	0	1	0	0	0
147	Phosphatidylcholine-sterol acyltransferase [1a]	0	0	0	0	0	13	2	0	0	0	0	0	0	0	10	0	0	0
148	Phosphatidylinositol-glycan-specific phospholipase D [GS1a]	0	0	0	0	0	0	0	19	10	0	0	0	0	0	0	1	0	13
149	Plasma kallikrein heavy chain [GS]	0	0	0	5	15	0	0	14	24	0	0	0	8	0	0	0	8	18
150	Plasma protease C1 inhibitor [GS]	0	0	2	0	0	0	5	2	6	0	0	0	0	0	1	7	0	8
151	Plasma serine protease inhibitor [GS]	0	0	0	0	0	0	0	0	10	0	0	0	0	0	0	0	0	13
152	Plasminogen [GS]	0	0	67	55	0	0	0	0	0	0	2	77	40	26	0	0	40	0
153	Pregnancy zone protein [GS1a]	0	0	0	0	0	0	0	20	52	0	0	0	0	0	0	0	0	57
154	Pregnancy-specific beta-1-glycoprotein 1 [GS]	0	0	0	0	0	0	0	0	0	0	0	19	12	6	4	0	12	0
155	Prenylcysteine oxidase 1 [G]	0	0	0	0	0	0	0	0	0	0	0	0	0	0	0	0	0	2
156	Protein AMBP [GS]	0	0	0	13	15	15	20	17	9	0	0	4	16	1	17	23	16	13
157	Protein S100-A8 [1a]	0	0	0	0	0	0	0	0	0	2	0	0	0	1	0	0	0	0
158	Protein S100-A9	0	0	0	0	0	0	0	0	0	5	0	0	0	2	0	0	0	1
159	Protein Z-dependent protease inhibitor [G1a]	0	0	0	0	0	5	0	2	0	0	0	0	0	0	0	0	0	5
160	Prothrombin	0	6	6	37	20	12	3	10	15	1	8	7	21	5	14	4	21	11
161	Retinol-binding protein 4 *	0	0	6	9	8	7	7	1	0	0	0	12	9	4	8	4	9	4
163	Secreted phosphoprotein 24[G 1a]	0	0	0	0	0	0	0	0	0	0	0	4	0	1	0	0	0	0
164	Selenoprotein P [G1a]	0	0	10	4	0	0	0	0	0	0	0	12	5	4	0	2	5	0
165	Serotransferrin [GS]	0	0	103	105	47	23	14	18	14	0	0	132	113	44	37	18	113	16
166	Serpin B3 *	0	0	0	0	0	0	0	0	0	1	0	0	0	0	0	0	0	0

167	Serum albumin [G]	6	8	32	110	98	101	90	78	66	3	10	26	216	13	114	94	216	78
168	Serum amyloid A-1 protein [GS]	0	0	0	0	0	0	0	0	0	0	0	0	5	0	0	0	5	0
169	Serum amyloid A-4 protein [GS]	0	0	0	1	6	3	5	2	3	0	0	0	9	0	6	4	9	2
170	Serum amyloid P-component [GS]	0	0	0	0	21	12	12	7	10	0	0	0	2	0	13	9	2	8
171	Serumparaoxonase/ arylesterase 1 [GS]	0	0	0	0	0	12	12	11	10	0	0	0	0	0	17	12	0	11
172	Serumparaoxonase/ lactonase 3 [G]	0	0	0	0	0	1	4	4	0	0	0	0	0	0	3	5	0	1
173	Sex hormone-binding globulin	0	0	0	0	10	0	0	0	0	0	0	0	0	0	0	0	0	0
174	Tetranectin [G]	0	0	10	9	3	0	0	0	0	0	0	10	5	3	0	0	5	0
175	Transthyretin *	0	0	0	0	0	0	1	3	4	0	0	0	0	0	0	3	0	2
176	Trypsin-1 [1a]	0	7	0	0	5	0	0	0	0	0	0	0	0	0	0	0	0	0
177	Ubiquitin*	0	0	8	20	18	10	10	10	2	0	0	3	19	1	5	5	19	0
178	Vitamin D-binding protein [GS]	7	9	9	8	9	9	5	7	9	7	8	7	10	7	7	4	10	7
179	Vitamin K-dependent protein C [1a]	2	0	0	0	0	0	0	0	0	3	0	0	0	1	0	0	0	0
180	Vitamin K-dependent protein S	0	0	0	17	10	0	0	0	0	0	0	0	30	0	0	0	30	0
181	Vitamin K-dependent protein Z [GS1a]	0	0	0	12	9	0	0	0	0	0	0	0	13	0	0	0	13	0
182	Vitronectin [GS]	0	0	0	0	0	24	9	6	6	0	0	0	0	0	23	14	0	7
183	von Willebrand factor [1a GS]	0	0	9	0	0	0	0	0	0	0	0	21	4	7	0	0	4	0
184	Zinc-alpha-2-glycoprotein [GS]	1	0	0	25	23	16	12	13	14	0	0	3	34	1	13	10	34	12

G, glycoprotein; GS, sialylated glycoprotein; 1a, low abundance protein (few ng to sub μg/mL level); *, non-glycoprotein.

TABLE 4

PROTEINS IDENTIFIED BY LC-MS/MS ANALYSIS OF THE MAL-II CAPTURED PROTEINS FROM DISEASE –FREE AND CANCER SERA AND FRACTIONATED ON THE RPC COLUMN.. DATA ON GS WERE FROM REFS. [2, 12, 16, 23, 24, 27, 43, 45, 51, 56, 57, 59-61]

		Average Spectral count for disease-free serum								Average Spectral count for cancer serum							
	Identified proteins (AAL)	Fr # 1	Fr # 2	Fr # 3	Fr # 4	Fr # 5	Fr # 6	Fr # 7	Fr # 8	Fr # 1	Fr # 2	Fr # 3	Fr # 4	Fr # 5	Fr # 6	Fr # 7	Fr # 8
1	Actin, cytoplasmic 1 *	2	5	0	0	0	0	0	0	0	0	0	0	0	0	0	0
2	Afamin [GS]	0	0	0	0	15	11	0	0	0	0	0	0	17	10	0	0
3	Alpha-1-acid glycoprotein 1 [GS]	0	5	4	0	0	2	0	0	0	4	3		3	0	0	0
4	Alpha-1-acid glycoprotein 2 [GS]	0	4	5	4	3	3	3	0	0	5	5	4	4	4	2	2
5	Alpha-1-antichymotrypsin [GS]	0	0	0	0	8	14	12	9	0	0	0	0	5	14	11	9
6	Alpha-1-antitrypsin [GS]	3	2	3	6	17	24	24	14	2	2	0	2	8	25	21	17
7	Alpha-1B-glycoprotein [GS]	0	0	10	0	2	0	2	0	0	2	9	3	3	3	2	2
8	Alpha-2-antiplasmin [GS]	0	0	0	0	0	3	8	3	0	0	0	0	0	4	11	10
9	Alpha-2-HS-glycoprotein [GS]	0	3	6	5	6	6	7	5	0	5	6	5	7	7	6	6
10	Alpha-2-macroglobulin [GS]	0	0	0	0	0	3	51	50	0	0	0		0	7	50	55
11	Alpha-enolase	2	0	0	0	0	0	0	0	0	0	0	0	0	0	0	0
12	Alpha-S1-casein	0	0	0	0	0	0	0	0	0	0	2	0	0	0	0	0
13	Angiotensinogen [GS]	0	0	0	0	0	2	6	0	0		0	0	0	4	8	4
14	Annexin A2 [1a]	3	0	0	0	0	0	0	0	0	0	0	0	0	0	0	0
15	Antithrombin-III [GS]	0	0	0	7	14	3	4	4	0	0	0	8	8	3	2	2
16	Apolipoprotein A-I [GS]	0	3	7	7	23	29	25	21	2	3	6	10	27	33	25	24

17	Apolipoprotein A-II *	0	0	3	4	4	3	3	4	2	2	3	4	3	3	4	4
18	Apolipoprotein A-IV *	6	11	8	6	11	18	14	3	5	5	5	0	10	19	18	16
19	Apolipoprotein B-100 [GS]	0	0	0	0	3	2	9	100	0	0	0		0	3	6	39
20	Apolipoprotein C-I*	0	2	3	2	0	2	2	0	0	2	4	4	3	2	4	3
21	Apolipoprotein C-II*	0	0	0	0	3	2	0	0	2	2	0	2	2	2	0	0
22	Apolipoprotein C-III [G]	0	0	2	2	2	2	2	2	0	2	0	2	2	3	0	2
23	Apolipoprotein D [GS]	0	0	0	2	7	7	6	2	0	0	0	3	7	7	6	6
24	Apolipoprotein E [G]	0	0	0	0	0	5	12	11	2	0	0	0	0	7	14	15
25	Apolipoprotein L1 [G]	0	0	2	4	4	2	3	3	0	0	2	4	2	2	6	8
26	Apolipoprotein M [GS]	0	0	0	4	4	2	4	0	0	0	0	5	3	3	4	3
27	Arginase-1	3	0	0	0	0	0	0	0	0	0	0	0	0	0	0	0
28	Beta-2-glycoprotein 1 [GS]	9	10	5	4	3	2	2	0	11	9	3	4	3	2	0	2
29	Beta-2-microglobulin [GS]	2	0	0	0	0	0	0	0	2	0	0	0	0	0	0	0
30	Beta-Ala-His dipeptidase [1a]	0	0	0	0	0	0	4	0	0	0	0	0	0	0	8	9
31	Bone marrow proteoglycan [GS]	0	0	0	0	0	0	0	0	0	0	0	0	0	2	0	0
32	Carboxypeptidase B2 [G 1a]	0	0	0	0	2	2	0	0	0	0	0	0	3	0	0	0
33	Carboxypeptidase N catalytic chain [G1a]	0	0	0	3	4	0	0	0	0	0	0	6	2	0	0	0
34	Carboxypeptidase N subunit 2 [G]	0	0	0	0	0	0	2	3	0	0	0	0	0	0	0	5
35	Cartilage oligomeric matrix protein [G1a]	0	0	0	0	3	0	0	0	0	0	0	0	2	0	0	0
36	Cathelicidin antimicrobial peptide [1a]	0	0	0	0	0	0	0	0	0	0	0	3	0	0	0	0
37	CD5 antigen-like*	0	0	0	0	2	0	0	0	0	0	0	0	3	4	2	3
38	Ceruloplasmin [GS]	0	0	5	25	21	19	21	12	0	0	3	24	23	21	16	19
39	Cholinesterase [1a]	0	0	0	0	2	0	2	2	0	0	0	0	2	0	2	2
40	Clusterin [GS]	0	0	0	9	9	3	3	0	0		0	9	7	4	2	2
41	Coagulation factor IX [GS1a]	0	0	0	0	0	0	0	0	0	0	0	7	0	0	3	0
42	Coagulation factor X [GS]	0	3	0	0	0	0	0	0	0	2	0	0	0	0	0	0
43	Coagulation factor XII [GS]	0	0	5	2	0	0	2	0	0	0	8	3	0	0	0	0
44	Complement C1r subcomponent [GS]	0	0	3	0	0	0	0	0	0	0	3	0	0	2	0	0
45	Complement C1s subcomponent G [GS]	0	0	0	14	8	5	2	0	0	0	0	19	7	5	2	3
46	Complement C2 G	0	0	0	0	0	0	0	0	0	0	0	0	0	0	2	2
47	Complement C3 G	0	0	6	6	45	45	97	59	0	0	0	0	57	59	106	93
48	Complement C4-A [GS]	0	0	0	0	0	0	2	0	0	0	0	0	0	2	0	0

49	Complement C4-B G	0	0	0	0	32	38	43	21	0	0	0		37	60	48	41
50	Complement C5 G	0	0	0	0	0	0	20	10	0	0	0	0	0	3	24	27
51	Complement component C6 G	0	0	10	4	0	0	0	0	0	0	9	8	0	0	0	0
52	Complement component C7 G	0	0	7	12	0	0	0	0	0	0	10	13	0	0	0	0
53	Complement component C8 alpha chain G	0	0	0	7	4	3	0	0	0		0	8	3	3	0	2
54	Complement component C8 beta chain G	0	0	0	8	0	0	0	0	0	0	0	8	0	0	0	0
55	Complement component C8 gamma chain G	0	0	0	5	0	0	0	0	0	0	0	6	0	2	0	0
56	Complement component C9 [G]	0	0	0	0	16	10	7	3	0	0	0	2	16	11	7	7
57	Complement factor B [G]	0	0	0	23	19	10	10	2	0	0	0	22	19	7	9	8
58	Complement factor H [GS]	0	8	2	0	0	0	2	0	2	22	2	0	0	0	0	0
59	Complement factor H-related protein 1 [GS]	0	0	0	0	0	0	0	0	2	0	0	0	0	0	0	0
60	Complement factor H-related protein 2 [G]	0	2	0	0	0	0	0	0	0	0	0	0	0	0	0	0
61	Complement factor I [G]	0	0	16	13	10	6	9	2	0	0	19	13	8	6	6	5
62	Corneodesmosin [GS]	0	2	0	0	0	0	0	0	0	0	0	0	0	0	0	0
63	Cornifin-A	0	2	0	0	0	0	0	0	0	0	0	0	0	0	0	0
64	Corticosteroid-binding globulin G	0	0	0	0	0	0	3	2	0	0	0	0	0	0	4	2
65	Dermcidin [1a]	3	0	0	0	0	2	2	0	2	2	0	0	0	0	0	3
66	Desmocollin-1[G 1a]	0	0	0	0	0	0	0	0	0	0	0	0	4	0	2	0
67	Desmoglein-1[G1a]	0	0	0	0	0	0	0	0	0	7	0	8	0	0	0	0
68	Desmoplakin *[1a]	36	26	0	0	0	0	0	4	0	3	0	0	0	0	2	6
69	Extracellular matrix protein 1 [G1a]	0	3	0	0	0	0	0	0	0	8	0	0	0	0	0	0
70	Fatty acid-binding protein, epidermal [G]	0	5	0	0	0	0	0	0	0	0	0	0	0	0	0	0
71	Fetuin-B [GS 1a]	0	0	2	2	2	0	0	0	0	0	2	2	0	0	0	0
72	Fibrinogen alpha chain [G]	3	0	0	0	0	0	0	0	3	0	0	0	0	0	0	0
73	Fibronectin [GS]	0	0	0	0	3	2	7	11	0	0	0	0	2	4	5	8
74	Ficolin-3 [GS1a]	0	0	0	0	3	3	5	3	0	0	0	0	3	4	4	4
75	Filaggrin [1a]	2	0	0	0	0	0	0	0	0	0	0	0	0	0	0	0
76	Filaggrin-2 [1a]	3	2	0	0	0	0	0	0	0	0	0	0	0	0	0	2
77	Galectin-3-binding protein[1a GS]	0	0	0	0	0	0	0	0	0	0	0	0	0	0	0	2
78	Galectin-7 [1a]	0	0	0	0	0	0	0	0	0	0	0	0	4	0	1	0
79	Gelsolin *	0	0	0	2	4	0	0	0	0	0	0	2	3	0	0	0
80	Glyceraldehyde-3-phosphate dehydrogenase [1a]	4	0	0	0	0	0	0	0	0	0	0	0	0	0	0	0

81	Haptoglobin [GS]	2	20	25	25	24	24	23	20	2	21	24	24	23	23	19	20
82	Haptoglobin-related protein *	0	0	4	4	3	4	4	2	0	0	4	3	4	4	4	2
83	Hemoglobin subunit alpha [G]	0	0	0	0	2	0	0	0	0	0	0	6	5	2	0	3
84	Hemoglobin subunit beta [G]	0	0	0	2	0	0	0	0	0	0	0	8	6	6	4	4
85	Hemopexin [GS]	0	0	14	10	6	7	6	2	0	0	15	9	8	6	3	5
86	Heparin cofactor 2 [GS]	0	0	0	0	2	8	7	3	0	0	0	0	4	7	6	6
87	Histidine-rich glycoprotein [GS]	0	3	4	4	2	3	3	0	0	3	4	4	2	3	3	2
88	Histone H4 [1a]	0	2	0	0	0	0	0	0	0	0	0	0	0	0	0	0
89	Hornerin *[1a]	10	4	0	2	0	2	0	2	0	3	0	0	0	0	0	2
90	Hyaluronan-binding protein 2	0	0	5	2	0	0	0	0	0	0	5	2	0	0	0	0
91	Ig alpha-1 chain C region	0	0	0	9	8	8	9	7	0	0	4	9	8	10	10	9
92	Ig gamma-1 chain C region	0	0	3	5	6	6	7	6	0	0	3	6	6	6	7	7
93	Ig kappa chain C region *	0	3	0	5	5	5	6	5	0	3	4	6	5	7	6	5
94	Ig mu chain C region [GS]	0	0	0	6	9	5	10	6	0	0	2	12	10	7	12	11
95	Immunoglobulin J chain [GS]	0	0	0	2	3	0	2	0	0	0	0	3	3	4	3	3
96	Immunoglobulin lambda-like polypeptide 5	0	3	2	5	5	4	5	4	0	2	2	6	5	5	5	4
97	Insulin-like growth factor-binding protein complex acid labile subunit	0	0	0	0	0	0	3	0	0	0	0	0	0	0	5	0
98	Inter-alpha-trypsin inhibitor heavy chain H1	0	0	2	2	12	15	17	8	0	0	0	0	14	20	14	10
99	Inter-alpha-trypsin inhibitor heavy chain H2 [GS]	3	3	3	3	5	19	22	9	0	3	0	0	3	27	22	13
100	Inter-alpha-trypsin inhibitor heavy chain H3 [GS]	0	0	0	0	5	3	0	0	0	0	0	0	6	3	0	0
101	Inter-alpha-trypsin inhibitor heavy chain H4 [GS]	0	0	3	10	6	17	15	16	0	0	3	10	8	27	17	21
102	Junction plakoglobin *[1a]	0	0	0	0	0	0	0	0	0	0	0	7	0	0	8	0
103	Kallistatin [GS]	0	0	0	0	0	5	12	4	0	0	0	0	0	11	10	3
104	Keratin, type I cytoskeletal 10 *[1a]	19	20	10	17	14	21	18	18	16	18	13	17	15	21	20	20
105	Keratin, type I cytoskeletal 13 [1a]	0	0	0	2	0	2	0	0	0	0	4	0	0	0	0	0
106	Keratin, type I cytoskeletal 14* [1a]	23	22	2	12	8	12	8	15	13	18	4	7	5	11	14	18
107	Keratin, type I cytoskeletal 16 *[1a]	10	13	0	0	0	0	2	7	5	11	2	0	0	5	3	5
108	Keratin, type I cytoskeletal 17 *[1a]	2	3	0	2	0	0	0	3	0	3	0	0	0	0	2	2
109	Keratin, type I cytoskeletal 9*	30	28	9	20	14	19	13	19	17	20	12	11	12	22	23	19
110	Keratin, type I microfibrillar	0	0	0	0	0	0	0	0	0	0	0	0	0	7	0	0
111	Keratin, type II cuticular Hb3	0	0	0	0	0	0	0	0	0	0	0	0	0	3	0	0

112	Keratin, type II cytoskeletal 1	36	34	18	31	22	30	24	32	23	32	23	23	20	26	30	33
114	Keratin, type II cytoskeletal 2 epidermal*	22	15	10	18	12	22	16	24	15	22	13	16	13	20	19	24
115	Keratin, type II cytoskeletal 4	2	0	0	0	0	0	0	0	0	2	0		0	0	0	0
116	Keratin, type II cytoskeletal 5 *[1a]	33	32	4	14	7	13	9	22	15	24	6	8	5	12	14	25
117	Keratin, type II cytoskeletal 6A *	2	2	0	0	0	0	0	0	2	2	0	0	0	0	0	0
118	Keratin, type II cytoskeletal 6C *	19	17	0	5	0	0	4	7	11	15	2	0	0	5	3	5
120	Keratin, type II cytoskeletal 78*	6	2	0	0	0	0	0	0	0	0	0	0	0	0	0	0
121	Keratin, type II cytoskeletal 80	4	2	0	0	0	0	0	0	0	0	0	0	0	0	0	0
122	Keratin, type II microfibrillar	0	0	0	0	0	0	0	0	0	0	0	0	0	6	0	0
123	Keratin, type II microfibrillar	0	0	0	0	0	0	0	0	0	0	0	0	0	2	0	0
124	Keratinocyte proline-rich protein	0	3	0	0	0	0	0	0	0	0	0	0	0	2	0	0
125	Leucine-rich alpha-2-glycoprotein [GS]	0	0	0	0	2	0	0	0	0	0	0	0	10	0	0	0
126	LMW of Kininogen-1 [GS]	3	19	25	24	19	22	20	10	4	24	26	26	23	22	21	22
127	Lumican G [GS]	0	0	0	8	0	0	0	0	0	0	0	7	0	0	0	0
128	Mannan-binding lectin serine protease*[1a]	0	0	0	0	2	0	0	0	0	0	0	0	2	0	0	0
129	N-acetylmuramoyl-L-alanine amidase G [GS]	0	0	0	0	5	3	0	0	0	0	0		6	0	0	0
130	Ovalbumin [GS]	4	5	6	7	8	11	12	11	3	4	2	6	10	11	11	9
131	Peroxiredoxin-1 *	2	2	0	0	0	0	0	0	0	0	0	0	0	0	0	0
132	Peroxiredoxin-2*	3	0	0	0	0	0	0	0	0	0	0	0	4	4	2	0
133	Phosphatidylcholine-sterol acyltransferase [1a]	0	0	0	0	2	0	0	0	0	0	0	0	2	0	0	0
134	Phosphatidylinositol-glycan-specific phospholipase D [GS1a]	0	0	0	0	0	0	6	0	0	0	0	0	0	0	7	6
135	Pigment epithelium-derived factor	0	0	0	0	0	0	4	0	0	0	0	0	0	0	6	3
136	Plasma kallikrein heavy chain [GS]	0	0	0	0	0	0	3	0	0	0	0	0	0	0	0	3
137	Plasma protease C1 inhibitor [GS]	0	0	0	0	2	2	3	2	0	0	0	0	5	5	7	6
138	Plasma serine protease inhibitor	0	0	0	0	0	0	0	0	0	0	0	0	0	0	2	3
139	Plasminogen [GS]	0	18	33	14	12	5	3	0	0	25	30	9	4	4	4	3
140	Platelet-activating factor acetylhydrolase	0	0	0	0	3	0	0	0	0	0	0	0	0	0	0	0
141	Plectin *	0	2	0	0	0	0	0	0	0	0	0	0	0	0	0	0
142	Plexin domain-containing protein 2 [G]	0	0	0	0	0	0	0	0	0	0	0	2	0	0	0	0
143	Pregnancy zone protein [G] s26[1a]	0	0	0	0	0	0	0	11	0	0	0	0	0	0	0	12
144	Pregnancy-specific beta-1-glycoprotein 1 [G S]	0	0	0	0	0	0	0	0	0	0	0	3	0	0	0	0

145	Pregnancy-specific beta-1-glycoprotein 9 [GS]	0	0	0	0	0	0	0	0	0	0	0	3	0	0	0	0
146	Prenylcysteine oxidase 1[G]	0	0	0	0	0	0	0	0	0	0	0	0	0	0	0	2
147	Protein AMBP [GS]	0	0	4	6	8	5	7	2	0	0	5	6	6	9	7	5
148	Protein POF1B	2	0	0	0	0	0	0	0	0	0	0	0	0	0	0	0
149	Protein S100-A7 [1a]	0	3	0	0	0	0	0	0	0	0	0	2	0	0	0	0
150	Protein S100-A8 [1a]	0	0	0	0	0	0	0	0	0	0	0	4	0	0	2	0
151	Protein S100-A9	0	0	0	0	0	0	0	0	0	0	0	3	0	0	0	0
152	Protein-glutamine gamma-glutamyltransferase E	0	2	0	0	0	0	0	0	0	0	0	0	0	0	0	0
153	Prothrombin	0	0	7	2	2	0	3	3	5	0	3	2	3	2	3	4
154	Trypsin	4	4	4	4	4	4	4	4	4	4	4	4	4	4	4	3
155	Retinol-binding protein 4 *	0	4	7	7	7	9	8	3	0	5	9	8	8	9	7	7
156	Serotransferrin [GS]	0	23	41	22	22	13	14	3	0	34	42	22	18	16	17	14
157	Serpin B12 *	3	0	0	0	0	0	0	0	0	0	0	0	0	0	0	0
158	Serpin B3 *	0	2	0	0	0	0	0	0	0	0	0	0	0	0	0	0
159	Serum albumin	20	0	3	0	5	0	0	0	0	0	9	0	18	0	0	7
160	Serum amyloid A-4 protein [GS]	0	0	0	5	3	4	3	2	0	0	0	5	3	2	4	4
161	Serum amyloid P-component [GS]	0	0	0	6	6	5	6	5	0	0	2	7	6	6	5	5
162	Serum paraoxonase/arylesterase 1 [GS]	0	0	0	0	5	5	5	4	0	0	0	0	6	6	5	4
163	Serum paraoxonase/lactonase 3 [G]	0	0	0	0	0	0	0	0	0	0	0	0	0	3	2	0
164	Sex hormone-binding globulin [G]	0	0	0	3	0	0	0	0	0	0	0	4	0	0	0	0
165	Small proline-rich protein 2A [G]	0	2	0	0	0	0	0	0	0	0	0	0	0	0	0	0
166	Sulfhydryl oxidase 1 [1a]	0	0	0	0	0	0	0	0	0	0	0	0	2	0	0	0
167	Tetranectin [GS]	0	3	4	2	0	0	0	0	0	4	4	0	0	0	0	0
168	Thioredoxin	2	0	0	0	0	0	0	0	0	0	0	0	0	0	0	0
169	Transferrin receptor protein 1 [1a]	0	0	0	0	0	0	3	0	0	0	0	0	0	0	3	0
170	Transthyretin *	0	4	5	4	3	3	4	0	0	0	7	7	7	7	2	2
171	Ubiquitin*	0	3	0	0	0	0	0	0	0	0	0	0	0	0	0	0
172	Vitamin D-binding protein [GS]	0	0	10	10	2	0	0	0	0	0	15	12	3	0	0	0
173	Vitamin K-dependent protein [GS]	0	0	0	0	5	3	2	0	0	0	0		6	7	4	2
174	Vitronectin [GS]	0	0	7	7	4	3	4	0	0	0	6	7	4	3	4	4
175	Zinc-alpha-2-glycoprotein [GS]	0	5	3	0	0	0	0	0	0	4	3	0	0	0	0	0

G, glycoprotein; GS, sialylated glycoprotein; 1a, low abundance protein (few ng to sub μg/mL level); *, non-glycoprotein

TABLE 5

UNIQUE PROTEINS IDENTIFIED IN THE RPC FRACTIONS OF THE SNA CAPTURED PROTEINS FROM DISEASE-FREE SERUM WITH AND WITHOUT DEPLETION COLUMNS. DATA ON GS WERE FROM REFS. [10, 12, 25, 30, 32, 43, 51, 56, 57, 59, 60, 62]

Without depletion	With depletion
Catalase [1a]	Actin, cytoplasmic 1 *
Complement C1r subcomponent	Afamin [GS]
Complement C5 [GS]	Alpha-2-macroglobulin [GS]
Cystatin-A [1a]	Annexin A2 [1a]
Desmocollin-1 [1a]	Antileukoproteinase
Desmoglein-1 [1a]	Apolipoprotein A-I [GS]
Desmoplakin [1a]	Apolipoprotein F [G]
Extracellular matrix protein 1 [1a]	Beta-2-microglobulin [GS]
Filaggrin-2 [1a]	Biotinidase [GS]
Gamma-B of Fibrinogen gamma chain	Calmodulin-like protein 5 [1a]
Glyceraldehyde-3-phosphate dehydrogenase [1a]	Carboxypeptidase B2 [GS1a]
Homo sapiens SNC73 protein (SNC73) mRNA	Cartilage acidic protein 1 [1aG]
Ig kappa chanin V-IV region Len	Cathelicidin antimicrobial peptide [1a]
Ig gamma chain-2 C region	Cholinesterase [1a]
Ig kappa chain V-III region WOL *	Coagulation factor V [GS1a]
Ig lambda-2 chain C regions *	Coagulation factor VII [GS]
Ig mu chain C region	Coagulation factor X [GS]
Ig alpha-2 chain C region G	Coagulation factor XII [GS]
Ig gamma-1 chain C region G	Complement C2 [G]
Ig kappa chain V-III region WOL *	Complement C4-A [GS]
Ig heavy chain V-I region EU	Complement C4-B [GS]
Ig gamma-3 chain C region [G]	Complement C5 [G]
Ig heavy chain V-III region GAL	Complement component C8 alpha chain [G]
Ig heavy chain V-I region HG3	Complement component C8 beta chain [G]
IGK@ protein	Complement component C8 gamma chain [G]
Inter-alpha (Globulin) inhibitor H2, isoform CRA_a	Complement component C9 [G]
Keratin, type I cytoskeletal 13	Complement factor H-related protein 2 [GS]
Keratin, type II cytoskeletal 1b	Complement factor H-related protein 3 [GS]
Keratin, type II cytoskeletal 78	Complement factor H-related protein 5 [GS]
Keratin, type II cytoskeletal 80	Corticosteroid-binding globulin

Kininogen-1 [GS]	Cystatin-C [GS]
Long of Complement factor H-related protein 2	Cysteine-rich secretory protein 3 [GS]
Peroxiredoxin-2	Dermcidin [1a]
Phospholipid transfer protein	Desmoplakin [1a]
Protein-glutamine gamma-glutamyltransferase E	Extracellular matrix protein 1 [G1a]
Protein-glutamine gamma-glutamyltransferase K	Extracellular superoxide dismutase [Cu-Zn] [GS 1a]
Prothrombin (Fragment)	Fibrinogen alpha chain [GS]
Putative uncharacterized protein	Ficolin-2 [GS]
Putative uncharacterized protein DKFZp686I04196 (Fragment)	Galectin-7 [GS1a]
Putative uncharacterized protein DKFZp686I15212	Gamma-A of Fibrinogen gamma chain [GS]
Putative uncharacterized protein DKFZp686L19235	Gelsolin [1a]
Putative uncharacterized protein DKFZp686P15220	Hemoglobin subunit delta [G]
SAA2-SAA2 protein	Hepatocyte growth factor-like protein [G]
Scavenger receptor cysteine-rich type 1 protein M130	Hydrocephalus-inducing protein homolog
suprabasin [1a]	Ig alpha-1 chain C region G
Triosephosphate isomerase [1a]	Ig gamma-1 chain C region G
Uncharacterized protein	Ig kappa chain C region *
Uncharacterized protein	Immunoglobulin lambda-like polypeptide 5
Uncharacterized protein	Insulin-like growth factor-binding protein 3 [GS]
	Insulin-like growth factor-binding protein complex acid labile subunit [GS]
	Inter-alpha-trypsin inhibitor heavy chain H2 [GS]
	Inter-alpha-trypsin inhibitor heavy chain H3 [GS]
	Intercellular adhesion molecule 2 [1a]
	Keratin, type II cytoskeletal 6B
	Keratin, type II cytoskeletal 6C
	Leucine-rich alpha-2-glycoprotein [GS]
	Leukocyte immunoglobulin-like receptor subfamily A member 3 [G]
	LMW of Kininogen-1 [GS]
	Low affinity immunoglobulin gamma Fc region receptor III-A [G]
	Lumican [GS]
	Lysozyme C [1a]
	Mannan-binding lectin serine protease 2 [1a]
	Mannose-binding protein C
	Monocyte differentiation antigen CD14
	N-acetylglucosamine-1-phosphotransferase subunit gamma [GS1a]

	N-acetylmuramoyl-L-alanine amidase [GS]
	Ovalbumin [GS]
	Peroxiredoxin-2
	Phosphatidylcholine-sterol acyltransferase [1a]
	Phosphatidylinositol-glycan-specific phospholipase D [GS1a]
	Plasma serine protease inhibitor [GS]
	Pregnancy-specific beta-1-glycoprotein 1 [GS]
	Prenylcysteine oxidase 1 [G]
	Protein S100-A8 [GS]
	Protein S100-A9
	Protein Z-dependent protease inhibitor [G1a]
	Prothrombin
	Retinol-binding protein 4
	Scavenger receptor cysteine-rich type 1 protein M130
	Secreted phosphoprotein 24 [G1a]
	Serpin B3
	Serum amyloid A-1 protein [GS]
	Serum amyloid A-4 protein [GS]
	Serum paraoxonase/lactonase 3
	Thyroxine-binding globulin
	Transforming growth factor-beta-induced protein ig-h3 [1a]
	Transthyretin
	Trypsin [1a]

G, glycoprotein; GS, sialylated glycoprotein; 1a, low abundance protein (few ng to sub μg/mL level); *, non-glycoprotein.

TABLE 6

UNIQUE PROTEINS IDENTIFIED IN THE RPC FRACTIONS OF THE SNA CAPTURED PROTEINS FROM DISEASE-FREE SERUM WITH AND WITHOUT DEPLETION COLUMNS. DATA ON GS WERE FROM REFS. [10, 12, 25, 30, 32, 43, 51, 56, 57, 59, 60, 62]

Without depletion	With Depletion
Attractin [1a]	Actin, cytoplasmic 1
C4b-binding protein alpha chain	Afamin
Cadherin-5 [1a]	Alpha-2-macroglobulin
Catalase [1a]	Alpha-enolase
Clusterin [GS]	Alpha-S1-casein
Coagulation factor XIII B chain [1a]	Annexin A2 [1a]
Complement C5 [GS]	Arginase-1
Complement factor H-related protein 4 [1a]	Beta-2-microglobulin
Cystatin-A [1a]	Bone marrow proteoglycan
Fibrinogen beta chain	Carboxypeptidase B2 [1a]
Fibronectin [GS]	Cartilage oligomeric matrix protein [1a]
Fibulin-1	Cathelicidin antimicrobial peptide [1a]
Gamma-B of Fibrinogen gamma chain	Cholinesterase [1a]
Homo sapiens SNC73 protein (SNC73) mRNA	Clusterin [GS]
IGK@ protein	Coagulation factor X
Kininogen-1 [GS]	Coagulation factor XII
Long of Complement factor H-related protein 2 [GS]	Complement C2
Mannan-binding lectin serine protease 1 [1a]	Complement C4-A
Phospholipid transfer protein	Complement C4-B
Protein-glutamine gamma-glutamyltransferase K	Complement C5
Putative uncharacterized protein	Complement component C8 alpha chain
Putative uncharacterized protein DKFZp686I04196 (Fragment)	Complement component C8 beta chain
Putative uncharacterized protein DKFZp686I15212	Complement component C8 gamma chain

Putative uncharacterized protein DKFZp686L19235	Complement component C9
Putative uncharacterized protein DKFZp686P15220	Complement factor H-related protein 2
SAA2-SAA2 protein	Corneodesmosin
Scavenger receptor cysteine-rich type 1 protein M130	Cornifin-A
selenoprotein P isoform 2	Corticosteroid-binding globulin
suprabasin isoform 1 precursor	Dermcidin [1a]
Triosephosphate isomerase	Extracellular matrix protein 1 [1a]
Uncharacterized protein	Fatty acid-binding protein, epidermal
Uncharacterized protein	Fibrinogen alpha chain
Uncharacterized protein	Fibronectin
Vitamin K-dependent protein C [1a]	Filaggrin [1a]
Vitamin K-dependent protein Z	Galectin-3-binding protein[1a]
Ig kappa chain V-I region EU *	Gelsolin
Ig kappa chain V-III region WOL*	Histone H4 [1a]
Ig kappa chain V-IV region *	Ig gamma-1 chain C region
Ig lambda chain V-I region WAH*	Ig kappa chain C region
Ig lambda chain V-III region LOI *	Immunoglobulin lambda-like polypeptide 5
Ig lambda chain V-III region SH *2	Insulin-like growth factor-binding protein complex acid labile subunit
	Inter-alpha-trypsin inhibitor heavy chain H2
	Inter-alpha-trypsin inhibitor heavy chain H3
	Keratin, type I microfibrillar
	Keratin, type II cuticular Hb3
	Keratin, type II cytoskeletal 4
	Keratin, type II cytoskeletal 6C
	Keratin, type II microfibrillar
	Keratin, type II microfibrillar
	Kininogen-1
	Leucine-rich alpha-2-glycoprotein
	Lumican
	Mannan-binding lectin serine protease[1a]
	N-acetylmuramoyl-L-alanine amidase
	Ovalbumin
	Peroxiredoxin-1
	Phosphatidylcholine-sterol acyltransferase [1a]
	Phosphatidylinositol-glycan-specific phospholipase D [1a]

	Pigment epithelium-derived factor
	Plasma serine protease inhibitor
	Platelet-activating factor acetylhydrolase
	Plectin
	Plexin domain-containing protein 2
	Pregnancy-specific beta-1-glycoprotein 1
	Pregnancy-specific beta-1-glycoprotein 9
	Prenylcysteine oxidase 1
	Protein POF1B
	Protein S100-A7 [1a]
	Protein S100-A8 [1a]
	Protein S100-A9
	Retinol-binding protein 4
	Serpin B12
	Serpin B3
	Serum amyloid A-4 protein
	Serum paraoxonase/lactonase 3
	Skin-specific protein 32
	Small proline-rich protein 2A
	Sulfhydryl oxidase 1 [1a]
	Tetranectin
	Thioredoxin
	Transferrin receptor protein 1 [1a]
	Trypsin [1a]
	Ubiquitin
	Vitamin D-binding protein
	Vitamin K-dependent protein S

G, glycoprotein; GS, sialylated glycoprotein; 1a, low abundance protein (few ng to sub μg/mL level); *, non-glycoprotein.

TABLE 7

DIFFERENTIALLY EXPRESSED PROTEINS CAPTURED BY THE SNA COLUMN.

DATA ON GS WERE FROM REFS.[10, 25, 43, 52, 57, 61, 62]

Fractions which differential expression was found (Down or up)	Identified Proteins	Accession Number	Mol. Wt.	Up/ down regulated	Total of average spectral counts from different fractions (DFS)	Total of average spectral counts from different fractions (CS)
F1-Up	Actin cytoplasmic	ACTB_HUMAN	42 kDa	Up	0	7
F5-Up	Afamin [GS]	AFAM_HUMAN	69 kDa	Up	0	4
F6-Down	Alpha-1-antichymotrypsin [GS]	AACT_HUMAN	48 kDa	Down	23	8
F4,F5,F6,F8-Down	Alpha-1-antitrypsin [GS]	A1AT_HUMAN	47 kDa	Down	285	63
F3,F7- Down	Antithrombin-III [GS]	ANT3_HUMAN	53 kDa	Down	32	10
F5,F6,F9-Up	Apolipoprotein A-I [GS]	APOA1_HUMAN	31 kDa	Up	170	255
F2, F3, F4-Down	Apolipoprotein A-IV	APOA4_HUMAN	45 kDa	Down	67	42
F9- Down	Apolipoprotein B-100 [GS]	APOB_HUMAN	516 kDa	Down	156	112
F4,F6-Up	Apolipoprotein C-I	APOC1_HUMAN	9 kDa	Up	12	30
F5-Up	Apolipoprotein D [GS]	C9JF17_HUMAN	24 kDa	Up	10	7
F2, F7-Down	Apolipoprotein E [G]	APOE_HUMAN	36 kDa	Down	15	25
F4-Up	Clusterin [GS]	CLUS_HUMAN	58 kDa	Up	7	17
F5-Up	Coagulation factor IX [1aGS]	FA9_HUMAN	52 kDa	Up	6	0
F3-Up	Coagulation factor X [1aGS]	FA10_HUMAN	55 kDa	Up	0	8
F1-Down ,F4,F5-Up	Complement C1r subcomponent [GS]	C1R_HUMAN	80 kDa	Down	40	57

F9-Down	Complement C2 [G]	CO2_HUMAN	83 kDa	Down	3	0
F1,F2,F4,F5,F6-Down	Complement C3 [G]	CO3_HUMAN	187 kDa	Down	187	66
F7,F9-Up	Complement C4-B [GS]	CO4B_HUMAN	193 kDa	Up	107	174
F2,F4,F8-Up	Complement factor H [GS]	CFAH_HUMAN	139 kDa	Up	17	78
F2-Up	Complement factor H-related protein 1 [GS]	FHR1_HUMAN	38 kDa	Up	2	8
F2-Up	Complement factor H-related protein 3 [GS]	FHR3_HUMAN	31 kDa	Up	5	0
F3-Up	Extracellular matrix protein [G1a]	ECM1_HUMAN	64 kDa	Up	8	17
F1,F3-Down	Fibronectin [GS]	FINC_HUMAN	240 kDa	Down	12	3
F5-Up	Hemopexin [GS]	HEMO_HUMAN	52 kDa	Up	13	73
F2-Up	Ig kappa chain C region	IGKC_HUMAN	12 kDa	Up	2	6
F5-Up	Ig mu chain C [GS]	IGHM_HUMAN	49 kDa	Up	17	0
F4,F6,F8,F9-Up	Inter-alpha-trypsin inhibitor heavy chain H4 [GS]	ITIH4_HUMAN	103 kDa	Up	113	113
F3-Up	Pregnancy-specific beta-1-glycoprotein [GS]	PSG1_HUMAN	48 kDa	Up	0	19
F4-Up	Kininogen-1 [GS]	KNG1_HUMAN	48 kDa	Up	75	89
F4-Down	Plasminogen [GS]	PLMN_HUMAN	91 kDa	Down	55	40
F4-Down	Prothrombin	THRB_HUMAN	70 kDa		37	21
F5-Up	Serum amyloid A-4 protein [GS]	SAA4_HUMAN	15 kDa	Up	6	0
F4-Up	Vitamin D-binding protein [GS]	VTDB_HUMAN	55 kDa	Up	17	30
F3-Up	Vitamin K-dependent protein Z [GS]	PROZ_HUMAN	47 kDa	Up	9	21

G, glycoprotein; GS, sialylated glycoprotein; 1a, low abundance protein (few ng to sub μg/mL level); *, non-glycoprotein.

TABLE 8

DIFFERENTIALLY EXPRESSED PROTEINS CAPTURED BY MAL-II COLUMN.

DATA ON GS WERE FROM REFS. [10, 25, 26, 30, 32, 43, 52, 56, 63, 64]

Fractions which differential expression was found(Down or up)	Identified Proteins	Accession Number	Mol. Wt.	Up/down regulated	Total of average spectral counts from different fractions (DFS)	Total of average spectral counts from different fractions (CS)
F4,F5- Down	Alpha-1-antitrypsin [GS]	A1AT_HUMAN	47 kDa	Down	23	10
F3-Down	Alpha-1B-glycoprotein [GS]	A1BG_HUMAN	54 kDa	Down	10	9
F4-Up	Antithrombin-III	ANT3_HUMAN	53 kDa	Up	7	8
F5-Up	Apolipoprotein A-I [GS]	APOA1_HUMAN	31 kDa	Up	23	27
F2,F4- Down	Apolipoprotein A-IV	APOA4_HUMAN	45 kDa	Down	17	5
F8-Down	Apolipoprotein B-100 [GS]	APOB_HUMAN	516 kDa	Down	100	39
F4-Up	Apolipoprotein M [GS]	APOM_HUMAN	21 kDa	Up	4	5
F1-Up	Beta-2-glycoprotein 1 [GS]	APOH_HUMAN	38 kDa	Up	9	11
F4-Up	Carboxypeptidase N catalytic chain [GS]	CBPN_HUMAN	52 kDa	Up	3	0
F8-Up	Complement C3 [GS]	CO3_HUMAN	187 kDa	Up	59	93
F2-Up	Complement factor H [GS]	CFAH_HUMAN	139 kDa	Up	7	22
F1-Down	Desmoplakin [1a]	DESP_HUMAN	332 kDa	Down	36	0
F2-Up	Extracellular matrix protein 1 [G1a]	ECM1_HUMAN	61 kDa	Up	2	8
F1-Down	Glyceraldehyde-3-phosphate dehydrogenase [1a]	G3P_HUMAN	36 kDa	Down	4	0

F3,F6-Down	Haptoglobin [GS]	HPT_HUMAN	45 kDa	Down	50	45
F4-Up	Hemoglobin subunit beta	HBB_HUMAN	16 kDa	Up	2	8
F1-Down	Hornerin [1a]	HORN_HUMAN	282 kDa	Down	10	0
F4-Up	Ig mu chain C region [GS]	IGHM_HUMAN	49 kDa	Up	0	12
F6-Up	Inter-alpha-trypsin inhibitor heavy chain H4 [GS]	ITIH4_HUMAN	103 kDa	Up	17	27
F1-Down	Junction plakoglobin [G1a]	PLAK_HUMAN	82 kDa	Down	8	0
F1,F2,F5-Up	Kininogen-1 [GS]	KNG1_HUMAN	48 kDa	Up	42	51
F3,F5,F6-Down	Plasminogen [GS]	PLMN_HUMAN	91 kDa	Down	50	38
F1-Up	Prothrombin	THRB_HUMAN	70 kDa	Up	0	5
F2-Up	Serotransferrin [GS]	TRFE_HUMAN	77 kDa	Up	23	34

G, glycoprotein; GS, sialylated glycoprotein; 1a, low abundance protein (few ng to sub μg/mL level); *, non-glycoprotein.

TABLE 9

DEP UNIQUE TO SNA LECTIN AND MAL-II LECTIN AND COMMON TO BOTH LECTINS. DATA ON GS WERE FROM REFS. [10, 25, 27, 28, 43, 51, 59, 61, 65]

DEP only in SNA lectin	**DEP common to both lectins**	**DEP only in MAL lectin**
Actin cytoplasmic	Alpha-1-antitrypsin GS	Alpha-1-antitrypsin GS
Afamin GS	Antithrombin-III GS	Alpha-1B-glycoprotein GS
Alpha-1-antichymotrypsin GS	Apolipoprotein A-I GS	Antithrombin-III
Alpha-1-antitrypsin GS	Apolipoprotein A-IV	Apolipoprotein A-I GS
Antithrombin-III GS	Apolipoprotein B-100 GS	Apolipoprotein A-IV
Apolipoprotein A-I GS	Complement C3 GS	Apolipoprotein B-100 GS
Apolipoprotein A-IV	Complement factor H GS	Apolipoprotein M GS
Apolipoprotein B-100 GS	Extracellular matrix protein G1a	Beta-2-glycoprotein 1 GS
Apolipoprotein C-I	Kininogen-1 GS	Carboxypeptidase N catalytic chain GS
Apolipoprotein D GS	Plasminogen GS	Complement C3 GS
Apolipoprotein E G	Prothrombin	Complement factor H GS
Clusterin GS	Alpha-1-antitrypsin GS	Desmoplakin 1a
Coagulation factor IX	Antithrombin-III GS	Extracellular matrix protein 1

1aGS		G1a
Coagulation factor X 1aGS	Apolipoprotein A-I GS	Glyceraldehyde-3-phosphate dehydrogenase 1a
Complement C1r subcomponent GS	Apolipoprotein A-IV	Haptoglobin GS
Complement C2 G	Apolipoprotein B-100 GS	Hemoglobin subunit beta
Complement C3 G	Complement C3 GS	Hornerin 1a
Complement C4-B GS	Complement factor H GS	Ig mu chain C region GS
Complement factor H GS	Extracellular matrix protein G1a	Inter-alpha-trypsin inhibitor heavy chain H4 GS
Complement factor H-related protein 1GS	Kininogen-1 GS	Junction plakoglobin G1a
Complement factor H-related protein 3 GS	Plasminogen GS	Kininogen-1 GS
Extracellular matrix protein G1a	Prothrombin	Plasminogen GS
Fibronectin GS	Alpha-1-antitrypsin GS	Prothrombin
Hemopexin GS	Antithrombin-III GS	Serotransferrin GS
Ig kappa chain C region	Apolipoprotein A-I GS	Alpha-1-antitrypsin GS
Ig mu chain C GS	Apolipoprotein A-IV	Alpha-1B-glycoprotein GS
Inter-alpha-trypsin inhibitor heavy chain	Apolipoprotein B-100 GS	Antithrombin-III

H4 GS		
Kininogen-1 GS	Complement C3 GS	Apolipoprotein A-I GS
Plasminogen GS	Complement factor H GS	Apolipoprotein A-IV
Pregnancy-specific beta-1-glycoprotein GS	Extracellular matrix protein G1a	Apolipoprotein B-100 GS
Prothrombin	Kininogen-1 GS	Apolipoprotein M GS
Serum amyloid A-4 protein GS	Plasminogen GS	Beta-2-glycoprotein 1 GS
Vitamin D-binding protein GS	Prothrombin	Carboxypeptidase N catalytic chain GS
Vitamin K-dependent protein Z GS	Alpha-1-antitrypsin GS	Complement C3 GS
Actin cytoplasmic	Antithrombin-III GS	Complement factor H GS
Afamin GS	Apolipoprotein A-I GS	Desmoplakin 1a
Alpha-1-antichymotrypsin GS	Apolipoprotein A-IV	Extracellular matrix protein 1 G1a
Alpha-1-antitrypsin GS	Apolipoprotein B-100 GS	Glyceraldehyde-3-phosphate dehydrogenase 1a
Antithrombin-III GS		Haptoglobin GS

G, glycoprotein; GS, sialylated glycoprotein; 1a, low abundance protein (few ng to sub μg/mL level); *, non-glycoprotein.

References

1. Fuster, M.M. and J.D. Esko, *The sweet and sour of cancer: glycans as novel therapeutic targets.* Nat Rev Cancer, 2005. **5**(7): p. 526-542.
2. Tian, Y., F.J. Esteva, J. Song, and H. Zhang, *Altered Expression of Sialylated Glycoproteins in Breast Cancer Using Hydrazide Chemistry and Mass Spectrometry.* Mol. Cell. Proteom., 2012. **11**(6).
3. Zhao, J., D.M. Simeone, D. Heidt, M.A. Anderson, and D.M. Lubman, *Comparative Serum Glycoproteomics Using Lectin Selected Sialic Acid Glycoproteins with Mass Spectrometric Analysis: Application to Pancreatic Cancer Serum.* Journal of Proteome Research, 2006. **5**(7): p. 1792-1802.
4. Kullolli, M., W.S. Hancock, and M. Hincapie, *Preparation of a high-performance multi-lectin affinity chromatography (HP-M-LAC) adsorbent for the analysis of human plasma glycoproteins.* J. Sep. Sci., 2008. **31**(14): p. 2733-2739.
5. Selvaraju, S. and Z. El Rassi, *Tandem lectin affinity chromatography monolithic columns with surface immobilised concanavalin A, wheat germ agglutinin and Ricinus communis agglutinin-I for capturing sub-glycoproteomics from breast cancer and disease-free human sera.* J. Sep. Sci., 2012. **35**(14): p. 1785-1795.
6. Selvaraju, S. and Z.E. Rassi, *Targeting human serum fucome by an integrated liquid-phase multicolumn platform operating in "cascade" to facilitate comparative mass spectrometric analysis of disease-free and breast cancer sera.* Proteomics, 2013. **13**(10-11): p. 1701-1713.

7. Lee, L.Y., M. Hincapie, N. Packer, M.S. Baker, W.S. Hancock, and S. Fanayan, *An optimized approach for enrichment of glycoproteins from cell culture lysates using native multi-lectin affinity chromatography.* J. Sep. Sci., 2012. **35**(18): p. 2445-2452.

8. Shibuya, N., I.J. Goldstein, W.F. Broekaert, M. Nsimba-Lubaki, B. Peeters, and W.J. Peumans, *The elderberry (Sambucus nigra L.) bark lectin recognizes the Neu5Ac(alpha 2-6)Gal/GalNAc sequence.* J.Biol. Chem., 1987. **262**(4): p. 1596-601.

9. Geisler, C. and D.L. Jarvis, *Letter to the Glyco-Forum: Effective glycoanalysis with Maackia amurensis lectins requires a clear understanding of their binding specificities.* Glycobiology, 2011. **21**(8): p. 988-993.

10. Yamamoto, K., Y. Konami, and T. Irimura, *Sialic Acid-Binding Motif of Maackia amurensis Lectins.* J. Biochem., 1997. **121**(4): p. 756-761.

11. Gunasena, D.N. and Z. El Rassi, *Hydrophilic diol monolith for the preparation of immuno-sorbents at reduced nonspecific interactions.* Journal of Separation Science, 2011. **34**(16-17): p. 2097-2105.

12. Ueda, K., et al., *Targeted serum glycoproteomics for the discovery of lung cancer-associated glycosylation disorders using lectin-coupled ProteinChip arrays.* Proteomics, 2009. **9**(8): p. 2182-2192.

13. Fanayan, S., M. Hincapie, and W.S. Hancock, *Using lectins to harvest the plasma/serum glycoproteome.* Electrophoresi, 2012. **33**(12): p. 1746-1754.

14. Durham, M. and F.E. Regnier, *Targeted glycoproteomics: Serial lectin affinity chromatography in the selection of O-glycosylation sites on proteins from the human blood proteome.* J. Chromatogr. A, 2006. **1132**(1–2): p. 165-173.

15. Yoshida, K.-i., S. Sumi, M. Honda, Y. Hosoya, M. Yano, K. Arai, and Y. Ueda, *Serial lectin affinity chromatography demonstrates altered asparagine-linked sugar chain structures of γ-glutamyltransferase in humaa renal cell carcinoma.* J. Chromatogr. B, 1995. **672**(1): p. 45-51.

16. Tian, Y. and H. Zhang, *Characterization of disease-associated N-linked glycoproteins.* Proteomics, 2013. **13**(3-4): p. 504-511.

17. Zeng, Z., M. Hincapie, S.J. Pitteri, S. Hanash, J. Schalkwijk, J.M. Hogan, H. Wang, and W.S. Hancock, *A Proteomics Platform Combining Depletion, Multi-lectin Affinity Chromatography (M-LAC), and Isoelectric Focusing to Study the Breast Cancer Proteome.* Anal. Chem., 2011. **83**(12): p. 4845-4854.

18. Selvaraju, S. and Z. El Rassi, *Tandem lectin affinity chromatography monolithic columns with surface immobilised concanavalin A, wheat germ agglutinin and Ricinus communis agglutinin-I for capturing sub-glycoproteomics from breast cancer and disease-free human sera.* J. Sep. Sci., 2012. **35**(14): p. 1785-1795.

19. Block, T.M., et al., *Use of targeted glycoproteomics to identify serum glycoproteins that correlate with liver cancer in woodchucks and humans.* Proceedings of the National Academy of Sciences of the United States of America, 2005. **102**(3): p. 779-784.

20. Stelzl, U., et al., *A Human Protein-Protein Interaction Network: A Resource for Annotating the Proteome.* Cell, 2005. **122**(6): p. 957-968.

21. Stumpf, M.P.H., T. Thorne, E. de Silva, R. Stewart, H.J. An, M. Lappe, and C. Wiuf, *Estimating the size of the human interactome.* Proc Nat. Academy Sci., 2008. **105**(19): p. 6959-6964.

22. Shetty, V., Z. Nickens, P. Shah, G. Sinnathamby, O.J. Semmes, and R. Philip, *Investigation of Sialylation Aberration in N-linked Glycopeptides By Lectin and Tandem Labeling (LTL) Quantitative Proteomics.* Anal. Chem., 2010. **82**(22): p. 9201-9210.

23. Boehm, T., J. Folkman, T. Browder, and M.S. O'Reilly, *Antiangiogenic therapy of experimental cancer does not induce acquired drug resistance.* Nature, 1997. **390**: p. 404-407.

24. Pisano, C., *Undersulfated, low-molecular-weight glycol-split heparin as an antiangiogenic VEGF antagonist.* Glycobiology, 2005. **15**: p. 1C-6C.

25. McGrath, R.T., T.A.J. McKinnon, B. Byrne, R. O'Kennedy, V. Terraube, E. McRae, R.J.S. Preston, M.A. Laffan, and J.S. O'Donnell, *Expression of terminal α2-6–linked sialic acid on von Willebrand factor specifically enhances proteolysis by ADAMTS13.* Blood, 2010. **115**(13): p. 2666-2673.

26. Faiers, A.A., A.Y. Loh, and D.H. Osmond, *Microheterogeneity and sialic acid in human plasma angiotensinogens in various physiological states.* Canadian J. Biochem., 1978. **56**(9): p. 892-899.

27. Ricci, G., A.D. Ambrosi, D. Resca, M. Masotti, and V. Alvisi, *Comparison of serum total sialic acid, C-reactive protein, α1-acid glycoprotein and β2-microglobulin in patients with non-malignant bowel diseases.* Biomedicine & Pharmacotherapy, 1995. **49**(5): p. 259-262.

28. Gout, E., et al., *Carbohydrate Recognition Properties of Human Ficolins: Glycan array screening reveals the sialic acid binding specificity of m-ficolin.* J. Biol. Chem., 2010. **285**(9): p. 6612-6622.

29. Depauw, P., C. Neyt, E. Vanderwinkel, R. Wattiez, and P. Falmagne, *Characterization of Human Serum N-Acetylmuramyl-L-alanine Amidase Purified by Affinity Chromatography.* Protein Expression and Purification, 1995. **6**(3): p. 371-378.

30. Pirie-Shepherd, S.R., E.A. Jett, N.L. Andon, and S.V. Pizzo, *Sialic Acid Content of Plasminogen 2 Glycoforms as a Regulator of Fibrinolytic Activity: .* J. Biol. Chem., 1995. **270**(11): p. 5877-5881.

31. Farrah, T., et al., *A High-Confidence Human Plasma Proteome Reference Set with Estimated Concentrations in PeptideAtlas.* Mol. Cell. Proteomics, 2011. **10**(9).

32. Nazifi, S., A. Oryan, M. Ansari-Lari, M.R. Tabandeh, A. Mohammadalipour, and M. Gowharnia, *Evaluation of sialic acids and their correlation with acute-phase proteins (haptoglobin and serum amyloid A) in clinically healthy Iranian camels (Camelus dromedarius).* Comparative Clin. Pathol., 2012. **21**(4): p. 383-387.

33. Polanski, M., N.L. Anderson, M. Polanski, and N.L. Anderson, *A List of Candidate Cancer Biomarkers for Targeted Proteomics.* Biomarker Insights, 2007. **1**(BMI-1-Anderson-Supplemetary Material): p. 1-48.

34. Clark, G.F., P. Grassi, P.-C. Pang, S. Schedin-Weiss, W. Sun, and A. Dell, *Tumor Biomarker Glycoproteins in the Seminal Plasma of Healthy Human Males Are Endogenous Ligands for DC-SIGN.* Mol. Cell. Proteomics., 2012. **11**(1).

35. Wu, J., X. Xie, S. Nie, R.J. Buckanovich, and D.M. Lubman, *Altered Expression of Sialylated Glycoproteins in Ovarian Cancer Sera Using Lectin-based ELISA Assay and Quantitative Glycoproteomics Analysis.* J. Proteom. Res., 2013. **12**(7): p. 3342-3352.

36. Cho, W., K. Jung, and F.E. Regnier, *Sialylated Lewis x Antigen Bearing Glycoproteins in Human Plasma.* J Proteome Res, 2010. **9**(11): p. 5960-5968.

37. von Schoultz, B. and T. Stigbrand, *Characterization of the "pregnancy zone protein" in relation to other α2-globulins of pregnancy.* Biochim. Biophys. Acta (BBA) - Protein Structure, 1974. **359**(2): p. 303-310.

38. Serada, S., M. Fujimoto, A. Ogata, and F. Terabe, *iTRAQ-based proteomic i dentification of leucine-rich α-2 glycoprotein as a novel inflammatory biomarker in autoimmune diseases.* Annals of the Rheumatic Diseases, 2010. **69**(4): p. 770-774.

39. Qiu, Y., T.H. Patwa, L. Xu, K. Shedden, and . *Plasma Glycoprotein Profiling for Colorectal Cancer Biomarker Identification by Lectin Glycoarray and Lectin Blot.* J. Proteome. Res., 2008. **7**(4): p. 1693-1703.

40. Yang, L., K. Rudser, L. Higgins, H. Rosen, A. Zaman, L. David, and G. Gourley, *Novel Biomarker Candidates to Predict Hepatic Fibrosis in Hepatitis C Identified by Serum Proteomics.* Digestive Diseases and Sciences, 2011. **56**(11): p. 3305-3315.

41. Imre, T., G. Schlosser, G. Pocsfalvi, R. Siciliano, É. Molnár-Szöllősi, T. Kremmer, A. Malorni, and K. Vékey, *Glycosylation site analysis of human alpha-*

1-acid glycoprotein (AGP) by capillary liquid chromatography—electrospray mass spectrometry. J. Mass Spectrom., 2005. **40**(11): p. 1472-1483.

42. Stenflo, J., *A new vitamin K-dependent protein. Purification from bovine plasma and preliminary characterization.* J. Biol. Chem., 1976. **251**(2): p. 355-363.

43. Kurogochi, M., T. Matsushista, M. Amano, J.-i. Furukawa, Y. Shinohara, M. Aoshima, and S.-I. Nishimura, *Sialic Acid-focused Quantitative Mouse Serum Glycoproteomics by Multiple Reaction Monitoring Assay.* Mol Cell Proteomics, 2010. **9**(11): p. 2354-2368.

44. Nafee, A.M., S.M.A. El Aal, and N.A. Mostafa, *Clinical significance of serum clusterin as a biomarker for evaluating diagnosis and metastasis potential of viral-related hepatocellular carcinoma.* Clin Biochem, 2012. **45**(13–14): p. 10701074.

45. Opstal-van Winden, A., et al., *Searching for early breast cancer biomarkers by serum protein profiling of pre-diagnostic serum; a nested case-control study*. BMC Cancer, 2011. **11**(1): p. 381.

46. Kester, H., B.-J. ven der Leede, P. van der Saag, and B. van der Burg, *Novel progesterone target genes identified by an improved differential display technique suggest that progestin-induced growth inhibition of breast cancer cells coincides with enhancement of differentiation.* J Biol Chem, 1997. **272**: p. 16637 - 16643.

47. Cao, M., Z. Gui, K. Sun, and Z. Wu. *Application of iTRAQ quantitative proteomics in identification of serum biomarkers in breast cancer*. in *Biomedical Engineering and Informatics (BMEI), 2011 4th International Conference on*. 2011.

48. Sung, H.-J., J.-M. Ahn, Y.-H. Yoon, T.-Y. Rhim, C.-S. Park, J.-Y. Park, S.-Y. Lee, J.-W. Kim, and J.-Y. Cho, *Identification and Validation of SAA as a Potential Lung Cancer Biomarker and its Involvement in Metastatic Pathogenesis of Lung Cancer.* J. Proteome. Res., 2010. **10**(3): p. 1383-1395.

49. Jackson, D., R.A. Craven, R.C. Hutson, I. Graze, H. Dieplinger, P.J. Selby, and R.E. Banks, *Proteomic Profiling Identifies Afamin as a Potential Biomarker for Ovarian Cancer.* Clin. Cancer Res., 2007. **13**(24): p. 7370-7379.

50. Khalil, A.A., *Biomarker discovery: A proteomic approach for brain cancer profiling.* Cancer Sci., 2007. **98**(2): p. 201-213.

51. Qiu, R.Q. and F.E. Regnier, *Comparative glycoproteomics of N-linked complex-type glycoforms containing sialic acid in human serum.* Anal. Chem., 2005. **77**(22): p. 7225-7231.

52. Raval, G.N., L.J. Parekh, D.D. Patel, F.P. Jha, R.N. Sainger, and P.S. Patel, *Clinical usefulness of alterations in sialic acid, sialyl transferase and sialoproteins in breast cancer.* Indian J Clin Biochem : IJCB, 2004. **19**(2): p. 60-71.

53. Ito, M., K. Ikeda, Y. Suzuki, K. Tanaka, and M. Saito, *An Improved Fluorometric High-Performance Liquid Chromatography Method for Sialic Acid Determination: An Internal Standard Method and Its Application to Sialic Acid Analysis of Human Apolipoprotein E.* Anal. Biochem., 2002. **300**(2): p. 260-266.

54. Pagnan, G., *Delivery of c-myb antisense oligodeoxynucleotides to human neuroblastoma cells via disialoganglioside GD(2)-targeted immunoliposomes: antitumor effects.* J. Natl Cancer Inst., 2000. **92**: p. 253-261.

55. Li, J., et al., *Independent validation of candidate breast cancer serum biomarkers identified by mass spectrometry*. Clin Chem, 2005. **51**: p. 2229 - 2235.

56. Zhao, J., D.M. Simeone, D. Heidt, M.A. Anderson, and D.M. Lubman, *Comparative Serum Glycoproteomics Using Lectin Selected Sialic Acid Glycoproteins with Mass Spectrometric Analysis: Application to Pancreatic Cancer Serum.* J. Proteome. Res., 2006. **5**(7): p. 1792-1802.

57. *Clinical usefulness of alterations in sialic acid, sialyltransferase and sialoproteins in breast cancer.* Indian J. Med. Res., 2005. **121**: p. 127-127.

58. Angata, K. and M. Fukuda, *Polysialyltransferases: major players in polysialic acid synthesis on the neural cell adhesion molecule.* Biochimie, 2003. **85**: p. 195-206.

59. Crocker, P.R., *Siglecs: sialic-acid-binding immunoglobulin-like lectins in cell-cell interactions and signalling.* Curr. Opin. Struct. Biol., 2002. **12**: p. 609-615.

60. Higashi, H., Y. Hirabayashi, Y. Fukui, M. Naiki, M. Matsumoto, S. Ueda, and S. Kato, *Characterization of N-Glycolylneuraminic Acid-containing Gangliosides as Tumor-associated Hanganutziu-Deicher Antigen in Human Colon Cancer.* Cancer Res., 1985. **45**(8): p. 3796-3802.

61. Pirie-Shepherd, S.R., E.A. Jett, N.L. Andon, and S.V. Pizzo, *Sialic Acid Content of Plasminogen 2 Glycoforms as a Regulator of Fibrinolytic Activity: I.* J. Biol. Chem., 1995. **270**(11): p. 5877-5881.

62. Brinkman-Van der Linden, E.C. and A. Varki, *New aspects of siglec binding specificities, including the significance of fucosylation and of the sialyl-Tn epitope. Sialic acid-binding immunoglobulin superfamily lectins.* J. Biol. Chem., 2000. **275**: p. 8625-8632.

63. Shah, P., S. Yang, S. Sun, P. Aiyetan, K.J. Yarema, and H. Zhang, *Mass Spectrometric Analysis of Sialylated Glycans with Use of Solid-Phase Labeling of Sialic Acids.* Anal. Chem., 2013. **85**(7): p. 3606-3613.

64. Zoli, A.P., J.F. Beckers, P. Wouters-Ballman, J. Closset, P. Falmagne, and F. Ectors, *Purification and characterization of a bovine pregnancy-associated glycoprotein.* Biology of Reproduction, 1991. **45**(1): p. 1-10.

65. Luo, C., et al., *Recombinant human complement subcomponent C1s lacking .beta.-hydroxyasparagine, sialic acid, and one of its two carbohydrate chains still reassembles with C1q and C1r to form a functional C1 complex.* Biochemistry, 1992. **31**(17): p. 4254-4262.

CHAPTER V

MULTI COLUMN LIQUID PHASE BASED PLATFORM FOR THE ONLINE ENRICHMENT AND FRACTIONATION OF SIALOGLYCOPROTEINS FROM DISEASE FREE AND BREAST CANCER SERUM – EFFECT OF LECTIN COLUMNS ORDER AND REVERSED PHASE COLUMN PERFORMANCE

Introduction

This chapter is a continuation to Chapter IV aiming at investigating the effect of the order of the lectin columns in the multi column platform (described in Chapter IV) on the number and identity of the captured proteins. Also, this chapter examines the effect of the performance of the RPC column used in the fractionation of the captured proteins by the two-lectin columns. In this regards, an ODA-TRIM monolithic column with incorporated multi wall carbon nanotubes that proved superior in the RPC of proteins than its counterpart ODA-TRIM column without incorporated nanotubes (introduced in Chapter III) has been evaluated in terms of its usefulness in revealing additional differentially expressed proteins as well as low abundance proteins.

Experimental

The experimental design was the same as in Chapter IV. The following summarizes the major experimental parts and their equivalent in previous chapters:

- The instruments and reagents were same as in chapter IV
- The monolithic RPC column preparation was described in chapter III
- RPC fractionation of captured proteins was the same as in chapter IV
- The preparation and immobilization of lectins were described in chapter IV
- The LC-MS/MS conditions were same as in chapter IV
- LC-MS/MS data analysis was the same as in chapter IV

Arrangement of the lectin affinity columns in the multi column platform

The SNA and MAL-II columns were used for capturing the human serum sialoglycoproteins. The proteins were first captured in the order SNA column → MAL-II column, and then the order was changed to MAL-II column → SNA column. Additionally, the RPC fractionation of the captured proteins was performed using an optimized ODA/TRIM column that incorporated 12.5 mg of MWCNTs (with a serial number SN 6957838) and the monolith thus prepared is designated M13, see chapter III.

Results and Discussion

LC-MS/MS identification of proteins captured by the lectin columns arranged in the order SNA→ MAL-II

Identification of proteins captured by the SNA columns. The captured proteins by the SNA column were eluted stepwise with the haptenic sugar lactose to the RPC column. The fractionation of RPC column was subsequently conducted with a linear ACN gradient at increasing ACN concentration in the mobile phase by going from 0-75% mobile phase B in mobile phase A for 12 min. The fractions were collected using a fraction collector starting at 7.5 min of the gradient and ended at 12 min (end of the gradient). Fractions of 0.5 mL each were collected at each 50 sec in Eppendorf tubes previously washed with ACN. Chromatograms of the RPC fractionation of the SNA captured proteins from disease free and cancer sera are shown in Fig. 1. The various fractions were evaporated to dryness using SpeedVac and then submitted for the LC-MS/MS analysis. In the LC-MS/MS scaffold report, the proteins reported were those with protein identification probability of at least 99%, and peptide identification probability of not less than 95% and containing at least two unique peptides. The false discovery rate for the peptide identification was 0.1% for both SNA and MAL-lectins. The identified proteins from disease free and cancer sera are listed in Table 1. The Venn diagram in Fig. 2 shows the number of proteins captured by the SNA column from disease free and cancer sera totaling 182 and 210 non-redundant proteins, respectively, with 30 and 58 unique proteins, respectively, and 152 common proteins for both type of sera.

Among the captured proteins, 155 proteins were reported to be glycosylated including 85 sialoglycoproteins and 83 low abundance proteins [1-26]. In the SNA captured proteins some novel biomarkers for breast cancer have been reported such as, cadherin-5, zinc-alpha-2-glycoprotein, cathepsin D, and galectin-7 [11, 27-31].

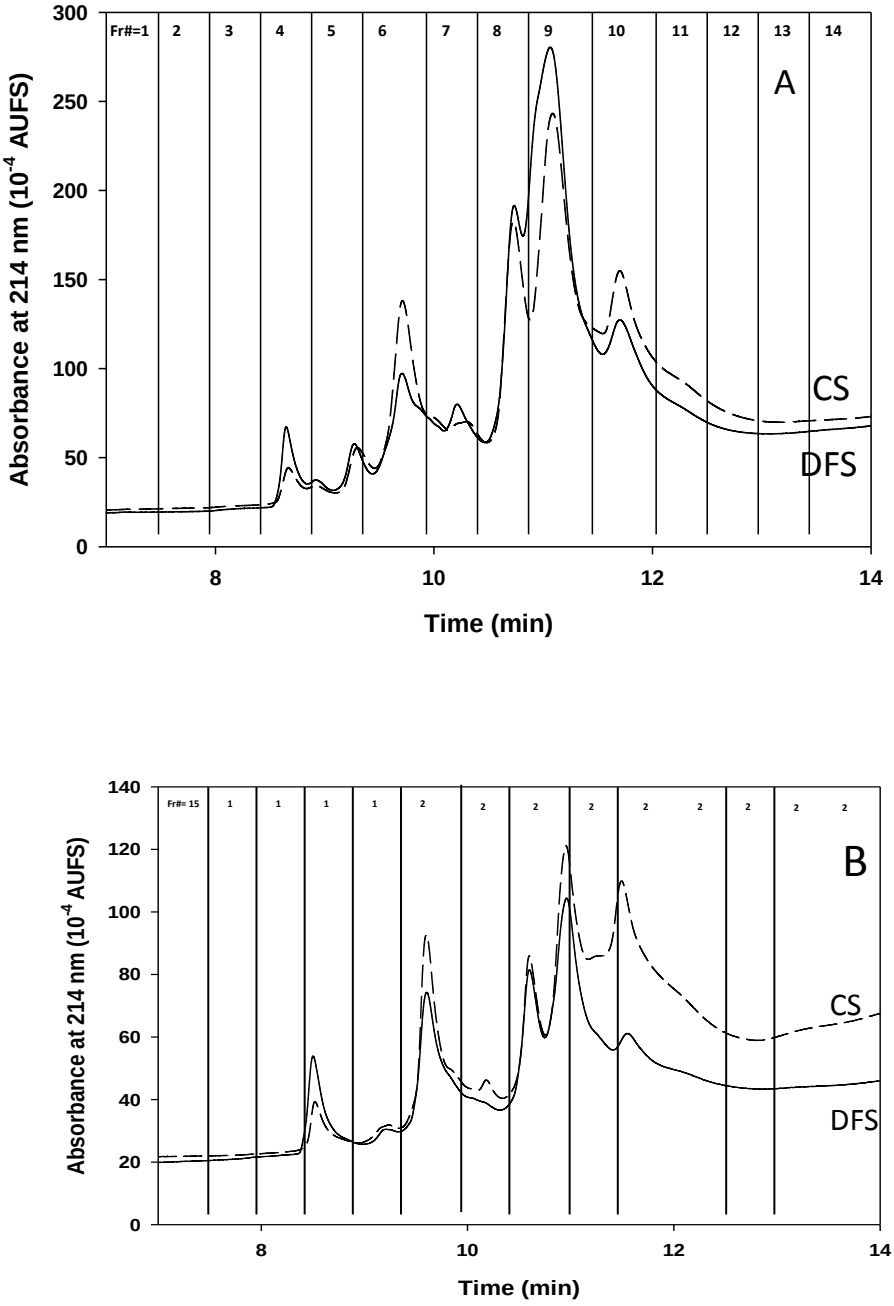

Figure 1. *Chromatograms of the RPC fractionation of proteins captured by SNA column (A) and MAL-II column (B) from disease free (DFS) and breast cancer sera (CS). The RPC fractionation was carried out by a linear gradient elution at increasing ACN*

concentration in the mobile phase by going from 0-75% of mobile phase B in 12 min. Mobile phase A consisted of H_2O/ACN (95:5 v/v) containing 0.1% TFA and mobile phase B consisted of ACN/H_2O (95:5 v/v) containing 0.1% TFA. Flow rate, 1 mL/min; UV detection, 214 nm.

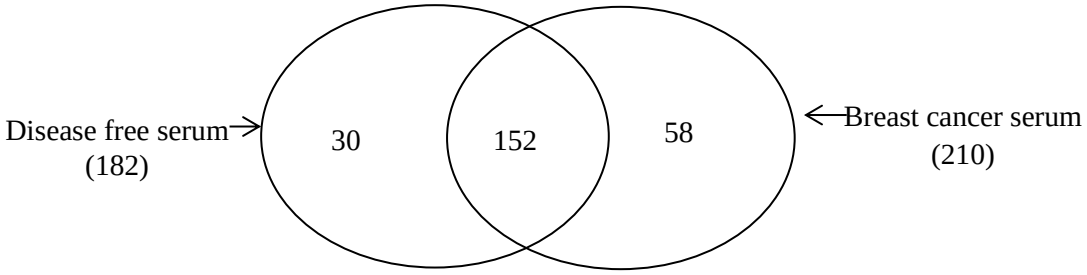

Figure 2. *Venn diagram for the LC-MS/MS identified proteins captured by the SNA lectin.*

Furthermore, apolipoprotein B-100, ceruloplasmin and fibronectin were reported as lung cancer biomarkers [32]. Plectin which is a low abundance protein was qualified as a pancreatic cancer biomarker [33]. Clusterin, leucine-rich-alpha-2-glycoprotein and complement H were identified as ovarian cancer biomarkers [34]. Calmodulin like protein, caspase 14, corneodesmosin were identified as biomarkers for the neuro-degerative diseases such as schizophrenia and Parkinson's disease [35]. Filaggrin-2 is a low abundance protein was associated with skin cancer [36]. Finally, semenogelin-1 was reported as a biomarker for prostate cancer [37].

Proteins, which have a reported concentration in the range of a few ng to less than 1 μg were considered as low abundance proteins. To cite a few of these low abundance proteins one can mention filaggrin-2 (4.6 ng/mL), desmolegein-2 and desmocolin-2 (2.7 ng/mL), plectin-1 (2.8 ng/mL). The concentration for these typical low abundance

proteins can be found in the human plasma proteome reference set that has non redundant set of 1929 protein sequences [38].

Identification of proteins captured by the MAL-II column. Using the same methodology as that reported above, proteins were eluted from the MAL-II column and then fractionated on the RPC column using a linear gradient elution at increasing ACN concentration from 0-75% mobile phase B in mobile phase A for 12 min, see Fig. 1-B for the resulting chromatograms. In this set of experiments, 138 and 163 proteins were identified in disease free and cancer sera, respectively, in the collected fractions by LC-MS/MS analysis using protein identification probability of 99% with peptide identification probability of 95% containing at least two unique peptides. These identified proteins are listed in Table 2. In the collected fractions, the number of proteins unique to disease free and cancer sera were 15 and 40 proteins, respectively, while 123 proteins were common to both sera, see the Venn diagram in Fig. 3. Among these identified proteins, 50 proteins were reported to be of the low abundance types and 57 were sialoglycoproteins [13, 39-42]. Among the captured low abundance proteins, one can mention the following sialoglycoproteins: cartilage acidic protein 1, cartilage oligomeric protein, coagulation factor IX, coagulation factor X, coagulation factor XII B chain, complement C1r subcomponent like proteincyctatin A, fetuin B, phosphatidylinositol-glycan-specific phospholipase D, pregnancy zone protein, and prolactin inducible protein [41, 43-45]. The sialylated low abundance protein such as pregnancy zone protein, prolactin inducible protein, cartilage oligomeric matrix protein and cystatin A were previously reported as breast cancer biomarkers [46-49]. Beta ala his dipepetidase and caspase 14 were also reported to increase in breast cancer serum [50, 51]. Cartilage acidic

protein, tetranectin, and cartilage acidic protein were identified as cancer biomarkers [52]. According to the protein atlas by Farrah et al. [38], the concentrations of some typical low abundance proteins are mentioned here including caspase 14 (1.9 ng/mL), filaggrin (0.82 ng/mL) plexin domain containing protein 2 (1.6 ng/mL), serpin B3 (6.1 ng/mL) and suprabesin (4.5 ng/mL),.

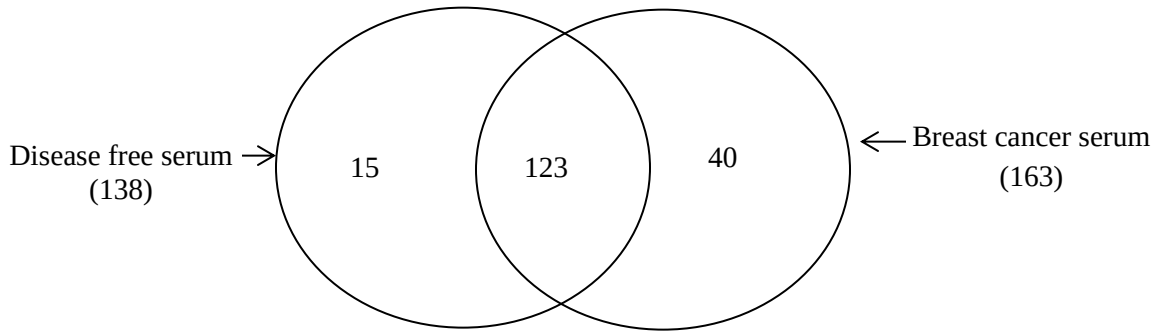

Figure 3. *Venn diagram for LC-MS/MS identified proteins captured by the MAL lectin.*

In the preceding chapter (i.e., Chapter IV), the RPC fractionation of captured proteins was performed using ODA/TRIM column without addition of nanoparticles. The preparation of the RPC column was described in chapter III and the column was designated as M3. In this chapter, a novel version of the M3 RPC column was used. It involved the addition of multi walled carbon nanotubes and the column was designated as M13. In both cases depleted disease free and breast cancer sera were analyzed. When compared to the RPC fractionation using the M3 column, the RPC on the M13 column facilitated the identification by LC-MS/MS of higher number of total proteins as well as sialoglycoproteins and low abundance proteins for both disease free and cancer sera. For instance, the SNA captured proteins when fractionated using the M3 column yielded for

disease free and breast cancer sera 180 and 182 identified proteins, respectively. Among these identified proteins, 125 of them were found to be glycoproteins including 83 sialoglycoproteins as well as 43 low abundance proteins. Fractionation *via* M13 column of the SNA captured proteins from disease free and breast cancer sera permitted the identification of 183 and 210 proteins by LC-MS/MS analysis, respectively. In these identified proteins, 155 proteins were glycoproteins including 85 sialoglycoproteins as well as 83 low abundance proteins. From these data obtained from the SNA captured proteins that were subsequently fractionated on the M13 one can assess the higher number of total proteins and sialoglycoproteins than in the case of fractionation on the M3 column. Also, the number of low abundance proteins that was identified by LC-MS/MS subsequent to RPC fractionation on the M13 column was almost the double of that identified by LC-MS/MS subsequent to the RPC fractionation on the M3 column.

The total number of proteins identified in the RPC fractions obtained on the M3 column after capturing these proteins by MAL-II column from disease free and breast cancer sera were 153 and 157, respectively, while the total number of proteins identified in the RPC fractions obtained on the M13 column after capturing these proteins by the same lectin column (i.e., MAL-II column) from the same sera were 138 and 163 proteins, respectively. In the case of RPC fractionation *via* M3 column, a total of 94 glycoproteins were identified including 63 sialoglycoproteins as well as 37 low abundance proteins. These numbers changed to 82 glycoproteins with 57 sialoglycoproteins and 50 low abundance proteins when performing the fractionation on the M13 while keeping other conditions the same.

In the case of RPC fractionation on M3 column, and using Uniprot software and NetNGly-predictor, which was used to predict the N-glycosylation sites of the protein one can find in the SNA captured proteins from disease free serum 75% of these proteins as glycoproteins and 25% as non-glycoproteins. For the SNA captured proteins from breast cancer serum, 81% of the identified proteins were found to be glycoproteins while 19% were non-glycoproteins. For the MAL-II captured proteins from disease free serum 74% of the identified proteins were found to be glycoproteins while 26 % were non-glycoproteins.

On the other hand, in the case of RPC fractionation on the M13 column, and relying on the same software mentioned above, the percentage of glycoproteins found among the captured proteins by MAL-II column from the normal serum were lower than that found in the fractions obtained with the M3 column. Oppositely, the percentage of glycoproteins in the factions obtained on the M13 column was higher for the cancer serum than that in the fractions of the M3 column. However, sialoglycoproteins were higher with the M3 column than the M13 column but a higher number of low abundance proteins were identified in the fractions of the M13 column.

Differentially expressed proteins for the column order SNA → MAL-II

The RPC chromatograms of the captured proteins by SNA and MAL-II columns from disease free and cancer sera are shown in Fig. 1 A and B, respectively. By simple visual inspection of the chromatograms one can readily identify differences in the peak intensity and shouldering in the chromatograms. The DEPs in the SNA and MAL-II columns in the cancer serum relative to the disease free serum were identified by taking

into consideration only proteins with 99.9% protein identification probability, 95% peptide identification probability and minimum of five unique peptides. The DEPs captured by the SNA column are shown in Table 3. These DEPs were identified using the quantitative Q-Q scatterplots which plot the normalized spectral count for each protein found in the breast cancer serum versus the normalized spectral count of that same protein found in disease free serum. The proteins that are two standard deviation away in cancer serum relative to the disease free serum are considered as DEPs. The scatterplot method for identifying DEPs was initially proposed by Selvaraju and El Rassi [17], and proved successful in identifying candidate biomarkers.

Using the Q-Q scatterplots, 37 proteins were identified in the SNA captured fractions as DEPs in breast cancer serum relative to the disease free serum, see Table 3. Among the identified proteins, 26 were down regulated while 11 proteins were up regulated. Among the DEPs, alpha-1-antichymotrypsin, alpha-1-antitrypsin, ant thrombin-III, Apolipoprotein B-100, cadherin-5, carboxypeptidase N catalytic chain, carboxypeptidase N subunit 2, coagulation factor IX, coagulation factor XIII B chain, complement C3, desmoglein-1, plasma kallikrein heavy chain, plasminogen and serotransferrin have been previously reported as sialoglycoproteins. The DEP galectin-3-binding protein is a low abundance protein. It has been previously reported of having enhanced levels in breast cancer patients [53]. Cadherin 5 is up regulated in breast cancer serum relative to disease free serum. The overexpression of cadherin family proteins was found indicative of invasive breast carcinomas [54]. In a recent study using multi lectin affinity chromatography with agarose bound wheat germ agglutinin and jacalin lectin for the identification of multiple glycoprotein biomarker candidates in depleted serum from

breast cancer patients, pregnancy zone protein, apolipoprotein C-III, and alpha-1-antichymotrypsin were present in higher concentration in breast cancer serum relative to the disease free serum [47]. Another recent study reported alpha-1-antitrypsin as a novel biomarker for the breast cancer and down regulated in stage 1 and in later stages (stage II and III) of breast cancer it was shown to be up regulated [55]. In our work, it is observed that alpha-1-antitrypsin is up regulated in the SNA captured protein fractions.

Similarly, using Q-Q scatterplots, 18 DEPs were identified in MAL-II captured fractions either up regulated or down regulated in the cancer serum relative to the disease free serum, see Table 4 for the DEPs. Afamin, alpha-1-antitrypsin, antithrombin-III, apolipoprotein B-100, ceruloplasmin, clusterin, complement C5, serotransferrin, and inter-alpha-trypsin inhibitor heavy chain H2 have been previously reported as sialoglycoproteins. The DEPs Desmoplakin, carboxypeptidase N catalytic chain, and C4b-binding protein alpha chain are low abundance proteins.

Recently identified breast cancer biomarker alpha-1-antitrypsin was down regulated in cancer serum relative to disease free serum. Afamin is a vitamin D binding protein and was found at elevated levels in breast cancer patients [56] which agrees with our present findin^{GS} whereby afamin was also found significantly up-regulated in breast cancer serum. Clusterin, which is up-regulated in the current study, was reported up regulated in breast, lung and colon cancer patients [57, 58]. The up-regulated sialoglycoprotein serotransferrin has been reported as differentially expressed in cancer patients [59, 60]. The DEP desmoplakin was identified as a lung cancer biomarker [61].

The SNA column has captured 25 unique DEPs, MAL has captured 6 unique DEPs while 12 DEPs were common to both lectins. A panel of 43 DEP has been

identified with both lectins and can be viewed as candidate biomarkers for breast cancer, see Table 5. Among the 43 DEPs, 11 were previously reported in the literature as breast cancer biomarkers. Therefore, this investigation has revealed 32 new potential biomarkers for breast cancer.

Differentially expressed proteins captured from SNA column using the M3 and M13 column were 32 and 37, respectively. Among the 32 DEPs captured by the SNA column and fractionated on the M3 column only three of them were low abundance proteins. Among the 37 DEPs in the fractions of the M13 column, 9 low abundance proteins were found, see Table 3 for DEPs captured by SNA lectin and fractionated on the M13 column. The DEPs captured by the MAL-II column and fractionated on the M 3 and M 13 columns were 24 and 18, respectively, with 5 and 3 low abundance proteins for M3 and M13 column, respectively, see Table 3 for DEPs captured by MAL lectin and fractionated on the M13 column. It has been observed that the RPC fractionation of SNA captured proteins using M13 column yielded higher number of DEPs with higher number of low abundance proteins than those found in the fractions of the M3 column. By comparing the identified DEPs in the fractions of M3 column and M13 column it is observed that the M13 column exhibited a better performance.

LC-MS/MS identification of proteins captured by the lectin columns arranged in the order of MAL-II → SNA

Identification of proteins captured by the MAL-II columns. The captured proteins by the MAL-II column were eluted stepwise with the haptenic sugar lactose and subsequently fractionated on the M13 RPC column as described above. The RPC

chromatograms obtained for MAL-II and SNA lectins are shown in Fig. 5. The identified proteins are those with protein identification probability of at least 99% with peptide identification probability of not less than 95% and containing at least two unique peptides. The identified proteins are listed in Table 6. The number of identified proteins from disease free and breast cancer sera are 180 and 191, respectively. In the MAL-II captured fractions, the identified proteins that were unique to disease free and cancer sera were 29 and 40, respectively, see Fig. 6. Among the captured proteins, 119 proteins were identified as glycoproteins including 78 sialoglycoproteins and 97 low abundance proteins. 40 proteins were identified as non-glycoproteins. It is observed that previously identified low abundance proteins as well as new low abundance proteins were identified. In the tandem lectin affinity format SNA lectin was connected followed by MAL-II lectin. By changing the order of lectin columns it is expected to see changes in the number of captured proteins, glycoproteins, sialoglycoproteins, low abundance proteins and DEPs. The proteins captured by the lectin columns were subjected to LC/MS/MS analysis after fractionation on the RPC column. The identified proteins are listed in Table 7. Using the same approach as in the above sections, 176 and 188 non-redundant proteins were found in the proteins captured by the SNA column from the disease free and breast cancer sera, respectively.

In the SNA fractions, the identified proteins that were unique to the disease free serum and the breast cancer serum were 17 and 29 for the disease free and cancer sera, respectively. Among the captured proteins, 110 were glycoproteins including 84 sialoglycoproteins and 66 were identified as low abundance proteins. Upon inverting the order of the lectin columns to Mal-II → SNA, the SNA lectin has captured 66 low

abundance proteins as compared to 83 low abundance proteins when the lectin columns order was SNA → MAL-II. On the other hand, MAL-II lectin has captured 97 proteins when the order was MAL-II → SNA as compared to 50 captured proteins in the reverse order (i.e., SNA → MAL-II).

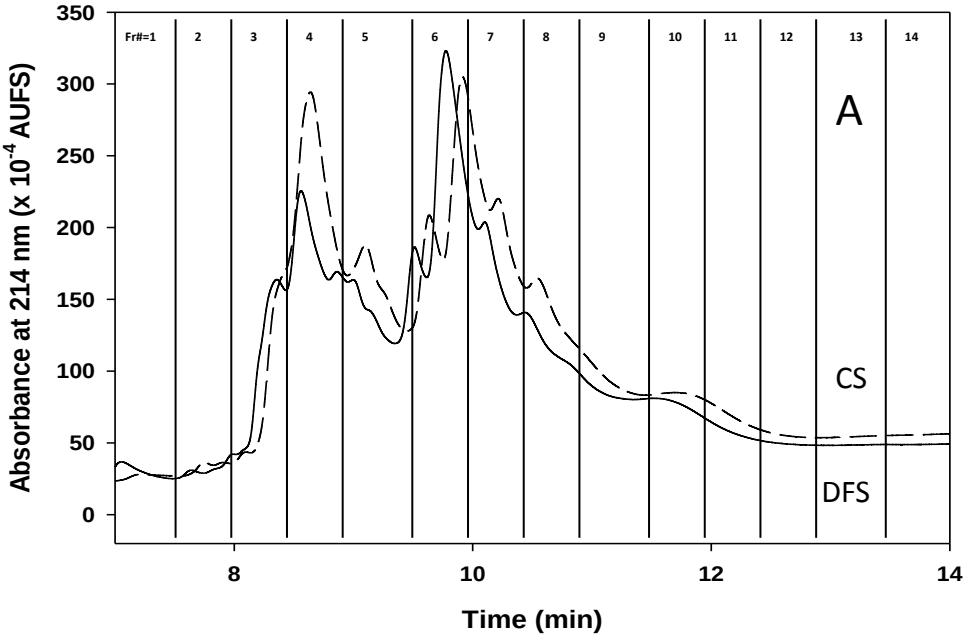

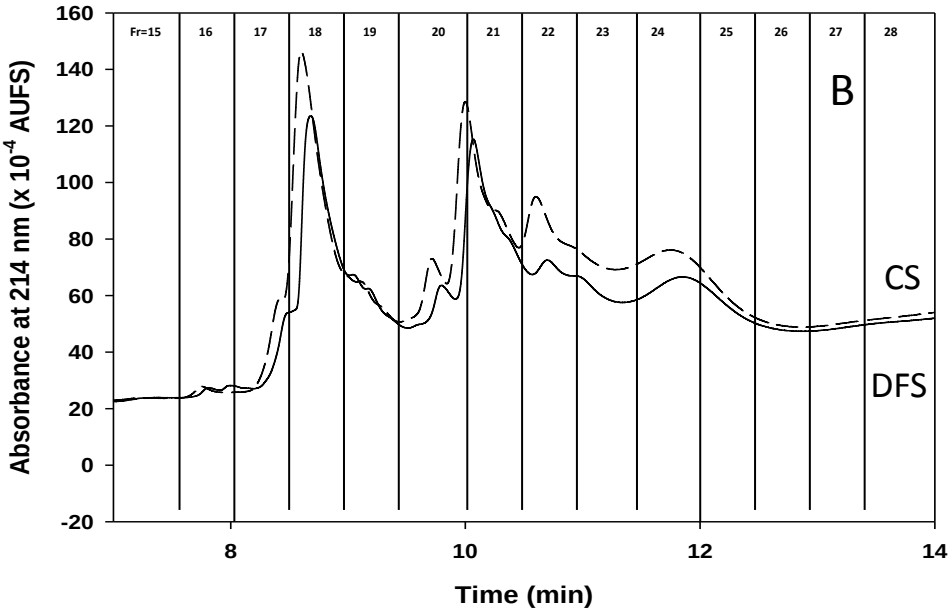

Figure 4. *Chromatograms of the RPC fractionation of proteins captured by MAL-II column (A) and SNA column (B) from disease free (DFS) and breast cancer sera (CS). All other conditions as in Fig. 1.*

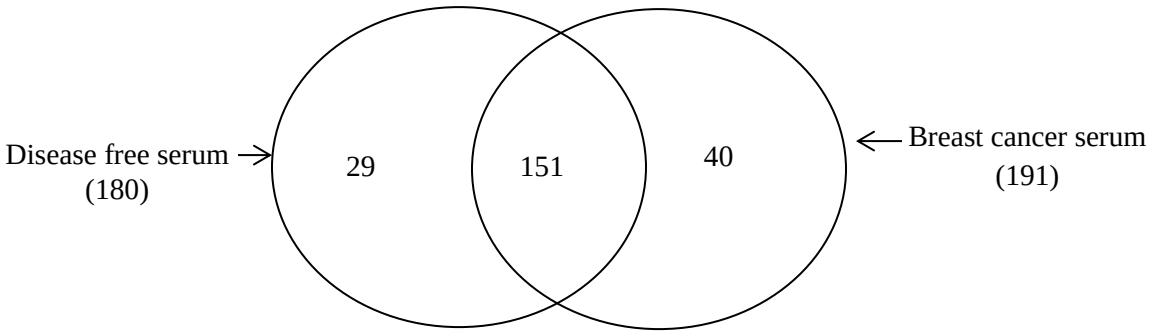

Figure 5. *Venn diagram for LC-MS/MS identified proteins captured by MAL-II lectin arranged in the reversed order (i.e., MAL-II → SNA).*

Using the Uniprot database and NetNgly predictor, which predicts the N-glycosylation sites in proteins, the majority of identified proteins were found to be glycoproteins and certain number were non-glycoproteins. For the disease free serum, and when MAL-II column was arranged as the first column, 66% of the identified proteins were glycoproteins while 34% were non-glycoproteins. For the breast cancer serum, 73% were identified as glycoproteins and 27% were identified as non-glycoproteins. For the SNA lectin placed in the reversed order (MAL-II→ SNA), 58% of the captured proteins were identified as glycoproteins while 42% of the proteins were non-glycoproteins for the disease free serum. With breast cancer serum, 64% of the

captured proteins by the SNA column were identified as glycoproteins while 36 % were non-glycoproteins. When considering the percentage of captured glycoproteins, it was noticed that the order SNA column → MAL-II column is better for capturing a higher amount of glycoproteins. Overall, comparing the total number of captured glycoproteins, sialoglycoproteins and low abundance proteins, it is observed that the lectin columns connected in the order SNA column → MAL-II column have captured higher number of glycoproteins and the order is the most suitable for capturing sialoglycoproteins.

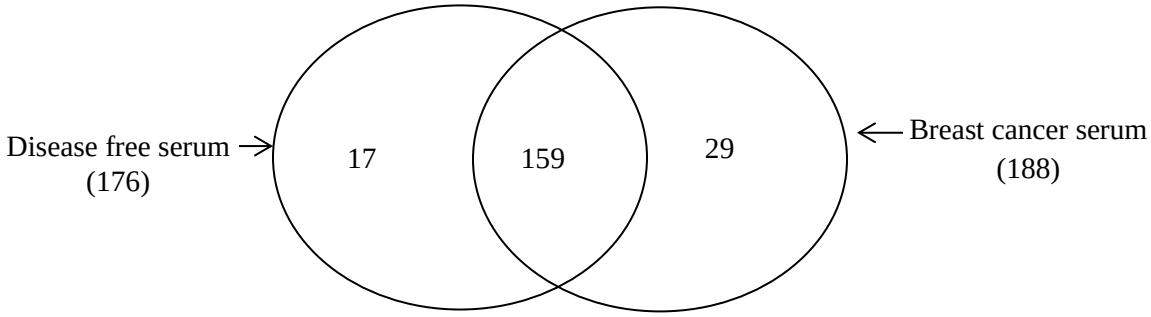

Figure 6. *Venn diagram for LC-MS/MS identified proteins captured by the SNA lectin with the reversed order (i.e., MAL-II→SNA)*

Differentially expressed proteins for the column order MAL-II → SNA The RPC chromatograms of the captured proteins by MAL-II → SNA columns from disease free and cancer sera are shown in Fig. 5 A and B. The two overlapping chromatograms exhibit differences in peak intensity, retention times and peak shouldering. DEPs from cancer serum were found relative to the disease free serum with 99.9% protein identification probability, 95% peptide identification probability with a minimum of five unique peptides. The DEPs were identified using the Q-Q scatterplot by plotting the

normalized spectral count of proteins in breast cancer serum relative to the disease free serum for the same fractions and same proteins. The DEPs were for proteins identified with $p < 0.05$ and that are more than two standard deviations away from being the same in both categories in the Q-Q scatterplots [17].

The MAL-II column, which was connected as the first lectin column has captured 27 DEPs, see Table 8. The DEPs were either up or down regulated. Among these captured DEPs, 20 proteins were sialoglycoproteins and four low abundance proteins. The low abundance DEPs were coagulation factor IX, coagulation factor XIIB chain, fibronectin, and vitronectin. For the SNA column 26 DEPs were identified with 15 sialoglycoproteins and seven low abundance DEPs, see Table 9. The captured low abundance proteins were annexin 1, fibronectin, hemoglobin subunit beta, junction plakoglobin, phosphatidylinisito-1-glycan-specific phospholiphase D, protein S100-A7, and vitamin D-binding protein.

Table 10 summarizes the DEPs unique to MALII (17 DEPs), those unique to SNA (21 DEPs) and those common to both columns (12 DEPs). Therefore, a panel of 50 DEPs was identified as candidate biomarkers for breast cancer. 11 DEPs were previously identified as candidate breast cancer biomarkers. As a result, 39 novel potential candidate biomarkers were revealed in this investigation.

To summarize, 22 common DEPs were identified for both lectin column orders, with 21 unique DEPs for the order SNA column → MAL column and 28 unique DEPs for the order MAL column → SNA column. Therefore, the order of columns seems to lead to a significant difference not only in the total numbers of captured DEPs but also in the identity of the captured DEPs. As a result, a broader panel of DEPs could be obtained

by considering both column orders. That is; a panel of 71 DEPs for both orders of columns, which is a broader panel than that of each column order.

Conclusions

This chapter has shown the importance of the RPC fractionation step of the proteins captured by the two lectin columns prior to LC-MS/MS analysis. The M13 RPC column with incorporated MWCNTs provided better fractionation than the M3 RPC column without incorporated nanotubes, since it has captured higher number of glycoproteins, sialoglycoproteins and low abundance proteins from the disease free and breast cancer sera. Regarding the order of the lectin columns, the investigation demonstrated that is beneficial to identify the DEPs for both column orders; that is SNA column → MAL column and MAL column → SNA column.

TABLE 1

IDENTIFIED BY THE LC-MS/MS ANALYSIS OF THE SNA CAPTURED PROTEINS FRACTIONATED ON THE RPC COLUMN FROM DISEASE- FREE AND CANCER SERA USING M13.DATA ON GS WERE FROM REFS. [15, 19, 24-26, 32, 34, 39, 40, 42, 46, 47, 51, 62-69]

		Average spectral count for disease-free serum						Average spectral for cancer serum					
#	Identified Proteins	Fr # 1	Fr # 2	Fr # 3	Fr # 4	Fr # 5	Fr# 6	Fr #1	Fr #2	Fr #3	Fr #4	Fr#5	Fr#6
1	14-3-3 protein beta/alpha [1 a]	0	0	0	0	0	0	0	0	2	0	0	0
2	14-3-3 protein zeta/delta [1a]	0	0	0	0	0	0	0	0	3	0	0	0
3	Actin, cytoplasmic 1 *	0	0	0	0	5	0	0	0	12	0	2	5
4	Afamin[GS]	0	0	4	16	0	0	0	0	0	4	3	0
5	Alpha-1-acid glycoprotein 1[GS]	0	5	4	2	0	0	0	4	3	2	0	0
6	Alpha-1-acid glycoprotein 2 [GS]	0	5	5	6	0	2	0	5	6	5	3	0
7	Alpha-1-antichymotrypsin[GS]	0	0	0	2	8	7	0	0	0	8	13	9
8	Alpha-1-antitrypsin [GS]	5	5	11	14	23	19	5	8	14	25	25	22
9	Alpha-1B-glycoprotein [GS]	0	11	8	5	2	2	2	11	10	6	2	2
10	Alpha-2-HS-glycoprotein [GS]	0	6	6	5	5	5	0	6	5	4	6	5
11	Alpha-2-antiplasmin [GS]	0	2	0	0	11	10	0	0	2	0	11	11
12	Alpha-2-macroglobulin [GS]	0	0	0	0	28	59	0	0	0	0	55	50
13	Alpha-2-macroglobulin-like protein 1 [GS]	0	0	0	0	0	0	0	0	3	0	0	0
14	Angiotensinogen[GS]	0	0	0	0	9	5	0	0	0	2	11	8
15	Apolipoprotein A-I [GS]	5	11	17	23	29	31	2	11	11	24	28	28
16	Apolipoprotein A-II	3	2	6	5	7	7	0	3	4	6	7	7

17	Apolipoprotein A-IV	6	14	20	19	30	26	11	15	17	21	25	27
18	Apolipoprotein B-100 GS	0	7	0	2	8	56	0	11	3	3	45	42
19	Apolipoprotein C-I	0	5	6	4	4	4	0	4	3	4	3	4
20	Apolipoprotein C-II	0	3	5	5	3	4	0	3	5	5	2	3
21	Apolipoprotein C-III G	2	5	5	5	3	4	2	3	6	4	2	3
22	Apolipoprotein C-IV	0	1	0	0	0	0	0	0	0	0	0	0
23	Apolipoprotein D GS	0	6	7	7	7	5	0	6	5	7	6	5
24	Apolipoprotein E G	3	5	9	8	19	22	2	3	5	11	15	20
25	Apolipoprotein F G	0	2	2	2	0	0	0	2	0	0	0	0
26	Apolipoprotein M GS	0	0	5	6	3	4	0	0	5	5	3	4
27	Apolipoprotein(a) 1a	2	2	2	0	0	0	2	3	2	0	0	0
28	Beta-2-glycoprotein 1 GS	8	9	6	9	3	5	9	9	7	5	3	3
29	Beta-Ala-His dipeptidase 1a	0	0	0	0	0	10	0	0	0	0	2	8
30	Bleomycin hydrolase 1a	0	0	0	0	0	0	3	0	0	0	0	0
31	C4b-binding protein alpha chain G	0	10	12	11	5	5	0	5	10	5	3	4
32	CD5 antigen-like	0	0	0	4	6	4	0	0	0	2	3	4
33	Cadherin-5 GS1a	0	8	4	4	0	0	0	6	2	0	0	0
34	Calmodulin-like protein 3	0	0	0	0	0	0	0	0	2	0	0	0
35	Calmodulin-like protein 5 1a	0	0	0	0	0	0	0	0	2	0	0	0
36	Calpain-1 catalytic subunit 1a	0	0	0	0	0	0	2	0	0	0	0	0
37	Carboxypeptidase N catalytic chain GS1a	0	0	10	12	4	3	0	0	5	11	7	4
38	Carboxypeptidase N subunit 2 GS	0	0	0	0	0	13	0	0	0	0	10	8
39	Caspase-14	0	0	0	0	0	0	6	0	0	0	0	0
40	Cathelicidin antimicrobial peptide 1a	0	0	2	2	0	0	0	0	2	3	0	0

41	Ceruloplasmin [GS]	0	6	28	34	24	26	0	10	28	33	22	20
42	Cholinesterase [1a]	0	0	0	0	2	0	0	0	0	0	0	0
43	Coagulation factor IX [GS1a]	0	3	12	11	2	0	0	6	8	6	0	0
44	Coagulation factor V G[1a]	0	5	2	2	0	0	0	5	0	0	0	0
45	Coagulation factor X [1a]	0	3	0	0	0	0	0	3	0	0	0	0
46	Coagulation factor XII [GS]	0	3	6	4	2	2	0	3	4	2	6	2
47	Coagulation factor XIII B chain [1a]	20	32	12	14	4	2	21	31	14	7	2	4
48	Complement C1r subcomponent [GS]	0	9	24	21	7	3	0	9	18	16	13	4
49	Complement C1r subcomponent-like protein [GS1a]	0	2	2	2	0	0	0	0	0	0	0	0
50	Complement C1s subcomponent [GS]	0	0	14	15	6	2	0	0	17	19	6	3
51	Complement C2 G	0	0	0	0	0	2	0	0	0	0	0	0
52	Complement C3 G	2	7	2	12	58	98	3	15	15	50	82	88
53	Complement C4 beta chain G	0	0	0	8	46	36	0	0	0	15	37	38
54	Complement C4-B G	0	0	0	0	2	3	0	0	0	0	2	2
55	Complement component C6 G	0	3	12	8	0	0	0	3	11	3	0	0
56	Complement component C7 G	0	0	4	4	0	0	0	0	4	0	0	0
57	Complement component C8 alpha chain G	0	0	0	2	0	0	0	0	0	0	0	0
58	Complement component C8 gamma chain G	0	0	0	2	0	0	0	0	0	0	0	0
59	Complement component C9 G	0	0	0	4	0	0	0	0	0	5	2	0

60	Complement factor B G	0	2	11	13	6	3	0	0	11	13	2	4
61	Complement factor H	45	52	36	31	20	24	53	52	30	16	16	19
62	Complement factor H-related protein 1 GS	4	3	0	0	0	0	2	4	0	0	0	0
63	Complement factor H-related protein 2 GS	2	2	0	0	0	0	0	2	0	0	0	0
64	Complement factor H-related protein 3 1aG	2	5	0	0	0	0	3	5	2	0	0	0
65	Complement factor H-related protein 4 1aG	0	1	0	0	0	0	0	0	0	0	0	0
66	Complement factor I G	0	5	22	17	9	4	0	10	17	14	5	6
67	Corneodesmosin 1a GS	0	0	0	0	0	0	2	0	0	0	0	0
68	Cornifin-A	0	0	0	0	0	0	0	0	2	0	0	0
69	Cystatin-A 1aGS	0	0	0	0	0	0	2	0	0	0	0	0
70	Desmoglein-1 1aGS	0	0	0	0	0	0	11	0	0	0	0	0
71	Desmoplakin 1a	5	0	0	0	0	0	23	0	8	0	3	3
72	Elongation factor 1-alpha 1 1a	0	0	0	0	0	0	0	0	2	0	0	0
73	Extracellular serine/threonine protein kinase FAM20C	0	0	2	0	0	0	0	0	0	0	0	0
74	Fetuin-B GS1a	0	4	8	7	0	0	0	4	7	7	0	0
75	Ficolin-2 1aGS	0	2	4	4	0	0	0	0	0	0	0	0
76	Filaggrin-2 1a	0	2	0	2	0	0	9	0	0	0	0	2
77	Galectin-3-binding protein GS1a	0	3	0	0	0	6	0	2	0	0	7	14
78	Galectin-7 1aGS	0	0	0	0	0	0	0	0	3	0	0	0
79	Gamma-glutamylcyclotransferase	0	0	0	0	0	0	2	0	0	0	0	0

80	Gasdermin-A	0	0	0	0	0	0	3	0	0	0	0	0
81	Glutathione peroxidase 3 [1a]	0	0	2	0	0	0	0	0	0	0	0	0
82	Glyceraldehyde-3-phosphate dehydrogenase [1a]	0	0	0	0	0	0	4	0	5	0	0	0
83	Haptoglobin [GS]	3	25	28	28	23	21	8	24	28	28	23	22
84	Heat shock protein HSP 90-beta [1a]	0	0	0	0	0	0	0	0	2	0	0	0
85	Heat shock protein beta-1 [1a]	0	0	0	0	0	0	0	0	2	0	0	0
86	Hemopexin [GS]	0	13	18	12	5	4	0	12	14	11	5	4
87	Heparin cofactor 2 [GS]	0	0	0	0	2	2	0	0	0	0	4	3
88	Histidine-rich glycoprotein [GS]	0	19	12	13	7	8	0	20	15	10	5	6
89	Histone H2A type 1-B/E [1a]	0	0	0	0	0	0	0	0	2	0	0	0
90	Histone H4 [1a]	0	0	0	0	0	0	0	0	4	0	0	0
91	Hornerin [1a]	3	0	0	2	0	0	0	0	2	0	0	2
92	Ig alpha-1 chain C region G	0	1	10	11	10	9	0	0	8	11	12	9
93	Ig alpha-2 chain C region G	0	0	2	2	0	0	0	0	0	2	0	1
94	Ig gamma-1 chain C region	0	2	2	2	2	4	4	3	6	0	2	3
95	Ig gamma-2 chain C region	0	0	0	0	0	0	0	0	3	0	0	0
96	Ig heavy chain V-III region	0	0	0	0	2	2	0	0	0	2	2	2
97	Ig heavy chain V-III region VH26	0	0	0	2	0	2	0	0	0	2	2	0
98	Ig kappa chain C region *	3	5	6	7	7	6	3	5	6	7	7	7
99	Ig kappa chain V-I region EU *	0	0	0	2	0	0	0	0	0	0	0	0
100	Ig kappa chain V-II region TEW *	0	0	0	2	0	0	0	0	0	0	0	0
101	Ig kappa chain V-III region B6*	0	0	0	0	0	0	0	0	0	2	0	0

102	Ig kappa chain V-III region WOL *	2	2	2	3	3	2	2	2	0	2	2	3
103	Ig kappa chain V-IV region Len *	0	0	0	2	0	2	0	0	0	0	0	1
104	Ig lambda chain V-I region HA *	0	2	0	0	2	0	0	2	0	2	2	2
105	Ig lambda chain V-III region LOI *	0	0	0	2	0	0	0	0	0	2	0	1
106	Ig lambda chain V-III region SH *	0	0	0	2	0	0	0	0	0	2	2	0
107	Ig lambda-2 chain C regions *	0	2	2	2	2	2	0	2	0	2	2	2
108	Ig mu chain C region [GS]	0	0	7	13	13	13	0	0	4	13	13	14
109	Immunoglobulin J chain [GS]	0	0	3	3	3	3	0	0	0	3	3	3
110	Immunoglobulin lambda-like polypeptide 5 *	2	3	4	4	4	5	2	2	3	5	5	4
111	Insulin-like growth factor-binding protein 3	2	0	0	0	0	0	0	0	0	0	0	0
112	Inter-alpha-trypsin inhibitor heavy chain H1 [GS]	0	2	0	5	26	12	0	2	2	20	24	18
113	Inter-alpha-trypsin inhibitor heavy chain H2 [GS]	2	3	0	2	29	17	3	3	3	12	27	18
114	Inter-alpha-trypsin inhibitor heavy chain H4 [1aGS]	0	4	10	10	24	23	0	4	7	8	18	22
115	Fibronectin [GS]	3	4	2	10	47	40	4	4	3	7	36	43
116	Desmocollin-1 [1aGS]	0	0	0	0	0	0	4	0	0	0	0	1
117	Disintegrin and metalloproteinase with thrombospondin motifs 13	0	0	2	3	0	0	0	0	0	0	0	0
118	Alpha-actinin-1 [GS 1a]	0	0	0	0	0	0	0	0	3	0	0	0

119	Annexin A2 [1a]	0	0	0	0	0	0	4	0	0	0	0	0
120	Apolipoprotein L1 G	0	0	5	6	5	10	0	0	4	5	6	9
121	Arginase-1	0	0	0	0	0	0	2	0	0	0	0	0
122	Asialoglycoprotein receptor 2 G[1a]	0	2	0	0	0	0	0	0	0	0	0	0
123	Attractin [1a]	0	0	4	3	0	0	0	0	3	0	0	0
124	C4b-binding protein beta chain [G]	0	2	0	0	0	0	0	2	0	0	0	0
125	Cartilage acidic protein 1[1aG]	0	0	4	2	0	0	0	0	2	0	0	0
126	Clusterin [GS]	0	4	17	18	8	10	0	5	13	19	10	8
127	Dermcidin [1a]	2	2	0	0	0	0	2	2	0	0	0	0
128	EGF-containing fibulin-like extracellular matrix protein 1 G	0	0	0	0	0	2	0	0	0	0	0	0
129	Fibrinogen alpha chain [GS]	5	3	4	2	0	2	5	3	3	0	0	0
130	Ficolin-3 [GS]	0	0	2	3	4	4	0	0	0	3	3	4
131	Haptoglobin-related protein [1a*]	0	0	5	5	4	4	0	0	5	5	3	4
132	Histidine ammonia-lyase	0	0	0	0	0	0	2	0	0	0	0	0
133	Histone H2B type 2-F	0	0	0	0	0	0	0	0	2	0	0	0
134	Hyaluronan-binding protein 2 *	0	9	6	4	2	0	0	8	6	2	0	2
135	Ig delta chain C region [1a]G	0	0	0	0	0	0	0	0	2	0	0	0
136	Insulin-like growth factor-binding protein complex acid labile subunit [GS]	0	0	0	0	6	0	2	0	0	0	3	6
137	Inter-alpha-trypsin inhibitor heavy chain H3 [GS]	0	0	0	0	0	0	0	0	0	2	0	0
138	Mannan-binding lectin	0	0	2	3	0	0	0	0	0	0	0	0

	serine protease 1 [1a]												
139	N-acetylmuramoyl-L-alanine amidase [GS]	0	0	0	2	0	0	0	0	0	3	0	0
140	Semenogelin-1 [1a]	0	2	0	0	0	0	0	2	0	0	0	0
141	Vitamin K-dependent protein Z [1aGS]	0	8	9	8	4	3	0	2	0	0	0	0
142	Calumenin [GS]	0	3	0	0	0	0	0	0	0	0	0	0
143	Extracellular matrix protein 1 [GS1a]	3	3	0	0	0	0	2	3	0	0	0	0
144	Pregnancy-specific beta-1-glycoprotein 1 [GS]	0	6	5	5	0	0	0	0	0	0	0	0
145	Collectin-11 [1a]	0	0	0	2	0	0	0	0	0	0	0	0
146	Coagulation factor VII [1a]	0	0	0	3	0	0	0	0	0	3	0	0
147	Fibulin-1 [GS]	0	0	4	4	0	0	0	0	3	3	0	0
148	Gamma-A of Fibrinogen gamma chain [GS]	0	0	2	2	0	0	0	0	2	0	0	0
149	Kininogen-1 [GS]	5	26	22	22	15	11	7	22	20	17	13	15
150	Alpha-enolase [1a]	0	0	0	0	0	0	0	0	3	0	0	0
151	Junction plakoglobin [1a]	0	0	0	0	0	0	4	0	0	2	0	0
153	Kallistatin [GS]	0	0	0	0	6	3	0	0	0	0	2	4
154	Keratin, type I cytoskeletal 14 [1a*]	17	12	3	10	9	10	24	11	25	15	6	14
155	Keratin, type I cytoskeletal 15 [1a*]	0	0	0	0	0	0	0	0	3	0	0	0
156	Keratin, type I cytoskeletal 16 [1a*]	8	7	0	0	2	0	15	5	11	10	0	7
157	Keratin, type I cytoskeletal 17 [1a*]	2	2	0	0	0	0	7	0	14	2	0	3
158	Keratin, type II cytoskeletal 1b *	0	4	0	0	0	0	17	0	0	0	0	1

159	Keratin, type II cytoskeletal 5 [1a*]	14	7	3	5	4	4	21	6	21	8	6	10
160	Keratin, type II cytoskeletal 6A*	6	3	0	0	0	0	5	2	5	2	0	2
161	Keratin, type II cytoskeletal 6B *	20	8	2	3	5	2	25	3	29	15	3	15
162	Keratin, type II cytoskeletal 78 *	0	0	0	0	0	0	7	0	0	0	0	0
163	Keratin, type II cytoskeletal 80*	0	0	0	0	0	0	9	0	0	0	0	0
164	Keratinocyte proline-rich protein	0	2	0	0	0	0	6	0	0	0	2	3
165	Leucine-rich alpha-2-glycoprotein [GS]	0	0	0	3	0	0	0	0	0	3	0	0
166	Lipopolysaccharide-binding protein [1a]	0	0	0	0	0	3	0	0	0	0	0	0
167	Lumican [GS]	0	0	7	3	0	0	0	0	4	3	0	0
168	Mannan-binding lectin serine protease 2	0	1	0	0	0	0	0	0	0	0	0	0
169	Monocyte differentiation antigen CD14 [1a]	0	0	0	0	0	0	0	0	0	3	0	0
170	Myosin-9 [1a]	0	0	0	0	0	0	0	0	2	0	0	0
171	N-acetylglucosamine-1-phosphotransferase [GS]	0	0	2	2	0	0	0	0	0	0	0	0
172	Neutrophil defensin 1	0	0	0	0	0	0	0	0	0	0	0	1
173	Out at first protein homolog	0	0	2	2	0	0	0	0	2	0	0	0
174	Phosphatidylcholine-sterol acyltransferase [1a]	0	0	0	4	3	3	0	0	0	4	2	3
175	Phosphatidylinositol-glycan-specific	0	0	0	0	11	17	0	0	0	0	9	12

	phospholipase D [GS1a]												
176	Phosphoglycerate mutase 2 [1a]	0	0	0	0	0	0	0	0	3	0	0	0
177	Phospholipid transfer protein G[1a]	0	0	0	0	0	3	0	0	0	0	3	2
178	Plasma kallikrein heavy chain	0	0	7	7	5	4	0	0	3	0	4	5
179	Plasma protease C1 inhibitor	0	0	0	0	11	9	0	0	0	0	9	8
181	Plasma serine protease inhibitor [1a]	0	0	0	0	0	6	0	0	0	0	0	3
182	Plasminogen	0	35	8	8	2	2	0	30	21	2	2	2
183	Plectin [1a]	0	0	0	0	0	0	2	0	0	0	0	0
184	Plexin domain-containing protein 2 [1a]	0	0	0	2	0	0	0	0	0	0	0	0
185	Pregnancy zone protein [GS1a]	0	0	0	0	0	20	0	0	0	0	17	17
186	Pregnancy-specific beta-1-glycoprotein 2 [GS]	0	0	2	3	0	0	0	0	0	0	0	0
187	Prenylcysteine oxidase 1 G[1a]	0	0	0	0	0	4	0	0	0	0	0	2
188	Protein AMBP [GS]	0	5	7	9	11	5	0	5	7	12	9	8
189	Protein S100-A11 [1a]	0	0	0	0	0	0	0	0	2	0	0	0
190	Protein S100-A7 [1a]	0	0	0	0	0	0	0	0	3	0	3	0
191	Protein S100-A8	0	0	0	0	0	0	0	0	2	0	0	0
192	Protein S100-A9	0	0	2	3	0	0	0	0	5	2	2	2
193	Protein Z-dependent protease inhibitor G[1a]	0	0	0	0	2	3	0	0	0	3	3	2
194	Protein-glutamine gamma-glutamyltransferase E [1a]	0	0	0	0	0	0	7	0	0	0	0	0
195	Protein-glutamine gamma-glutamyltransferase K	0	0	0	0	0	0	3	0	0	0	0	0

196	Prothrombin	2	6	20	21	6	6	2	6	11	19	4	5
197	Alpha-S1-casein	0	2	0	4	0	0	2	0	2	0	0	0
198	Alpha-S2-casein	0	0	0	2	0	0	0	0	0	0	0	0
199	Alpha-lactalbumin	0	4	0	0	0	0	0	4	0	0	0	0
200	Antithrombin-III [GS]	0	4	16	18	7	5	2	7	9	22	12	6
201	Beta-2-microglobulin [GS]	2	2	0	0	0	0	0	2	0	0	0	0
202	Beta-casein	0	0	0	2	0	0	0	0	0	0	0	0
203	Catalase [1a]	0	0	0	0	0	0	3	0	0	0	0	0
204	Cathepsin D [GS]	0	0	0	0	0	0	2	0	0	0	0	0
205	Cationic trypsin	3	0	0	0	0	0	2	0	0	0	0	0
206	Complement C5	0	0	0	0	2	14	0	0	0	0	27	16
207	Gelsolin [1a]	0	0	0	3	0	0	0	0	0	0	0	0
208	Glutathione S-transferase P [1a]	0	0	0	0	0	0	0	0	2	0	0	0
209	Hemoglobin subunit alpha G	0	0	7	8	4	4	0	0	3	2	0	3
210	Hemoglobin subunit beta G	0	2	9	10	7	6	0	0	3	3	0	6
211	Keratin, type I cytoskeletal 10 [1a]	19	22	20	24	23	19	25	20	20	24	26	24
212	Keratin, type I cytoskeletal 9*	17	14	13	19	14	16	23	15	15	18	14	20
213	Keratin, type II cytoskeletal 1*	27	26	22	29	23	26	36	25	24	29	27	28
214	Keratin, type II cytoskeletal 2 epidermal *	26	25	19	26	19	23	44	26	24	26	26	34
215	Peptidyl-prolyl cis-trans isomerase A [1a]	0	0	0	0	0	0	0	0	2	0	0	0
216	Retinol-binding protein 4	0	4	5	3	4	2	0	4	4	4	3	4
217	Serotransferrin [GS]	3	43	46	30	13	14	0	41	31	22	10	13

218	Serum albumin	10	33	55	52	42	40	17	45	57	50	41	39
219	Thioredoxin [1a]	0	0	0	0	0	0	3	0	0	0	0	0
220	Trypsin [1a]	4	4	4	4	2	3	4	4	4	3	3	3
221	Ubiquitin *	0	0	0	0	0	0	2	0	0	0	0	0
222	Secreted phosphoprotein 24 [1a]	0	3	0	0	0	0	0	2	0	0	0	0
223	Selenoprotein P G	5	7	5	5	0	4	3	7	2	0	0	0
224	Serpin B12	0	0	0	0	0	0	3	0	0	0	0	0
225	Serum amyloid A-1 protein [GS]	0	0	3	2	0	0	0	0	0	0	0	0
226	Serum amyloid A-4 protein [GS]	0	2	5	5	3	3	0	0	4	6	4	4
227	Serum amyloid P-component [GS]	0	0	6	7	5	5	0	0	6	6	4	5
228	Serum paraoxonase/arylesterase 1 [GS]	0	0	3	5	9	8	0	0	0	5	9	8
229	Serum paraoxonase/lactonase 3 [1aGS]	0	0	0	2	3	3	0	0	0	0	2	3
230	Sex hormone-binding globulin [1aG]	0	0	2	2	0	0	0	0	2	0	0	0
231	Small proline-rich protein 2E G	0	0	0	0	0	0	0	0	0	0	2	0
232	Suprabasin [1a]	0	0	0	0	0	0	2	0	0	0	0	0
233	Tetranectin	0	7	4	2	0	0	0	7	5	2	0	0
234	Transthyretin	0	8	9	8	4	3	5	8	9	8	6	6
235	Tubulin alpha-1B chain	0	0	0	0	0	0	0	0	5	0	0	0
236	Tubulin beta-4A chain [1a]	0	0	0	0	0	0	0	0	3	0	0	0

237	Vitamin D-binding protein GS	0	0	0	0	0	0	0	0	15	7	0	0
238	Vitamin K-dependent protein C 1a	0	7	4	2	0	0	0	0	7	6	0	0
239	Vitamin K-dependent protein S	0	0	0	0	0	0	0	0	0	10	6	4
240	Vitronectin GS	4	4	4	4	2	3	0	8	11	7	6	4
241	Zinc-alpha-2-glycoprotein GS	2	5	0	0	0	0	0	6	0	0	0	0

G, glycoprotein; GS, sialylated glycoprotein; 1a, low abundance protein (few ng to sub μg/mL level); *, non-glycoprotein.

TABLE 2

PROTEINS IDENTIFIED BY THE LC-MS/MS ANALYSIS OF THE SNA CAPTURED PROTEINS FRACTIONATED ON THE RPC COLUMN FROM DISEASE- FREE AND CANCER SERA USING M13 COLUMN. DATA ON GS WERE FROM REFS.[15, 24, 34, 39, 40, 42, 56, 62, 63, 67, 69-72]

		Average spectral count for disease-free serum						Average spectral count for cancer serum					
#		Fr # 1	Fr # 2	Fr # 3	Fr # 4	Fr # 5	Fr # 6	Fr # 1	Fr # 2	Fr #3	Fr # 4	Fr # 5	Fr #6
1	Actin, aortic smooth muscle *	0	0	0	0	0	0	0	0	0	2	0	0
2	Afamin [GS]	0	3	12	4	0	0	0	6	19	18	0	0
3	Alpha-1-acid glycoprotein 1 [GS]	0	3	0	0	0	0	4	0	0	0	0	0
4	Alpha-1-acid glycoprotein 2 [GS]	0	3	2	3	3	2	5	6	3	2	2	0
5	Alpha-1-antichymotrypsin [GS]	5	2	13	12	10	10	0	2	12	11	8	5
6	Alpha-1-antitrypsin [GS]	17	14	28	29	28	22	6	19	28	27	20	15
7	Alpha-1B-glycoprotein [GS]	0	8	0	2	0	0	6	5	0	0	0	0
8	Alpha-2-antiplasmin [GS]	0	0	2	6	5	2	2	0	2	7	7	2
9	Alpha-2-HS-glycoprotein [GS]	3	7	6	6	7	7	5	7	6	6	5	4
10	Alpha-2-macroglobulin [GS]	28	0	0	21	48	59	0	0	3	39	51	58
11	Alpha-S1-casein	0	0	0	0	0	2	0	0	0	0	0	2
12	Angiotensinogen	0	0	2	6	8	6	0	0	2	6	4	2
13	Antithrombin-III [GS]	6	4	10	7	7	5	0	12	7	5	0	0
14	Apolipoprotein A-I [GS]	19	29	33	35	35	33	14	31	33	36	33	31
15	Apolipoprotein A-II *	4	3	6	6	6	7	3	6	6	7	7	7

16	Apolipoprotein A-IV *	12	17	24	29	28	24	12	22	25	26	24	17
17	Apolipoprotein B-100 [GS]	26	0	2	4	38	60	0	0	0	10	26	34
18	Apolipoprotein C-I *	2	4	2	3	2	3	4	5	4	4	5	4
19	Apolipoprotein C-II *	2	2	2	0	0	2	2	5	2	2	2	3
20	Apolipoprotein C-III [G]	0	5	2	0	2	3	3	4	3	3	3	3
21	Apolipoprotein D [GS]	4	8	8	8	6	8	3	8	9	7	7	5
22	Apolipoprotein E [G]	6	8	11	15	14	15	4	13	18	20	17	11
23	Apolipoprotein F [G]	2	0	0	0	0	0	0	0	0	0	0	0
24	Apolipoprotein L1 [G]	4	3	4	5	7	7	4	4	4	7	10	4
25	Apolipoprotein M [GS]	2	5	3	3	3	3	2	6	4	3	3	0
26	Apolipoprotein(a) [1a]	2	0	0	0	0	0	0	0	0	0	0	0
27	Arginase-1	0	0	0	0	0	0	0	0	0	0	2	0
28	Beta-2-glycoprotein 1 [GS]	6	5	3	2	2	2	6	7	7	3	3	2
29	Beta-Ala-His dipeptidase [1a]	0	0	0	0	6	8	0	0	0	3	12	0
30	C4b-binding protein alpha chain[G]	0	15	6	4	5	5	6	12	6	5	3	3
31	C4b-binding protein beta chain[G]	0	2	0	2	0	0	0	0	0	0	0	0
32	Carboxypeptidase N catalytic chain [1a]	2	0	5	6	3	0	0	8	5	2	0	0
33	Carboxypeptidase N subunit 2 [GS]	5	0	0	0	4	12	0	0	0	0	5	8
34	Cartilage acidic protein 1 [1aG]	0	0	0	0	0	0	0	2	0	0	0	0
35	Cartilage oligomeric matrix protein [1a GS]	0	0	0	2	2	2	0	0	2	0	0	0
36	Caspase-14 [1a*]	0	0	0	0	0	0	0	3	0	0	4	3
37	Cationic trypsin	3	2	2	3	0	0	0	0	0	0	0	4
38	CD5 antigen-like *	0	0	0	2	2	3	0	0	7	7	3	0

39	Ceruloplasmin [GS]	4	12	17	21	17	12	4	29	24	22	11	7
40	Clusterin [GS]	6	9	13	9	8	7	5	16	9	6	4	3
41	Coagulation factor IX [1a GS]	0	0	0	0	0	0	0	3	0	0	0	0
42	Coagulation factor X [1a GS]	0	0	0	0	0	0	2	0	0	0	0	0
43	Coagulation factor XII [GS]	0	2	0	3	3	0	0	8	2	3	0	0
44	Coagulation factor XIII B chain [1a GS]	3	4	0	0	0	0	2	0	0	0	0	0
45	Complement C1r subcomponent [GS]	0	5	2	3	3	0	0	17	6	3	0	0
46	Complement C1r subcomponent-like protein [1a GS]	0	0	0	0	0	0	0	0	2	0	0	0
47	Complement C1s subcomponent	2	6	4	6	5	2	0	11	6	5	0	2
48	Complement C3 [GS]	26	24	41	81	93	96	3	16	51	96	120	88
49	Complement C4 beta chain [G]	3	2	31	40	42	38	0	6	42	45	34	24
50	Complement C4-B [GS]	0	0	0	0	0	0	0	0	2	2	2	0
51	Complement C5	4	0	0	4	11	21	0	0	0	5	16	10
52	Complement component C6 [G]	0	4	0	0	0	0	0	8	0	0	0	0
53	Complement component C7 [G]	0	4	0	0	0	0	0	7	0	0	0	0
54	Complement component C8 alpha chain [G]	0	0	0	0	2	0	0	3	0	0	0	0
55	Complement component C8 gamma chain [G]	0	0	0	0	0	0	0	3	0	0	0	0
56	Complement component C9 [G]	0	0	3	2	2	0	0	2	4	0	0	0
57	Complement factor B [G]	2	2	7	5	0	0	0	9	6	5	0	0
58	Complement factor H [GS]	60	54	18	23	21	25	47	44	32	25	21	8
59	Complement factor H-related protein 1 [GS]	3	2	0	0	0	0	2	0	0	0	0	0
60	Complement factor I [G]	4	19	10	9	10	8	6	22	13	11	7	2
61	Cystatin-A [1a GS]	0	0	0	0	0	0	2	2	0	0	0	0

62	Dermcidin [1a]	0	2	0	0	0	2	0	2	0	0	0	3
63	Desmocollin-1 [1a]	0	0	0	0	0	0	2	0	0	0	4	2
64	Desmoglein-1 [1a G]	2	0	0	0	0	0	0	0	0	0	5	3
65	Desmoplakin [1a *]	5	2	2	0	0	2	4	2	0	2	3	20
66	Extracellular matrix protein 1	0	0	0	0	0	0	2	0	0	0	0	0
67	Fetuin-B [1a GS]	2	8	3	3	2	2	3	8	3	4	2	0
68	Fibrinogen alpha chain	3	0	0	0	0	0	2	0	0	0	0	0
69	Fibronectin	4	0	8	16	21	25	0	0	14	24	25	12
70	Fibulin-1 [GS]	0	0	0	4	0	0	0	2	3	0	0	2
71	Ficolin-3	2	0	0	2	3	3	0	2	3	3	2	3
72	Filaggrin-2 [1a]	3	2	0	2	0	2	3	2	0	2	9	5
73	Galectin-3-binding protein [1a GS]	0	0	0	0	0	5	0	0	0	0	2	3
74	Gelsolin	0	0	0	2	0	0	0	2	0	0	0	0
75	Glyceraldehyde-3-phosphate dehydrogenase [1a]	0	0	0	0	0	0	0	0	0	0	4	2
76	Haptoglobin [GS]	20	24	20	19	21	20	22	25	19	21	18	16
77	Haptoglobin-related protein [1a]	0	3	4	4	4	5	0	5	4	5	4	2
78	Hemoglobin subunit alpha	0	0	0	0	0	0	0	4	2	2	0	0
79	Hemoglobin subunit beta	0	0	0	0	0	0	0	4	7	5	3	3
80	Hemopexin [GS]	4	9	3	5	4	3	3	10	6	4	3	0
81	Heparin cofactor 2 [GS]	0	0	3	3	2	0	0	0	3	4	0	0
82	Histidine-rich glycoprotein [GS]	2	9	3	5	4	5	5	9	8	5	3	2
83	Hornerin *[1a]	2	3	2	0	0	2	2	6	0	0	2	6
84	Hyaluronan-binding protein 2	0	5	0	0	0	0	4	6	2	0	0	0
85	Ig alpha-1 chain C region [G]	8	7	9	10	12	11	2	11	13	14	10	9
86	Ig gamma-1 chain C region [G]	2	4	7	6	7	7	0	4	6	6	7	7
87	Ig gamma-2 chain C region [G]	0	0	0	0	0	0	0	0	0	2	0	0
88	Ig gamma-3 chain C region [G]	0	0	0	2	2	0	0	0	2	0	0	0

89	Ig heavy chain V-II region ARH-77 *	0	0	0	0	0	2	0	0	0	2	0	0
90	Ig heavy chain V-III region BRO *	0	0	0	2	2	2	0	0	0	2	2	0
91	Ig heavy chain V-III region GAL *	0	0	0	0	0	0	0	0	0	2	0	0
92	Ig heavy chain V-III region TIL *	0	0	0	0	0	0	0	0	2	2	0	0
93	Ig kappa chain C region *	4	5	6	8	7	7	3	8	8	8	7	7
94	Ig kappa chain V-I region EU *	0	0	0	0	0	0	0	0	0	2	0	0
95	Ig kappa chain V-II region RPMI 6410 *	0	0	0	0	0	0	0	0	0	2	0	0
96	Ig kappa chain V-III region WOL [*]	2	0	2	2	2	2	0	2	2	3	2	2
97	Ig kappa chain V-IV region Len *	0	0	0	0	0	2	0	0	0	0	0	0
98	Ig lambda chain V region 4A [1a*]	0	0	0	0	0	0	0	0	0	2	2	0
99	Ig lambda-2 chain C regions *	4	3	6	5	6	5	2	5	5	5	5	5
100	Ig mu chain C region	6	4	9	11	11	13	0	8	12	11	12	11
101	Immunoglobulin J chain	0	0	3	4	4	4	0	2	4	4	3	2
102	Immunoglobulin lambda-like polypeptide 5 *	0	0	2	0	0	2	0	0	0	0	0	0
103	Insulin-like growth factor-binding protein complex acid labile subunit	2	0	0	0	0	0	0	0	0	0	0	0
104	Inter-alpha-trypsin inhibitor heavy chain H1 [GS]	4	4	10	18	19	9	0	2	13	20	11	5
105	Inter-alpha-trypsin inhibitor heavy chain H2 [GS]	5	2	15	24	26	17	0	3	19	32	14	9
106	Inter-alpha-trypsin inhibitor	0	0	0	4	0	0	0	0	4	0	0	0

	heavy chain H3												
107	Inter-alpha-trypsin inhibitor heavy chain H4 [GS]	8	5	14	15	14	16	4	10	18	18	14	14
108	Junction plakoglobin	0	0	0	0	0	0	0	0	0	0	0	2
109	Junction plakoglobin [1a]	0	0	0	0	0	0	0	0	0	0	0	5
110	Kallistatin [GS]	0	0	5	5	5	0	0	0	3	10	3	0
111	Keratin, type I cytoskeletal 10 [1a*]	22	25	22	21	23	22	23	20	19	25	27	27
112	Keratin, type I cytoskeletal 13 [1a*]	0	0	0	0	2	8	0	0	0	0	0	0
113	Keratin, type I cytoskeletal 14 [1a*]	6	10	8	4	3	6	6	5	7	7	7	9
114	Keratin, type I cytoskeletal 16 [1a*]	16	26	16	5	7	17	18	13	11	12	11	22
115	Keratin, type I cytoskeletal 17 [1a*]	4	6	2	0	0	2	3	3	0	3	0	4
116	Keratin, type I cytoskeletal 9*	19	25	25	21	18	22	19	23	22	22	17	28
117	Keratin, type II cytoskeletal 1	31	33	35	29	27	28	32	27	24	30	31	36
118	Keratin, type II cytoskeletal 1b*	3	0	0	0	0	0	2	0	0	3	3	0
119	Keratin, type II cytoskeletal 2 epidermal	27	29	28	27	35	25	33	22	21	32	42	41
120	Keratin, type II cytoskeletal 4	0	2	0	0	0	3	0	0	0	0	0	0
121	Keratin, type II cytoskeletal 5 [1a*]	15	13	14	7	9	16	13	5	6	9	16	19
122	Keratin, type II cytoskeletal 6A*	2	2	0	0	0	0	0	0	0	0	0	2
123	Keratin, type II cytoskeletal 6B *	0	2	0	0	0	0	0	0	0	0	0	0
124	Keratin, type II cytoskeletal 6C*	15	19	13	4	4	15	12	10	7	11	5	20

125	Keratin, type II cytoskeletal 78 *	0	0	0	0	0	0	0	0	0	0	0	2
126	Keratin, type II cytoskeletal 80 *	0	0	0	0	0	0	0	0	0	0	3	0
127	Keratinocyte proline-rich protein	2	0	0	2	2	0	0	0	0	3	6	5
128	LMW of Kininogen-1 [GS]	8	23	16	15	15	13	22	26	19	20	11	10
129	Lumican [GS]	0	2	0	0	0	0	0	7	0	0	0	0
130	Lysozyme C [1a]	0	0	0	0	0	0	0	0	0	0	0	2
131	Mannan-binding lectin serine protease 1 [1a *]	0	0	0	0	0	0	0	0	3	0	0	0
132	Ovalbumin	0	0	0	2	2	0	0	0	2	0	0	0
133	Pepsin A	0	0	0	0	2	0	0	0	0	0	0	0
134	Peroxiredoxin-2 [1a*]	0	0	0	0	0	0	0	0	2	0	0	2
135	Phosphatidylcholine-sterol acyltransferase [1a]	0	0	0	0	0	0	0	0	3	0	0	0
136	Phosphatidylinositol-glycan-specific phospholipase D [1a GS]	0	0	0	0	3	7	0	0	0	5	8	4
137	Plasma kallikrein heavy chain [GS]	0	0	0	3	0	0	0	0	3	3	0	0
138	Plasma protease C1 inhibitor [GS]	0	0	8	9	11	11	0	2	10	9	5	5
139	Plasma serine protease inhibitor [1a]	0	0	0	0	4	2	0	0	0	0	5	0
140	Plasminogen [GS]	2	28	2	3	3	3	25	16	8	4	2	0
141	Plexin domain-containing protein 2 [1aG]	0	0	0	0	0	0	0	4	2	0	0	0
142	Pregnancy zone protein [1a GS]	5	0	0	0	3	20	0	0	0	0	5	20
143	pregnancy-specific beta-1-glycoprotein 1 [GS]	0	0	0	0	0	0	7	5	3	2	0	0

144	Prenylcysteine oxidase 1 [1a G]	0	0	0	0	0	3	0	0	0	0	0	0
145	Prolactin-inducible protein [1a GS]	0	0	0	0	0	6	0	0	0	0	0	0
146	Protein AMBP [GS]	2	5	5	8	9	3	2	7	9	7	4	2
147	Protein S100-A7 [1a]	0	0	0	0	0	2	0	0	0	0	0	2
148	Protein S100-A8 [1a]	0	0	0	0	0	0	0	0	0	0	0	2
149	Protein S100-A9	0	2	0	0	2	3	0	3	2	2	2	4
150	Protein-glutamine gamma-glutamyltransferase E [1a]	0	0	0	0	0	0	0	0	0	0	3	0
151	Prothrombin	0	3	2	3	2	0	2	4	3	2	0	0
152	Retinol-binding protein 4 *	3	6	6	5	6	7	5	6	7	7	6	4
153	Secreted Ly-6/uPAR-related protein 1 [1a*]	0	0	0	0	0	0	0	2	0	0	0	0
154	Selenoprotein P [1a]	2	3	0	0	0	0	3	3	0	0	0	0
155	Serotransferrin [GS]	5	30	14	12	8	7	27	27	49	13	7	24
156	Serpin B3 [1a]	2	0	0	0	0	0	0	0	0	0	0	0
158	Serum albumin	36	64	52	49	43	43	47	62	51	42	41	32
159	Serum amyloid A-1 protein [GS]	0	2	0	0	0	0	2	2	0	0	0	0
160	Serum amyloid A-4 protein [GS]	3	6	4	2	4	4	3	5	4	4	3	4
161	Serum amyloid P-component [GS]	5	6	7	6	6	7	4	7	6	6	4	5
162	Serum paraoxonase/arylesterase 1 [GS]	3	2	4	6	6	7	0	3	7	6	6	6
163	Serum paraoxonase/lactonase 3 [1a]	0	0	0	3	2	2	0	0	3	3	0	0
164	Short of Complement factor H-related protein 2	2	0	0	0	0	0	0	2	0	0	0	0
165	Skin-specific protein 32	0	0	0	0	0	0	0	0	0	0	4	0
166	Sulfhydryl oxidase 1 [1a]	0	0	0	3	0	0	0	0	7	0	0	0
167	Suprabasin [1a]	0	0	0	0	0	0	0	0	0	0	3	0

168	Tetranectin [GS]	0	7	2	2	2	3	4	2	2	2	0	0
169	Transthyretin *	0	6	3	4	3	4	3	9	7	5	2	0
170	Trypsin [1a]	5	4	3	3	3	3	4	3	3	3	4	4
171	Ubiquitin-60S ribosomal protein L40 [G]	0	0	0	0	0	0	0	0	0	2	0	0
172	Vitamin D-binding protein [GS]14	0	5	0	0	0	0	2	12	0	0	0	0
173	Vitamin K-dependent protein C [1a]	0	3	0	0	0	0	0	7	0	0	0	0
174	Vitamin K-dependent protein S	0	2	3	8	2	0	0	3	11	3	2	0
175	Vitronectin [GS]	2	8	3	4	5	5	6	7	6	7	5	5
176	Zinc-alpha-2-glycoprotein [GS]	0	0	0	0	0	0	3	0	0	0	3	2

G, glycoprotein; GS, sialylated glycoprotein; 1a, low abundance protein (few ng to sub μg/mL level); *, non-glycoprotein.

TABLE 3

DIFFERENTIALLY EXPRESSED PROTEINS IN THE SNA FRACTIONS FROM DISEASE FREE SERUM (DFS) AND CANCER SERUM (CS). DATA ON GS WERE FROM REFS.[26, 34, 39, 40, 42, 62, 63, 67]

Fractions which differential expression was found (Down or up)	Identified Proteins	Accession Number	Mol. Wt.	Up/down regulated	Total of average spectral counts from different fractions (DFS)	Total of average spectral counts from different fractions (CS)
F3-Down	Actin, cytoplasmic 1	ACTB_HUMAN	42 kDa	Down	12	2
F4-Up	Alpha-1-antichymotrypsin [GS]	AACT_HUMAN	48 kDa	Up	7	13
F4-Up	Alpha-1-antitrypsin [GS]	A[1a]T_HUMAN	47 kDa	Up	14	25
F5-up	Alpha-2-macroglobulin	A2MG_HUMAN	163 kDa	Down	28	55
F2-Down	Alpha-lactalbumin	LALBA_BOVIN	16 kDa	Down	5	0
F1- Down	Annexin A2 [1a]	ANXA2_HUMAN	40 kDa	Down	5	0
F2-Down	Antithrombin-III [GS]	ANT3_HUMAN	53 kDa	Down	8	4
F5-Down	Apolipoprotein B-100 [GS]	APOB_HUMAN	516 kDa	Down	56	42
F2- Up	Apolipoprotein C-III [G]	B0YIW2_HUMAN	13 kDa	Up	5	10
F2- Up	C4b-binding protein alpha chain [G]	C4BPA_HUMAN	67 kDa	Up	5	12
F2- Up	Cadherin-5 [GS]	CADH5_HUMAN	88 kDa	Up	4	9
F2- Up	Calumenin	CALU_HUMAN	38 kDa	Up	0	4

F3-Up	Carboxypeptidase N catalytic chain [GS]	CBPN_HUMAN	52 kDa		5	10
F1-Down	Carboxypeptidase N subunit 2 [GS]	CPN2_HUMAN	61 kDa	Down	5	0
F2-Down	Coagulation factor IX [GS1a]	FA9_HUMAN	52 kDa	Down	6	3
F4-Up	Coagulation factor XIII B chain [GS1a]	F13B_HUMAN	76 kDa	Up	7	14
F2, F3 -Down	Complement C3 [GS]	CO3_HUMAN	187 kDa	Down	30	9
F5, F6-Down	Complement C5 [G]	CO5 _HUMAN	188 kDa	Down	43	2
F2,F4-Down	Complement component C6	CO6_HUMAN	105 kDa	Down	14	11
F2-Down	Complement factor I	CFAI_HUMAN	66 kDa	Down	10	5
F1- Down	Desmoglein-1 [GS1a]	DSG1_HUMAN	114 kDa	Down	11	1
F1, F3,F4-Down	Desmoplakin [1a]	DESP_HUMAN	332 kDa	Down	31	5
F1- Down	Filaggrin-2 [1a]	FILA2_HUMAN	248 kDa	Down	9	2
F6-Down	Galectin-3-binding protein [1a]	LG3BP_HUMAN	65 kDa	Up	6	14
F3-Up	Hemoglobin subunit alpha	HBA_HUMAN	15 kDa	Up	3	7
F3-Up	Hemoglobin subunit beta	HBB_HUMAN	16 kDa	Up	3	9
F1- Down	Ig gamma-1 chain C region	IGHG1_HUMAN	36 kDa		4	0
F4-Down	Inter-alpha-trypsin inhibitor heavy chain H1	ITIH1_HUMAN	101 kDa	Down	20	5
F1,- Down	Inter-alpha-trypsin inhibitor heavy chain H2	ITIH2_HUMAN	106 kDa	Down	17	3
F1- Down	Junction plakoglobin [1a]	PLAK_HUMAN	82 kDa	Down	6	0
F4-Up	Plasma kallikrein heavy chain [GS]	H0YAC1_HUMAN	77 kDa	Up	2	10
F4-Up, F3-Down	Plasminogen [GS]	PLMN_HUMAN	91 kDa	Up	37	10
F5-Up	Pregnancy zone	PZP_HUMAN	164 kDa	Up	0	17

	protein [GS1a]					
F2- Up	Pregnancy-specific beta-1-glycoprotein 1 [G]	PSG1_HUMAN	48 kDa	Up	0	6
F3-Up	Serotransferrin [GS]	TRFE_HUMAN	77 kDa	Up	31	46
F2-Down	Serum albumin	ALBU_HUMAN	69 kDa	Down	45	33
F1- Down	Transthyretin	TTHY_HUMAN	16 kDa	Down	5	0

G, glycoprotein; GS, sialylated glycoprotein; 1a, low abundance protein (few ng to sub μg/mL level); *, non-glycoprotein.

TABLE 4

DIFFERENTIALLY EXPRESSED PROTEINS IN THE MAL FRACTIONS FROM DISEASE-FREE SERUM (DFS) AND CANCER SERUM (CS) M13 COLUMN. DATA ON GS WERE FROM REFS. [26, 39, 42, 56, 62, 63]

Fractions which differential expression was found(Down or up)	Identified Proteins	Accession Number	Mol. Wt.	Up/down regulated	Total of average spectral counts from different fractions (DFS)	Total of average spectral counts from different fractions (CS)
F3-up	Afamin [GS]	AFAM_HUMAN	69 kDa	Up	4	18
F4,F5-Down	Alpha-1-antitrypsin [GS]	A[1a]T_HUMAN	47 kDa	Down	46	57
F3-Up	Alpha-2-macroglobulin	A2MG_HUMAN	163 kDa	Up	0	3
F1-Down	Antithrombin-III [GS]	ANT3_HUMAN	53 kDa	Down	6	0
F5-Down	Apolipoprotein B-100 [GS]	APOB_HUMAN	516 kDa	Down	38	26
F3-Up	Apolipoprotein C-I	APOC1_HUMAN	9 kDa	Up	2	5
F4- Down	C4b-binding protein alpha chain [1a]	C4BPA_HUMAN	67 kDa	Up	6	2
F1-Up	Carboxypeptidase N catalytic chain [1a]	CBPN_HUMAN	52 kDa	Up	2	8
F1-Up	Ceruloplasmin [GS]	CERU_HUMAN	122 kDa	Up	4	12
F2-Up	Clusterin [GS]	CLUS_HUMAN	58 kDa	Up	9	16
F2-Up	Complement C1r subcomponent	C1R_HUMAN	80 kDa	Up	5	17
F5, F6-Down	Complement C5 [GS]	CO5 _HUMAN	188 kDa	Down	33	26

F5-Down	Complement factor I	CFAI_HUMAN	66 kDa	Down	8	2
F6-Up	Desmoplakin [1a]	DESP_HUMAN	332 kDa	Up	2	20
F3-Up	Hemoglobin subunit beta	HBB_HUMAN	16 kDa	Up	0	7
F5-Down	Inter-alpha-trypsin inhibitor heavy chain H1	ITIH1_HUMAN	101 kDa	Down	19	11
F5,F6-Down	Inter-alpha-trypsin inhibitor heavy chain H2 [GS]	ITIH2_HUMAN	106 kDa	Down	43	25
F2-Up	Serotransferrin [GS]	TRFE_HUMAN	77 kDa	Up	30	49

G, glycoprotein; GS, sialylated glycoprotein; 1a, low abundance protein (few ng to sub μg/mL level); *, non-glycoprotein.

TABLE 5

DEPS UNIQUE TO SNA LECTIN AND MAL LECTIN AND COMMON TO BOTH LECTINS.

DATA ON GS WERE FROM REFS. [15, 32, 39, 56, 62, 63, 70, 73, 74]

DEPs unique to SNA lectin	**DEPs common to both lectins**	**DEPs unique to MAL lectin**
Actin, cytoplasmic 1	Alpha-1-antitrypsin [GS]	Afamin [GS]
Alpha-1-antichymotrypsin [GS]	Alpha-2-macroglobulin	Apolipoprotein C-I
Alpha-lactalbumin	Antithrombin-III [GS]	Carboxypeptidase N catalytic chain [1a]
Annexin A2 [1a]	Apolipoprotein B-100 [GS]	Ceruloplasmin [GS]
Apolipoprotein B-100 [GS]	C4b-binding protein alpha chain G	Clusterin [GS]
Apolipoprotein C-III G	Complement C5 [GS]	Complement C1r subcomponent
Cadherin-5 [GS]	Complement factor I	
Calumenin	Desmoplakin [1a]	
Carboxypeptidase N catalytic chain [GS]	Hemoglobin subunit beta	
Carboxypeptidase N subunit 2 [GS]	Inter-alpha-trypsin inhibitor heavy chain H1	
Coagulation factor IX [GS1a]	Inter-alpha-trypsin inhibitor heavy chain H2 [GS]	
Coagulation factor XIII B chain [GS1a]	Serotransferrin [GS]	
Complement C3 [GS]		
Complement C5 G		
Complement component C6		
Desmoglein-1 [GS1a]		

Filaggrin-2 [1a]		
Galectin-3-binding protein [1a]		
Hemoglobin subunit alpha		
Ig gamma-1 chain C region		
Junction plakoglobin [1a]		
Plasma kallikrein heavy chain [GS]		
Plasminogen [GS]		
Pregnancy zone protein [GS1a]		
Pregnancy-specific beta-1-glycoprotein 1 G		
Serotransferrin [GS]		
Serum albumin		
Transthyretin		

G, glycoprotein; GS, sialylated glycoprotein; 1a, low abundance protein (few ng to sub μg/mL level); *, non-glycoprotein.

TABLE 6

PROTEINS IDENTIFIED BY THE LC/MS ANALYSIS OF THE MAL-II CAPTURED PROTEINS FRACTIONATED ON THE RPC COLUMN FROM DISEASE- FREE AND CANCER SERA USING M13 COLUMN. DATA ON GS WERE FROM REFS. [14, 15, 24, 26, 32, 39, 40, 42, 56, 62-64, 69, 70, 73]

		Average Spectral count for disease-free serum						Average Spectral count for cancer serum					
		Fr #1	Fr #2	Fr #3	Fr #4	Fr #5	Fr #6	Fr #1	Fr #2	Fr #3	Fr #4	Fr #5	Fr #6
1	14-3-3 protein beta/alpha [1a]	0	0	2	0	0	0	0	0	0	0	0	0
2	14-3-3 protein zeta/delta [1a]	0	0	3	0	0	0	0	0	0	0	0	0
3	A disintegrin and metalloproteinase with thrombospondin motifs 13 [1a] [GS]	0	0	0	0	0	0	0	0	2	3	0	0
4	Actin, cytoplasmic 1 *	0	0	12	0	2	0	0	0	0	0	5	0
5	Afamin [GS]	0	0	0	18	3	0	0	0	4	16	0	0
6	Alpha-1-acid glycoprotein 1 [GS]	0	4	3	2	0	0	0	5	4	2	0	0
7	Alpha-1-acid glycoprotein 2 [GS]	0	5	6	5	3	0	0	6	5	6	0	2
8	Alpha-1-antichymotrypsin [GS]	0	0	0	8	13	9	0	0	0	2	8	7
9	Alpha-1-antitrypsin [GS]	5	8	14	25	25	22	5	5	11	14	23	19
10	Alpha-1B-glycoprotein [GS]	2	11	10	6	2	2	0	11	8	5	2	2
11	Alpha-2-antiplasmin [GS]	0	0	2	0	11	11	0	3	0	0	11	10
12	Alpha-2-HS-glycoprotein [GS]	0	6	5	4	6	5	0	6	6	5	5	5
13	Alpha-2-macroglobulin [GS]	0	0	0	0	55	57	0	0	0	0	28	59

14	Alpha-2-macroglobulin-like protein 1 [GS]	0	0	3	0	0	0	0	0	0	0	0	0
15	Alpha-actinin-1 [1a]	0	0	3	0	0	0	0	0	0	0	0	0
16	Alpha-lactalbumin [GS]	0	4	0	0	0	0	0	0	0	0	0	0
17	Alpha-S1-casein	2	0	2	0	0	0	0	2	0	4	0	0
18	Alpha-S2-casein	0	0	0	0	0	0	0	0	0	2	0	0
19	Angiotensinogen [GS]	0	0	0	2	11	7	0	0	0	0	9	5
20	Annexin A2 [1a]	4	0	0	0	0	0	0	0	0	0	0	0
21	Antithrombin-III [GS]	2	7	9	22	12	5	0	2	16	18	7	5
22	Apolipoprotein A-I [GS]	2	11	11	24	28	28	5	11	17	23	29	31
23	Apolipoprotein A-II *	0	3	4	6	7	7	3	2	6	5	7	7
24	Apolipoprotein A-IV*	11	15	17	21	25	26	6	14	20	19	30	26
25	Apolipoprotein B-100 [GS]	0	11	3	3	45	54	0	6	0	2	8	56
26	Apolipoprotein C-I *	0	4	3	4	3	3	0	6	6	4	4	4
27	Apolipoprotein C-II *	0	3	5	5	2	3	0	4	5	5	3	4
28	Apolipoprotein C-III [G]	2	3	6	4	2	3	2	5	5	5	3	4
29	Apolipoprotein C-IV *	0	0	0	0	0	0	0	2	0	0	0	0
30	Apolipoprotein D [GS]	0	6	5	7	6	5	0	5	7	7	7	5
31	Apolipoprotein E [G]	2	3	5	11	15	20	3	5	9	8	19	22
32	Apolipoprotein F [G]	0	2	0	0	0	0	0	2	2	2	0	0
33	Apolipoprotein L1 [G]	0	0	4	5	6	10	0	0	5	6	5	10
34	Apolipoprotein M [GS]	0	0	5	5	3	4	0	0	5	6	3	4
35	Apolipoprotein(a) [1a]	2	3	2	0	0	0	2	2	2	0	0	0
36	Arginase-1 [1a]	2	0	0	0	0	0	0	0	0	0	0	0
37	Asialoglycoprotein receptor 2 [1a G]	0	0	0	0	0	0	0	2	0	0	0	0
38	Attractin [1a]	0	0	3	0	0	0	0	0	4	3	0	0
39	Beta-2-glycoprotein 1 [GS]	9	9	7	5	3	3	8	9	6	9	3	5
40	Beta-2-microglobulin [GS]	0	2	0	0	0	0	2	0	0	0	0	0

41	Beta-Ala-His dipeptidase [1a]	0	0	0	0	2	11	0	0	0	0	0	10
42	Beta-casein	0	0	0	0	0	0	0	0	0	2	0	0
43	Bleomycin hydrolase [1a]	3	0	0	0	0	0	0	0	0	0	0	0
44	C4b-binding protein alpha chain [G]	0	5	10	5	3	3	0	11	12	11	5	5
45	C4b-binding protein beta chain [G]	0	2	0	0	0	0	0	2	0	0	0	0
46	Cadherin-5 [1a GS]	0	6	2	0	0	0	0	9	4	4	0	0
47	Calmodulin-like protein 3	0	0	2	0	0	0	0	0	0	0	0	0
48	Calmodulin-like protein 5 [1a]	0	0	2	0	0	0	0	0	0	0	0	0
49	Calpain-1 catalytic subunit [1a]	2	0	0	0	0	0	0	0	0	0	0	0
50	Calumenin [GS]	0	0	0	0	0	0	0	3	0	0	0	0
51	Carboxypeptidase N catalytic chain [1a GS]	0	0	5	11	7	4	0	0	10	12	4	3
52	Carboxypeptidase N subunit 2 [GS]	0	0	0	0	10	10	0	0	0	0	0	13
53	Cartilage acidic protein 1 [1a G]	0	0	2	0	0	0	0	0	4	2	0	0
54	Caspase-14 [1a *]	6	0	0	0	0	0	0	0	0	0	0	0
55	Catalase [1a]	3	0	0	0	0	0	0	0	0	0	0	0
56	Cathelicidin antimicrobial peptide [1a]	0	0	2	3	0	0	0	0	2	2	0	0
57	Cathepsin D [GS]	2	0	0	0	0	0	0	0	0	0	0	0
58	Cationic trypsin	2	0	0	0	0	0	3	0	0	0	0	0
59	CD5 antigen-like *	0	0	0	2	3	3	0	0	0	4	6	4
60	Ceruloplasmin [GS]	0	10	28	33	22	19	0	5	28	34	24	26
61	Cholinesterase [1a]	0	0	0	0	0	0	0	0	0	0	2	0
62	Clusterin [GS]	0	5	13	19	10	8	0	4	17	18	8	10
63	Coagulation factor IX [1a GS]	0	6	8	6	0	0	0	2	12	11	2	0
64	Coagulation factor V [1a G]	0	5	0	0	0	0	0	5	2	2	0	0
65	Coagulation factor VII [1a]	0	0	0	3	0	0	0	0	0	3	0	0
66	Coagulation factor X [1a]	0	3	0	0	0	0	0	3	0	0	0	0

67	Coagulation factor XII [GS]	0	3	4	2	6	2	0	0	6	4	2	2
68	Coagulation factor XIII B chain [1a]	21	31	14	7	2	0	20	33	12	14	4	2
69	Collectin-11 [1a]	0	0	0	0	0	0	0	0	0	2	0	0
70	Complement C [GS]	0	0	0	0	27	20	0	0	0	0	2	14
71	Complement C1r subcomponent [GS]	0	9	18	16	13	4	0	0	24	21	7	3
72	Complement C1r subcomponent-like protein [1a GS]	0	0	0	0	0	0	0	3	2	2	0	0
73	Complement C1s subcomponent [GS]	0	0	17	19	6	2	0	0	14	15	6	2
74	Complement C2 [G]	0	0	0	0	0	0	0	0	0	0	0	2
75	Complement C3 [G]	3	15	15	50	82	99	2	4	2	12	58	98
76	Complement C4 beta chain [G]	0	0	0	15	37	36	0	0	0	8	46	36
77	Complement C4-B [G]	0	0	0	0	2	2	0	0	0	0	2	3
78	Complement component C6 [G]	0	3	11	3	0	0	0	0	12	8	0	0
79	Complement component C7 [G]	0	0	4	0	0	0	0	0	4	4	0	0
80	Complement component C8 alpha chain [G]	0	0	0	0	0	0	0	0	0	2	0	0
81	Complement component C8 gamma chain [G]	0	0	0	0	0	0	0	0	0	2	0	0
82	Complement component C9 [G]	0	0	0	5	2	0	0	0	0	4	0	0
83	Complement factor B [G]	0	0	11	13	2	3	0	3	11	13	6	3
84	Complement factor H [G]	53	52	30	16	16	19	45	52	36	31	20	24
85	Complement factor H-related protein 1 [GS]	2	4	0	0	0	0	4	3	0	0	0	0
86	Complement factor H-related protein 2 [G]	0	2	0	0	0	0	2	2	0	0	0	0
87	Complement factor H-related protein 3 [1aG]	3	5	2	0	0	0	2	5	0	0	0	0

88	Complement factor H-related protein 4 [1a G]	0	0	0	0	0	0	0	2	0	0	0	0
89	Complement factor I [G]	0	10	17	14	5	6	0	3	22	17	9	4
90	Corneodesmosin [1a GS]	2	0	0	0	0	0	0	0	0	0	0	0
91	Cornifin-A [1a]	0	0	2	0	0	0	0	0	0	0	0	0
92	Cystatin-A [1a GS]	2	0	0	0	0	0	0	0	0	0	0	0
93	Dermcidin [1a]	2	2	0	0	0	0	2	0	0	0	0	0
94	Desmocollin-1 [1a GS]	4	0	0	0	0	2	0	0	0	0	0	0
95	Desmoglein-1 [1a GS]	11	0	0	0	0	0	0	0	0	0	0	0
96	Desmoplakin [1a *]	23	0	8	0	3	4	5	0	0	0	0	0
97	EGF-containing fibulin-like extracellular matrix protein 1 [1a G]	0	0	0	0	0	0	0	0	0	0	0	2
98	Elongation factor 1-alpha 1 [1a]	0	0	2	0	0	0	0	0	0	0	0	0
99	Extracellular matrix protein 1 [1aG]	2	3	0	0	0	0	3	3	0	0	0	0
100	Extracellular serine/threonine protein kinase FAM20C [G]	0	0	0	0	0	0	0	0	2	0	0	0
101	Fetuin-B [1a GS]	0	4	7	7	0	0	0	4	8	7	0	0
102	Fibrinogen alpha chain [GS]	5	3	3	0	0	0	5	3	4	2	0	2
103	Fibronectin [GS]	4	4	3	7	36	41	3	4	2	10	47	40
104	Fibulin-1 [GS]	0	0	3	3	0	0	0	0	4	4	0	0
105	Ficolin-2 [1a GS]	0	0	0	0	0	0	0	2	4	4	0	0
106	Ficolin-3 [1aGS]	0	0	0	3	3	4	0	0	2	3	4	4
107	Filaggrin-2 [1a]	9	0	0	0	0	3	0	2	0	2	0	0
108	Galectin-3-binding protein [1a GS]	0	2	0	0	7	8	0	3	0	0	0	14
109	Galectin-7 [1a GS]	0	0	3	0	0	0	0	0	0	0	0	0
110	Gamma-A of Fibrinogen gamma chain [GS]	0	0	2	0	0	0	0	0	2	2	0	0
111	Gamma-glutamylcyclotransferase	2	0	0	0	0	0	0	0	0	0	0	0

112	Gasdermin-A	3	0	0	0	0	0	0	0	0	0	0	0
113	Gelsolin [1a]	0	0	0	0	0	0	0	0	0	3	0	0
114	Glutathione peroxidase 3	0	0	0	0	0	0	0	0	2	0	0	0
115	Glutathione S-transferase P [1a]	0	0	2	0	0	0	0	0	0	0	0	0
116	Glyceraldehyde-3-phosphate dehydrogenase [1a]	4	0	5	0	0	0	0	0	0	0	0	0
117	Haptoglobin [GS]	8	24	28	28	23	22	3	25	28	28	23	21
118	Haptoglobin-related protein [1a *]	0	0	5	5	3	4	0	0	5	5	4	4
119	Heat shock protein beta-1 [1a]	0	0	2	0	0	0	0	0	0	0	0	0
120	Heat shock protein HSP 90-beta [1a]	0	0	2	0	0	0	0	0	0	0	0	0
121	Hemoglobin subunit alpha [G]	0	0	3	2	0	2	0	0	7	8	4	4
122	Hemoglobin subunit beta [G]	0	0	3	3	0	6	0	3	9	10	7	6
123	Hemopexin [GS]	0	12	14	11	5	3	0	13	18	12	5	4
124	Heparin cofactor 2 [GS]	0	0	0	0	4	3	0	0	0	0	2	2
125	Histidine ammonia-lyase	2	0	0	0	0	0	0	0	0	0	0	0
126	Histidine-rich glycoprotein [GS]	0	20	15	10	5	6	0	19	12	13	7	8
127	Histone H2A type 1-B/E [1a]	0	0	2	0	0	0	0	0	0	0	0	0
128	Histone H2B type 2-F [1a]	0	0	2	0	0	0	0	0	0	0	0	0
129	Histone H4 [1a]	0	0	4	0	0	0	0	0	0	0	0	0
130	Hornerin [1a*]	0	0	2	0	0	3	3	0	0	2	0	0
131	Hyaluronan-binding protein 2 *	0	8	6	2	0	0	0	10	6	4	2	0
133	Ig alpha-1 chain C region [G]	0	0	8	11	12	9	0	2	10	11	10	9
134	Ig alpha-2 chain C region [G]	0	0	0	2	0	2	0	0	2	2	0	0
135	Ig delta chain C region [1aG]	0	0	2	0	0	0	0	0	0	0	0	0
136	Ig gamma-1 chain C region [G]	4	3	6	0	2	3	0	2	2	2	2	4
137	Ig gamma-2 chain C region [G]	0	0	3	0	0	0	0	0	0	0	0	0
138	Ig heavy chain V-III region BRO *	0	0	0	2	2	2	0	0	0	0	2	2
139	Ig heavy chain V-III region VH26	0	0	0	2	2	0	0	0	0	2	0	2

	*												
140	Ig kappa chain C region *	3	5	6	7	7	7	3	5	6	7	7	6
141	Ig kappa chain V-I region EU*	0	0	0	0	0	0	0	0	0	2	0	0
142	Ig kappa chain V-II region TEW*	0	0	0	0	0	0	0	0	0	2	0	0
143	Ig kappa chain V-III region B6 *	0	0	0	2	0	0	0	0	0	0	0	0
144	Ig kappa chain V-III region WOL*	2	2	0	2	2	3	2	2	2	3	3	2
145	Ig kappa chain V-IV region Len *	0	0	0	0	0	2	0	0	0	2	0	2
146	Ig lambda chain V-I region HA *	0	2	0	2	2	0	0	0	0	0	2	0
147	Ig lambda chain V-III region LOI*	0	0	0	2	0	2	0	0	0	2	0	0
148	Ig lambda chain V-III region SH *	0	0	0	2	2	0	0	0	0	2	0	0
149	Ig lambda-2 chain C regions *	0	2	0	2	2	2	0	2	2	2	2	2
150	Ig mu chain C region [GS]	0	0	4	13	13	14	0	0	7	13	13	13
151	Immunoglobulin J chain [GS]	0	0	0	3	3	3	0	0	3	3	3	3
152	Immunoglobulin lambda-like polypeptide 5 *	2	2	3	5	5	4	2	3	4	4	4	5
153	Insulin-like growth factor-binding protein 3	0	0	0	0	0	0	2	0	0	0	0	0
154	Insulin-like growth factor-binding protein complex acid labile subunit [GS]	2	0	0	0	3	0	0	0	0	0	6	0
155	Inter-alpha-trypsin inhibitor heavy chain H1 [GS]	0	2	2	20	24	15	0	0	0	5	26	12
156	Inter-alpha-trypsin inhibitor heavy chain H2 [GS]	3	3	3	12	27	14	2	2	0	2	29	17
157	Inter-alpha-trypsin inhibitor heavy chain H3 [GS]	0	0	0	2	0	0	0	0	0	0	0	0
158	Inter-alpha-trypsin inhibitor heavy chain H4 [1a GS]	0	4	7	8	18	22	0	4	10	10	24	23
159	Junction plakoglobin [1a*]	4	0	0	2	0	0	0	0	0	0	0	0

160	Kallistatin [GS]	0	0	0	0	2	3	0	0	0	0	6	3
161	Keratin, type I cytoskeletal 10 [1a*]	25	20	20	24	26	24	19	22	20	24	23	19
162	Keratin, type I cytoskeletal 14 [1a*]	24	11	25	15	6	16	17	12	3	10	9	10
163	Keratin, type I cytoskeletal 15 [1a*]	0	0	3	0	0	0	0	0	0	0	0	0
164	Keratin, type I cytoskeletal 16 [1a*]	15	5	11	10	0	9	8	8	0	0	2	0
165	Keratin, type I cytoskeletal 17 [1a*]	7	0	14	2	0	3	2	3	0	0	0	0
166	Keratin, type I cytoskeletal 9*	23	15	15	18	14	22	17	14	13	19	14	16
167	Keratin, type II cytoskeletal 1*	36	25	24	29	27	29	27	26	22	29	23	26
168	Keratin, type II cytoskeletal 1b*	17	0	0	0	0	2	0	5	0	0	0	0
169	Keratin, type II cytoskeletal 2 epidermal*	44	26	24	26	26	40	26	25	19	26	19	23
170	Keratin, type II cytoskeletal 5 [1a*]	21	6	21	8	6	12	14	7	3	5	4	4
171	Keratin, type II cytoskeletal 6A *	5	2	5	2	0	3	6	3	0	0	0	0
172	Keratin, type II cytoskeletal 6B *	25	3	29	15	3	18	20	9	2	3	5	2
173	Keratin, type II cytoskeletal 78*	7	0	0	0	0	0	0	0	0	0	0	0
174	Keratin, type II cytoskeletal 80 *	9	0	0	0	0	0	0	0	0	0	0	0
175	Keratinocyte proline-rich protein	6	0	0	0	2	4	0	2	0	0	0	0
176	Kininogen-1 [GS]	7	22	20	17	13	15	5	27	22	22	15	11
177	Leucine-rich alpha-2-glycoprotein [GS]	0	0	0	3	0	0	0	0	0	3	0	0
178	Lipopolysaccharide-binding protein [1a]	0	0	0	0	0	0	0	0	0	0	0	3
179	Lumican [GS]	0	0	4	3	0	0	0	0	7	3	0	0
180	Mannan-binding lectin serine protease 1 [1a]	0	0	0	0	0	0	0	0	2	3	0	0
181	Mannan-binding lectin serine protease 2	0	0	0	0	0	0	0	2	0	0	0	0
182	MBP-1 of Alpha-enolase	0	0	3	0	0	0	0	0	0	0	0	0

183	Monocyte differentiation antigen CD14 [1a]	0	0	0	3	0	0	0	0	0	0	0	0
184	Myosin-9 [1a]	0	0	2	0	0	0	0	0	0	0	0	0
185	N-acetylglucosamine-1-phosphotransferase subunit gamma [1a GS]	0	0	0	0	0	0	0	0	2	2	0	0
186	N-acetylmuramoyl-L-alanine amidase [GS]	0	0	0	3	0	0	0	0	0	2	0	0
187	Neutrophil defensin 1	0	0	0	0	0	2	0	0	0	0	0	0
188	Out at first protein homolog	0	0	2	0	0	0	0	0	2	2	0	0
189	Peptidyl-prolyl cis-trans isomerase A [1a G]	0	0	2	0	0	0	0	0	0	0	0	0
190	Phosphatidylcholine-sterol acyltransferase [1a]	0	0	0	4	2	0	0	0	0	4	3	3
191	Phosphatidylinositol-glycan-specific phospholipase D [1a GS]	0	0	0	0	9	12	0	0	0	0	11	17
192	Phosphoglycerate mutase 2 [1a]	0	0	3	0	0	0	0	0	0	0	0	0
193	Phospholipid transfer protein [1aG]	0	0	0	0	3	3	0	0	0	0	0	3
194	Plasma kallikrein heavy chain	0	0	3	0	4	4	0	0	7	7	5	4
195	Plasma protease C1 inhibitor	0	0	0	0	9	7	0	0	0	0	11	9
196	Plasma serine protease inhibitor [1a]	0	0	0	0	0	4	0	0	0	0	0	6
197	Plasminogen	0	30	21	2	2	0	0	36	8	8	2	2
198	Plectin [1a]	2	0	0	0	0	0	0	0	0	0	0	0
199	Plexin domain-containing protein 2 [1a]	0	0	0	0	0	0	0	0	0	2	0	0
200	Pregnancy zone protein [1a GS]	0	0	0	0	17	23	0	0	0	0	0	20
201	Pregnancy-specific beta-1-glycoprotein 1 [GS]	0	0	0	0	0	0	0	7	5	5	0	0
202	Pregnancy-specific beta-1-	0	0	0	0	0	0	0	0	2	3	0	0

	glycoprotein 2 [GS]												
203	Prenylcysteine oxidase 1 [1a G]	0	0	0	0	0	3	0	0	0	0	0	4
204	Protein AMBP [GS]	0	5	7	12	9	7	0	4	7	9	11	5
205	Protein S100-A11 [1a]	0	0	2	0	0	0	0	0	0	0	0	0
206	Protein S100-A7 [1a]	0	0	3	0	3	0	0	0	0	0	0	0
207	Protein S100-A8 [1a]	0	0	2	0	0	0	0	0	0	0	0	0
208	Protein S100-A9	0	0	5	2	2	3	0	0	2	3	0	0
209	Protein Z-dependent protease inhibitor [1a G]	0	0	0	3	3	2	0	0	0	0	2	3
210	Protein-glutamine gamma-glutamyltransferase E [1a]	7	0	0	0	0	0	0	0	0	0	0	0
211	Protein-glutamine gamma-glutamyltransferase K	3	0	0	0	0	0	0	0	0	0	0	0
212	Prothrombin	2	6	11	19	4	5	2	6	20	21	6	6
213	Retinol-binding protein 4	0	4	4	4	3	0	0	4	5	3	4	2
214	Secreted phosphoprotein 24 [1a]	0	2	0	0	0	0	0	3	0	0	0	0
215	Selenoprotein P [1aG]	3	7	2	0	0	0	5	7	5	5	0	4
216	Semenogelin-1 [1a]	0	2	0	0	0	0	0	0	0	0	0	0
217	Serotransferrin [GS]	0	41	31	22	10	13	3	43	46	30	13	14
218	Serpin B12	3	0	0	0	0	0	0	0	0	0	0	0
219	Serum albumin	17	45	57	50	41	39	10	29	55	52	42	40
220	Serum amyloid A-1 protein [GS]	0	0	0	0	0	0	0	0	3	2	0	0
221	Serum amyloid A-4 protein [GS]	0	0	4	6	4	5	0	2	5	5	3	3
222	Serum amyloid P-component [GS]	0	0	6	6	4	5	0	0	6	7	5	5
223	Serum paraoxonase/arylesterase 1 [GS]	0	0	0	5	9	7	0	0	3	5	9	8
224	Serum paraoxonase/lactonase 3 [1a G]	0	0	0	0	2	3	0	0	0	2	3	3
225	Sex hormone-binding globulin [1a G]	0	0	2	0	0	0	0	0	2	2	0	0

226	Small proline-rich protein 2E G	0	0	0	0	2	0	0	0	0	0	0	0
227	Suprabasin [1a]	2	0	0	0	0	0	0	0	0	0	0	0
228	Tetranectin	0	7	5	2	0	0	0	7	4	2	0	0
229	Thioredoxin [1a]	3	0	0	0	0	0	0	0	0	0	0	0
230	Transthyretin	5	8	9	8	6	6	0	8	9	8	4	3
231	Trypsin [1a]	4	4	4	3	3	3	4	4	4	4	2	3
232	Tubulin alpha-1B chain	0	0	5	0	0	0	0	0	0	0	0	0
233	Tubulin beta-4A chain [1a]	0	0	3	0	0	0	0	0	0	0	0	0
234	Ubiquitin*	2	0	0	0	0	0	0	0	0	0	0	0
235	Vitamin D-binding protein [GS]	0	0	15	7	0	0	0	0	18	13	0	0
236	Vitamin K-dependent protein C [1a]	0	0	7	6	0	0	0	0	8	8	0	0
237	Vitamin K-dependent protein S	0	0	0	10	6	3	0	0	3	8	6	7
238	Vitamin K-dependent protein Z [1a] [GS]	0	2	0	0	0	0	0	3	0	0	0	0
239	Vitronectin [GS]	0	8	11	7	6	4	0	9	12	10	5	5
240	Zinc-alpha-2-glycoprotein [GS]	2	5	0	0	0	0	0	7	0	0	0	0

G, glycoprotein; GS, sialylated glycoprotein; 1a, low abundance protein (few ng to sub μg/mL level); *, non-glycoprotein.

TABLE 7

PROTEINS IDENTIFIED BY THE LC/MS ANALYSIS OF THE SNA CAPTURED PROTEINS FRACTIONATED ON THE RPC COLUMN FROM DISEASE- FREE AND CANCER SERA USING M13 COLUMN. DATA ON GS WERE FROM REFS. [6, 14, 15, 24, 26, 32, 34, 39, 42, 48, 56, 62-64, 67, 70, 73, 74]

		Average spectral count for disease-free serum						Average spectral for cancer serum					
#	Identified proteins	Fr# 1	Fr#2	Fr#3	Fr#4	Fr#5	Fr#6	Fr#1	Fr#2	Fr#3	Fr#4	Fr#5	Fr#6
1	Actin, cytoplasmic 1 *	0	0	0	0	0	0	0	0	0	0	0	11
2	Afamin [GS]	0	32	41	7	0	0	0	23	38	13	0	0
3	Alpha-1-acid glycoprotein 1 [GS]	12	11	5	2	3	0	15	10	8	5	3	0
4	Alpha-1-acid glycoprotein 2 [GS]	8	10	0	0	0	0	10	14	0	0	0	0
5	Alpha-1-antichymotrypsin [GS]	0	10	44	28	22	22	0	10	24	26	19	12
6	Alpha-1-antitrypsin [GS]	28	86	141	107	58	49	13	67	98	100	52	27
7	Alpha-1B-glycoprotein [GS]	22	15	4	4	3	3	17	18	6	5	4	0
8	Alpha-2-antiplasmin [GS]	3	0	10	14	13	9	0	0	15	24	34	3
9	Alpha-2-HS-glycoprotein [GS]	23	21	21	17	17	11	17	21	15	12	14	13
10	Alpha-2-macroglobulin [GS]	6	4	17	64	134	161	0	2	11	56	157	115
11	Alpha-S1-casein	0	0	0	5	0	0	0	0	0	0	0	0
12	Angiotensinogen [GS]	0	0	14	18	17	10	0	0	8	20	16	5
13	Annexin A1 [1a]	0	0	0	0	0	0	0	0	0	0	0	14

14	Annexin A2 [1a]	0	0	0	0	0	4	0	0	0	0	0	4
15	Antithrombin-III [GS]	4	47	27	19	13	11	3	35	21	8	9	4
16	Apolipoprotein A-I [GS]	30	92	145	128	88	79	21	91	141	119	99	61
17	Apolipoprotein A-II *	8	10	18	17	17	17	5	13	17	17	19	10
18	Apolipoprotein A-IV *	33	42	57	52	43	32	25	38	50	41	48	30
19	Apolipoprotein B-100 [GS]	17	17	18	81	120	125	5	7	6	17	71	34
20	Apolipoprotein C-I *	10	16	3	4	4	4	7	14	4	0	7	2
21	Apolipoprotein C-II *	5	14	6	3	4	3	3	12	4	0	4	4
22	Apolipoprotein C-III [G]	10	12	6	3	4	4	7	12	5	0	5	0
23	Apolipoprotein D [GS]	6	11	20	11	8	7	2	10	19	13	9	4
24	Apolipoprotein E [G]	9	31	25	25	23	23	9	19	20	19	26	11
25	Apolipoprotein F [G]	0	0	0	0	0	0	3	0	0	0	0	0
26	Apolipoprotein L1 [G]	0	11	4	5	6	6	0	10	6	6	13	4
27	Apolipoprotein M [GS]	0	13	5	5	5	4	0	14	5	4	5	0
28	Apolipoprotein(a) [1a]	3	4	0	0	0	0	3	2	0	0	0	0
29	Attractin [1a]	0	9	2	0	0	0	0	12	3	0	0	0
30	Beta-2-glycoprotein 1 [GS]	37	11	10	6	5	3	38	17	15	8	10	3
31	Beta-2-microglobulin [GS]	4	0	0	0	0	0	6	0	0	0	0	0
32	Beta-Ala-His dipeptidase [1a]	0	0	0	3	5	0	0	0	0	0	15	0
33	Beta-casein	0	0	0	0	0	0	0	0	0	3	0	0
34	C4b-binding protein alpha chain [G]	2	13	14	5	6	0	0	5	2	0	2	2
35	C4b-binding protein beta chain [G]	0	3	0	0	0	0	0	0	0	0	0	0
36	Carboxypeptidase B2 [1a GS]	0	0	4	0	0	0	0	0	7	0	0	0
37	Carboxypeptidase N catalytic chain [1a GS]	0	17	15	4	4	3	0	27	17	4	5	0
38	Carboxypeptidase N subunit 2 [GS]	0	0	0	4	20	25	0	0	0	8	22	14
39	Cartilage oligomeric matrix	0	0	0	0	0	0	0	0	3	0	0	0

	protein [1a GS]												
40	Cationic trypsin	3	0	0	0	0	0	0	0	0	0	0	0
41	CD5 antigen-like *	0	4	10	9	6	3	0	0	10	7	11	3
42	Ceruloplasmin [GS]	6	69	65	42	37	36	5	83	65	54	45	30
43	Cholinesterase [1a]	0	0	4	0	0	0	0	0	4	4	4	3
44	Clusterin [GS]	11	31	20	16	11	7	9	28	15	8	10	6
45	Coagulation factor IX [1a GS]	0	3	0	0	0	0	0	4	0	0	0	0
46	Coagulation factor V [1a GS]	3	0	0	0	0	0	0	0	0	0	0	0
47	Coagulation factor XII [GS]	4	8	10	10	6	0	4	13	5	0	4	0
48	Coagulation factor XIII B chain [1a GS]	13	0	0	0	0	0	9	0	0	0	0	0
49	Complement C1r subcomponent [GS]	14	32	24	20	4	0	14	44	16	11	3	0
50	Complement C1r subcomponent-like protein [1a GS]	0	5	4	4	0	0	0	7	4	0	0	0
51	Complement C1s subcomponent [GS]	0	26	11	6	3	0	0	28	12	4	3	0
52	Complement C2 [G]	0	0	0	2	6	0	0	0	0	7	12	0
53	Complement C3 [GS]	13	81	154	213	248	196	8	37	153	214	342	148
54	Complement C4-A [GS]	0	0	104	82	0	0	0	0	0	0	0	0
55	Complement C4-B [GS]	0	33	106	84	67	66	0	25	93	111	91	61
56	Complement C5 [G]	0	0	2	12	28	28	0	0	0	7	51	20
57	Complement component C6 [G]	7	12	0	0	0	0	8	20	0	0	0	0
58	Complement component C7 [G]	0	2	0	0	0	0	0	9	0	0	0	0
59	Complement component C8 alpha chain [G]	0	18	6	3	4	2	0	9	5	3	3	0
60	Complement component C8 beta chain [G]	0	0	0	0	0	0	0	4	0	0	0	0

61	Complement component C8 gamma chain [G]	0	14	8	3	3	2	0	8	3	0	2	0
62	Complement component C9 [G]	0	2	3	0	0	0	0	3	4	0	0	0
63	Complement factor B [G]	5	35	17	8	7	0	10	41	23	12	15	4
64	Complement factor H [GS]	173	76	64	55	48	19	153	84	61	36	38	30
65	Complement factor H	76	0	0	0	0	0	69	0	0	0	0	0
66	Complement factor H-related protein 1 [GS]	26	8	8	0	0	0	21	12	6	0	0	0
67	Complement factor H-related protein 2 [GS]	15	4	5	0	0	0	17	6	3	2	0	0
68	Complement factor H-related protein 3 [1a GS]	10	0	0	0	0	0	10	0	0	0	0	0
69	Complement factor I [G]	23	44	28	22	14	7	25	65	25	18	17	11
70	Corticosteroid-binding globulin	0	0	0	4	4	2	0	0	0	3	4	3
71	Cystatin-B [1a GS]	0	0	0	0	0	0	0	0	0	0	0	5
72	Dermcidin [1a]	2	0	3	0	0	0	0	0	0	0	0	4
73	Desmocollin-1 [1a GS]	0	0	0	0	0	3	0	0	0	0	0	0
74	Desmoglein-1 [1a GS]	0	0	0	0	0	8	0	0	2	0	0	3
75	Desmoplakin [1a*]	6	5	0	0	3	22	0	0	4	0	5	25
76	Elongation factor 1-alpha 1 [1a]	0	0	0	0	0	0	0	0	0	0	0	4
77	Extracellular matrix protein 1G	0	0	0	0	0	0	7	0	0	0	0	0
78	Fetuin-B [1a GS]	6	14	10	4	2	0	4	15	6	4	4	0
79	Fibrinogen alpha chain [GS]	7	0	0	0	0	0	6	0	0	0	0	0
80	Fibronectin [GS]	26	24	92	88	83	66	9	12	50	61	68	61
81	Fibulin-1 [GS]	0	0	3	0	0	0	0	2	3	0	0	0
82	Ficolin-2 [1a GS]	0	0	0	0	0	0	0	3	0	0	0	0
83	Ficolin-3 [1a GS]	0	3	5	7	10	7	0	3	5	8	11	4
84	Filaggrin-2 [1a]	0	0	0	0	4	5	0	0	4	3	4	4

85	Galectin-3-binding protein [1a]	0	0	0	0	6	5	0	0	0	0	6	9
86	Gelsolin *	5	8	5	0	0	0	0	4	4	0	0	0
87	Glyceraldehyde-3-phosphate dehydrogenase [1a]	0	0	0	0	0	2	0	0	0	0	0	0
88	Haptoglobin [GS]	79	96	83	75	68	59	74	96	79	72	65	56
89	Haptoglobin-related protein [1a*]	38	48	46	44	43	33	0	52	40	41	38	33
90	Heat shock protein beta-1 [1a G]	0	0	0	0	0	0	0	0	0	0	0	4
91	Hemoglobin subunit alpha G	0	9	0	0	0	0	9	32	13	8	7	5
92	Hemoglobin subunit beta G	0	10	7	4	2	0	10	26	16	14	15	12
93	Hemoglobin subunit delta	0	0	0	0	0	0	0	14	0	0	0	0
94	Hemopexin [GS]	35	53	19	14	11	8	23	56	17	14	16	8
95	Heparin cofactor 2 [GS]	0	0	17	13	10	7	0	4	17	16	12	9
96	Hepatocyte growth factor activator [1a GS]	6	0	0	0	0	0	0	0	0	0	0	0
97	Histidine-rich glycoprotein [GS]	32	33	23	21	12	10	20	26	13	14	13	5
98	Hornerin [1a *]	0	3	4	0	0	5	0	3	5	0	2	2
99	Hyaluronan-binding protein 2 *	6	7	0	0	0	0	7	11	0	0	0	0
100	Ig alpha-1 chain C region [G]	11	37	42	40	29	30	11	43	36	42	39	28
101	Ig alpha-2 chain C region [G]	0	29	33	35	24	0	0	33	28	30	31	0
102	Ig delta chain C region [G]	0	3	0	0	0	0	0	0	0	0	0	0
103	Ig gamma-1 chain C region [G]	4	3	10	13	12	7	4	4	7	8	8	8
104	Ig heavy chain V-II region ARH-77 *	0	0	0	4	3	4	0	0	3	0	4	5
105	Ig heavy chain V-III region BRO [*]	0	4	2	3	3	3	0	0	3	3	0	4
106	Ig heavy chain V-III region GAL [*]	0	2	4	0	3	0	0	0	4	3	3	0
107	Ig heavy chain V-III region TIL *	0	0	3	4	3	3	0	3	3	3	4	3
108	Ig kappa chain C region *	11	19	24	27	27	26	10	22	23	25	25	22

109	Ig kappa chain V-I region DEE *	0	0	0	0	0	0	0	0	3	0	0	0
110	Ig kappa chain V-II region RPMI 6410 *	0	0	3	0	0	0	0	0	0	0	0	0
111	Ig kappa chain V-III region HAH *	0	4	4	5	2	0	0	3	4	4	3	4
112	Ig kappa chain V-IV region Len *	0	3	4	2	3	3	0	3	4	0	2	0
113	Ig lambda chain V region 4A [1a *]	0	0	3	3	0	3	0	0	3	3	4	0
114	Ig lambda chain V-I region NEW*	0	0	3	0	0	0	0	0	0	0	0	0
115	Ig lambda chain V-I region WAH *	0	0	3	3	0	0	0	2	3	0	0	0
116	Ig lambda chain V-III region LOI *	0	0	4	3	4	0	0	2	3	3	3	0
117	Ig lambda chain V-III region SH*	0	3	6	2	3	0	0	3	4	0	4	0
118	Ig lambda-2 chain C regions [GS]	0	15	18	15	17	15	10	15	17	15	17	15
119	Ig mu chain C region [GS]	5	23	35	39	42	28	0	23	37	42	47	28
120	IgGFc-binding protein [1a G]	0	0	0	0	0	0	0	0	0	0	3	6
121	Immunoglobulin J chain [GS]	3	5	5	6	6	4	0	4	5	7	5	5
122	Immunoglobulin lambda-like polypeptide 5	6	11	15	11	13	10	8	10	14	14	12	10
123	Insulin-like growth factor-binding protein 3 [GS]	5	0	0	0	0	0	0	0	0	0	0	0
124	Insulin-like growth factor-binding protein complex acid labile subunit [GS]	2	0	0	0	0	0	0	0	0	6	5	0
125	Inter-alpha-trypsin inhibitor heavy chain H1 [GS]	3	33	55	42	27	16	0	13	48	54	39	18
126	Inter-alpha-trypsin inhibitor heavy chain H2 [GS]	14	9	57	48	35	14	5	8	55	66	43	14

127	Inter-alpha-trypsin inhibitor heavy chain H3 [GS]	0	5	14	0	0	0	0	2	15	0	0	0
128	Inter-alpha-trypsin inhibitor heavy chain H4 [1a GS]	10	45	50	33	35	34	9	48	77	64	68	39
129	Junction plakoglobin [1a]	0	0	0	0	0	7	0	0	0	0	0	4
130	Junction plakoglobin	0	0	0	0	0	38	0	0	0	0	0	0
131	Kallistatin [GS]	0	0	10	13	7	3	0	4	9	25	14	4
132	Keratin, type I cuticular Ha3-II [1a]	0	0	0	0	0	0	0	0	0	0	9	0
133	Keratin, type I cytoskeletal 10 [1a]	58	59	64	44	57	83	38	56	64	57	63	57
134	Keratin, type I cytoskeletal 13 [1a]	0	22	0	0	20	0	0	0	0	16	14	60
135	Keratin, type I cytoskeletal 14 [1a]	33	38	31	31	31	70	17	22	38	29	36	42
136	Keratin, type I cytoskeletal 16 [1a]	36	47	25	32	35	77	0	19	34	31	39	50
137	Keratin, type I cytoskeletal 17 [1a]	24	27	21	20	23	52	0	0	28	21	23	38
138	Keratin, type I cytoskeletal 9	65	64	52	35	43	111	32	50	48	40	55	53
139	Keratin, type II cuticular Hb4	0	0	0	0	0	0	0	0	0	0	8	0
140	Keratin, type II cuticular Hb6	0	0	0	0	0	0	0	0	0	0	5	0
141	Keratin, type II cytoskeletal 1	83	74	74	49	71	104	42	70	72	71	77	78
142	Keratin, type II cytoskeletal 1b	0	0	0	0	0	0	0	0	0	5	0	0
143	Keratin, type II cytoskeletal 2 epidermal	71	59	67	37	57	89	27	54	60	52	74	64
144	Keratin, type II cytoskeletal 4	0	8	0	0	5	0	0	0	0	0	6	72
145	Keratin, type II cytoskeletal 5 [1a]	41	37	37	22	32	69	11	26	38	26	40	63
146	Keratin, type II cytoskeletal 6A	34	36	0	25	33	81	0	0	37	25	43	64
147	Keratin, type II cytoskeletal 6B	33	36	20	21	31	82	9	18	39	22	45	67
148	Keratin, type II cytoskeletal 78	0	0	0	0	0	5	0	0	0	0	0	5
151	Keratinocyte proline-rich protein	0	2	5	0	3	7	0	2	3	5	4	4
152	Kininogen-1	63	60	42	23	20	16	76	81	52	32	38	23
153	Leucine-rich alpha-2-	0	3	0	0	0	0	0	7	0	0	0	0

	glycoprotein [GS]												
154	Leucine-rich repeat-containing protein 15 [GS]	0	0	0	0	0	0	0	0	0	0	4	0
155	Lipopolysaccharide-binding protein [1a]	0	0	0	0	0	4	0	0	0	0	3	3
156	Lumican [1a GS]	0	3	0	0	0	0	0	10	0	0	0	0
157	Lysozyme C [1a]	3	0	0	0	0	2	3	0	0	0	0	4
158	Mannan-binding lectin serine protease 1 [1a *]	0	0	0	5	0	0	0	9	5	0	0	0
159	N-acetylmuramoyl-L-alanine amidase [GS]	0	5	2	0	0	0	0	5	0	0	0	0
160	Neutrophil defensin 1	0	0	0	0	0	3	0	0	0	3	0	0
161	Ovalbumin [GS]	0	0	0	0	0	0	0	0	3	0	0	0
162	Peroxiredoxin-1 [1a]	0	0	0	0	0	0	0	0	0	0	0	4
163	Peroxiredoxin-2 [1a]	0	0	0	0	0	3	0	0	4	5	0	0
164	Phosphatidylcholine-sterol acyltransferase [1a]	0	0	7	0	0	0	0	0	6	0	0	0
165	Phosphatidylinositol-glycan-specific phospholipase D [1a GS]	0	0	0	9	11	4	0	0	0	11	14	16
166	Phospholipid transfer protein [1a G]	0	0	0	0	0	3	0	0	0	0	0	0
167	Pigment epithelium-derived factor [GS]	0	0	0	0	0	0	0	0	0	0	2	0
168	Plasma kallikrein heavy chain [GS]	0	0	6	4	7	3	0	13	5	4	7	3
169	Plasma protease C1 inhibitor [GS]	0	5	18	29	18	18	0	4	14	19	16	15
170	Plasma retinol-binding protein [G]	7	23	23	14	6	6	13	22	22	18	15	5
171	Plasma serine protease inhibitor [1a GS]	0	0	0	11	7	6	0	0	0	7	17	0
172	Plasminogen [GS]	69	33	9	7	3	0	58	37	5	3	5	0
173	Pregnancy zone protein [1a GS]	0	0	0	0	29	47	0	0	0	0	43	33

174	Pregnancy-specific beta-1-glycoprotein 1 [GS]	0	0	0	0	0	0	3	4	3	0	0	0
175	Prenylcysteine oxidase 1 [1a G]	0	0	0	0	0	0	0	0	0	0	5	0
176	Prolactin-inducible protein [1a G]	0	0	0	0	0	2	0	0	0	0	0	2
177	Protein AMBP [GS]	18	21	22	21	17	6	14	20	20	20	17	7
178	Protein S100-A7 [1a]	0	0	0	0	0	4	0	0	0	9	0	0
179	Protein S100-A8 [1a]	0	0	0	0	0	0	0	0	0	4	0	6
180	Protein S100-A9	3	4	4	3	4	6	0	3	3	11	4	9
181	Protein Z-dependent protease inhibitor [1a G]	0	0	4	0	0	0	0	0	3	2	3	0
182	Protein-glutamine gamma-glutamyltransferase E [1a]	0	0	0	0	0	0	0	0	0	0	0	3
183	Prothrombin	16	16	6	5	5	3	6	8	5	3	5	2
184	Selenoprotein P [1a G]	5	0	0	0	0	0	6	0	0	0	0	0
185	Semenogelin-1 [1a]	0	0	0	0	0	5	0	0	0	0	0	0
186	Serotransferrin [GS]	120	85	42	24	19	22	99	95	31	20	24	32
187	Serpin B12	0	0	0	0	0	2	0	0	0	0	0	0
188	Serum albumin	0	18	0	0	0	0	0	23	0	0	0	0
189	Serum albumin	171	240	137	101	92	90	156	258	138	119	129	69
190	Serum amyloid A-4 protein [GS]	3	13	8	7	6	5	4	14	7	0	3	2
191	Serum amyloid P-component [GS]	0	24	18	15	11	9	8	21	16	14	13	9
192	Serum paraoxonase/arylesterase 1 [GS]	0	7	19	14	12	13	0	10	15	14	14	10
193	Serum paraoxonase/lactonase 3 [1a G]	0	0	0	0	0	0	0	0	4	5	4	0
194	Sex hormone-binding globulin [1a G]	0	3	0	0	0	0	0	3	0	0	0	0
195	Small proline-rich protein 3 [G]	0	0	0	0	0	0	0	0	0	0	0	4
196	Sulfhydryl oxidase 1 [1a]	0	0	4	0	0	0	0	0	4	0	0	0
197	Tetranectin [GS]	8	4	3	0	0	0	9	5	4	4	2	0

198	Thyroxine-binding globulin [GS]	0	0	0	5	0	0	0	0	0	3	2	0
199	Transthyretin *	14	17	13	8	4	4	8	23	11	8	7	0
200	Trypsin [1a]	14	12	12	9	11	10	12	13	13	12	12	13
201	Vitamin D-binding protein [GS]	2	62	5	6	0	0	4	32	0	0	0	0
202	Vitamin K-dependent protein C [1a]	4	14	0	0	0	0	5	16	0	0	0	0
203	Vitamin K-dependent protein S	0	13	36	13	6	6	0	13	35	16	11	7
204	Vitamin K-dependent protein Z [1a GS]	0	0	0	0	0	0	4	0	0	0	0	0
205	Vitronectin [GS]	11	17	11	10	11	5	9	18	11	8	10	7
206	von Willebrand factor [1a GS]	0	0	3	0	0		0					
207	Zinc-alpha-2-glycoprotein [GS]	12	3	3	0	0	0	15	6	3	0	0	0

G, glycoprotein; GS, sialylated glycoprotein; 1a, low abundance protein (few ng to sub μg/mL level); *, non-glycoprotein.

TABLE 8

DIFFERENTIALLY EXPRESSED PROTEINS IN THE MAL FRACTIONS FROM DISEASE-FREE SERUM (DFS) AND CANCER SERUM (CS) FOR THE COLUMN ORDER MAL-II → SNA. DATA ON GS WERE FROM REFS. [14, 22, 34, 56, 62, 63, 67, 68, 70]

Fractions which differential expression was found(Down or up)	Identified Proteins	Accession Number	Mol. Wt.	Up/down regulated	Total of average spectral counts from different fractions (DFS)	Total of average spectral counts from different fractions (CS)
F4,F5,F6-Down	Alpha-1-antichymotrypsin [GS]	AACT_HUMAN	48 kDa	Down	30	17
F3,F4,F5,F6-Down	Alpha-1-antitrypsin [GS]	A[1a]T_HUMAN	47 kDa	Down	86	47
F2,F5,F3-Down	Alpha-1B-glycoprotein [GS]	A1BG_HUMAN	54 kDa	Down	23	19
F5-Down	Alpha-2-macroglobulin [GS]	A2MG_HUMAN	163 kDa	Down	55	28
F3-Up	Antithrombin-III [GS]	ANT3_HUMAN	53 kDa	Up	9	16
F3-Up	Apolipoprotein A-I [GS]	APOA1_HUMAN	31 kDa	Up	11	17
F4-Up	Apolipoprotein E[G]	APOE_HUMAN	23 KDa	Up	5	11
F4-Down	Apolipoprotein B 100 [GS]	APOB_HUMAN	516 KDa	Down	45	8
F2-Down	Apolipoprotein L1[G]	APOL1_HUMAN	21 kDa	Down	10	5
F2-Up	Beta-2-glycoprotein 1 [GS]	APOH_HUMAN	38 kDa	Up	5	9
F4-Up	Coagulation factor IX [GS1a]	FA9_HUMAN	52 kDa	Up	6	11
F5-Down	Coagulation factor XII [GS]	FA12_HUMAN	68 kDa	Down	6	2
F4-Uo	Coagulation factor XIII B[GS1a]	F13B_HUMAN	76 kDa	Up	7	14

F6-Up	Complement C1r subcomponent [GS]	C1R_HUMAN	80 kDa	Up	16	21
F3-Down	Complement C1s subcomponent [GS]	C1S_HUMAN	77 kDa	Down	18	12
F3,F4-Down	Complement C3 [G]	CO3_HUMAN	187 kDa	Down	65	15
F5,F6-Up	Fibronectin [1aGS]	FINC_HUMAN	240 kDa	Up	43	57
F4-Up	Hemoglobin subunit alpha [G]	HBA_HUMAN	15 kDa	Up	2	8
F4,F5-Down	Inter-alpha-trypsin inhibitor heavy chain H1 [GS]	ITIH1_HUMAN	101 kDa	Down	44	31
F1,F3,F4,F5-Down	Inter-alpha-trypsin inhibitor heavy chain H2 [GS]	ITIH2_HUMAN	106 kDa	Down	45	31
F2-Up	Clusterin [GS]	CLUS_HUMAN	58 kDa	Up	12	17
F2-Up	Pregnancy-specific beta-1-glycoprotein 1 [GS]	PSG1_HUMAN	48 kDa	Up	2	7
F6-Up	Phosphatidylinositol-glycan-specific phospholipase [GS]	PHLD_HUMAN	92 kDa	Up	9	17
F3-Up	Plasma kallikrein heavy chain	H0YAC1_HUMAN	77 kDa	Up	3	7
F2,F3,F4-Down	Plasminogen	PLMN_HUMAN	91 kDa	Up	53	42
F2,F6-Up	Serotransferrin [GS]	TRFE_HUMAN	77 kDa	Up	72	89
F4-Up	Vitronectin [GS1a]	VTNC_HUMAN	54 kDa	Up	7	10

G, glycoprotein; GS, sialylated glycoprotein; 1a, low abundance protein; *, non-glycoprotein.

TABLE 9

DIFFERENTIALLY EXPRESSED PROTEINS IN THE SNA FRACTIONS FROM DISEASE-FREE SERUM (DFS) AND CANCER SERUM (CS) FOR THE COLUMN ORDER MAL-II → SNA. DATA ON GS WERE FROM REFS. [14, 34, 56, 62, 63, 67, 68, 70]

Fractions which differential expression was found(Down or up)	Identified Proteins	Accession Number	Mol. Wt.	Up/down regulated	Total of average spectral counts from different fractions (DFS)	Total of average spectral counts from different fractions (CS)
F2-Down	Afamin [GS]	AFAM_HUMAN	69 kDa	Down	32	23
F3-Down	Alpha-1-antichymotrypsin [GS]	AACT_HUMAN	48 kDa		44	24
F5-Up	Alpha-2-antiplasmin [GS]	A2AP_HUMAN	55 kDa	Up	13	34
F6-Up	Annexin A1 [1a]	ANXA1_HUMAN	39 kDa	Up	6	14
F4-Down	Antithrombin-III [GS]	ANT3_HUMAN	53 kDa	Down	19	8
F1,F2,F3,F4,F5,F6-Down	Apolipoprotein B-100 [GS]	APOB_HUMAN	516 kDa	Down	388	158
F2,F3-Down	C4b-binding protein alpha chain [G]	C4BPA_HUMAN	67 kDa	Down	27	7
F3-Up	Carboxypeptidase B2 [GS]	CBPB2_HUMAN	48 kDa		5	9
F4-Down	Coagulation factor XII [GS]	FA12_HUMAN	68 kDa	Down	10	2
F5-Up	Complement C2 [G]	CO2_HUMAN	83 kDa	Up	6	12
F2-Down	Complement C3 [GS]	CO3_HUMAN	187 kDa	Down	81	37
F4-Down	Complement C4-A [GS]	CO4A_HUMAN	193 kDa	Down	82	10

F5-Up	Complement C5 [G]	CO5_HUMAN	188 kDa	Up	67	91
F3-Down	Complement component C8 gamma chain	CO8G_HUMAN	22 kDa		14	8
F2-Up	Complement factor H [G]	CFAH_HUMAN	139 kDa	Up	76	84
F1,F2,F3,F5-Down	Fibronectin 1[GS1a]	FINC_HUMAN	240 kDa	Down	225	135
F2,F3-Up	Hemoglobin subunit alpha [G]	HBA_HUMAN	15 kDa	Up	9	45
F1,F2,F3,F4-Up	Hemoglobin subunit beta [1a]	HBB_HUMAN	16 kDa	Up	21	66
F2-Down	Inter-alpha-trypsin inhibitor heavy chain H1 [GS]	ITIH1_HUMAN	101 kDa	Down	33	13
F3,F4,F5-Up	Inter-alpha-trypsin inhibitor heavy chain H4 [GS]	ITIH4_HUMAN	103 kDa		118	209
F6-Down	Junction plakoglobin [1a]	5GWP8_HUMAN	66 kDa	Down	38	4
F5-Up	Kininogen-1 [GS]	KNG1_HUMAN	48 kDa	Up	20	38
F2-Up	Lumican [GS]	LUM_HUMAN	38 kDa	Up	3	10
F6-Up	Phosphatidylinositol-glycan-specific phospholipase D [1aGS]	PHLD_HUMAN	92 kDa	Up	4	16
F4-Up	Protein S100-A7 [1a]	S10A7_HUMAN	11 kDa	Up	6	11
F2-Down	Vitamin D-binding protein [1a]	D6RF35_HUMAN	53 kDa	Down	62	32

G, glycoprotein; GS, sialylated glycoprotein; 1a, low abundance protein (few ng to sub μg/mL level); *, non-glycoprotein.

TABLE 10

DEPS UNIQUE TO MAL LECTIN AND SNA LECTIN AND COMMON TO BOTH LECTINS FOR THE COLUMN ORDER MAL-II → SNA. DATA ON GS WERE FROM REFS. [14, 22, 32, 34, 39, 56, 62, 63, 67, 68, 70, 73, 74]

DEPs unique to MAL lectin	**DEPs common to both lectins**	**DEPs unique to SNA lectin**
Alpha-1-antitrypsin [GS]	Alpha-1-antichymotrypsin[GS]	Actin, cytoplasmic 1
Apolipoprotein A-I [GS]	Alpha-1B-glycoprotein [GS]	Afamin [GS]
Apolipoprotein EG	Alpha-2-macroglobulin [GS]	Alpha-2-antiplasmin [GS]
Apolipoprotein L1G	Antithrombin-III [GS]	Annexin A1 [1a]
Beta-2-glycoprotein 1 [GS]	Apolipoprotein B 100 [GS]	Apolipoprotein B-100 [GS]
Clusterin [GS]	Coagulation factor XII [GS]	Carboxypeptidase B2 [GS]
Coagulation factor IX [GS1a]	Complement C3 G	Inter-alpha-trypsin inhibitor heavy chain H4 [GS]
Coagulation factor XIII B[GS1a]	Fibronectin [1aGS]	Complement C2 G
Complement C1r subcomponent [GS]	Hemoglobin subunit alpha G	Complement C4-A[GS]
Complement C1s subcomponent [GS]	Inter-alpha-trypsin inhibitor heavy chain H1 [GS]	Complement C5 G
Inter-alpha-trypsin inhibitor heavy chain H2 [GS]	Phosphatidylinositol-glycan-specific phospholipase [GS]	Complement component C8 gamma chain
Phosphatidylinositol-glycan-specific phospholipase [GS]	Plasma kallikrein heavy chain	Complement factor H G
Plasma kallikrein heavy chain		Hemoglobin subunit beta [1a]
Plasminogen		Kininogen-1 [GS]
Pregnancy-specific beta-1-glycoprotein 1 [GS]		Lumican [GS]

Serotransferrin [GS]		Phosphatidylinositol-glycan-specific phospholipase D [1aGS]
Vitronectin [GS1a]		Junction plakoglobin [1a]
		Plasma kallikrein heavy chain
		Protein S100-A7 [1a]
		Protein S100-A9
		Vitamin D-binding protein [1a]

G, glycoprotein; GS, sialylated glycoprotein; 1a, low abundance protein (few ng to sub μg/mL level); *, non- glycoprotein.

References

1. Al-Mehdi, A.B., *Intravascular origin of metastasis from the proliferation of endothelium-attached tumor cells: a new model for metastasis.* Nature Med., 2000. **6**: p. 100-102.
2. Brinkman-Van der Linden, E.C. and A. Varki, *New aspects of siglec binding specificities, including the significance of fucosylation and of the sialyl-Tn epitope. Sialic acid-binding immunoglobulin superfamily lectins.* J. Biol. Chem., 2000. **275**: p. 8625-8632.
3. Fukuda, M.N., *A peptide mimic of E-selectin ligand inhibits sialyl Lewis X-dependent lung colonization of tumor cells.* Cancer Res., 2000. **60**: p. 450-456.
4. Girnita, L., *Inhibition of N-linked glycosylation down-regulates insulin-like growth factor-1 receptor at the cell surface and kills Ewing's sarcoma cells: therapeutic implications.* Anticancer Drug Des., 2000. **15**: p. 67-72.
5. Granovsky, M., *Suppression of tumor growth and metastasis in Mgat5-deficient mice.* Nature Med., 2000. **6**: p. 306-312.
6. Pagnan, G., *Delivery of c-myb antisense oligodeoxynucleotides to human neuroblastoma cells via disialoganglioside GD(2)-targeted immunoliposomes: antitumor effects.* J. Natl Cancer Inst., 2000. **92**: p. 253-261.

7. Sanderson, R.D., *Heparan sulfate proteoglycans in invasion and metastasis.* Semin. Cell Dev. Biol., 2001. **12**: p. 89-98.

8. Saxon, E. and C.R. Bertozzi, *Cell surface engineering by a modified Staudinger reaction.* Science, 2000. **287**: p. 2007-2010.

9. Schachter, H., *The joys of HexNAc. The synthesis and function of N- and O-glycan branches.* Glycoconj. J., 2000. **17**: p. 465-483.

10. Tumova, S., A. Woods, and J.R. Couchman, *Heparan sulfate proteoglycans on the cell surface: versatile coordinators of cellular functions.* Int. J. Biochem. Cell Biol., 2000. **32**: p. 269-288.

11. Fry, S.A., J. Sinclair, J.F. Timms, A.J. Leathem, and M.V. Dwek, *A targeted glycoproteomic approach identifies cadherin-5 as a novel biomarker of metastatic breast cancer.* Cancer Lett., 2013. **328**(2): p. 335-344.

12. Fuster, M.M. and J.D. Esko, *The sweet and sour of cancer: glycans as novel therapeutic targets.* Nat Rev Cancer, 2005. **5**(7): p. 526-542.

13. Liu, F.T. and G.A. Rabinovich, *Galectins as modulators of tumour progression.* Nature Rev. Cancer, 2005. **5**: p. 29-41.

14. Pisano, C., *Undersulfated, low-molecular-weight glycol-split heparin as an antiangiogenic VEGF antagonist.* Glycobiology, 2005. **15**: p. 1C-6C.

15. Qiu, R.Q. and F.E. Regnier, *Comparative glycoproteomics of N-linked complex-type glycoforms containing sialic acid in human serum.* Anal. Chem., 2005. **77**(22): p. 7225-7231.

16. Ramanathan, R.K., *Phase I study of a MUC1 vaccine composed of different doses of MUC1 peptide with SB-AS2 adjuvant in resected and locally advanced pancreatic cancer.* Cancer Immunol. Immunother., 2005. **54**: p. 254-264.

17. Selvaraju, S. and Z.E. Rassi, *Targeting human serum fucome by an integrated liquid-phase multicolumn platform operating in "cascade" to facilitate comparative mass spectrometric analysis of disease-free and breast cancer sera.* Proteomics, 2013. **13**(10-11): p. 1701-1713.

18. Uematsu, R., J.-i. Furukawa, H. Nakagawa, Y. Shinohara, K. Deguchi, K. Monde, and S.-I. Nishimura, *High Throughput Quantitative Glycomics and Glycoform-focused Proteomics of Murine Dermis and Epidermis.* Mol. Cell. Proteome., 2005. **4**(12): p. 1977-1989.

19. Yeh, L.-K., W.-L. Chen, W. Li, E.M. Espana, J. Ouyang, T. Kawakita, W.W.-Y. Kao, S.C.G. Tseng, and C.-Y. Liu, *Soluble Lumican Glycoprotein Purified from Human Amniotic Membrane Promotes Corneal Epithelial Wound Healing.* Invest. Ophthal. Vis. Sci., 2005. **46**(2): p. 479-486.

20. Ching, I.S., W. Ching-Ho, S. Shih-Cheng, L. Hsiu-Chin, L. Jiunn-Wang, and S. Hong-Lin, *The Infection of Chicken Tracheal Epithelial Cells with a H6N1 Avian Influenza Virus.* PLoS ONE, 2011. **6**(5): p. 1-7.

21. Geisler, C. and D.L. Jarvis, *Letter to the Glyco-Forum: Effective glycoanalysis with Maackia amurensis lectins requires a clear understanding of their binding specificities.* Glycobiology, 2011. **21**(8): p. 988-993.

22. Pacchiarotta, T., et al., *Fibrinogen alpha chain O-glycopeptides as possible markers of urinary tract infection.* J. Proteome. Res., 2012. **75**(3): p. 1067-1073.

23. Zeng, Z., M. Hincapie, S.J. Pitteri, S. Hanash, J. Schalkwijk, J.M. Hogan, H. Wang, and W.S. Hancock, *A Proteomics Platform Combining Depletion, Multi-lectin Affinity Chromatography (M-LAC), and Isoelectric Focusing to Study the Breast Cancer Proteome.* Anal. Chem., 2011. **83**(12): p. 4845-4854.

24. Dutta, G., D.S. Barber, P. Zhang, N.J. Doperalski, and B. Liu, *Involvement of dopaminergic neuronal cystatin C in neuronal injury-induced microglial activation and neurotoxicity.* J. Neurochem., 2012. **122**(4): p. 752-763.

25. Linnartz, B., J. Kopatz, A.J. Tenner, and H. Neumann, *Sialic Acid on the Neuronal Glycocalyx Prevents Complement C1 Binding and Complement Receptor-3-Mediated Removal by Microglia.* J. Neurosci., 2012. **32**(3): p. 946-952.

26. Nazifi, S., A. Oryan, M. Ansari-Lari, M.R. Tabandeh, A. Mohammadalipour, and M. Gowharnia, *Evaluation of sialic acids and their correlation with acute-phase proteins (haptoglobin and serum amyloid A) in clinically healthy Iranian camels (Camelus dromedarius).* Com. Clin. Path., 2012. **21**(4): p. 383-387.

27. Geyer, H., R. Geyer, M. Odenthal-Schnittler, and H.-J. Schnittler, *Characterization of human vascular endothelial cadherin glycans.* Glycobiology, 1999. **9**(9): p. 915-925.

28. Yoshimura, M., Y. Ihara, Y. Matsuzawa, and N. Taniguchi, *Aberrant glycosylation of E-cadherin enhances cell-cell binding to suppress metastasis.* J. Biol. Chem., 1996. **271**: p. 13811-13815.

29. Delort, L., S. Perrier, V. Dubois, H. Billard, T. Mracek, C. Bing, M.P. Vasson, and F. Caldefie-Chezet, *Zinc-alpha2-glycoprotein: a proliferative factor for breast cancer? In vitro study and molecular mechanisms.* Oncol Rep, 2013. **29**(5): p. 2025-9.

30. Abbott, D.E., et al., *Reevaluating Cathepsin D as a biomarker for breast cancer: Serum activity levels versus histopathology.* Cancer Biol. Ther., 2010. **9**(1): p. 23-30.

31. Campion, C.G., M. Labrie, G. Lavoie, and Y. St-Pierre, *Expression of Galectin-7 Is Induced in Breast Cancer Cells by Mutant p53.* PLoS ONE, 2013. **8**(8): p. e72468.

32. Ueda, K., et al., *Targeted serum glycoproteomics for the discovery of lung cancer-associated glycosylation disorders using lectin-coupled ProteinChip arrays.* Proteomics, 2009. **9**(8): p. 2182-2192.

33. Pan, S., T.A. Brentnall, K. Kelly, and R. Chen, *Tissue proteomics in pancreatic cancer study: Discovery, emerging technologies, and challenges.* Proteomics, 2013. **13**(3-4): p. 710-721.

34. Wu, J., X. Xie, S. Nie, R.J. Buckanovich, and D.M. Lubman, *Altered Expression of Sialylated Glycoproteins in Ovarian Cancer Sera Using Lectin-based ELISA*

Assay and Quantitative Glycoproteomics Analysis. J.proteome.Res., 2013. **12**(7): p. 3342-3352.

35. Raiszadeh, M.M., et al., *Proteomic Analysis of Eccrine Sweat: Implications for the Discovery of Schizophrenia Biomarker Proteins.* J.proteome.res., 2012. **11**(4): p. 2127-2139.

36. Gerber, P.A., et al., *Systematic Identification and Characterization of Novel Human Skin-Associated Genes Encoding Membrane and Secreted Proteins.* PLoS ONE, 2013. **8**(6): p. e63949.

37. Migita, T. and S. Inoue, *Implications of the Golgi apparatus in prostate cancer.* Int.J Biochem. Cell Biol., 2012. **44**(11): p. 1872-1876.

38. Farrah, T., et al., *A High-Confidence Human Plasma Proteome Reference Set with Estimated Concentrations in PeptideAtlas.* Mol. Cell. Proteome., 2011. **10**(9).

39. Shetty, V., Z. Nickens, P. Shah, G. Sinnathamby, O.J. Semmes, and R. Philip, *Investigation of Sialylation Aberration in N-linked Glycopeptides By Lectin and Tandem Labeling (LTL) Quantitative Proteomics.* Anal.Chem., 2010. **82**(22): p. 9201-9210.

40. Pirie-Shepherd, S.R., E.A. Jett, N.L. Andon, and S.V. Pizzo, *Sialic Acid Content of Plasminogen 2 Glycoforms as a Regulator of Fibrinolytic Activity: .* J. Biol. Chem., 1995. **270**(11): p. 5877-5881.

41. Faiers, A.A., A.Y. Loh, and D.H. Osmond, *Microheterogeneity and sialic acid in human plasma angiotensinogens in various physiological states.* Canadian J. Biochem., 1978. **56**(9): p. 892-899.

42. Ito, M., K. Ikeda, Y. Suzuki, K. Tanaka, and M. Saito, *An Improved Fluorometric High-Performance Liquid Chromatography Method for Sialic Acid Determination: An Internal Standard Method and Its Application to Sialic Acid Analysis of Human Apolipoprotein E.* Anal. Biochem., 2002. **300**(2): p. 260-266.

43. Kurogochi, M., T. Matsushista, M. Amano, J.-i. Furukawa, Y. Shinohara, M. Aoshima, and S.-I. Nishimura, *Sialic Acid-focused Quantitative Mouse Serum Glycoproteomics by Multiple Reaction Monitoring Assay.* Mol. Cell. Proteome., 2010. **9**(11): p. 2354-2368.

44. von Schoultz, B. and T. Stigbrand, *Characterization of the "pregnancy zone protein" in relation to other α2-globulins of pregnancy.* Biochim. Biophys. Acta, 1974. **359**(2): p. 303-310.

45. Madera, M., Y. Mechref, I. Klouckova, and M.V. Novotny, *Semiautomated High-Sensitivity Profiling of Human Blood Serum Glycoproteins through Lectin Preconcentration and Multidimensional Chromatography/Tandem Mass Spectrometry.* J. Proteome. Res., 2006. **5**(9): p. 2348-2363.

46. Yang, Z. and W.S. Hancock, *Approach to the comprehensive analysis of glycoproteins isolated from human serum using a multi-lectin affinity column.* J. Chromatogr. A, 2004. **1053**(1–2): p. 79-88.

47. Yang, Z., L.E. Harris, D.E. Palmer-Toy, and W.S. Hancock, *Multilectin Affinity Chromatography for Characterization of Multiple Glycoprotein Biomarker Candidates in Serum from Breast Cancer Patients.* Clin. Chem., 2006. **52**(10): p. 1897-1905.

48. Alexander, H., A.L. Stegner, C. Wagner-Mann, G.C. Du Bois, S. Alexander, and E.R. Sauter, *Proteomic Analysis to Identify Breast Cancer Biomarkers in Nipple Aspirate Fluid.* Clin. Cancer Res., 2004. **10**(22): p. 7500-7510.

49. Hamler, R.L., K. Zhu, N.S. Buchanan, P. Kreunin, M.T. Kachman, F.R. Miller, and D.M. Lubman, *A two-dimensional liquid-phase separation method coupled with mass spectrometry for proteomic studies of breast cancer and biomarker identification.* Proteomics, 2004. **4**(3): p. 562-577.

50. Zeng, Z., M. Hincapie, B.B. Haab, S. Hanash, S.J. Pitteri, S. Kluck, J.M. Hogan, J. Kennedy, and W.S. Hancock, *The development of an integrated platform to identify breast cancer glycoproteome changes in human serum.* J. Chromatogr. A, 2010. **1217**(19): p. 3307-3315.

51. Olofsson, M.H., et al., *Cytokeratin-18 Is a Useful Serum Biomarker for Early Determination of Response of Breast Carcinomas to Chemotherapy.* Clin Cancer Res., 2007. **13**(11): p. 3198-3206.

52. Veenstra, T.D., T.P. Conrads, B.L. Hood, A.M. Avellino, R.G. Ellenbogen, and R.S. Morrison, *Biomarkers: Mining the Biofluid Proteome.* Mol. Cell. Proteome., 2005. **4**(4): p. 409-418.

53. Iurisci, I., N. Tinari, C. Natoli, D. Angelucci, E. Cianchetti, and S. Iacobelli, *Concentrations of Galectin-3 in the Sera of Normal Controls and Cancer Patients.* Clin. Cancer Res., 2000. **6**(4): p. 1389-1393.

54. Paredes, J., A. Albergaria, J.T. Oliveira, C. Jerónimo, F. Milanezi, and F.C. Schmitt, *P-Cadherin Overexpression Is an Indicator of Clinical Outcome in Invasive Breast Carcinomas and Is Associated with CDH3 Promoter Hypomethylation.* Clin. Cancer Res., 2005. **11**(16): p. 5869-5877.

55. Hamrita, B., K. Chahed, M. Trimeche, C.L. Guillier, P. Hammann, A. Chaïeb, S. Korbi, and L. Chouchane, *Proteomics-based identification of α1-antitrypsin and haptoglobin precursors as novel serum markers in infiltrating ductal breast carcinomas.* Clinica Chimica Acta, 2009. **404**(2): p. 111-118.

56. Opstal-van Winden, A., et al., *Searching for early breast cancer biomarkers by serum protein profiling of pre-diagnostic serum; a nested case-control study.* BMC Cancer, 2011. **11**(1): p. 381.

57. Leskov, K.S., D.Y. Klokov, J. Li, T.J. Kinsella, and D.A. Boothman, *Synthesis and Functional Analyses of Nuclear Clusterin, a Cell Death Protein.* J. Biol. Chem., 2003. **278**(13): p. 11590-11600.

58. July, L.V., E. Beraldi, A. So, L. Fazli, K. Evans, J.C. English, and M.E. Gleave, *Nucleotide-based therapies targeting clusterin chemosensitize human lung adenocarcinoma cells both in vitro and in vivo.* Mol. Cancer Ther., 2004. **3**(3): p. 223-232.

59. Ahmed, N., K.T. Oliva, G. Barker, P. Hoffmann, S. Reeve, I.A. Smith, M.A. Quinn, and G.E. Rice, *Proteomic tracking of serum protein isoforms as screening biomarkers of ovarian cancer*. Proteomics, 2005. **5**(17): p. 4625-4636.

60. Sun, Z.-L., Y. Zhu, F.-Q. Wang, R. Chen, T. Peng, Z.-N. Fan, Z.-K. Xu, and Y. Miao, *Serum proteomic-based analysis of pancreatic carcinoma for the identification of potential cancer biomarkers.* Biochim. Biophys., 2007. **1774**(6): p. 764-771.

61. Cho, J.-Y. and H.-J. Sung, *Proteomic approaches in lung cancer biomarker development.* Expert Rev. Proteome., 2009. **6**(1): p. 27-42.

62. Tian, Y., F.J. Esteva, J. Song, and H. Zhang, *Altered Expression of Sialylated Glycoproteins in Breast Cancer Using Hydrazide Chemistry and Mass Spectrometry.* Mol. Cell. Biol., 2012. **11**(6).

63. Tian, Y. and H. Zhang, *Characterization of disease-associated N-linked glycoproteins.* Proteomics, 2013. **13**(3-4): p. 504-511.

64. Janosi, J.B.M., S.M. Firth, J.J. Bond, R.C. Baxter, and P.J.D. Delhanty, *N-Linked Glycosylation and Sialylation of the Acid-labile Subunit:*. J. Biol. Chem., 1999. **274**(9): p. 5292-5298.

65. Jalkanen, S. and M. Jalkanen, *Lymphocyte CD44 binds the COOH-terminal heparin-binding domain of fibronectin.* J. Cell Biol., 1992. **116**: p. 817-825.

66. Bharadwaj, D., R.J. Harris, W. Kisiel, and K.J. Smith, *Enzymatic Removal of Sialic Acid from Human Factor IX and Factor X Has No Effect on Their Coagulant Activity.* J. Biol. Chem., 1995. **270**(12): p. 6537-6542.

67. Xu, L., W. Xu, G. Xu, Z. Jiang, L. Zheng, Y. Zhou, W. Wei, and S. Wu, *Effects of cell surface α2-3 sialic acid on osteogenesis.* Glycoconjugate Journal, 2013. **30**(7): p. 677-685.

68. Zauner, G., M. Hoffmann, E. Rapp, C.A.M. Koeleman, I. Dragan, A.M. Deelder, M. Wuhrer, and P.J. Hensbergen, *Glycoproteomic Analysis of Human Fibrinogen Reveals Novel Regions of O-Glycosylation.* J. Proteome. Res., 2012. **11**(12): p. 5804-5814.

69. Millar, J.S., *The sialylation of plasma lipoproteins.* Atherosclerosis, 2001. **154**(1): p. 1-13.

70. Boehm, T., J. Folkman, T. Browder, and M.S. O'Reilly, *Antiangiogenic therapy of experimental cancer does not induce acquired drug resistance.* Nature, 1997. **390**: p. 404-407.

71. Li, J., et al., *Independent validation of candidate breast cancer serum biomarkers identified by mass spectrometry.* Clin Chem, 2005. **51**: p. 2229 - 2235.

72. Adachi, T., T. Kodera, H. Ohta, K. Hayashi, and K. Hirano, *The heparin binding site of human extracellular-superoxide dismutase.* Arch. Biochem. Biophys., 1992. **297**(1): p. 155-161.

73. Ueda, K., T. Katagiri, T. Shimada, S. Irie, T.-A. Sato, Y. Nakamura, and Y. Daigo, *Comparative Profiling of Serum Glycoproteome by Sequential Purification of Glycoproteins and 2-Nitrobenzenesulfenyl (NBS) Stable Isotope Labeling: A New Approach for the Novel Biomarker Discovery for Cancer.* J. Proteome. Res., 2007. **6**(9): p. 3475-3483.

74. Yoshida, K.-i., S. Sumi, M. Honda, Y. Hosoya, M. Yano, K. Arai, and Y. Ueda, *Serial lectin affinity chromatography demonstrates altered asparagine-linked sugar chain structures of γ-glutamyltransferase in humaa renal cell carcinoma.* J. Chromatogr. B: , 1995. **672**(1): p. 45-51.

VITA

Erandi Prashani Mayadunne

Candidate for the Degree of

Doctor of Philosophy

Thesis: NON POLAR AND AFFINITY MONOLITHIC STATIONARY PHASES FOR HPLC OF LARGE AND SMALL MOLECULES AND THEIR USE IN A MULTI COLUMN LIQUID PHASE SEPARATION PLATFORM FOR THE CAPTURING AND FRACTIONATION OF SIALOGLYCOPROTEINS FROM HUMAN SERUM

Major Field: Chemistry

Biographical:

Education:

Completed the requirements for the Doctor of Philosophy in Analytical at Oklahoma State University, Stillwater, Oklahoma in December 2013.

Completed the requirements for the Bachelor of Science in your major Pharmacy at University of Colombo, Sri Lanka in 2007.

Experience:
Graduate Teaching Assistant, Oklahoma State University, Department of Chemistry, January 2009 to present
Assistant Lecture in University of Colombo, Sri Lanka from January 2008-December 2008.

Name: Erandi Prashani Mayadunne Date of Degree: December, 2013

Institution: Oklahoma state University location: Stillwater, Oklahoma

Title of study: Non Polar and Affinity Monolithic Stationary Phases for HPLC of Large and Small Molecules and Their Use in a Multi Column Liquid Phase Separation Platform for the Capturing and Fractionation of Sialoglycoproteins from Human Serum

Pages in Study: 304 Candidate for the Degree of Doctor of Philosophy

Major Field: Chemistry

Scope and Method of Study:

The major objective of this investigation was to develop novel nonpolar and affinity monolithic stationary phases for HPLC of small and large molecules, and the evaluation of their potentials in proteomics. The monolithic stationary phases were based on the *in situ* co-polymerization of methacrylate/acrylate monomers in the presence of adequately chosen porogens. The nonpolar monoliths for reversed phase chromatography (RPC) involved the co-polymerization of (i) octadecyl acrylate (ODA) and trimethyloyl propane triacrylate (TRIM) with or without incorporated multiwall carbon nanotubes (MWCNTs) and (ii) glyceryl methacrylate (GMM) and ethylene glycol dimethacrylate (EDMA) incorporated with MWCNTs. The affinity monoliths were based on the co-polymerization of GMM and pentaerythritol triacrylate (PETA) which were further modified with (i) surface immobilized lectins such as *Sambucus nigra* agglutinin (SNA) or *Maakia amurensis* lectin (MAL) and (ii) antibodies or microbial proteins for the depletion of high abundance proteins, e.g., albumin and immunoglobulins (Igs). These columns were assembled in a multi column platform consisting of high precision HPLC pumps and switching valves to perform the on line the depletion of albumin and Igs, followed by the capturing of sialoglycoproteins from human serum and the subsequent fractionation of these captured proteins by RPC. The RPC fractions were analyzed by liquid chromatography – tandem mass spectrometry (LC-MS/MS) to identify the sialoglycoproteins and to determine their differential expression in breast cancer serum with respect to disease free serum.

Findings and Conclusions:

The major findings and conclusions were as follows: while GMM/EDMA-MWCNTs monolith proved useful for RPC separations of small chiral and achiral molecules on the basis of hydrophobic and π-π interactions, the ODA/TRIM monoliths with or without MWCNTs were very effective is separating proteins with improved selectivity when the monolith has incorporated MWCNTs. The lectin monolithic columns specific for sialoglycoproteins captured selectively these targeted proteins. These captured proteins, which were further fractionated by RPC, were readily identified by LC-MS/MS. In total, the multi column platform in combination with LC-MS/MS facilitated the identification of 71 differentially expressed proteins in breast cancer serum with respect to healthy serum, thus representing 71 candidate breast cancer biomarkers.

ADVISOR'S APPROVAL: Dr. ZIAD EL RASSI